# High Density Mapping Of Ventricular Scar- Insights Into Mechanisms Of Ventricular Tachycardia

**By**

**Sachin Nayyar**

**MBBS, MD, DM**

**Centre for Heart Rhythm Disorders**

**University of Adelaide and Royal Adelaide Hospital**

**A thesis submitted to the Faculty of Health Science, University of Adelaide in total fulfillment of the requirements of the degree of DOCTOR OF PHILOSOPHY**

**Department of Cardiology, Royal Adelaide Hospital**

**Discipline of Medicine, University of Adelaide,**

**Adelaide, South Australia**

**Australia**

**December 2013**

**To my wife Pallavi**

**& Parents**

**Urmila and Raj Kumar Dham**

# ABSTRACT

Ventricular tachyarrhythmias related to structural heart disease are the most common cause of sudden cardiac death. Many of these occur in patients with ventricular scarring, related predominantly to coronary artery disease or dilated cardiomyopathies. These regions of scarring remodel over time with ongoing collagen turnover and do not stay stable, such that patients are often subject to repeated episodes of the arrhythmia.

Ventricular scars are composed of variable regions of dense interstitial fibrosis that create conduction block, interspersed with viable myocyte channels with diminished coupling which produce substrate for circuitous slow conduction pathways that promote reentry. During sinus rhythm, these channels can be identified by the presence of late potentials and long stimulus to QRS intervals during pacing in the channel. A high density of sampling in the left ventricle allows recording of small amplitude electrograms that are of fundamental emphasis in ventricular substrate mapping. Several studies have characterized channels in patients with ventricular scar and ventricular tachycardia (VT). However, there has been no assessment on the functional characteristics of these channels and whether channels that are critical to the VT circuit differ from non-VT channels.

Chapter 1 reviews literature on arrhythmic burden and epidemiology of scar related VT, its cellular mechanisms, substrate characterization, techniques of VT mapping and gaps in the current knowledge. Chapter 2 presents the high density characterization of substrate in ischemic cardiomyopathy (ICM) patients with VT and compares the features of VT supporting channels with channels that do not support VT. This study showed that compared to non-VT channels, VT channels are more often located in the dense scar, longer in length, have long stimulus to QRS latencies and slower conduction velocity. Chapter 3 describes the electrogram properties in

regions of VT channels, and development of a stepwise model from multiple electrogram properties to ensemble regions supporting VT(s) during sinus rhythm. It also discusses the application of Shannon entropy, a fundamental measure of information content in signals, to map VT channels in sinus rhythm. This system of ablation along with high density mapping will significantly advance VT mapping and help individualize substrate based ablation. Chapter 4 presents data on high density characterization of substrate in ICM patients with VT and compares with those who do not have spontaneous VT. It showed that patients without spontaneous VT have fewer channels with shorter lengths and faster conduction, compared to VT patients. These observations partly explain the relative higher predilection of few selected surviving myocyte channels in the post infarct ventricles to sustain VT.

Structural heterogeneity in the scar produces spatial and temporal disturbances in ventricular repolarization over multiple time scales. Chapter 5 evaluates the role of acute autonomic modulation on beat-to-beat QT variability in patients with heart failure with and without VT, and contrasts it with patients without structural heart disease. It showed that acute pacing and humoral modulation including beta-blockade fail to bring down high repolarization instability in heart failure patients and VT.

Catheter ablation is the mainstay for treatment of recurrent ventricular arrhythmias in patients with structural heart disease. Chapter 6 analyses published literature on ventricular arrhythmia storm ablation in a systematic review and meta-analysis. It showed that the interventions are safe and patients often need multiple procedures including non-radiofrequency ablation measures. Although patients who had successful ablation had good long-term outcomes, a failed procedure portended an early and high rate of mortality compared with medically managed historic controls. It raised a pertinent concern of possible harmful effects of catheter ablation in a high risk patient population.

In summary, this thesis has developed innovative insights into the surviving myocyte channels in patients with ischemic cardiomyopathy. It describes a novel tool for

ventricular substrate mapping that is readily applicable in the clinical laboratory. The repolarization instability is elevated in these patients and is resistant to modulation by acute beta-blocker treatment. Finally, catheter ablation is safe and should be advised in most patients with ventricular arrhythmia storm.

# DECLARATION

I certify that this work contains no material which has been accepted for the award of any other degree or diploma in any university or other tertiary institution and, to the best of my knowledge and belief, contains no material previously published or written by another person, except where due reference has been made in the text. I certify that no part of this work will, in the future, be used in a submission for any other degree or diploma in any university or other tertiary institution without the prior approval of the University of Adelaide and where applicable, any partner institution responsible for the joint-award of this degree.

The work was performed at Centre for Heart Rhythm Disorders, University of Adelaide and Royal Adelaide Hospital, Adelaide, Australia.

I certify that the writing of this thesis, the results, interpretation, opinions and suggestions are entirely my own work. This thesis does not exceed the length of 80,000 words exclusive of tables, figures and bibliography.

I give consent to this copy of my thesis, when deposited in the University Library, being made available for loan and photocopying, subject to the provisions of the Copyright Act 1968. The author acknowledges that copyright of published works contained within this thesis resides with the copyright holder(s) of those works. I also give permission for the digital version of my thesis to be made available on the web, via the University's digital research repository, the Library catalogue and also through web search engines, unless permission has been granted by the University to restrict access for a period of time.

Signature…….. Date……

(Sachin Nayyar)

# ACKNOWLEDGEMENTS

I would like to thank Professor Prashanthan Sanders, Dr Kurt Roberts-Thomson and Dr Anthony Brooks for their guidance, support and encouragement as my supervisors and mentors over this exciting period. It has indeed been a privilege to work side by side with distinguished clinical researchers. Their dedication to work and research continues to inspire me. I am also grateful to Professor Jaganmohan Tharakan, a renowned scholar and a clinician, and Professor Mohan Nair, a distinguished cardiologist, from my training institutes back in India for their workmanship and directive roles that has culminated in undertaking this thesis.

I am also grateful to the University of Adelaide for affording me a scholarship for the duration of my PhD studies. These studies could not have been performed if not for the many patients, who often at times of significant illness, participated in our understanding of the disease.

I want to acknowledge the important role of Dr Glenn Young, whose teaching, appreciation and encouragement motivated me, and who also provided many of the patients and session times for study protocols.

I wish to advance special sincere thanks to Dr Kurt Roberts-Thomson for his stupendous planning, prudence and patience in helping conduct this difficult study in high risk patients. Special thanks to Dr Pawel Kuklik for his exceptional support, and developing a novel computational model to enable signal mapping, that singularly added clinical application from otherwise observational results. Thanks to Thomas Sullivan for his statistical advice and support. A very special appreciation for Dr Anand Ganesan, whose disruptive intelligence and perseverance helped me nurture as a diligent and intensive researcher focused on goals. My sincere thanks to Dr Mathias Baumert from School of Electrical and Electronic engineering, who helped me build a scientific grasp in the technique and interpretation of body surface electrocardiography. I am also thankful to all other co-fellows, who helped me

develop a spirited insight while learning electrophysiology, and made me recognize value of entitlement.

My sincere appreciation to the electrophysiology laboratory technical team at the Royal Adelaide Hospital, Lauren Wilson, Ksenya Wojewidka, Simon Stolcman, and industry support staff, Darius Chapman, Rayed Kutieleh whose determined support and organization helped conducting these cases. A sincere thanks to the nursing staff, Judith, Karen, Christine, Jake, Sam, Arun, Reeba, Ravish, Crystal, Julia and many other special people associated with the laboratory for throughout selfless support.

My warm gratitude to my esteemed parents Dr Raj Kumar Dham and Urmila Dham, whose tremendous encouragement and belief helped me commission and complete this work. Without their youthful feelings and inspirations, it was virtually unmanageable to undertake and perform at the expected levels.

Most importantly, I wish to thank my beloved wife Pallavi, who despite her own bright career prospects, has always endeavored to stay by my side. I appreciate her for her unconditional love and understanding throughout the trying times. The masterful role of my son Sabeer over the last three years cannot be undervalued for his intelligences over stress management. I cannot help but thank Him to have this little angel who forgot his pleasures to help me achieve my academic ambitions.

# TABLE OF CONTENTS

# PUBLICATIONS AND COMMUNICATIONS TO LEARNED SOCIETIES

Chapter 2

- **Manuscript** accepted for publication in Circulation Arrhythmia Electrophysiology
- 
- **Presented** as an oral at Annual Heart Rhythm Society meeting, 2012 & 2013, USA, and **published** in abstract form (*Heart Rhythm*.2012;9:S329-S356) (*Heart Rhythm*.2013;10:S85)
- 
- **Best Clinical paper award** at Annual Asia Pacific Heart Rhythm Society meeting, 2012, Taiwan.

- **Best Poster Award** at Annual Cardiac Society of Australia and New Zealand meeting, 2012, and published in abstract form (Heart, Lung and Circulation, 2012;21:S1-S330)

- Ralph Reader Young Investigator Award, Clinical, Finalist at Annual Cardiac Society of Australia and New Zealand meeting, 2013

Chapter 3

- **Presented** as an moderated and innovation posters at Annual Heart Rhythm Society meeting, 2013, USA, and **published** in abstract form (*Heart Rhythm*.2013;10:S482)

- **NIMMO First Prize**, 2013 for Full Time Research, Royal Adelaide Hospital

- Best Poster award, Catheter ablation at Annual Asia Pacific Heart Rhythm Society meeting, 2013, Hong Kong

- **Manuscript** organized for publication

Chapter 4

- **Manuscript** organized for publication

Chapter 5

- **Presented** as a poster at Annual Heart Rhythm Society meeting, 2013, USA, and **published** in abstract form (*Heart Rhythm*.2013;10:S388-S433)
- **Manuscript** published as Original Research article in American Journal of Physiology- Heart and Circulatory Physiology:. *Autonomic modulation of repolarization instability in patients with heart failure prone to ventricular tachycardia.* Nayyar S, Roberts-Thomson KC, Hasan MA, et al. Am J Physiol Heart Circ Physiol. doi:10.1152/ajpheart.00448.2013

Chapter 6

- **Manuscript published** as Clinical Update & Reviews in European Heart Journal: *Venturing into ventricular arrhythmia storm: a systematic review and meta-analysis.* Nayyar S, Ganesan AN, Brooks AG, et al. European Heart Journal 2013; 34: 560-569

- **Presented** as a poster at Annual Heart Rhythm Society meeting, 2012, Boston, and **published** in abstract form, Heart Rhythm.2012;9:S357–S388

- **Presented** as a poster at Annual Asia Pacific Heart Rhythm Society meeting, 2012, Taiwan.

# ABBREVIATIONS

AP: Action potential

ECG: Electrocardiogram

EF: Ejection fraction

ICD: Implantable cardioverter defibrillator

ICM: Ischemic cardiomyopathy

DCM: Dilated cardiomyopathy

LV: Left ventricle

QTV: QT variability

RV: Right ventricle

ShEn: Shannon entropy

S-QRS: Stimulus-QRS

VA: Ventricular arrhythmia

VF: Ventricular fibrillation

VT: Ventricular tachycardia

# CHAPTER 1. REVIEW OF LITERATURE

## ABSTRACT

Sudden cardiac death (SCD) due to ventricular arrhythmias (VA) [ventricular tachycardia (VT) or ventricular fibrillation (VF)] is a major public health problem in industrialized societies. Over the last four decades, substantial progress has been made in the understanding of basic pathophysiologic mechanisms of these arrhythmias, as well as their diagnosis and management. Identification and treatment of patients who have survived an episode of VA has now become well established. Catheter ablation and implantable cardioverter defibrillator (ICD) have assumed an increasing important role in therapy of these arrhythmias, especially in patients with underlying structural heart disease. Increasing attention is being given to identifying and prophylactically treating individuals to prevent sudden death due to VT or VF. However, despite important advances, there are numerous limitations in the contemporary catheter ablation based management strategies of VA. This review explores the changing epidemiology of VA, current understanding of basic physiology and arrhythmia formation, application of existing VT mapping methods, new insights from recent advances in VT mapping and problems in the current therapies.

## 1.1 Epidemiology: Arrhythmic Burden of Ventricular Tachycardia In Ischemic Cardiomyopathy and Its Risk Assessment

### 1.1.1 Ventricular Arrhythmia and Sudden Cardiac Death

Ventricular arrhythmias were recognized as a mechanism of SCD in late 19th century, when James MacWilliam related various observations from epidemiology, pathology and experimental studies [1]. It was realized that death due to VT or VF in most cases was associated with pathologic abnormalities attributable to coronary artery disease (CAD). The incidence of VA related death is not precisely known, and is estimated by the prevalence of various forms of sudden cardiac death [2]. The theory that most VA related deaths are due to CAD is supported by retrospective death certificate data, as well as prospectively acquired autopsy evidence of CAD in SCD victims. These data suggest that 70-75% of SCDs are attributable to CAD [3-5]. Over the past fifty years, the rates of ventricular arrhythmia related SCD due to CAD are declining in many populations [5, 6], with ~60% reduction reported in the Framingham population aged 40-79 years. This may reflect the impact of improved primary and secondary prevention treatment strategies targeted at established CAD (e.g. thrombolysis, revascularization, heart failure management) [7] and its risk factors (e.g. hypertension, smoking, dyslipidemia) [8], and increasing implantation of ICDs [9, 10]. The recommendation for ICD treatment targeting asymptomatic patients at high risk for SCD and underlying CAD has accounted for significant proportion of reduced incidence of VA related deaths [11, 12]. This decline in CAD related SCD has contributed to the overall reduction in the SCD rates. Nonetheless, this decreased incidence may be balanced by increased prevalence of monomorphic VT as improved therapies prolong life in patients after MI.

Mortality in patients with ischemic cardiomyopathy (ICM) is primarily by pump failure or by SCD, of which more than 75% is due to VA [13]. Despite significant advances in management, mortality remains unacceptably high, with 40-70% of

patients dying due to SCD [14, 15]. The extent of infarction, and possibly location involving the septum, are the two important prognostic factors associated with malignant VAs [16, 17]. Although total mortality among patients who have mild heart failure is low, the relative proportion of patients dying suddenly is significant. Patients who have more advanced heart failure have a substantial annual mortality of 40-60%; however, the relative proportion of sudden death amounts to less than 30% of all causes of death [14, 18].

### 1.1.2 TIME COURSE OF VENTRICULAR ARRHYTHMIAS IN ISCHEMIC CARDIOMYOPATHY

With the availability of thrombolysis and primary angioplasty for acute infarction, the incidence of sustained monomorphic VT has decreased remarkably. Only 1% of patients experience an episode of sustained, tolerated VT in the year following infarction [19]. Among patients with CAD who present with sustained monomorphic VT, ~30% have their first episode within the first year following myocardial infarction (MI) [19]. Subsequently, there is consistent 3-5% per year incidence of VT occurrence over the next 15 years [19]. Few patients, especially those following inferior wall MI, present with first VT episode >15 years following their first infarction. The cycle lengths of the tachycardias occurring early after infarction, however, tend to be faster, and the tachycardia is more poorly tolerated. This may reflect evolving scar formation, which when completed, may sustain longer tachycardia cycle lengths, owing to newly established abnormalities of conduction. Nonetheless, as demonstrated in Dr. Josephson's laboratory, tachycardias initiated 2 weeks after infarction (even if spontaneous VT is not present) can be replicated by programmed stimulation a year later [20] and possess high risk for SCD [21]. Thus, some components of the anatomic substrate are relatively fixed once infarction has occurred, although they continue to evolve with development of new circuits and advanced heart failure [22].

The incidence of SCD due to VF related death has also reduced but less than that of sustained monomorphic VT. This is due to shift in patients from those who would have previously developed monomorphic VT to more presenting with cardiac arrest due to preservation of myocardium by early coronary perfusion [23]. Among survivors of acute MI with left ventricular dysfunction, the highest risk of SCD is in the first 12 months after the index infarction, and most events occur in the first few months [24]. The risk is highest in the first 30 days after myocardial infarction--1.4 % per month and dramatically decreases to 0.14% per month after 2 years [25]. This is in contrast to sustained monomorphic VT, that has a median time of onset at 15 months following infarction [19].

### 1.1.3 Identification of Patients At Risk of Ventricular Arrhythmia

The highest incidence of SCD occurs in survivors of out-of-hospital cardiac arrest and high-risk post infarction subgroups, but the greatest absolute numbers of SCD events occur in larger subgroups of patients with apparent lower risk. Risk stratification aims at identifying quantitative and qualitative measurements that can serve as sensitive and specific predictors to recognize risk factors for arrhythmic mortality among the large group of patients with CAD.

*A. Clinical and Demographic Data*

Several clinical variables have been demonstrated to be independent predictors of mortality in patients with ICM: Age, New York Heart Association (NYHA) class, atrial fibrillation (AF), QRS duration and blood urea nitrogen level [26-28]. Primary ICD therapy reduces mortality in the intermediate risk patients, while no benefit is achieved in low (no risk factor) and high-risk patients (> 3 risk factors) compared to conventional medical therapy [28].

*B. Left Ventricular Function*

Ventricular function as defined by the left ventricular ejection fraction (LVEF) has been recognized as a major determinant of late mortality for decades [29, 30]. An LVEF <35% has a positive predictive value of 28% for cardiac death or sustained VA on follow-up [31]. However, LVEF lacks sensitivity as a predictive measure for SCD. This is emphasized by the fact that less than 50% of infarct survivors who die suddenly have LVEF <30%. Additionally, ICM patients with LVEF < 30%, but with absence of other poor prognostic factors (advanced NYHA class, AF, non-sustained VT, heart failure) have favorable survival with 2-year arrhythmic death risk of <5%. These patients do not appear to derive as much benefit with ICD therapy, compared to those with additional risk factors [32]. However, caution should be applied during interpretation of this data, as it is based on a subgroup analysis and has not been validated in a prospective trial [32].

*C. Electrocardiographic Monitoring*

Ambulatory ECG recording or Holter monitoring was the first ECG based approach to determine the risk of patients and implement antiarrhythmic therapy [33]. Primary prevention of sudden death with ICD therapy was introduced by the MADIT and MUSTT trials in patients with documented nonsustained VT and inducibility of ventricular tachyarrhythmias [18, 34]. However, with the more recent MADIT II and SCD-HeFT trials, the incremental risk stratification value provided by spontaneous non-sustained ventricular arrhythmias in patients with LVEF <35% is unclear [35, 36].

*D. QRS duration and Signal Average ECG*

A broad QRS duration is associated with increased risk of mortality. In the presence of normal QRS duration on standard ECG, the presence of late potentials or prolonged filtered QRS duration on signal average ECG indicates increased risk of cardiac events [37]. Patients with LVEF <30% and filtered QRS duration >140ms have significantly high (~40%) cardiac and total mortality risk over 5 years [38].

### *E. Microvolt T-wave Alternans*

Microvolt T-wave alternans yields prognostic information in infarct survivor patients, even in those with preserved ventricular function. It carries a high negative predictive value (96-100%), such that over 24 months follow-up, no arrhythmic events or SCD were reported in patients with a negative test [39, 40].

### *F. Heart Rate Variability*

Prognostic value of various heart rate variability parameters in post-infarct patients has been tested in many studies [41-43]. Although depressed heart rate variability parameters strongly predict overall mortality in heart failure patients, association with arrhythmic sudden death is not very well reported.

### *G. Beat-to-Beat QT Variability*

Non-homogenous myocyte loss, diminished myocyte coupling, and ion channel dysfunction accompany scarring in the heart. This produces spatial heterogeneity in ventricular action potential repolarization and prolonged $QT_C$ interval that predisposes to ventricular arrhythmias and SCD [44-49]. Superimposed on this spatial heterogeneity, temporal (beat-to-beat) variation in cardiac repolarization across the ventricle was first recognized in the seminal work by Dr Berger and shown to be elevated in ischemia and heart failure [50-53]. The subtle inter-beat changes in QT interval, termed QT interval variability (QTV), have attracted increasing interest as they provide non-invasive insight into the temporal dynamics of ventricular activity. Importantly, augmented QTV is thought to signify compound spatio-temporal heterogeneity in repolarization and its assessment may yield independent and powerful marker for improved risk stratification for guiding ICD therapy. Increased QTV was found to predict appropriate device therapies in the MADIT-II (Multicenter Automatic Defibrillator Implantation Trial-II) study, as well as total and arrhythmic deaths in heart failure patients without defibrillators [54-57].

QT variability can be influenced by heart rate variability, autonomic changes and repolarization reserve, each of which has been studied in normal hearts [58-61]. There is evidence suggesting that enhanced beat-to-beat fluctuations in repolarization duration in heart failure do not reflect merely incidental changes in heart rate and electrical restitution [50-52]. As interventions that increase sympathetic stimulation shorten ventricular repolarization duration, increase spatial dispersion in repolarization and increase QTV in normal hearts [60, 62], the elevated QT interval variability in heart failure may result from enhanced sympathetic drive and subsequent diminution in repolarization reserve in these patients [63, 64]. On the other hand, primary reduction in repolarization reserve itself, which is commonly seen in structural heart disorders [65, 66] may be the principle driver of elevated QTV in these patients [67].

*Role of sympathetic nervous system and beta-blockers in heart failure*

Heart failure is accompanied by neurohormonal hyperactivity as a compensatory mechanism to maintain cardiac output [68]. This is evident by elevated plasma catecholamine levels, increased central sympathetic outflow and heightened norepinephrine spillover from the intrinsic cardiac nerve terminals into the circulation [68, 69]. In addition, there is $beta_1$- adrenoceptor downregulation and functional desensitization in the cardiac plasma membrane [70]. Chronic isoproterenol administration has been shown to promote myocyte apoptosis, interstitial fibrosis, reduction in $beta_1$-adrenoceptor mediated inotropic reserve, and induces left ventricular dilatation [71].

Chronic beta-blocker therapy reverses left ventricular remodeling, reduces risk of ventricular arrhythmias, improves coronary blood flow, reduces cardiac workload and protects against cardiotoxic overstimulation by the catecholamines [72]. These effects are mediated by: a) direct antagonism of adrenergic cardiotoxic effects, b) cardiac beta-adrenoceptor upregulation and restoration of their signaling, c) increase in inotropic reserve, d) suppression of adverse remodeling promoting renin-angiotensin system, and e) coronary blood flow enhancement by diastolic

prolongation [73]. Beta-blocker therapy effectively reduces the risk of sudden death in heart failure patients [74]. This could possibly be mediated in part by reverse remodeling and reduction in repolarization heterogeneity. Both carvedilol and metoprolol have been shown to reduce QTV in patients with prior myocardial infarction and in patients with chronic heart failure [75, 76].

### *H. Invasive Electrophysiological Testing*

The pioneering work by Dr Hein J Wellens demonstrated variable inducibility rates for induction of sustained monomorphic VT in patients with ICM [77]. In general, among patients presenting with sustained monomorphic VT, 95% patients have inducible VT in the laboratory [19, 78]. In addition, the reproducibility of initiation is consistent over 1 year from the initial study. Single or double ventricular extrastimuli initiate sustained VT in 60-85% of these patients [79]. Patients presenting with cardiac arrest in the setting of ICM have relative lower rate of inducibility for VT (50% patients). In such patients, induction of sustained monomorphic VT more often requires triple extrastimuli, and cycle length of induced VT is shorter compared to patients presenting with VT. Studies that have focused on all possible morphologies of uniform VT report an average yield of three to four morphologies per patient [80, 81]. Clinical relevance of induced VTs has been defined in different ways. A VT morphology is usually considered "clinically relevant", if it (a) matches the spontaneous VT (on the surface ECG or ICD electrograms) [82] (b) monomorphic [22], (d) reproducible, and (e) has slow rate (>270ms cycle length) [80]. Complete non-inducibility after catheter ablation for VT is considered as a prognostic marker for a favorable arrhythmia free survival patients with ICM and recurrent VT [80].

The incremental role of invasive electrophysiologic induction for VT in primary prevention in presence of other strong risk factors (e.g low LVEF) is limited. Although older trials relied on VT inducibility in the laboratory for decision on ICD therapy [18, 34, 83], current guidelines do not endorse electrophysiologic testing prior to ICD implantation in primary prevention patients [18, 36, 84]. Non-inducible patients have

considerable VT event rate and a higher VF event rate compared to inducible patients [22].

## 1.2 THE SUBSTRATE: MECHANISM OF VENTRICULAR IMPULSE PROPAGATION AND ARRYTHMOGENESIS

### 1.2.1. INTRODUCTION

Propagation of cardiac impulse requires cellular action potential (AP) generation, and activation and conduction in the syncytium of multicellular cardiac tissue [85]. Complex interactions between cellular electrical activity, cell-to-cell communication, and cardiac tissue organization determine AP conduction in health and its abnormal behavior in reentrant circuits. First recording of cardiac transmembrane AP was made by Coraboeuf and Wiedmann in 1949 [86]. In conjunction with the principles of nerve excitation by Hodgkin and Huxley [87], this made it possible to associate important properties of membrane ion-channels with the generation of AP. The discovery of gap junctions for intercellular electrical coupling, the dynamics of $Ca^{2+}$ conductance and the development of patch clamp techniques for studying properties of single membrane ion channels further enhanced the understanding of molecular mechanisms of cardiac AP generation and its propagation [88-92]. It has now become possible to relate the perturbations in gene expression and the structure and function of ion channel and gap junction proteins [93]. The electrical phenomenon observed at the level of whole heart result from complex interplay among many molecular events. In the context of ventricular arrhythmia research, computer modeling has provided crucial insights into the contribution of individual cellular and molecular events to the cardiac electrical function [94]. The following sections integrate the basic principles and mechanisms of normal and abnormal cardiac conduction, and the development of arrhythmogenic substrate for re-entrant ventricular tachycardia (VT), with a specific focus in ischemic cardiomyopathy.

### 1.2.2 Action Potential Generation By Single Myocytes

Action potential generation is a pre-requisite before propagation of activation in the multicellular cardiac tissue. It is accomplished by currents through membrane ion channels equilibrating with ionic milieu of the single cells [95]. For a single cardiac cell under space-clamp conditions, the following equation governs the transmembrane potential ($V_m$) to the total transmembrane cardiac current ($I_{ion}$)

$$\frac{dV_m}{dt} = -\frac{1}{C_m} . I_{ion} \qquad (1)$$

where $C_m$ is the capacitance (μF/cm$^2$) provided by the charge separation across the membrane [96]. It states that change in $V_m$ occurs by displacement of charges on the membrane capacitance caused by movement of ions across the cell membrane. This movement occurs via voltage gated ion channels, ATP dependent pumps, and exchangers, and $I_{ion}$ represents the sum total of all currents. A negative $I_{ion}$ (inward movement of positive ions) will cause a positive change (depolarize) in $V_m$, while a positive $I_{ion}$ (outward movement of positive ions) will reduce (repolarize) the $V_m$. The movement of ions occurs in a time, voltage and concentration dependent manner via various ion selective mechanisms, resulting in generation of the action potential [96]. A mathematical model of cardiac ventricular cell AP generation (such as the Luo-Rudy model) integrates these principles of ion movements across ion channels, pumps and exchangers [97, 98]. This model accounts for the dynamic changes in the ion concentration ($Na^+$, $Ca^{2+}$ and $K^+$), and forms the basis for a quantitative description of AP generation (Figure 1.1). The most important properties of these ionic currents are (i). $I_{Na}$ is characterized by fast activation and by fast and slow inactivation, and (ii). $I_{Ca(L)}$ is inactivated by both fast $Ca^{2+}$ dependent manner, and a slow voltage dependent process [99-101]. In re-entrant arrhythmias where the leading head of the activation wavefront interacts with the tail in phase of repolarization, the repolarizing $K^+$ currents may also become important determinants of impulse conduction, besides $I_{Na}$ and $I_{Ca(L)}$.

In addition to the Luo-Rudy model, many other mathematical models describe the AP formation in cardiac cells [102]. In general, these are based on the Hodgkin-Huxley method that computes the whole cell AP from individual transmembrane currents produced from many sources of ion currents.

### 1.2.3 Principles of Propagation

---

#### A. Normal Continuous Propagation

During AP generation in a space clamped single cardiac myocyte, the ion current is used only to change the local charge on the membrane capacitance. In contrast, in a multicellular structure, the current generated during depolarization of a given cell is divided between altering local membrane capacitance and depolarizing the membrane of the downstream cells via resistive gap junctions [94]. The simplest model of AP propagation is a linear well-coupled cellular structure in a continuous series, with components of cytoplasmic and axial intercellular (gap junctional) resistances, and devoid of major electrical discontinuities due to absence of gap junctions or anatomic separation by layers of fibrosis. The following equation relates the transmembrane ion current and the axial current that flows between cells in a linear chain

$$\boldsymbol{C_m}.\frac{\boldsymbol{\partial V_m}}{\boldsymbol{\partial t}} + \boldsymbol{I_{ion}} = \left(\frac{\boldsymbol{a}}{\boldsymbol{2r_i}}\right).\left(\frac{\boldsymbol{\partial^2 V_m}}{\boldsymbol{\partial x^2}}\right) \qquad (2)$$

It is a general equation describing reaction-diffusion systems, where $a$ is the fiber radius and $r_i$ is the axial resistance per unit length [94]. Here $V_m$ is the function of both time ($t$) and space ($x$). Under space clamp conditions, $V_m$ is constant in space, thus $\partial^2 V_m / \partial x^2 = 0$, and equation (2) reduces to equation (1). The left part of the equation (2) is the total transmembrane current, consisting of the capacitative current $\left(C_m.\frac{\partial V_m}{\partial t}\right)$ and the ionic current ($I_{ion}$). The right side computes the net gain or loss of axial current as it flows down the fiber. This equation thus states the charge

conservation principle that any change in axial current must be accounted by the current that crosses the membrane.

### B. Discontinuous propagation

Propagating electrical waves in the cardiac tissue interact with boundaries [103]. These may be physical boundaries such as cell membranes of variably oriented myocytes, connective tissue barriers or blood vessels, or a virtual boundary due to dispersion of current from a small strand to a large mass of tissue (current to load mismatch). Interactions at boundaries are of crucial importance and underlie the mechanisms of reentrant ventricular arrhythmias [104]. In addition, excitability of the individual cells also determines the success of conduction.

#### *i) Physical barriers*

The physical (sealed end) boundaries may produce a complete or partial barrier. Collision of the AP at the physical obstacle and its local reflection as an electrotonic current increases the rate of depolarization, $dV_m/dt_{max}$ and local velocity of conduction [105]. They reduce the electrical load on the cells proximal to the collision site. These variations reflect in the shape of the local extracellular electrogram [106]. There is concomitant decrease in maximal $I_{Na}$ caused by rapid inactivation of $Na^+$ channels due to fast depolarization and reduction in the electrochemical gradient. Thus, in contrast to continuous conduction, there is an inverse relation between depolarizing $Na^+$ current and $dV_m/dt_{max}$ at sites of collision [107].

#### *ii) Dispersion of current*

Dispersion of current during transition from a small to a large mass of tissue reduces the current density per unit membrane area because a small number of elements have to furnish current to a larger number of excitable elements downstream (current to load mismatch) [107, 108]. It slows down the local AP upstroke and reduces conduction velocity. A large mismatch between up and downstream elements can produce block in conduction. There is a direct relationship between $dV_m/dt_{max}$ and

depolarizing $Na^+$ current because of inactivation of $Na^+$ channels during the prolonged AP upstroke. However, just distal to the transition site, maximal $I_{Na}$ is increased due to reduced $V_m$ and resultant increase in the electrochemical gradient.

Another scenario, which is particularly relevant in the cardiac impulse propagation, is the interaction of the activation wavefront with the sites of partial collision as well as with the current dispersion [109]. In such situations, current tends to propagate through the low resistance elements. A large value of resistance, due to large discontinuity by fibrotic tissue or too large a number of downstream elements produces conduction block.

*iii) Excitability of cell membranes*

Excitability of the membranes in the distal elements also affects the success of conduction [94]. The interaction between determinants of excitability (number and function of ion channels, transporters and exchangers) and resistive properties (gap junctions, tissue structure) underlies the mechanism of slow conduction in cardiac tissue.

### C. The Safety of Propagation

For propagation to succeed, the excited cell (source current) must provide sufficient charge for depolarizing neighboring unexcited cells (electric sink/ load) to their excitation threshold [110]. Once the threshold is reached and AP generated, the load on the excited cell is removed, and the newly excited cell switches from being a sink to being a source for the downstream tissue, perpetuating AP propagation. The safety factor for conduction (SF) relates this source-sink relationship [111]. It is the ratio of charge generated to the charge consumed during the excitation of a single cell in the cardiac tissue:

$$\mathbf{SF} = \frac{\int_A I_c \mathbf{d}t + \int_A I_{out} \mathbf{d}t}{\int_A I_{in} \mathbf{d}t} \qquad (3)$$

$I_c$ is the capacitative current of the cell and $I_{in}$ and $I_{out}$ are the axial currents in and out of the cell [111]. The charge associated with each current is computed by the time integral of that current over an interval *A*. Safety factor > 1 indicates that more charge is produced during cellular excitation than the charge required to cause the excitation. This characterizes successful conduction. When SF falls below 1, conduction cannot be sustained, and conduction failure occurs.

### D. Propagation Along a Curvature

The foundational work by Fast and Kleber demonstrated that physical obstacles or functional zones of block in a sheet of cells cause activation wavefront to turn and follow a curved shape [112]. If the activation wavefront is curving outwards (convex), the propagation velocity slows down. This is because the local excitatory current provided by the cells in the front of the convexity of the wave diverges into larger tissue area downstream. In contrast, if the activation wavefront is curving inwards (concave), the excitatory current converges in front of the propagating wave producing faster membrane depolarization and a rapid propagation velocity. These phenomena are based on the principles of current to load mismatch and partial collisions governing discontinuous propagation in the tissue.

The degree of wavefornt curvature ($\rho$) can be defined as the negative reciprocal of the local radius of curvature (r),

$$\rho = -\frac{1}{r}$$

The dependence of conduction velocity ($\theta$) on the wavefront curvature in an excitable medium is given by the following equation

$$\theta = \theta_0 + D\rho \qquad (4)$$

The coefficient *D* is determined by the properties of the medium, and D is equal to $1/C_m S_V R_1$ where $C_m$ is the membrane capacitance, $S_V$ is the cell surface-to-volume ratio, and $R_1$ is the intracellular resistance [113]. The propagation velocity thus depends on the radius of curvature with slowing of conduction at progressively smaller radii of conduction. Conduction block occurs below a critically small radius ($r_c$). The presence of curvature associated with wavefronts interacting with obstacles is an

important determinant of conduction slowing, conduction block, and reentrant arrhythmias.

### 1.2.4 Factors affecting Action Potential Propagation: Structural Basis of Anisotropy

---

#### A. Orientation of Muscle Fibers

Anisotropic architecture of the ventricular tissue produces considerable variations in the propagation velocity within a given region [114-116]. The longitudinal conduction velocity ($\theta_L$) along the direction of the muscle fibers is faster than the transverse conduction velocity ($\theta_T$) orthogonal to the longitudinal axis. The anisotropic ratio ($\theta_L / \theta_T$) of propagation velocity ranges from ~10 in the crista terminalis of the right atrium to ~ 2 in the ventricles [117]. In the direction of the long cell axis, the ventricular specialized conduction system (Purkinje fibers) has the highest velocity (1.7-2.5m/s), while the lowest velocity is measured in the ventricle (0.48-0.61 m/s) [118].

#### B. Cellular Shape and Size

Cardiomyocytes in the ventricle have an elongated shape, either "brick"- like (adult myocytes) or fusiform appearance (neonatal myocytes). As detailed by Kleber, Janse and Fast in the Handbook of Physiology, 2002, there is a large variability in cellular size within different regions of the ventricular myocardium, with a consistent length: width ratio [117]. The functional connections (gap junctions) between normal adult cardiac cells show a high density preferential location at the longitudinal cell ends that accounts for the faster propagation velocity along the length of the fibers [119 120]. In contrast, neonatal myocytes show more regularly distributed and spaced connections all around the cell perimeter [121]. The pattern of distribution of gap junctions has a relatively small effect on the transverse conduction velocity.

However, cell size has significant effect on the conduction velocity, with transverse cell-to-cell conduction delay shown to be significantly greater in a network of larger cells compared to a network of smaller myocytes [122]. Cell size assumes significance in arrhythmogenesis during pathological changes in cell size due to cellular swelling or atrophy [123].

### C. Connexin Expression

The functional connections between cardiac myocytes, so called gap-junctions, vary in their molecular composition, degree of expression and distribution pattern [111, 120, 124, 125]. Connexin 43 (Cx43) is the most abundant protein expressed at gap junctions in the heart and plays an important role in the ventricles and the specialized conduction system. Cx40 is expressed in the specialized conduction system, and due to its large conductance contributes to high conduction velocity in the specialized conduction system. Colocalization of different connexins in gap junctions has been shown to produce multitude of electrical conductance states in vitro, however their functional role in vivo is unknown [126].

The expression and distribution of gap junctions can be remodeled by several factors. Unlike normal adult myocytes, surviving tissue in the infarcted areas show a uniform and spaced expression of connexins all around the cell perimeter [127, 128]. Due to a low density of connexins, the connectivity i.e., the average number of neighboring myocytes connected to an individual myocyte, is poor in the surviving tissue within infarcted area. The connectivity amounts to 11±3 cells in normal dog ventricle [119] versus 6.5 in the surviving tissue within infarcted areas of dog ventricle [129]. Remodeling of connexins also occurs with ventricular hypertrophy, mechanical stretch and heart failure that result in concomitant changes in conduction velocity [130, 131]. The role of gap junction conductance in propagation has been investigated in theoretical experiments. Decrease in gap junction conductance has been shown to produce junctional delay and marked slowing of propagation velocity [111].

### D. Ion Channel Clustering

Similar to the clustered localization of connexins on the membrane, ion channels participating in AP generation and propogation are confined to specific areas in the cell membrane. $Na^+$ and $K^+$ channels are concentrated close to gap junctions at the intercalated disks [132], while L type of $Ca^{2+}$ channels colocalize with the invaginating T tubules [133]. Clustering of $Na^+$ channels close to the gap junctions did not show any significant effect on the propagation velocity [122].

### E. Cell-to-Cell Interactions Between Myocytes and Nonmyocytes

Connective tissue layers of fibroblasts and vascular endothelial cells act functionally as electric insulators between myocytes. However, this paradigm has been questioned in the context of electric phenomenon observed across fibrous scars [134, 135]. Experimental evidence of Cx43 based cell-to-cell coupling between myocytes and nonmyocytes has been obtained in vitro; direct proof in vivo is still lacking [136, 137]. Myocyte-to-nonmyocyte coupling is suggested in neonatal rate myocyte monolayers by slow current propagation locally in region of nonmyocyte, with an electrotonic "action potential" of very slow upstroke in the nonmyocyte cell [138]. The fact that the inexcitable nonmyocyte cell only consumes the local current produces a distinct local slowing of conduction.

Following myocardial infarction, myocytes have been shown to lose much of Cx43 [139, 140]. In addition, inflammatory responses to infarction transform resident cardiac fibroblasts to myofibroblasts, which are involved in the normal immune response to inflammation and tissue repair [141]. This transformation includes rapid proliferation of myofibroblasts. Myofibroblasts produce IL-1β, which in turn downregulates Cx43 in the intact heart [142]. Studies in intact heart failed to show any direct coupling between myofibroblasts and myocytes. Conduction abnormalities in regions of myofibroblasts were predominantly due to reduction of Cx43 in adjacent myocytes [142].

### 1.2.5 Action Potential Propagation and Extracellular Electrogram Generation

The principles governing discontinuous conduction determine the shape of the transmembrane AP [143]. In a detailed simulation two-dimensional model of cellular network, the effect of discontinuities formed by cell borders and selective presence of gap junctions produced distinct profiles of propagation velocity, $I_{Na}$, and thus the steepness of the AP upstroke [144]. The effect of discontinuities is observed even at the subcellular level, where the conduction velocity is not homogenous throughout the cell. There is a slight decrease in conduction velocity after the local current flowing through the gap junction is dispersed into the cell. Inversely, there is local increase of conduction velocity as impulse approaches the cell-to-cell connections because of reflection of axial currents by cell borders at these sites (partial collision). Similarly the steepness in the transmembrane AP, reflected as $dV_m/dt_{max}$, is lowest at dispersion sites beyond gap junctions and highest at sites of partial collision and reflection of intracellular electrotonic current before gap junctions [122, 144]. Modifications of elements of discontinuity by modifications in the low resistance elements (the cell) and high resistance elements (intercellular connections) will affect the $dV_m/dt_{max}$ and slope of the AP. In response to a progressive decrease in gap junction coupling, $dV_m/dt_{max}$ initially increases due to greater confinement of depolarizing charge to individual cells. The later decrease in $dV_m/dt_{max}$ at very high levels of intercellular resistance, is due to decreasing electrotonic currents flowing into the cells [111, 122].

The shape of transmembrane AP also depends on the direction of impulse propagation. Higher degree of discontinuity in the transverse direction produces higher values for $dV_m/dt_{max}$ [109, 122]. Additionally, cell size is a major determinant of $dV_m/dt_{max}$, with higher values measured in large cells compared to small cells [122].

### 1.2.6 Local Activation Analyses From Extracellular Electograms

In a multicellular fiber with continuous conduction and normal cellular coupling, the extracellular electrogram is smooth, and is indistinguishable from that generated in a continuous syncytium. It does not reflect the underlying discrete structure of the multicellular fiber. The time of local activation is taken as the moment of steepest negative deflection of the unipolar electrogram [145], which coincides with the steepest portion of the upstroke of local AP ($dV_m/dt_{max}$) and maximum local depolarizing $Na^+$ current ($I_{Na}$) (Figure 1.2). This relationship does not hold true in tissues with reduced cell-to-cell coupling, and there is no unique local activation time [108, 146, 147]. With reduced intercellular coupling, irregularities appear in both membrane potential and local extracellular electrogram as depolarization and propagation events of the individual neighboring cells become separated in time to be evident as distinct deflections in the extracellular electrogram. This situation is characteristic of the inhomogeneous substrate associated with myocardial infarction, where increased uncoupling between myofiber bundles occurs due to replacement fibrosis. The seminal works by Spach et al in 1986 and then Dillon et al in 1988 described the formation of 'fractionated' electrograms recorded in this setting reflecting the discontinuity of conduction between fiber bundles [148, 149].

### 1.2.7 Mechanisms of Slow Conduction

Slow conduction in the ventricular muscle in pathophysiological settings is associated with arrythmogenesis. It is an important determinant of the size of the reentrant circuits, wavelength of excitation $\lambda$, which is given by the product

$$\lambda = \theta \times t_r \qquad (5)$$

where $\theta$ is the conduction velocity and $t_r$ is the refractory period of the tissue [94].

### A. Slow Conduction Due to Reduced Membrane Excitability

The most important determinant of reduced excitability is reduced availability of $Na^+$ channels leading to a reduction in $I_{Na}$. This happens in the presence of ischemia [150, 151], hyperkalemia, acidosis, hypoxia [152], and antiarrhythmic drugs ($Na^+$ channel blockers e.g. tetrodotoxin) [153]. It can also be the consequence of genetic mutations that result in loss of $Na^+$ channel function [154]. A progressive reduction in the membrane density of excitable $Na^+$ channels decreases conduction velocity and SF of propagation in a non-linear "all-or-none" manner [111]. Initially, SF decreases very slowly and is relatively insensitive to moderate changes in $Na^+$ channel availability, because sufficient current is generated to reach excitation threshold. However, at extreme reduction in channel availability, the generated depolarizing charge is not sufficient to depolarize the membrane to excitation threshold and SF drops rapidly towards 1. When SF falls below 1, it cannot sustain conduction and leads to abrupt conduction failure. The minimum conduction velocity that can be sustained during a simulation with reduced membrane excitability prior to conduction block has been shown to be 0.17 m/s, a reduction by a factor of 3 relative to control velocity (0.54 m/s) at full membrane excitability [111, 155]. Thus, reduced membrane excitability cannot sustain very slow conduction.

#### *Role of $Ca^{2+}$ Current During Slow Conduction Caused by Reduced $Na^+$ Current*

L-type $Ca^{2+}$ current tends to support membrane conduction slowed down by $I_{Na}$ suppression. At depressed membrane availability of $Na^+$ channels, the $I_{Ca(L)}$ acts to increase the electrotonic drive force, and consequently, the depolarizing current to downstream tissue [111]. However, despite $Na^+$ channels suppression, $I_{Na}$ is the dominating current driving conduction and contribution by $I_{Ca(L)}$ is small. The contribution of $Ca^{2+}$ current to propagation is increased by the presence of epinephrine [151, 156].

### *Reduced Membrane Excitability by Acute Myocardial Ischemia*

The seminal works by Janse, Kleber and Wit have shaped the description of pathophysiological changes during acute ischemia. They demonstrated reduction in membrane excitability and AP propagation in the early phase of myocardial ischemia [157, 158]. As the acute phase of ischemia does not involve gap junction uncoupling (up to first 10-15 min) or laying down of fibrosis, reentrant arrhythmias during this phase primarily result from abnormal membrane excitability [159, 160]. This is due to hyperkalemia, intra- and extracellular acidosis, and anoxia with a decrease in intracellular ATP levels, all of which promote inactivation of $Na^+$ channels. These changes are not uniform and are different in the ischemic centre and its periphery [161]. Additional factors, such as epinephrine and $I_{Ca(L)}$ supported propagation, and variations in the heart rate, that effect availability of excitable $Na^+$ channels are responsible for dynamic changes in reentrant circuits during acute ischemia [162, 163].

## B. Slow Conduction Due to Reduced Cell-to-Cell Coupling

Reduced cell-to-cell electrical coupling contributes to slow conduction in many pathophysiological conditions such as acute ischemia (after first 15min) [160], post-infarct surviving tissue [127], ventricular hypertrophy [164] and heart failure [131]. This may be due to decrease in conductance of gap junctions secondary to ischemia [160], hypoxia [165], acidosis [166] or increase in intracellular $Ca^{2+}$ [167, 168], or it may be brought about by changes in expression or distribution patterns of gap junction proteins [169, 170].

### *Paradoxical High Safety For Propagation with Reduced Cell-to-Cell Coupling*

Analogous to reduced membrane excitability, reduced cell-to-cell coupling produces reduction in conduction velocity of AP [111]. However, quantitatively, the slowing of conduction is more severe following uncoupling than during reduced excitability [111, 147]. The change in the SF of propagation follows a biphasic pattern. Safety factor initially increases to maximum as cell coupling is reduced and the velocity is

significantly slowed, followed by a fall when conduction block occurs. The minimum conduction velocity before block occurs during a simulation with reduced coupling has been observed to be 0.26 x $10^{-2}$ m/s. In contrast to tissue with depressed excitability, very slow conduction can therefore be sustained with high safety of propagation and robust conduction in a tissue with reduced cell-to-cell coupling [111, 156].

Mechanistically, high SF is the manifestation of discontinuous nature of propagation during this setting [111, 171]. As the cells become less coupled, there is greater confinement of current within the depolarizing cell with less electrotonic load and axial flow of current to the downstream cells. As a result, individual cells depolarize faster with a high safety margin but conduction proceeds slowly with long delays between cells. With extreme reduction in coupling, the membrane charging is slow due to reduced axial current. It allows time for $Na^+$ channel inactivation and eventually, when reduce $I_{Na}$ is not compensated for by the conservation of charge by reduced cell coupling, propagation fails. The slow conduction due to discontinuous propagation is reflected initially as increased $dV_m/dt_{max}$ because of faster depolarization, later followed by its decline at extreme degree of uncoupling. The long discontinuities in conduction between individual cells become analogous to 'saltatory' conduction, and produce multiple peak deflections in the local extracellular electrogram [111].

### *Role of $Ca^{2+}$ Current During Slow Conduction Caused by Cell-To-Cell Uncoupling*

Alterations in the gap junctions in a multicellular tissue can modulate membrane ionic currents. As the conduction delays between individual cells exceed the duration of the action potential upstroke, the relative contributions of $I_{Na}$ and $I_{Ca(L)}$ to depolarization and AP conduction change [172-174]. Due to slow activation caused by reduced cell coupling, the downstream cell starts activation when the upstream source cell is already in its plateau phase. During this phase, $I_{Na}$ is already inactivated

and $I_{Ca(L)}$ is the major inward current generating depolarization. Consequently, contribution from $I_{Ca(L)}$ becomes significant, and with further cell-to-cell uncoupling, $I_{Ca(L)}$ becomes the dominating current. The high $I_{Ca(L)}$ maintains a high plateau potential, and serves as a driving force to the downstream tissue forcing more source charge to the downstream depolarizing cell. The flow of $I_{Na}$, as determined by the kinetic properties of the $Na^+$ channels, is too rapid to provide the depolarizing charge for a sufficiently longer time, and flow of the slower $I_{Ca(L)}$ is necessary to sustain conduction. The switch from $Na^+$ supported conduction to a largely $Ca^{2+}$ supported conduction thus constitutes a feedback mechanism from the sink (load) to the source of excitation [94].

### C. Slow Conduction Related to Tissue Structure- Effect of Length and Branching

Dr de Bakker, through his work on infarcted human papillary muscles, elegantly elucidated conduction in the complex lattice of surviving myofibers in the scar [175]. Such myofibers have long effective conduction time due to zigzag pattern of conduction. Additionally, as demonstrated by Kucera et al, long length of a myofiber strand places distal sections of the strand remote from the source current, reducing the amount of charge available to excite distal tissue, thus slowing conduction in the distal segment [176]. Multiple side branches to a main strand also put charge load on the main strand. As conduction moves from the interconnecting segment of a main strand to the branching segment, a small mass of cells has to excite large mass in the branches. The local current in the main strand is thus dispersed and the conduction velocity in the main strand decreases (referred as 'pull' effect). Partial collision in the excited side branches, in turn, delivers excitatory charge to the next segment of the main strand, thus driving propagation and helping to maintain high safety of propagation (referred as 'push' effect) in the main strand [177]. These effects are more complex when the branching leads to other surviving main strands within the scar or into the larger excitable myocardium. These open-ended branches can feed activating currents and pre-excite the main strand, producing conduction block during a reentrant excitation. Such concepts have significant impact on the

extracellular electrograms expressed from individual channel components in a network of conducting channels within the scar [176]. Channels with paucity of side branches have less complex signals with narrow voltage distribution compared to those with multiple side branches. In addition, branched network channels have low safety of propagation at faster rates and cannot sustain reentrant VT [176]. In contrast, a long channel with paucity of side branches has high safety of propagation even during slow conduction at faster rates. These differences in the channel architecture and the expressed extracellular electrograms can be exploited to differentiate channels supporting VT from non-VT channels in the scar.

### 1.2.8 Mechanisms of Unidirectional Conduction Block

The heterogeneity in impulse conduction, as slow conduction or block in particular locations versus robust conduction at other sites in a tissue, provides conditions suitable for initiation of circulating excitation and maintenance of reentrant arrhythmias [178, 179]. Such conditions can occur in a homogenous tissue with uniform electric properties, when local cardiac excitation (e.g. produced a premature ventricular beat) interacts with the repolarizing tail of the preceding wave. The critical or the vulnerable window during which unidirectional block occurs falls in the relative refractory period of the propagating AP [180]. A premature stimulus outside this window either conducts bi-directionally (if too late), or is blocked in both directions (if too early). A stimulus within the vulnerable window generates critical $Na^+$ current that propagates in the retrograde direction where $Na^+$ channels are progressively more recovered, but blocks in the antegrade direction where $Na^+$ channels are progressively less excitable [179]. In normal tissue, this time window is very small and risk of maintenance of reentrant arrhythmia is negligible [178, 179]. Alterations in electric properties of the tissue such as membrane excitability and cell-to-cell coupling increase these functional heterogeneities in the tissue, and predispose to reentry formation [178].

### A. Heterogeneity in Membrane Excitability and Refractoriness

The width of vulnerable time window is increased by many pathophysiological conditions that alter membrane availability of excitable $Na^+$ channels. Ischemia is a key factor for the generation of unidirectional block and reentrant arrhythmias [157, 158, 163]. Conduction slowing due to prolonged recovery from inexcitability associated with elevation of extracellular [$K^+$], hypoxia, and acidosis decreases the availability of $Na^+$ channels for repetitive excitation [152, 163]. Both absolute and relative refractory periods are markedly prolonged; they exceed the duration of previous AP and lead to marked widening of the vulnerable window. Regional ischemia with gradient from the center to the border of the ischemic zone increases asymmetry in membrane excitability [158, 181].

Electrical remodeling with changes in the repolarizing $K^+$ channels, $Na^+/Ca^{2+}$ exchangers in the ventricles and resulting increased heterogeneity of repolarization also increase the probability of unidirectional block and reentry [65]. These changes occur in the setting of myocardial ischemia [182], ventricular hypertrophy, heart failure [183, 184] and genetic ion channel disorders [185]. The common denominator of these changes is widening of the time window of vulnerability.

### B. Heterogeneity in Tissue Architecture and Discontinuous Conduction

Structural discontinuities are present in most regions even in otherwise structurally normal ventricles. Dispersion of propagating wavefronts, from Purkinje fibers into large mass of myocardium [186] and structural discontinuities in the midmural layers in the form of thin tissue sheets interconnected by small trabeculae [103], produce slowing of conduction.

Pathologic alterations in the ventricular geometry produced by altered orientation of myofibers and lying down of connective tissue septa (scarring) characteristic of infarcted, hypertrophic, and failing myocardium, produce physical discontinuities and promote conduction block [187].

*Altered orientation of muscle fibers*

Conduction is slow in the transverse direction with prolonged refractoriness than in the longitudinal direction of the muscle fiber. A premature stimulus can therefore block transverse to the fiber orientation while it may continue to propagate in the excitable longitudinal direction [151, 188].

*Connective Tissue Septa and Pivoting of Propagation*

Connective tissue septa laid parallel with the length of muscle fibers do not affect the longitudinal conduction, however, transverse conduction collides and is blocked by a long uninterrupted fibrous septum [112]. Beyond the end of a resistive septum, wavefront can continue transversely, however, it tends to pivot slowly around the obstacle (Figure 1.3). This conduction slowing around the pivot point is because of transverse direction of impulse spread in relation to the fiber direction during the turn and convex curvature with concomitant dispersion of the local current at the wavefront [189]. The radius of curvature at the pivot point is limited by the requirements of critical curvature radius, $r_{c,}$ and it cannot be infinitely small [112]. The slowing of conduction at the pivot point is an important factor determining the behavior of circulating excitation and reentry [190].

A gap in the fibrous septum can allow transverse conduction [138, 191]. The conduction slows down and gets curved immediately beyond the gap due to the effect of dispersion. A decrease in width of the gap will produce a decrease in the radius of curvature of the emerging wavefront and eventually conduction block at the critical curvature [191, 192]. Due to its critical nature, the success of propagation through the gap is sensitive to changes in the depolarizing $I_{Na}$. An increase in the rate of stimulation produces conduction block at the gap width that still conducts impulse at a lower rate.

*Tissue Expansion*

Abrupt tissue expansion from a thin strand to a large sheet of muscle fibers behaves analogous to a conduction gap. Due to the effect of large current-to-load mismatch, the conduction slows down at the expansion point and assumes a curved shape [108, 193]. Propagation block occurs below a critical width of the source strand (unidirectional block). Conduction in the opposite direction, from the large mass of sheet to the thin strand, is always maintained. It is not accompanied by conduction delay since the convergence constitutes a reduction in electric load [108].

Slowing of conduction at pivot point at the end of the linear fibrous septum, through a gap, or at sites of abrupt tissue expansion is accompanied by switch in the role of $I_{Na}$ and $I_{Ca(L)}$ in depolarization, as $I_{Ca(L)}$ becomes the dominant current sustaining conduction [107, 108, 194]. Drugs that block $I_{Na}$ cause preferential conduction slowing at pivot points, and smaller levels of $I_{Na}$ block is sufficient to produce conduction block at these locations [195].

### 1.2.9 Basic Principles of Reentry

---

#### A. Leading circle concept, Scroll waves, Vortex shedding

Mines made first demonstration of reentry in heart muscle [196, 197]. He described one of the basic requirements for development of reentry as the establishment of unidirectional conduction block, and the excitation wave propagates around a large inexcitable obstacle such that the revolution time exceeds the refractory period. Reentrant circuits sustain excitation when the anatomical wavelength ($l$) exceeds the minimum reentrant wavelength, $\lambda$, given by equation 5. An excitable gap (difference between anatomical and reentrant wavelength) in a circus movement makes it stable with respect to its frequency of rotation as validated in the rabbit atrial muscle by Allessie et al [198, 199]. In the case, where $\lambda$ is longer than $l$, the excitation wave becomes extinct when it encounters not yet recovered refractory tissue. In the intermediate situation, when $\lambda \sim l$, the head of the following wavefront meets the

partially refractory tail of the preceding wavefront, there is no excitable gap. This is the smallest possible pathway (referred to as the "leading circle'') in which the impulse can continue to circulate and the stimulating efficacy of the wavefront is enough to excite the tissue ahead, which is still in its relative refractory phase [200]. Because the wavefront propagates through partially refractory tissue, the conduction velocity is reduced and period of revolution is relatively long.

In the cardiac tissue, reentrant waves, as theorized by Winfree, assume spiral shape referred as two-dimensional "spiral waves" or three-dimensional "scroll waves" [201]. Because velocity of a convex rotating wavefront is slower than a linear wavefront, and period of rotation remains constant in a stable rotating wave, the propagation velocity at the center (more convex) is slower than at the periphery (more linear) of the wave [202]. The extracellular electrograms from the center (referred as spiral wave rotor or scroll wave filament) shows multiple deflections for each rotation cycle [200, 203].

The heterogeneities in the cellular electric properties and tissue architecture contribute to the development of unidirectional conduction block [112, 157]. Reentrant activation can be tied to anatomical obstacles or to regions of functional block [204]. The condition can become favorable for reentry when a wavefront interacts with a refractory segment of temporary or functional block extending the otherwise small region of anatomical discontinuity. This refractory segment can force the propagating wave to deviate from its course and circumvent the inexcitable segment till it recovers from inexcitability [205]. Because functional reentrant pathways are not tied, they can change their location and size. In tissues with reduced excitability or decreased cell-to-cell coupling, there is greater susceptibility for formation of these lines of functional blocks following premature stimuli. If the critical radius of curvature at the pivoting point is large, as it may happen in an electrically inhomogeneous tissue, the returning wavefront encounters excitable tissue and detaches from the pivoting point [206]. This initiates spiral wave, a phenomenon called "vortex shedding", that has important role in formation of complex arrhythmia like ventricular fibrillation in ischemic hearts [207].

### B. PHASE SINGULARITY (ROTOR TIP)

Phase singularities play a crucial role in the spiral wave initiation [112, 208] (Figure 1.3). Propagation around a pivot point produces a radius of curvature, and the tip of the isochrones follows the spiral path that is detached from the pivot point, because propagation fails below a critical value of radius of curvature ($r_c$). At the spiral tip three phases of excitation fuse into a single point termed "phase singularity" or "wavebreak". These phases are: 1) the nonexcited zone in resting phase, between the spiral tip and the pivoting point 2) the excited state in phase of depolarization, which forms the wavefront head, and 3) the phase of repolarization, which forms the wavefront tail. The phase singularity rotates around a circular core of non-excited tissue [209].

Lines of block that anchor pivot points can be both anatomical and functional [210, 211]. In a excitable tissue without anatomical obstacles, a timed premature impulse that is blocked through interaction with the tail of the preceding excitation wave produces reentry by propagating retrograde and reentering into the refractory zone with formation of a phase singularity at the spiral tip [205] (Figure 1.4). The phase singularity moves in circular path around a core of resting tissue.

### C. ROLE OF EXCITABLE GAP

A gap of excitable tissue (length of the circuit segment, or time period) exists between head of the wavefront and tail of the preceding wavefront, if $l > \lambda$. This is referred as a "fully" excitable gap, when the tail of the preceding wave does not affect the head and the velocity of the following wave, and there is absence of a head-tail interaction [94]. In contrast, in a leading circle type reentry, with $l \sim \lambda$, there is presence of head-tail interaction [200]. The zone where the rotating wavefront can be captured by a local stimulus in the presence of head-tail interaction is referred to as "partial" excitable gap. The existence and extent of the excitable gap in a reentrant circuit enables modulation of the tachycardia spontaneously or by a locally applied stimulus and may be exploited to terminate the tachycardia [189, 212, 213]. The existence

of excitable gap has been clearly demonstrated in fixed macroscopic anatomical reentry as in post myocardial infarction ventricular tachycardia [213-215]. In functional reentry (e.g. spiral wave reentry) or a mixed form of reentry, the existence of excitable gap is debated. Although functional reentry can develop in a seemingly continuous medium with regularly spaced isochrones during normal rhythm, the underlying alterations in the microscopic morphological components (intrinsic tissue architecture, discontinuous gap junctions) that effect tissue electric properties are analogous to macroscopic obstacles on a smaller scale [189, 212, 216-218].

*Entrainment and Resetting*

Entrainment of a reentrant arrhythmia was originally defined as "an increase in the rate of tachycardia to a faster pacing rate, with resumption of the intrinsic tachycardia upon cessation of pacing", and is taken to indicate an underlying reentrant mechanism [219, 220]. The antidromic wavefront collides with each preceding orthodromic wave, and both waves annihilate locally. In the orthodromic direction, the premature stimulus from pacing continues to propagate. As a result at termination of pacing, the arrhythmia is reset, i.e., the propagation continues to circulate with the intrinsic frequency but with a phase shift caused by pacing [212, 221, 222]. The electrograms resulting from fusion of the orthodromically travelling intrinsic tachycardia waves and stimulated waves are used to define the forms of entrainment [223]. The return cycle may show prolongation or be of normal duration, depending on the location of the pacing stimulus in relation to reentrant circuit [223]. Conduction slowing within the circuit by a more premature impulse or due to the presence of a partially excitable gap can prevent resetting and produce long return interval [224]. A very early extrastimulus or faster pacing entering in the relative refractory period will block in orthodromic direction as it encounters the absolute refractory tissue. In the antidromic direction it is able to propagate till it encounters the preceding tachycardia wave and terminates the tachycardia [220]. Although pacing near the site of origin of a focal arrhythmia may also exhibit acceleration of the tachycardia to the pacing rate, the ability to repeatedly reset the tachycardia makes a focal tachycardia mechanism unlikely.

*Head-Tail Interactions, Restitution and Instability in Reentry*

The movement of the rotor tip (phase singularity) can be predicted by the relationship between the reentrant wavelength ($\lambda$), and the anatomical wavelength ($l$) that in turn depends on the radius of curvature ($l = 2\pi r_c$) [209]. When the trajectory ($l$) of the wave tip is longer than the $\lambda$, the head-to-tail interaction is minor, and the inner core of the spiral wave, characterized by the phase singularity, rotates around a circular core of non-excited tissue. If the length of the trajectory is similar to the reentrant wavelength, rotor movement becomes unstable resulting in a meandering trajectory of the phase singularity. In normal myocardium, with normal excitability, $\lambda >> l$, a stable Z-shaped line of block has been found in many studies [199, 224-226].

Dependence of conduction time in a segment, on the preceding diastolic interval in the circuit (conduction velocity restitution), produces cycle length oscillations. When the dependence is steep (negative slope < -1), instability and eventual termination occurs, while damping of oscillations is observed at less negative slopes [227]. Alternating deceleration and acceleration of the tachycardia is observed when the wavefront invades and retreats from the partially refractory tail of the preceding wave.

On a similar analogy to alteration of conduction velocity, the rotation period can oscillate with an alteration in the AP duration by the preceding diastolic interval [228, 229]. Damped oscillations are observed when the slope of the restitution curve of AP duration is <1, and instability is produced with a slope >1. Heterogeneities in cellular properties and variations in structural components in remodeled pathological substrates are major determinants of spatial dispersion of AP and conduction velocity restitution [94].

*Wave Splitting*

High AP restitution is considered responsible for instability of spiral waves and splitting or break-up of a “mother” wave into two or more daughter waves [230]. This is implicated as a crucial mechanism for multiple wavelet reentry described in the

seminal work by Moe [231], and is considered as an explanation for the transition of ventricular tachycardia to ventricular fibrillation [232].

### *Anchoring of Spiral Waves*

The spiral waves tend to drift towards regions of decreased excitability, and have been suggested to "anchor" to local resistive obstacles (small scar or blood vessel) [216, 233]. The size of the anchoring element can be significantly small relative to the wavefront. The anchoring of spiral waves potentially explain the stable or partially stable nature of many forms of functional reentry [234].

## 1.3 Mapping of Scar Related Ventricular Tachycardia In Ischemic Cardiomyopathy

### 1.3.1 Relevant Anatomy

The typical anatomic substrate for sustained monomorphic VT is extensive healed infarction with resultant LV dysfunction. The extent of myocardial scarring is an important determinant of arrhythmia risk after MI [235]. Patients with tolerated sustained VT have more extensive infarction, more frequent aneurysm formation, and more pronounced LV dysfunction than do patients with non-sustained VT or SCD [19]. In some cases, fixed anatomic structure such as the mitral valve annulus boundaries a band of myocardium along with adjacent scar, producing anatomical conditions suitable for peri-mitral reentry [235, 236] Early reperfusion following an acute infarct results in patchy scarring and is associated with relatively faster VT than non-perfused patients [23]. Scarring produces thinning and aneurysm formation, while sites with preserved myocardium retain thickness. Geometric structure studies by Ciaccio et al in the post-infarct ventricles have shown that most VT circuits form at most abrupt gradients of tissue thickness in the scar that is associated with greater curvature and slow conduction [237]. Additionally, non-uniform muscle contraction in the post infarction ventricles affects the sustainability of arrhythmias [238]. Stretch by the contractile normal myocardium is greatest at aneurysm boundaries that triggers premature beat formation at these sites and may account for greater frequency of VT circuits in the aneurysm boundaries.

### 1.3.2 Definition of Scar

The normal left ventricular bipolar electrograms, described by Cassidy et al. [239], have an amplitude of greater than 3 mV, a duration of less than 70 msec, and an

amplitude/duration ratio of greater than 0.045. After an MI, the tissue can be broadly divided into three zones: the dense scar, the surrounding normal live myocardial tissue, and the intervening borderzone [240-242]. A confluent site with bipolar electrogram amplitude of 0.5mV or less represents dense scar, 0.5 to 1.5mV is infarct borderzone, and electrograms >1.5mV are recorded in normal areas. This concept has been validated by statistical analysis of normal and abnormal bipolar electrograms, by comparison to nuclear perfusion imaging, and in porcine models of anterior infarction [240, 241, 243-245]. In the animal model, infarct size and topography by voltage mapping correlated with the functional (assessed by intracardiac echocardiography) and pathologic measurements. A bipolar voltage electrogram amplitude cut-off of 1.5mV also serves well to distinguish normal from infarcted tissue despite variations in the direction of wavefront propagation that result from different rhythms [e.g. sinus rhythm and ventricular paced (RV or biventricular) rhythm]. Only 8% of sites were reclassified from abnormal (≤1.5mV) to normal (>1.5mV) or vice-versa [246]. As unipolar mapping has a larger field of view, unipolar electrogram amplitude obtained by endocardial mapping is affected by the transmural distribution of scar [247, 248]. An endocardial bipolar voltage >1.9 mV and unipolar voltage <6.7 mV has been shown to have a high negative predictive value (91%) for detecting nonendocardial scar from either endocardial scar or no scar [249].

### 1.3.3 Relationship Between Scar And Borderzone

The borderzone is not only at the periphery of the dense scar, but it is located at any of the interfaces between the surviving myocardial tissue and dense scar. In the borderzone, electrically active preserved myocardial fibers are interspersed within the bed of fibrous tissue. These preserved fibers are characterized by abnormal electrophysiologic properties, including decreased cell-to-cell electrical coupling and slower conduction properties [94]. Some of these surviving tissues can be identified as visible small confluent islets of relatively preserved voltages surrounded by the scar. These islets may not necessarily participate in VT [250]; however, they are markers of

anatomic proximity to other buried surviving myofibers that may have role in perpetuation of VT.

### 1.3.4 Role of the Epicardium

In most patients with post-MI VT, the arrhythmogenic substrate is located on the endocardial surface of the heart. Surgical mapping studies have revealed that not all VT circuits can be eliminated by endocardial ablative strategies alone and a minority of post-MI patients requires an epicardial ablation approach to eliminate their VT [251, 252]. Most (90%) of these patients who have epicardial VT circuits had previous inferior wall MIs [253], the reasons for which are unclear. This might relate to the basal peri-mitral location of the scar, as is often seen in non-ischemic dilated cardiomyopathy [254]. The scarring disposes this already anatomically remote region in myocardium to further delayed activation, predisposing to development of reentrant circuits.

### 1.3.5 Role of the Endocavitary Structures

Although well established as a potential focus for origin of idiopathic left ventricular VT and premature ventricular beats, papillary muscles are occasionally implicated in scar related VT when involved in the infarct [255-257]. Mapping of VT circuits in or near papillary muscle can be challenging due to poor catheter stability and obstruction in catheter manipulation [258]. The role of papillary muscles as a stable stationary anchoring zone for rotational circuits during VF propagation has been investigated [259, 260]. The root of the papillary muscle remains electrically quiescent at the center while the reentrant wavefront propagates around this anisotropic anatomic obstacle.

### 1.3.6 CHANNELS IN THE SCAR AND THEIR LOCALIZATION

The pathogenesis of VT in most patients with a prior MI, is reentry involving these compartmentalized myocardial fibers within the scar. Macro reentrant circuits develop around an anatomically determined obstacle (scar) or a partially anatomic barrier combined with a functional barrier. Generally, the arrhythmogenic circuit is not a simple single circuit but rather an extensive sheet of surviving myocardial fibers in a bed of scar tissue with multiple potential entry and exit points that allow for multiple reentrant paths (i.e., different VTs) to traverse through scar [175, 241]. The slow conducting zones of the reentry circuit (referred as the isthmus) is located in dense scar in 90% of scar related VT, while entrance and exits sites are found in borderzone or normal myocardium [261]. Clinical studies in hemodynamically stable VT in patients with prior MI report average isthmus lengths as 31±7 mm, and the width as 16±8 mm [236, 261]. Clinically, surviving myocardial fiber channels within the scar can be mapped chiefly in two ways: a) Entrainment mapping b) Substrate mapping.

#### A. ENTRAINMENT MAPPING

The seminal work from Waldo's research group first developed the concept of entrainment mapping (originally in atrial flutter) in 1983 [219]. It is a fundamental electrophysiological maneuver to accurately find channels supporting ventricular tachycardia [223, 262]. The ability to entrain the tachycardia at rates faster than the tachycardia rate is considered as the hallmark for reentrant mechanism of tachycardia. Although there are multiple limitations in the application of entrainment that are related to the VT itself, entrainment mapping, when feasible, is perhaps superior to other methods (substrate mapping) for defining the relationship of a site to the VT circuit [263].

*Intervals In Entrainment Mapping*

The ability of an extrastimulus to influence the tachycardia depends on the tachycardia cycle length (TCL), the duration of excitable gap of the tachycardia, refractoriness at the stimulation site, and conduction time from the stimulation site to the tachycardia circuit. After the first stimulus in an overdrive pacing train that penetrates and resets the circuit ($n^{th}$ stimulus), subsequent stimuli interact with the reset circuit. Depending on the degree that the excitable gap is pre-excited by the $n^{th}$ stimulus, subsequent stimuli will fall on either fully excitable or partially excitable tissue. Entrainment is said to be present when two consecutive stimuli conduct orthodromically through the circuit while colliding antidromically with the preceding wavefront [19]. The orthodromic impulse of the last introduced stimulus propagates around the circuit to become the first complex of the resumed VT. The conduction time of this impulse to the exit site (or QRS) is termed the last entrained interval. The interval from the last stimulus to the first return electrogram at the pacing site [post pacing interval (PPI)] depends on the location of the pacing site in relation to the VT circuit, conduction delay from pacing site to the tachycardia circuit and conduction delay in the orthodromic wavefront during pacing. As faster pacing introduces conduction delays, pacing at cycle lengths 10-20ms shorter than the TCL minimizes the effect of conduction delays on PPI. As the time from the orthodromically activated electrogram during VT to the onset of the return cycle QRS or an intracardiac electrogram elsewhere (e.g. RV apex) remains constant, the stimulus to QRS (S-QRS) (or stimulus to RV apex) remains constant during pacing. In absence of recording an electrogram at the pacing site, these measurements can be used as surrogate to characterize the last entrained interval [264].

*QRS Morphology During Entrainment*

QRS morphology during pacing depends on the fusion of both the stimulated and tachycardia wavefronts. The degree of fusion depends on the pacing cycle length and anatomic location of the pacing site in relation to the protected isthmus (inner loop) of the VT circuit. Fusion is absent (concealed entrainment) when pacing site is within the protected isthmus as the myocardial capture by the pacing stimulus is

restricted to a small area. Pacing from elsewhere in the circuit (outer loop) or rest of the myocardium produces depolarization of myocardium by both the stimulated and paced wavefronts and manifest fusion. Fusion may be inapparent while pacing at longer cycle lengths, and progressive fusion is noted at faster pacing rates as surface ECG progresses from looking more like the VT complex to a entirely paced complex.

### *Activation Mapping for Mid-diastolic Electrograms*

During VT, the isthmus encompasses only diastolic potentials, and conduction time through the isthmus accounts for 57% to 81% of the tachycardia cycle length. Because of the limited myocardial area depolarized, the activation of the isthmus contributes negligibly to the surface electrocardiogram in sinus rhythm. Activation mapping in hemodynamically stable VT is targeted for sites demonstrating presystolic or mid-diastolic electrograms during VT [265]. A diastolic electrogram that drives, rather than follow, the VT QRS is likely from within the circuit [266]. Often, however, apparent absence of a local diastolic electrogram does not preclude location within a small channel, and entrainment can be useful [267].

### *Criteria For Entrainment*

Entrainment, while overdrive pacing, is said to be present when there is: (a) fixed fusion of the paced complexes at any cycle lengths, (b) progressive fusion, which is still fixed at any given paced cycle length, and (c) the resumption of the tachycardia following pacing with a nonfused complex at a return cycle length equal to the paced cycle length [78, 268-270]. Specific criteria are used clinically to evaluate relation of location of the pacing site to the reentrant circuit [262, 264]. A site is identified to be present within the circuit (inner loop or outer loop) when: (1) PPI –TCL ≤ 30ms, or (2) S-QRS and electrogram to QRS interval difference ±20ms, or (3) $n^{th}$ stimulus to n+1 QRS and $n^{th}$ electrogram to n+1 QRS interval difference ≤ 20ms. A site is identified to be present in the isthmus (inner loop) of the circuit when concealed fusion is present (QRS morphology during pacing matches the VT morphology). When expressed as a percentage of the TCL, the S-QRS interval also localizes the pacing site within the isthmus. Sites with S-QRS less than 30% of the TCL are near the

isthmus exit site, those 30-70% of the TCL are within the central isthmus, whereas those more than 70% of the TCL are near the isthmus entrance site. A site where concealed fusion is present but PPI-TCL is greater than 30ms is considered as the bystander component of the VT circuit.

*Clinical Studies*

Stevenson et al. provided the first clinical testing to assess importance of entrainment characteristics by catheter ablation and VT termination in post-MI VT [223]. Ablation was more likely to terminate VT at sites that demonstrated concealed entrainment, a PPI approximating the TCL, and a S-QRS greater than 60ms but less than 70% of the TCL. Concealed entrainment alone was not sufficient to guide ablation, because 25% of sites where concealed entrainment was present had long PPI, thus qualifying as bystander locations. Sites with isolated mid-diastolic potentials or continuous electrical activity were also demonstrated to be successful ablation targets. Ablation at sites where combinations of favorable characteristics were present resulted in VT termination in 35% of applications, compared with 4% when these characteristics were absent. In study by Bogun et al. [271], the predictive value increased to 70-90% in presence of combination of these favorable characteristics. The variation in success rate while ablation at sites deemed to be from the inner loop of the VT circuit could result from ineffective lesion formation, broader isthmus or insufficiently detailed mapping.

The acute success rate of entrainment mapping and ablation ranges from 67% to 96% in published studies and 30% to 46% VT recurrence rate over 2 to 3 year follow-up [80, 81, 223, 271-276]. Despite arrhythmia control, all-cause mortality remains high in these patients, ranging up to 30% at 3 years and ~ 50% at 5 years [81, 275, 276]. Majority of these deaths are caused by progressive cardiomyopathy and refractory heart failure.

### *Limitations of Entrainment Mapping*

Entrainment mapping has no limitations as a concept, however its application is restricted due to the several limitations related to the VT itself. In order to apply detailed entrainment mapping, VT must be reproducibly inducible, hemodynamically well tolerated to allow prolonged mapping during VT, and not accelerating or changing to different VT morphologies during entrainment [277]. Additional limitations include the need to be able to consistently capture local tissue in dense scar regions, the need to distinguish near-field from far-field capture, and failure to recognize the local electrogram due to amplifier ringing artifact at termination of pacing. Only 10-30% of patients with large infarcts have such stable VT [274, 278, 279]. Strategies to improve hemodynamic tolerance of VT (e.g. ventricular assist device, intraaortic balloon counterpulsation) have been described to assist entrainment mapping, however, increase the morbidity associated with the procedure [280, 281]. Single beat pacing and entrainment is useful alternative commonly used in patients with unstable VT [282].

## B. Substrate Mapping

The prerequisite conditions for entrainment mapping are often not met in contemporary patients undergoing catheter ablation. As an alternative, VT ablation is frequently led by the morphology of the VT itself and the distribution of the underlying substrate during sinus rhythm [283].

### *QRS morphology in VT*

The 12-lead QRS morphology during VT can help conceive general localization of the exit site of VT circuit [19, 283, 284]. The electrical information from the critical diastolic pathway in scar does not manifest as visible deflections on the conventional surface ECG. Exit site localization can however guide to a region of interest and planning diastolic pathway ablation. Briefly, VT morphology can be examined for a) bundle branch block pattern, b) frontal plane QRS axis, and c) precordial R wave transition.

In post infarct hearts, VTs virtually always arise from the LV or the interventricular septum. While right bundle branch block patterns arise from VTs in the LV, left bundle branch block pattern VTs arise in or adjacent to the interventricular septum exiting through the right side of the septum. Nevertheless, successful ablation is often accomplished from the left side of the septum in infarct related septal VTs. Septal VTs are generally narrower than the VTs originating in the free wall due to concurrent conduction in both directions and early engagement of the His-Purkinje system in the diastolic pathway. The frontal plane QRS axis during VT varies in the context of infarct location. Superior axis VT arises from the inferior LV (inferior wall or inferior portion of the septum) and inferior axis VT from the superior LV (anterior wall or superior septum). The axis becomes rightwards as the exit moves away from the midline towards the lateral wall. The frontal plane QRS does not discriminate between right bundle branch block VTs from apical lateral versus septal sites of origin that usually have right superior axis. Relative timing of the right ventricular apical activation determined from the implanted defibrillator lead may distinguish these sites [285]. The precordial R wave transition varies with the exit site location in an apex-to-base dimension. In VTs from near the mitral annulus (as in inferior and posterior lateral infarcts), a posterior structure, the impulse propagates from near the back to front and from base towards apex, and the precordial leads thus have large R waves usually from V2 through V4 and late precordial transition with persistence of r or R wave through V6 (positive concordance). Negative QRS (QS) complexes across the precordial leads (negative concordance), especially V4 to V6, signify origin from the apex, which is an anterior site. Right bundle branch block pattern VTs coming from the apex may have a qR in V1, or occasionally a monophasic R wave, but there is QS or QR in V2 and V3, often extending as QS across the precordium through V6. Left bundle branch VT from the anteroseptal infarct can present with QS complexes across the precordium possibly reflecting right ventricular exit from the septal VT circuit and transapical activation of remainder of the LV. It is always associated with initial Q waves in leads I and aVL. If an initial R wave is present in V1, along with a Q wave in aVL, the location of the exit site is more posterior in the middle of the septum.

Several factors can limit the ability of QRS morphology to localize VT: i) size of the infarct and extent of scarring, ii) shape of the heart (e.g. aneurysm formation) and its position within the thorax, and iii) conduction abnormalities (due to ischemia, anti-arrhythmic drugs, metabolic disturbances) affecting propagation from the site of VT. The accuracy of the ECG in localizing VT exit site in anterior infarction is much less than the inferior infarction due to greater degree of myocardial scarring. The R-S transition in the standard six precordial leads can be deceiving in a large dilated left ventricle. Criteria for discriminating endocardial versus epicardial circuit, although useful in non-ischemic tachycardias, they lack predictive value for post-infarction VT [286, 287]. None of the ECG features suggestive of epicardial VTs (QRS duration ≥198ms, pseudo delta wave ≥34ms, intrinsicoid deflection time in lead V2 ≥85ms, shortest RS complex duration ≥121ms and maximal peak deflection index ≥0.54) consistently predict epicardial location in infarct related VT. The presence of a Q wave in lead I and its absence in inferior leads is not considered specific for epicardial superior LV VT site. Often post infarct patients have multiple VTs, and sustained monomorphic VTs induced in the electrophysiology lab do not match with the clinical VT. When a 12-lead ECG of a VT is not available, correlation of the device generated intracardiac electrograms can be useful to decide the clinical relevance of an induced VT [82].

*Pace mapping*

VT morphology is widely emphasized to be relevant in planning ablation targets [282, 288, 289]. A long S-QRS interval can serve as a marker for slow conduction, and paced QRS morphology similar to the VT QRS morphology likely indicates location within a VT channel or its bystander component. The course of a channel can be traced by joining sites with matching paced QRS morphology in order of their S-QRS interval [282]. All sites with long paced latencies >40ms, particularly with latency >80ms, irrespective of the resulting QRS morphology are considered as good markers being adjacent to entrainment proven isthmuses of clinical VT [289]. Pacing directly within the scar serves to assess presence of surviving tissue within the scar [290]. Myocardial capture during pacing at sites at which it is difficult to determine whether a small

amplitude late potential is present, or has obscure significance can help ascertaining presence of thin surviving muscle bundles in the scar.

*Pitfalls of Pace Mapping*

It has been realized that analysis of paced QRS morphology does not provide incremental benefit over identification of a slow conducting zone to target catheter ablation. While paced QRS morphology similar to VT corresponds to location in the isthmus of VT or its blind-loop bystander and is mostly specific for the VT channel, in contrary, a mismatched paced QRS morphology does not imperatively rule out the location for clinical VT channel [282, 288]. This is possible as regions of functional block and wavefront collision, present during VT, may define propagation corridors during tachycardia but not during pace mapping as pace stimulation is generally done at rates much slower than VT [148]. Paced QRS morphology from sites within a channel may exit via the VT entrance site and thus have different morphologies. This can result in false interpretation as a non-VT channel. In addition, channels with multiple potential exits can manifest mixed QRS morphologies. Various criteria have been used to match paced QRS and VT morphology (9 to 11 out of 12 ECG leads) that can introduce error in the assessment of sites with matching morphology [289]. Conventionally, unipolar pacing with a 4mm tip catheter is used to eliminate far field capture from the anode [291]. However, the precision of mapping, particularly the lack of virtual electrode and small field of view, is better with smaller closely spaced bipolar electrodes [292, 293]. Pacing capture threshold can vary in different regions of scar depending on excitability, thickness, and orientation of surviving myocyte bundles within the scar. Pacing threshold >10mA is considered a feature of electrically unexcitable scar [290]. Threshold testing before pacing at each site is highly time consuming, thus pacing is generally performed at a fixed output of 10mA. Failure to recognize far field capture during high output pacing can result in misinterpretation of a pace map location. The response to pacing is assessed based on the resulting QRS response. Pacing within a slow conducting channel with long refractoriness, with large sink of current, or interrupted by fibrous septa can manifest as intermittent QRS response or local capture without global QRS response.

*Non-fluoroscopic Cardiac Mapping*

Accurate understanding of the ventricular substrate and mechanism of VT are a prerequisite for its successful treatment. Non-fluoroscopic cardiac mapping systems are designed to provide local electrical information in conjunction with spatio-anatomic information. During recent years, Ensite NavX (St Jude Medical Inc, St Paul, MN, USA) navigation and visualization technology and CARTO (Biosense Webster Inc. Diamond Bar, CA, USA) have evolved as the main representatives. Ensite Velocity is the latest released platform of the Ensite NavX technology [294]. It represents an open system that allows 3D visualization of multiple intracardiac catheters from different manufacturers. This is an impedance-based system and up to 128 electrodes can be visualized in the 3D space through a 5.6kHz signal emitted from three pairs of surface patch electrodes. Pace map sites, abnormal electrogram sites and lesion markers can be tagged to see continuity and their relation to the scar. A bipolar voltage cutoff of 1.5mV serves well to separate normal from scarred tissue [243, 295]. Voltage threshold below 0.5mV is arbitrarily defined as dense scar; this does not imply that this tissue does not contain surviving tissue. Indeed, this tissue often contains surviving myofibrils that express late potentials during sinus rhythm or mid-diastolic potentials during VT.

*Linear Ablation*

Marchlinski et al first described anatomically guided linear lesions anchoring dense scar across the borderzone to other anatomic barriers (or normal myocardium) and is traditionally considered as the closest approximation to surgical subendocardial resection [240]. The region of the VT circuit is identified by presumed exit site through pace mapping. Other investigators have modified this anatomic approach: i) a pair of crossing linear lesions, one extending from the exit site into the scar and the other tangentially along the border of the scar, ii) completely encircle the scar, iii) extending short linear lesions transecting identified isthmuses of VT circuits, or between islands of inexcitable segments (i.e. demonstrating failure to capture at higher outputs) [263, 290, 296]. Channels of preferential conduction often become evident by adjusting the scar voltage definition within 0.1-0.5mV range as bands of relatively

high voltage [261, 297, 298]. It is unknown if such offsetting of voltage reflects greater healthy intramural tissue or absence of subendocardial scar [299].

*Scar Related Electrograms*

Electrograms are classified according to the standard criteria [239, 241, 300] as:
i) normal (3 or fewer sharp intrinsic deflections from baseline, amplitude ≥3mV, duration <70ms, and/or amplitude: duration >0.046mV/ms),
ii) fractionated (multiple intrinsic deflections, amplitude ≤0.5mV, duration ≥133ms and/or amplitude: duration ≤0.005),
iii) late (any electrogram with a duration that extends beyond the end of surface QRS), and
iv) very late potentials (isolated component ≥100ms after the end of surface QRS). Any electrogram not fitting into one of these categories is classified as other abnormal electrograms. More recently, the term "localized abnormal ventricular activities" (or LAVA) has been introduced to qualify abnormal electrograms that can be buried within the local electrogram. Poor coupling to the local electrogram unmasked by programmed extra-stimulation characterizes these LAVA potentials [301].

Current substrate based ablation strategies for post-infarct VT emphasize high density mapping of the scar to identify and target all scar related abnormal electrograms by catheter ablation [301, 302]. These electrograms are considered indicative of underlying surviving myocyte bundles with discontinuous conduction [303]. However, information content pertinent to a VT supporting channel remains obscure in this simplistic way of composite electrogram classification. Although specific for identifying VT channels, these electrograms have poor sensitivity; not all such electrograms reside in the VT supporting channels and, in fact, many are bystanders [304, 305]. Conversely, only 50% of central, proximal or exit sites of reentry circuits have abnormal electrograms [306]. Targeting these electrograms often results in ablation of bystander sites (e.g. dead end pathways) and channels that may not be operative in any clinical VT (non-VT channels). This approach of ablation has shown

to improve VT free survival in these patients [301, 302]. No significant adverse effect on ventricular function is reported by ablation within already infarcted tissue.

### *Novel Electrogram Properties*

Additional measures of electrogram properties such as isochrones of activation time and activation gradient in surviving tissue within the scar have been studied during sinus rhythm [307-309]. Sites with late activation in the scar and regions of large temporal gradient in activation have been shown to be in anatomic proximity to critical segments of VT circuits [305, 310]. However, none of these properties have been systematically studied in large three dimensional electroanatomic maps of bipolar electrograms in human ventricles to identify targets of catheter ablation of VT. Moreover, analysis of scar electrograms in the voltage domain has not been performed. The information encoded in the inequalities of voltage distribution within the scar can perhaps be studied to differentiate channels supporting VT from innocent bystanders. Shannon entropy is a fundamental measure of inequalities described in information theory [311]. This has been recently studied in animal atrial fibrillation [312]. Signal voltage distribution and thus Shannon entropy, was shown to be higher at pivot region of a rotor compared to its periphery. The complex electrograms expressed from branched channel segments within the scar will have high Shannon entropy compared to electrograms from linear channels with paucity of side branches. Scar analysis in voltage domain for regions of minimum entropy, thus can improve localization of channel segments critical for maintaining VT.

### *Use of Multipolar Catheters*

Conventional mapping is done using a quadripolar catheter with 2 or 3 bipoles. It has to be positioned at several separate points to acquire detailed electrical information. Increasing the number of recording bipoles has the advantage of recording electrical information from the scar in detail and in shorter time. High density mapping of ventricles with a linear duo-decapolar catheter has been shown to improve identification of late potentials and characterization of the scar [250]. Noncontact mapping using a 64-electrode balloon array has larger field of view, however the

information obtained on the amplitude and timing of electrograms is limited by the fact that the electrograms are virtual (far-field) which are susceptible to errors towards the extremities of the mapping field. However, it can identify diastolic pathways and exit sites during VT, and correlates with the information obtained by contact mapping in sinus rhythm [313]. The physical interference to the movement of the ablation catheter and inferior location accuracy of the balloon array system are some of the limitations of this system.

*PentaRay™ Catheter*

The PentaRay™ catheter (Biosense-Webster Inc., Diamond Bar, CA, USA) is a 7F high density mapping catheter with 20 electrodes distributed over 5 soft radiating splines (1-mm electrodes separated by 4-4-4 or 2-6-2 mm inter-electrode spacing) that allow splaying of the catheter to cover a surface diameter of 3.5 cm (area 7 cm2). This close electrode spacing allows recording of very small amplitude electrograms, not recorded by wider spaced electrodes used in other channel mapping studies. The catheter is able to record from 15 bipolar electrodes during a single beat and is therefore able to create patterns of activation rapidly, that can assist in defining the tachycardia circuit and subsequent ablation. It has previously been used to map focal and macro-reentrant atrial tachycardias as well as atrial fibrillation [314]. A recent study described use of PentaRay™ catheter for substrate characterization in patients with post-infarct VT [301]. It can be positioned in LV either by transeptal access using steerable sheaths or retrogradely from aorta. When attached to electro-anatomic mapping system (Ensite NavX™, St Jude Medical Inc., St Paul, MN, USA), the ability of this catheter to record multiple activation points during a single beat allows acquisition of the 3-dimensional geometry and patterns of activation in a very short period of time. A potential limitation of this catheter is contact of all the splines may get restricted by the mitral apparatus including papillary muscles or in the tapering apex of the LV.

*Clinical Studies*

Several published clinical studies have evaluated the efficacy of substrate based ablation approach, although all are non-randomized observational studies [240, 263, 279, 295-297, 301, 302, 315-317]. The data are encouraging with acute success rate reported from 49% to 82%, and 23% to 47% VT recurrence rate at long-term follow-up. Two randomized studies (SMASH-VT, V-TACH) evaluated the role of prophylactic substrate ablation in patients undergoing ICD implantation for secondary prevention. [318, 319] Both studies showed a significant reduction in appropriate ICD interventions in the ablation arm. A trend towards mortality reduction with VT ablation was observed in SMASH-VT study. Large variation between the two studies in the long-term VT recurrence rates in the ablation groups (12% & 53% at 22-month follow-up) was mainly due to differences in the adopted ablation strategies. The actual efficacy of each of the individual approaches is not known and requires further study with prospective randomized clinical trials.

*Limitations of Substrate Mapping*

The most important limitation of substrate mapping in its present form is lack of electrical resolution within the scar. Its application is often elementary given the inability of the present day mapping methods to reliably distinguish electrograms that populate VT channels from those elsewhere within the scar, and requires extensive pace mapping and catheter ablation within the scar. As the ventricular scar volume can be frequently large, complete elimination of scar related electrograms or scar dechannelization remains technically difficult and time consuming.

### 1.3.7 INDICATIONS OF VENTRICULAR TACHYCARDIA ABLATION

Only 10% of patients with VT are appropriate candidates for VT ablation [274]. Considering the risk-benefit analysis of VT ablation, every attempt is made to optimize pharmacologic and antitachycardia pacing (ATP) therapy [320-322], and treat

reversible factors such as ischemia. Ablation is less attractive in patients with large infarctions and multiple clinically relevant VT morphologies. Patients with end-stage heart failure may be intolerant of protracted procedures. The typical patient considered for VT ablation has (i) frequent VT episodes resulting in ICD shocks due to rapid VT or ineffective ATP, (ii) has severe symptoms (palpitations, presyncope) despite effective ATP, or (iii) recurrent slow VT. Some investigators consider ablation alone (without ICD therapy) as a primary therapy for VT in patients who present with tolerated VT [323]; however, as ischemic heart disease is progressive and scar evolution can be unpredictable, most agree that ablation therapy is palliative and adjunctive to ICD therapy [324]. Presence of intra-cardiac thrombus is an absolute contraindication for performing catheter ablation of VT. Presence of severe peripheral vascular disease or mechanical prosthetic valve may limit ventricular access and increase the risk of complications.

#### VENTRICULAR TACHYCARDIA STORM

Ventricular tachycardia storm is defined as (i) recurrent VT in a short time (≥3 separate episodes in 24 hours, each requiring termination by intervention), (ii) frequent defibrillator therapies (≥3 separate episodes separated by 5 min in 24 hours), or (iii) incessant VT (continuous VT that recurred promptly despite intervention for termination over > 12 hours) [325, 326]. It is increasingly being recognized as a distinctive arrhythmia syndrome with its specific management issues and prognostic consequences that differ from ventricular tachycardia (VT) episodes unrelated to storm [326, 327]. Despite the presence of an ICD, the appearance of a VT storm still portends a high mortality [327-330]. The AVID study which followed secondary prevention ICD recipients observed a 5.6 fold relative increase in mortality in the first 12 weeks following development of VA storm and 2.4 fold over 3 years as compared to those who had VT episodes unrelated to storm [327]. Radiofrequency catheter ablation is evolving as the standard care in patients with VT storm, with VT free long term survival improved with early invasive intervention [331]. Other approaches such as transcoronary ethanol ablation generally remain as a treatment of last resort after failure of RFA [332]. Most of the published data on VA storm ablation are single center small series or case reports and has relative small representation within large

multicenter VT ablation series [279, 316]. Despite this relatively modest supporting evidence, current guidelines endorse the role of catheter ablation for VA storm management with a consensus on early intervention [326].

### 1.3.8 BIOPHYSICS OF CATHETER ABLATION IN THE VENTRICLE

Radiofrequency ablation is a principle tool implemented in clinical electrophysiology laboratories for treatment of cardiac arrhythmias. It has now been a standard of practice for managing ventricular tachycardia [333]. The results of these procedures are significantly improved with use of irrigated ablation as compared to non-cooled ablation [295, 334]. In the canine thigh model, Nakagawa et al have shown that the lesion is deeper and larger with the saline-irrigated ablation as compared to standard temperature controlled ablation as it allows delivery of higher power without rise in electrode-tissue interface impedance [335]. Radiofrequency ablation lesion formation results from resistive tissue heating at the electrode tissue interface and superficial tissue while passive heat conduction from superficial to deeper layers determines heating of deeper layers [336]. Resistive heating of tissue is directly proportional to power density and tissue impedance. A drop in tissue impedance will reduce heating and a rise in impedance will result in excessive heating and coagulum formation or boiling increasing risk of thromboembolic complications. Convective cooling of the electrode-blood interface by irrigation allows greater power delivery without tip temperature rise and sudden rise in impedance [337]. Irrigation is even more important in scarred issues as heating of the deeper tissues may remain poor in the presence of fibrous scarring. Despite irrigation, ablation lesions are smaller and superficial in infarcted myocardium compared to the normal ventricular muscle [338]. Irrigated radiofrequency ablation is now used as the primary ablation modality in the left ventricle. In the multicenter Cooled RF and Thermocool VT ablation trials, it was possible to ablate all VTs in 50-75% patients with 3-8% risk of major complications, that included stroke, pericardial tamponade and death [272, 279]. In a retrospective analysis that compared standard versus irrigated catheter ablation of

VT at isthmus sites, irrigated radiofrequency ablation had greater efficacy for terminating VT suggesting reentry circuit isthmuses often exceed the width and depth of a standard radiofrequency lesion. [334].

## 1.4 Recent Advances and New Technologies in Mapping of Scar Related Ventricular Tachycardia

### 1.4.1 New Imaging Technologies

The location and morphology of the infarcted tissue can be elucidated by preprocedural magnetic resonance imaging (MRI) or computed tomography (CT) with body surface mapping.

#### A. Contrast Enhanced Magnetic Resonance Imaging

MRI is a non-invasive, non-ionizing imaging modality that can provide detailed anatomic information with high spatial resolution. In relevance to substrate mapping, delayed enhancement contrast MRI (DE-MRI) can distinguish normal from chronically infarcted tissue with millimeter spatial resolution [273]. A preprocedural MRI can serve as a roadmap to guide substrate based catheter ablation [339]. The three-dimensional (3D) cardiac MRI can be integrated with electroanatomic mapping information to guide catheter navigation and place ablation lesions at channels in the scar in real time. This has been tested in vivo porcine experiments. It is now being studied in the clinical electrophysiological laboratory to guide substrate mapping and ablation of VT in a reliable manner, with shorter procedural times and less radiation exposure [340-346].

*Risk stratification*

DE-MRI has been used as a risk stratification tool in post-infarct patients with LV dysfunction. It improves prediction of monomorphic VT inducibility at electrophysiology study [347, 348], and of spontaneous ventricular arrhythmia and mortality, beyond that with LV ejection fraction [349].

*Mapping of Conducting Channels*

Patients with inducible VT have greater DE-MRI derived subendocardial scar area than patients without inducible VT [347, 350]. This is in accordance with electroanatomic mapping data. In a study, the MRI derived anatomy of LV was integrated with the electroanatomic mapping data (CARTOMERGE™, Biosense-Webster Inc., Diamond Bar, CA, USA), and a cutoff of 60% of the maximum pixel signal intensity on DE-MRI best differentiated dense scar and borderzone. This could also identify 69% of the conducting channels observed on the CARTOMERGE™. Matching improved to 81% of conducting channels when, instead of whole LV, only the subendocardial half of the LV was segmented. A Cohen kappa coefficient of 0.70 was obtained between location of each intracardiac electrogram bipolar voltage and 3D DE-MRI derived scar components [344]. Another study defined scar on DE-MRI as signal intensity greater than 3 SD than the remote normal myocardium. Sites with signal intensity 2 to 3 SD were labeled as heterogeneous tissue (scar with surviving myocytes) [351]. The heterogeneous tissue was more abundant in patients with VT and matched with the conducting channels identified by electroanatomic mapping. Critical isthmuses of VT were identified in relation to ~58% of these anatomical channels. In a recent study, critical components of VT circuits were reported in regions where the scar transmurality was greater than 25% [346]. Although MRI gives superior resolution, CT gives the feasibility to evaluate left ventricular and epicardial coronary anatomy. It is particularly useful in patients with implanted ICDs or pacemakers. Endocardial low voltage and abnormal ventricular electrograms have been shown to colocalize with CT defined thinned segments (<5mm wall thickness) of the LV myocardium [352, 353].

*Virtual Electrophysiologic Study*

More recently, DE-MRI has been used to characterize VT inducibility through a virtual electrophysiologic study [354]. In a porcine infarct model, normal areas, gray zones, and infarct cores were classified based on their signal intensity. In the computer model, gray zones were assigned slower conduction and longer action potential durations than normal myocardium, and virtual LV surface was

reconstructed. Virtual electrophysiological study was then performed by programmed extrastimuli introduced into the simulated scar structure. This compared well with the results of actual in vivo programmed stimulation and noncontact mapping. The simulated VT reentrant circuits approximated with the circuits seen on noncontact mapping.

### B. Body Surface Mapping

Body surface mapping is a novel non-invasive electrocardiographic imaging (ECGI) that reconstructs, from body surface potentials, epicardial electrograms over the surface of the heart [355, 356]. The ECGI methodology [357, 358] uses electrodes (n = 256) on strips that are applied to the torso of the patient. Computed tomography (CT) markers are attached to each electrode. All strips are connected to a portable mapping system (BioSemi, Amsterdam, the Netherlands; CardioInsight Technologies Inc, Cleveland, OH, USA). After electrodes application, patients undergo thoracic noncontrast gated CT with axial resolution of 3 mm. Patient-specific ventricular epicardial surface geometry and body surface electrode positions are digitized from CT images. The 256 channels of body surface potentials are sampled at 1-ms intervals from the start of the QRS complex through the ST segment (ventricular activation). Algorithms are used to noninvasively construct virtual unipolar epicardial electrograms and epicardial activation isochrones from body surface potentials and geometrical information. The ECGI is constructed on a beat-by-beat basis and does not require accumulating data from many identical beats. Electrocardiographic imaging has been shown to colocalize the epicardial electrical scar to the anatomic scar with a high degree of accuracy (sensitivity 89%, specificity 85%). It also demonstrates activation detouring and lines of block in sinus rhythm produced by epicardial scar. Fractionated and late potentials can also be identified within ventricular scar. ECGI is still a novel research tool, and has limited availability that precludes large clinical studies. However, it has huge potential role in arrhythmia risk stratification, identification of targets for ablation in the scar, and map stable VT [355, 359].

### 1.4.2 Human Stem Cells as Bench Models for Ventricular Tachycardia Mapping

Cultured cardiac cells in monolayers derived from animal tissue serve as a model for basic study of wave propagation and cardiac arrhythmias [360].They form a synthetic tissue system that can be manipulated structurally and functionally to evaluate various electrophysiological phenomenon at a scale that is intermediate between a single cell and the native tissue. However, animal-derived cultured tissues are different from intact human tissues, mainly because there is a difference in the ion channel types between the species, such as the HERG (human ether-a-go-go related gene) channel. Human pleuripotent stem cells have unlimited differentiation capacity and can be induced to form cardiomyocytes. These can be functionally integrated as complex cellular monolayers that can then be examined for cellular activation, reentrant arrhythmias and therapeutic modulation [361].

### 1.4.3 Gene Transfer

Altered connexin and ion channel expression in the healed infarct results in conduction slowing and increases reentrant VT susceptibility [362]. In an intact porcine infarct model [363], targeted manipulation of Cx43 levels by viral vector mediated direct gene transfer reduced electrogram fractionation, improved conduction velocity in the infarct borderzone and reduced ventricular tachycardia inducibility by 60%. In another study, gene transfer of the dominant negative KCNH2-G628S mutation to the infarct border caused localized prolongation of the effective refractory period and eliminated ventricular arrhythmia inducibility [364].

## 1.5 Limitations in The Current Knowledge And Research Objectives

### 1.5.1 Electrical Resolution Within Scar

Despite more than two decades of research, mapping of scar related VT has remained a challenge [365]. This results from complex structure of the scar and expanse of its distribution compounded by multiple clinical VT and high-risk procedures. Current substrate mapping methods advocate elimination of all scar related abnormal electrograms and lack rationalization in deciding the targets of ablation. This is an interesting problem; at one instance, there are convincing data that only specific regions in the scar possess electrophysiological properties suitable to sustain reentrant circuits, but with lacking tools to clearly resolve the problem, a comprehensive ablation of all excitable potentials in the scar is suggested. With a lack of well-defined end points, convincing elimination of all electrograms is therefore only conjectural and requires extensive long duration ablation [301, 302]. Upcoming technologies of catheter ablation such as contact force sensing [366, 367] and intramural needle ablation [368] can only partially eliminate these limitations and would still rely on high-definition mapping of the scar.

### 1.5.2 Poor Clinical Outcomes With Catheter Ablation

Clinical advancement in substrate based ablation strategies has failed to improve outcomes in these patients. It is anticipated that elimination of all abnormal electrograms will improve long-term clinical outcome in these patients. However, compared to historical controls, there is no improvement in the outcomes with almost 50% patients experiencing at least one episode of recurrent VT on follow-up [240, 290, 297, 301]. The results are duplicated even in highly experienced and dedicated

units for the treatment of scar related VT [317]. There is no data that catheter ablation for VT improves mortality [369]. The reported 6-10% acute major complication rate as cardiac perforation, pericardial tamponade and death in patients undergoing extensive substrate ablation remains undesirable [279, 301, 370].

Intuitively, it is conceivable that large majority of surviving myocyte channels that coexist in the scar possibly never mature to sustain clinical VT. It is unknown whether these "non-VT channels" differ from VT channels, and if they are only vestigial. Complete surgical endocardial resection of the scar successfully eliminates most scar related VT with few long-term recurrences, however has very high perioperative mortality [371, 372]. Present data do not suggest any adverse effect of extensive catheter ablation in the scar on ventricular function [373]. However, catheter based scar homogenization or dechannelization, if it has to match clean surgical scar results, would require rigorous elimination of mostly innocent surviving tissue in the scar. Incomplete scar dechannelization, that is often the case with the current available mapping and ablation tools, can potentially cause loss of large sink of current, only partially coalescing regions of conduction block and risk developing fast VT and VF that are more life-threatening. It was evident in the multicenter Thermocool-VT trial, where, post ablation, fast VT developed in 33% of patients [279]. Such vital evidence is alarming and is obvious acutely after routine VT catheter ablation procedures in all electrophysiological laboratories. However, impact of newly inducible fast VT on long-term outcomes has not been clearly evaluated in clinical studies.

### 1.5.3 Research Objectives

We therefore embarked on this project in post-infarct ventricles with the main objective of exploring electrophysiological properties of the scar in ultra high-density sinus rhythm maps, and to assess if there are intra-patient and inter-patient differences in the conducting channel properties. We aimed to contrast

electroanatomic properties of VT supporting channels with non-VT channels in the scar. We wanted to explore the relationship of conventional electrogram properties to the channel regions and test their predictive value to recognize VT channel regions. We also aimed to develop a set of novel multidimensional numeric and symbolic properties to reliably predict information on the topology of VT channels within the complex interacting system of scar and surviving myocytes. We compared the scar and channel properties in patients with and without spontaneous VT to explain why only few patients with scar develop VT. The focus of these research projects is to develop patient-oriented techniques for mapping life threatening VT channels in ischemic cardiomyopathy. The end objective is to expedite VT mapping and ablation, and offer a targeted management approach in those needing catheter ablation of VT.

We also aimed to study the surface electrocardiographic expression of intracardiac heterogeneity within the scar components in patients with cardiomyopathy. We employed electrocardiographic beat-to-beat QT variability recorded on the body surface to test the global activation-repolarization differences in the intramural scar. As sudden death in patients with ventricular scarring is mostly due to VT that degenerates to VF, assessment of QT variability is of significance in patients with scar related monomorphic VT. We assessed the effect of atrial pacing and pharmacologic modulation on the beat-to-beat activation-repolarization periodicity within the scar tissue components.

Finally, we performed a systematic review of literature on the invasive management of all high-risk ventricular arrhythmia storm patients, in order to evaluate the safety and efficacy of catheter ablation, and associate any potential adverse consequences that extensive but failed ablation may have in these patients. We chose to study the VT storm ablation outcomes to highlight the differences in the conduct of VT mapping and ablation procedures in the laboratories around the world. There is need for a scar based mapping method that allows rapid identification of critical regions supporting VT without using extensive pace mapping or mapping during unstable VTs.

## FIGURES

---

***FIGURE 1.1***

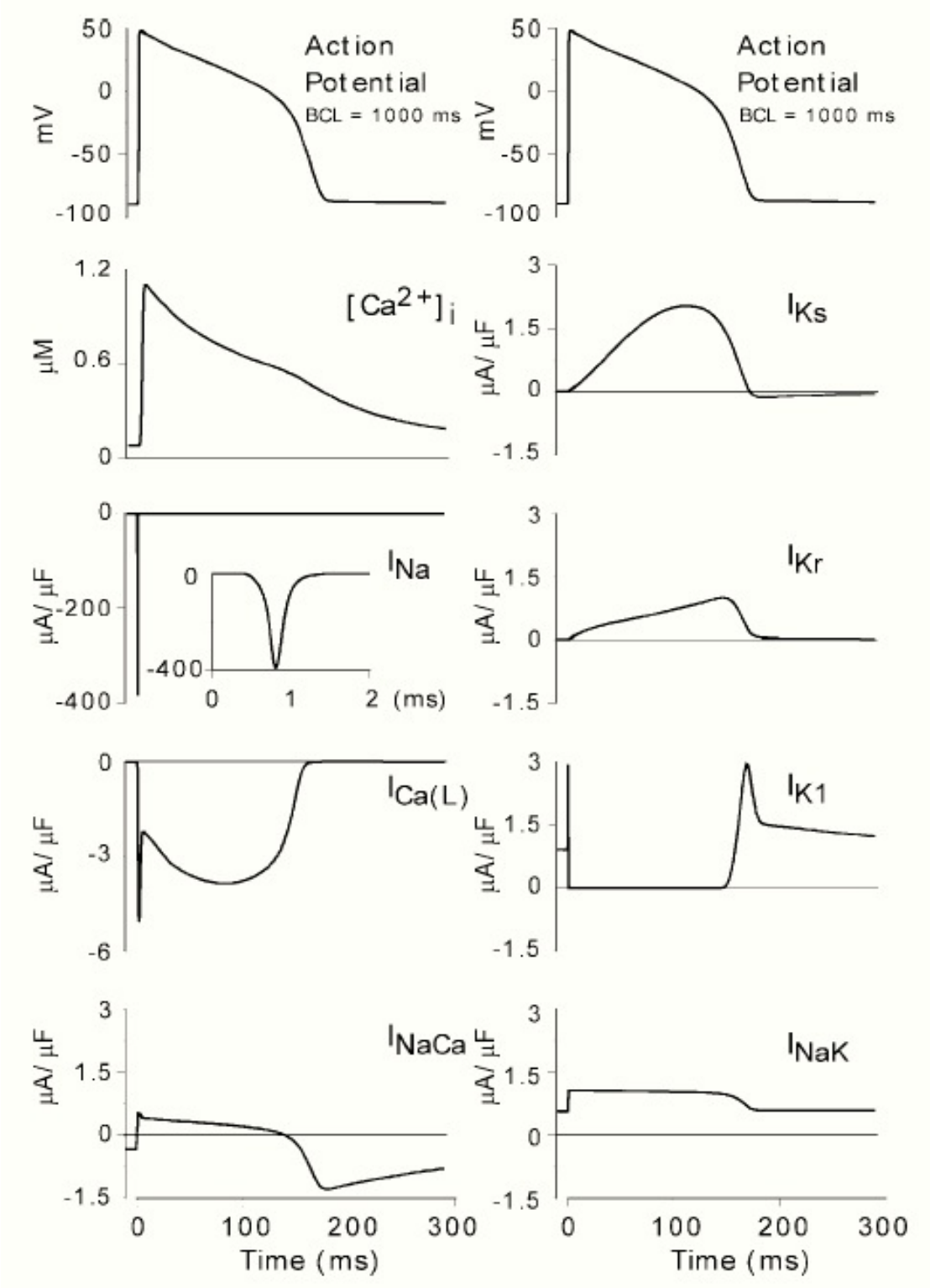

Figure 1.1 Ionic currents during action potential (AP) generation. Only selected ionic currents with major roles are included in the figure. Shown are the AP curves (copied at top of both columns for reference), the free calcium transient in the sarcoplasm $[Ca^{2+}]_i$ during AP, the selected ionic currents that determine the AP morphology. The inset in $I_{Na}$ shows the current on an expanded time scale. The simulated quantities of currents are based on Luo-Rudy model for the ventricular cell at constant steady state pacing at 1000ms. Once the threshold of activation is reached, the fast inward sodium current ($I_{Na}$) rapidly depolarizes the membrane and produce very fast AP upstroke. The $I_{Na}$ reaches its peak amplitude quickly (inset), after which it inactivates. When the $V_m$ upstroke reaches around -25mV, the inward L-type $Ca^{2+}$ current [$I_{Ca(L)}$] activates and provides a depolarizing current against repolarization produced by outward delayed potassium currents, $I_{Kr}$ (r=rapid) and $I_{Ks}$ (s=slow). The $I_{Ca(L)}$ is relatively slow in reaching its peak (spike), and does not contribute to the depolarizing phase of ventricular AP. However, its prolonged active state (dome) supports against the repolarization maintaining the plateau phase of AP. The $I_{Ca(L)}$ plays an important role in inducing $Ca^{2+}$ release from the sarcoplasmic reticulum, producing calcium transients and initiating muscle contraction. The two repolarizing currents, $I_{Kr}$ and $I_{Ks}$, gradually increase to dominate, before a large increase (late peak) of the inward potassium current ($I_{K1,}$ inward rectifier) brings the membrane AP down to its resting level. The sodium/calcium exchanger ($I_{NaCa}$) is an electrogenic process that moves $3Na^{2+}$ inwards for $1Ca^{2+}$ outwards. During the early phase of AP, it operates in reverse direction extruding $Na^{2+}$ and producing a small positive outward current. It then switches to its direct mode to extrude $Ca^{2+}$ and become a positive inward current that tends to slow AP repolarization and prolong the AP duration (From Rudy [85]).

***FIGURE 1.2***

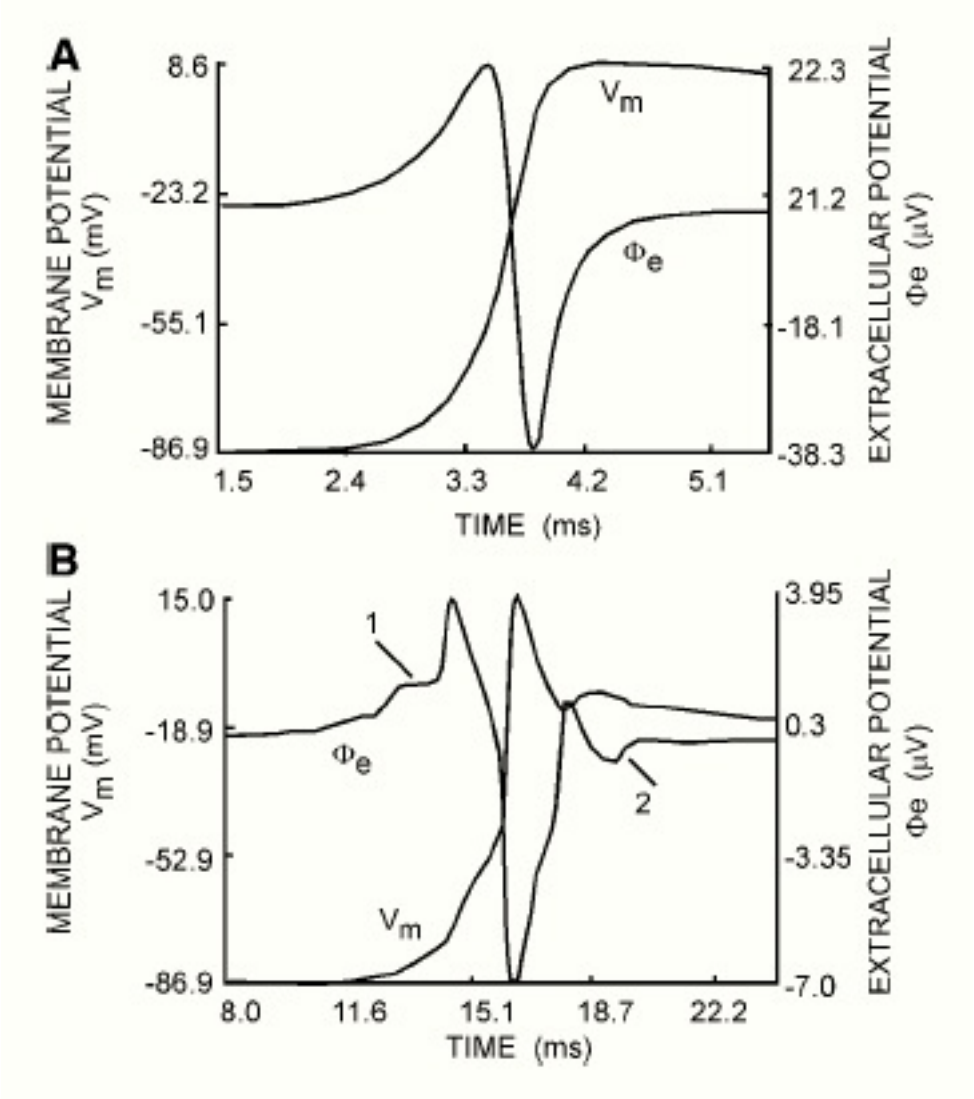


Figure 1.2. Relationship between upstroke of the transmembrane action potential ($V_m$) and the corresponding extracellular unipolar electrogram ($\Phi_e$) at different degrees of intercellular coupling. A: Normal coupling. B: coupling is reduced by a factor of 50. 1 and 2 indicate additional deflections in the unipolar electrogram produced by time-separated activation of upstream and downstream neighboring cells, respectively (From Rudy and Quan [147]).

***FIGURE 1.3***

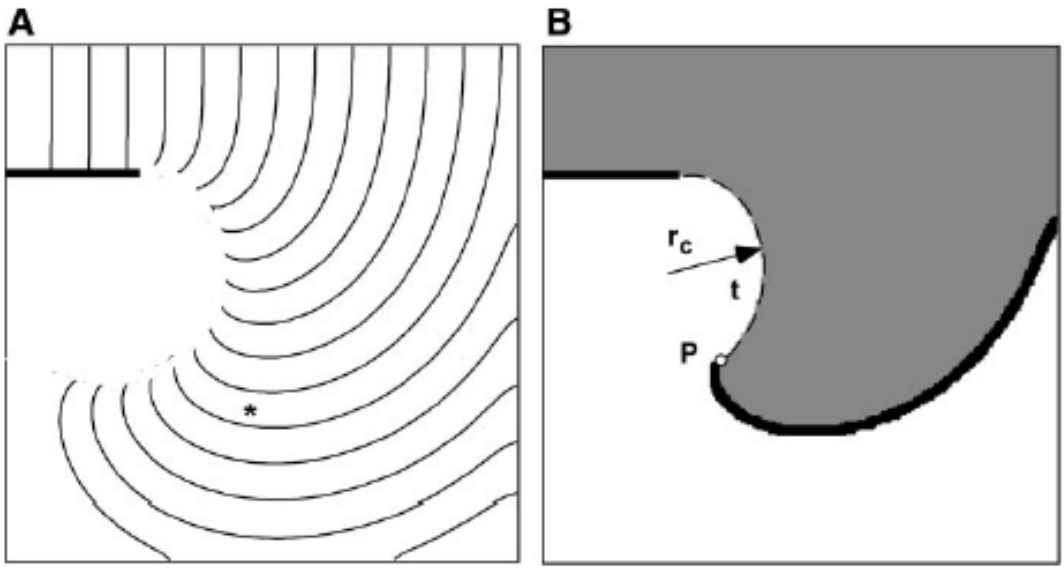


Figure 1.3. Propagation of a wave around a pivot point and formation of phase singularity. (*A*) Isochronal map of activation spread (*B*) Moment of activation marked by asterisk in *A.* Horizontal black line is anatomical (or functional) obstacle. The tip of the isochrones follows a path that is detached from the pivot point. The dashed line *t* shows the trajectory of the spiral wave tip with the radius $r_c$. The black color shows the depolarized area defined by activation of $I_{Na}$, the grey color shows the area in refractory state defined by inactivation of $I_{Na}$, and white color is area in resting state. Point *P* marks the phase singularity, where the three $I_{Na}$ phases meet each other. (From Fast and Kleber [112])

***FIGURE 1.4***

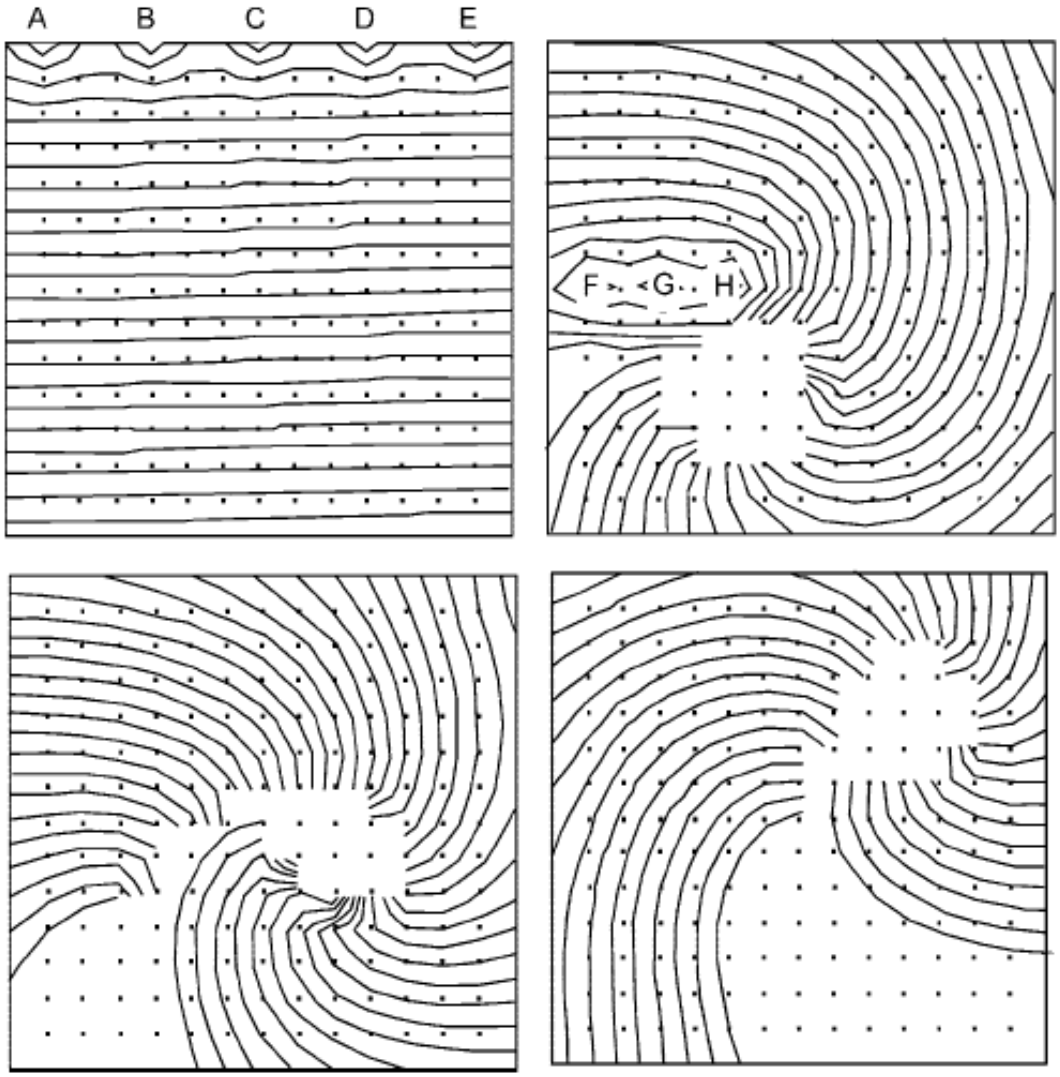


Figure 1.4. Initiation of spiral wave reentry: isochronal maps. *Top left*: linear wavefront propagation from top to bottom after simultaneous stimulation of sites *A-E*. *Top right*: after the initiation of wavefront from top to bottom, a second stimulus is applied simultaneously at sites *F-H*. This wave is blocked in the antegrade direction (below electrodes *F-H*) by the tail of the preceding wavefront but proceeds retrogradely and sets up the reentrant circuit. Activation during the subsequent reentry cycles is shown in the *bottom left* (2nd cycle) and *bottom right* panels (3rd cycle). (From van Capelle and Durrer [205])

# CHAPTER 2. HIGH DENSITY MAPPING OF VENTRICULAR SCAR IN ISCHEMIC CARDIOMYOPATHY- A COMPARISON OF CHANNELS THAT SUPPORT VENTRICULAR TACHYCARDIA WITH CHANNELS THAT DO NOT SUPPORT VT

## ABSTRACT

**Background.** Surviving myocytes within scar may form channels that support ventricular tachycardia (VT) circuits. There is little data on the properties of channels that comprise VT circuits and those which are non-VT supporting channels.

**Methods.** In 22 patients with ischemic cardiomyopathy and VT, high-density mapping was performed with the PentaRay™ catheter and Ensite NavX™ system during sinus rhythm. A channel was defined as a series of matching pace-maps with a stimulus (S) to QRS time of ≥40ms. Sites were determined to be part of a VT channel if there were matching pace-maps to the VT morphology. This was confirmed with entrainment mapping when possible.

**Results.** Of the 238 channels identified, 57 channels corresponded to an inducible VT. Channels that were part of a VT circuit were more commonly located within dense scar than non-VT channels (97% vs 82%, p=0.036). VT supporting channels were of greater length (mean±SEM 53±5 vs 33±4mm), had higher longest S-QRS (130±12 vs 82±12ms), longer conduction time (103±14 vs 43±13ms) and slower conduction velocity (0.87±0.23 vs 1.39±0.21m/s) than non-VT channels (p<0.001). Of all the fractionated (mean130±105), late (10±5) and very late (4±3) potentials located in scar, only 21%, 26% and 29% respectively were recorded within VT channels.

**Conclusion.** High-density mapping shows substantial differences among channels in ventricular scar. Channels supporting VT are more commonly located in dense scar, longer than non-VT channels, and have slower conduction velocity. Only a minority of scar related potentials participate in the VT supporting channels. These findings may provide a basis for more limited substrate ablation strategies.

## 2.1 INTRODUCTION

Scar related reentry is the most common mechanism of ventricular tachycardia (VT) in patients with ischemic cardiomyopathy (ICM) [277, 374]. The complex electroanatomic structure of scar [235, 350], with a meandering network of surviving myocyte channels interspersed in fibrous tissue, results in discontinuous and anisotropic slow conduction, non-uniform high restitution and altered excitability that lead to the development of reentrant VT [148, 175, 375, 376]. In clinical studies, these channels can be identified by several methods. Entrainment mapping has long been regarded as the gold standard [223, 262], but has limitations, in particular the need for hemodynamic stability. Pacing during sinus rhythm within dense scar can also identify channels [288, 290, 377]. Areas of paced latencies ≥40ms in scar are observed to collocate with isthmus sites, identified by entrainment mapping in patients with hemodynamically stable VT in ICM [288]. Similarly, bands of relatively preserved voltages in the scar have been shown to pair with slow conducting zones within the scar [261, 297, 298]. Many of these channels exhibit isolated potentials and fractionated electrograms that are often targeted during substrate based ablation [299, 301, 302, 306].

Recent substrate ablation strategies employ high density mapping with an objective to map and eliminate all scar related abnormal electrograms [250, 301, 302, 378, 379]. However, as only a finite number of sustained VT ensue in the setting of healed myocardial infarction, it is likely that only a subgroup of these channels will have satisfactory electrophysiological properties to perpetuate reentrant VT, while the vast majority are potential onlookers [304, 305, 380]. In this study, we performed high-density characterization of electrophysiologic substrate in patients with ICM and recurrent VT. We hypothesized that differences in the anatomy and physiology between channels will explain their differential likelihood to perpetuate reentrant VT. In addition, we examined the association between these channels and the scar related abnormal electrograms which may give an insight into substrate ablation techniques.

## 2.2 METHODS

This study was approved by the Human Research Ethics Committee of the Royal Adelaide Hospital and the University of Adelaide.

### 2.2.1 PATIENT POPULATION.

Twenty-two consecutive patients with ICM with recurrent VT or VT storm [≥3 episodes or implantable cardioverter defibrillator (ICD) therapies for VT in 24 hours] undergoing a clinically indicated catheter ablation procedure were studied. Patients with a previous VT ablation, acute coronary event within the preceding 1month, intracardiac thrombus, mechanical prosthetic valve and severe aorto-iliac peripheral vascular disease were excluded.

### 2.2.2 ELECTROPHYSIOLOGIC STUDY

The procedure was done in post-absorptive state under conscious sedation. Briefly, a quadripolar catheter and decapolar catheter were positioned at the right ventricular (RV) apex and coronary sinus, respectively. Programmed ventricular stimulation was performed from the RV apex at two drive cycle lengths (600ms and 400ms) with up to 3 extrastimuli. All sustained monomorphic VTs induced at baseline, during the course of the study and post-ablation were considered clinical VT [19]. A 20-pole catheter (PentaRay™, 2-6-2 mm interelectrode spacing, 1mm electrodes, Biosense Webster Inc, Diamond Bar, CA, USA) was introduced either retrogradely using standard sheaths or transeptally using the Agilis™NxT steerable introducer (St Jude Medical Inc., St Paul, MN, USA) into the left ventricle (LV) for mapping. Activated clotting time was maintained, with intravenous unfractionated heparin, between 250-300 seconds throughout the course of the study. After obtaining a left

ventricular geometry on the electro-anatomic mapping system (EnsiteNavX™, St Jude Inc., St Paul, MN, USA), an endocardial contact map was acquired in sinus rhythm. At each location, before signal acquisition, stability and adequate splaying of the PentaRay™ splines over the endocardium was confirmed fluoroscopically and ventricular ectopic beats were vigilantly excluded. Mapping was targeted to regions of low voltage (<1.5mV) and sufficient sampling was performed elsewhere to have fill threshold of 15mm. Additional points were taken with quadripolar ablation catheter if there were regions difficult to access with the PentaRay™ catheter. All points projecting > 10mm from the geometry were considered of inadequate contact and were excluded. Regular definitions were used to describe preserved voltage (>1.5mV), borderzone voltage (0.5-1.5mV) and dense scar (<0.5mV) [240]. Electrograms were classified according to the standard criteria [300] as:

i) normal (3 or fewer sharp intrinsic deflections from baseline, amplitude ≥3mV, duration <70ms, and/or amplitude: duration >0.046mV/ms),

ii) fractionated (multiple intrinsic deflections and amplitude: duration ≤0.005mV/ms),

iii) late (isolated component ≥20ms after the end of surface QRS), and

iv) very late potentials (isolated component ≥100ms after the end of surface QRS).

Any electrogram not fitting into one of these categories were classified as other abnormal electrograms. Figure 2.1 shows examples of each of the abnormal electrograms. Bipolar electrograms were filtered at 30 to 500 Hz, notch 50 Hz and presented at 100mm/s (LabSystem PRO v2.4a EP, Bard Inc., Lowell, MA, USA).

Bipolar pace mapping (MicroPace EPS 320 Cardiac Stimulator, Santa Ana, CA, USA) was performed at each location at 600ms cycle length or 50ms faster than the intrinsic sinus rate at constant output (10mA, 2ms) at sites with low voltage, fractionation and/or late electrograms. Pace-map locations were tagged on the electroanatomic surface. Entrainment mapping was performed whenever feasible at sites with abnormal electrograms, long S-QRS latencies and a paced QRS morphology matching VT. Standard criteria were used to define VT isthmus sites: concealed fusion with stimulus-QRS (S-QRS) interval that matched the electrogram-QRS interval (±20ms) and post pacing interval tachycardia cycle length difference (PPI-TCL) of

≤30ms [289]. If a mappable VT was rendered transiently non-inducible following PentaRay™ positioning in the zone of interest, entrainment pacing was reattempted with the ablation catheter.

### 2.2.3 RADIOFREQUENCY ABLATION

Catheter ablation then proceeded with 3.5mm tip irrigated ablation (CoolFlex, St Jude or Thermocool, Biosense Webster) targeting abnormal scar related electrograms and sites with long S-QRS intervals. Programmed ventricular stimulation was repeated following catheter ablation to evaluate procedural success. Complete success was defined as no inducible VT after ablation, abolition of one or more clinical VTs with other VTs remaining inducible was considered a partial success, and the inability to eliminate the clinical VT was considered as failure.

### 2.2.4 POST-PROCESSING OF MAPS

The surface areas of low voltage and dense scar were measured using the integrated software. Offline analysis of the digitally stored electrograms and pace maps was performed on the Bard EP system with the use of on-screen calipers at a sweep speed of 200mm/s. Electrogram timing, duration and peak-to-peak voltage were measured manually and the locations of fractionated, late and very late potentials were registered on the electroanatomic surface. Pace-maps were physically searched and matched for at least 11/12 lead matches in the surface ECG QRS morphology. If the morphology matched a spontaneous or inducible VT, it was considered as a VT channel; otherwise it was classified as non-VT channel. The S-QRS interval was measured manually to the onset of QRS in the ECG lead with the shortest S-QRS [282]. A channel was fashioned from an orthodromically-activated sequence of identical pace maps, including a minimum of two pace maps, with at least one pace map having a S-QRS ≥40ms [288]. So as not to overestimate the channel

length, the shortest endocardial distance, joining at least 60% of the pertinent pace maps, was used (Figure 2.2). This distance was determined using the incorporated software and was recorded as channel length. The remainder of the pace maps, if any extending beyond 1 cm of the main length, were considered as joint annexes to the channel. In stable VT, a channel was constructed connecting entrainment locations reasoned from isthmus sites in an orthodromic order of S-QRS latencies [223]. Conduction time and conduction velocity in the channel were ascertained as the difference between the longest and shortest S-QRS interval and the ratio of channel length to conduction time, respectively.

A pace-map location with multiple QRS morphologies was considered as a shared segment if remote pace-map locations with QRS morphologies corresponding to the index pace-map existed. Further, if two channels were perceived to cross each other on the anatomic surface, they were considered having a shared endocardial segment. As activation can exit in either direction of a channel with different QRS morphology, this may erroneously classify segments of VT channels as non-VT channels. To reduce such possibility, the electroanatomic properties of isolated non-VT channels which did not have any shared pace maps or shared anatomic segments with VT channels (referred to as unshared non-VT channels) were separately compared with VT channels.

Small confluent areas (≥2 sampled points) of relatively preserved voltage (>0.5mV) surrounded by dense scar were referred to as islets and their relationship with channels was determined [250]. Fractionated and late potentials were considered related to a channel location if they were sited within 1cm of the channel and their joint annexes.

### 2.2.5 FOLLOW-UP

All patients had or received ICDs and were monitored clinically at 3 monthly follow-ups with device interrogation. Recurrence was defined as the occurrence of sustained VT or appropriate ICD therapies.

### 2.2.6 STATISTICAL ANALYSIS

Baseline parameters are presented as mean ± standard deviation (SD) for continuous variables, proportion for categorical variables, and median with interquartile range (IQR) for count variables. To account for intrapatient clustering of data and interpatient differences, linear and non-linear mixed-effects models, clustered by patient identity (random effect), were used to examine the effect of channel type (fixed effect) on each of the outcomes. As several S-QRS intervals were recorded for each channel, to account for clustering within a channel, channel count within patient was also included as a random effect in the model comparing SQRS interval values between channel types. Linear, logistic and negative binomial mixed-effects models were used to explore the continuous, dichotomous and count outcomes, respectively. The results estimated from models are presented as mean ± standard error of mean (SEM) for continuous outcomes, proportions with their 95% confidence interval (95% CI) for dichotomous outcomes and mean with 95% CI for count outcomes. The S-QRS intervals of pace maps were ranked and $95^{th}$ percentile values were reported for each channel group. The sensitivity and specificity of abnormal electrogram properties compared to VT channel location were computed. Moreover, the measure of agreement between VT channel locations and abnormal electrogram distribution in the scar was evaluated by Cohen's kappa ($\kappa$) test, with values of $\kappa>0.4$ indicating agreement. All calculations were performed using SAS 9.3 (SAS Institute Inc., Cary, NC, USA). A value of $p<0.05$ was considered statistically significant.

## 2.3 RESULTS

### 2.3.1 BASELINE CLINICAL CHARACTERISTICS

The baseline characteristics of the twenty-two patients are presented in Table 2.1. Fifteen patients had frequent monomorphic VT, while seven had a history of VT storm. None of the patients required circulatory support. All patients had previous myocardial infarction (mean time to first infarct 14±10years) and eleven had coronary bypass surgery (10 remote, 1 recent within 30 days). All patients had undergone a recent non-invasive evaluation or coronary angiography to exclude active ischemia.

### 2.3.2 INDUCIBLE VENTRICULAR TACHYCARDIA

Programmed ventricular stimulation was performed on average 3.0±2.5 times during the study. All patients had one or more inducible, or spontaneous sustained monomorphic VT at baseline. Most patients had additional VTs induced during the course of study. Overall 73 different VTs were inducible, a mean of 3.3±1.6 VTs per patient, with a mean cycle length of 396±110ms. Twenty-six (36%) VTs in 11 patients were hemodynamically stable.

### 2.3.3 LEFT VENTRICULAR ENDOCARDIAL VOLTAGE MAPPING

A mean number of 760±205 sampling points were taken per patient with 431±137 points within dense scar. Of the total left ventricular area (324±69cm$^2$), 60±15% (204±73cm$^2$) had low voltage, and 37±11% (128±56cm$^2$) was formed by dense scar. Islets of relatively preserved voltages [median 3, IQR 1 to 4 per patient, mean voltage 1.2±1 mV] were identified within dense scar in 20 of the 22 patients.

### 2.3.4 MAPPING OF CHANNELS

#### A. PACE MAPPING

Pace mapping was performed in low voltage zones at 2507 sites, 114±62 per patient. Capture was absent at 670 sites (27%), 30±24 per patient. Of the captured sites, 1076 sites (median 38, IQR 19 to 61 per patient) had S-QRS interval ≥40ms that led to the construction of channels. Figure 2.3 illustrates the pace map series for an inducible VT. The distribution of pace maps among various channel types is given in Table 2.2 and Figure 2.4. Overall, 428 pace maps corresponded to 57 inducible VTs that formed the VT channel group while 838 pace maps belonged to the non-VT channel group. Matching pace maps to 16 inducible VTs could not be found. Despite relatively uniform pace mapping density in the scar, the mean pace map count was higher in the VT channels [7 (95% CI 5.4 to 10.2)] compared to the non-VT channel group [4 (95% CI 3.1 to 5.0), p=0.0001]. Pace maps with S-QRS interval ≥40ms [mean 6 (95% CI 4.4 to 8.4)] and ≥80ms [mean 1 (95% CI 0.7 to 2.7)] were more frequent in VT channels compared to non-VT channels [4 (95% CI 2.7 to 4.5) and 0.5 (95% CI 0.3 to 1.0) respectively, p<0.001]. These differences achieved greater significance when comparison was restricted to the unshared non-VT channels. Beat-to-beat variations in the S-QRS intervals were occasionally observed as varying degrees of exit block at paced sites with long latencies in the VT channel group (Figure 2.5).

#### B. ENTRAINMENT MAPPING

Entrainment mapping was feasible in 11 patients who had at least one potentially mappable VT. Overall, at the entrainment locations, diastolic potentials covering 52±22% of tachycardia cycle length could be identified within the PentaRay™ mapping catheter area. The participation of these diastolic potentials in the tachycardia circuit was demonstrated and isthmus locations could be confirmed in 6VTs (Figure 2.6).

### C. VT CHANNELS

The comparison between electroanatomic properties of VT channels, non-VT channels and unshared non-VT channels are presented in Table 2.3. Fifty-seven VT channels (3±1 per patient) were identified. Fifty-four VTs could be mapped in the LV, while 3 had matching pace maps in the RV. The majority (97%) of these channels resided in the dense scar, with 48% of channels having segments extending into the borderzone. The majority of the low-voltage area had voltages between 0.1 and 0.5mV and so altering the voltage to this range did not identify VT channels. Preserved voltage channels created by lowering the borderzone to 0.1-0.3 mV identified 33 voltage channels, of which 18 (55%) had lengths of mapped VT circuits. Conversely, 51% of mapped VT channels were within these voltage channels. Islets of relatively preserved voltages were identified in the close proximity to 40% of VT channels. Twenty VT channels (35%) had shared pace map locations (4 channels) or shared anatomic segments (16 channels) with at least one another VT channel. The odds of finding a longest S-QRS interval of >80ms were 5.9 times greater in a VT channel relative to an unshared non-VT channel (95% CI 2.6 to 13.6, p<0.0001). The joint annexes to the VT channels, identified in 24 VT channel regions, extended a mean of 18±7mm beyond the main length of the channel.

### D. NON-VT CHANNELS

All non-VT channels were mapped in the LV. Overall, 183 non-VT channels (8±6 channels per patient) were identified, with an average of 4.6 (95% CI 2 to 7) non-VT channels in a patient per VT channel. This included 33 non-VT channels (1±2 channels per patient) that shared pace maps (9 channels) or had shared anatomic segments with a VT channel (24 channels). The remaining 150 non-VT channels (7±5 channels per patient) belonged to the unshared non-VT channel group. The mapped VT and non-VT channels in a case example are illustrated in Figure 2.7.

Unlike VT channels, unshared non-VT channels had a wider distribution with 18% found in the borderzone voltage regions (p=0.02). Most of these channels (112/150,

75%) were located beyond 1cm of the VT channel regions. Islets of preserved voltages were identified in close proximity to a smaller proportion of unshared non-VT channels compared to VT channels (40% vs. 15%, p <0.001). Compared to the VT channels, the longest S-QRS interval (p<0.0001) and conduction time (p<0.0001) were shorter, the mapped channel length was shorter (p=0.0003) and conduction velocity (p=0.0008) was faster in unshared non-VT channels. Any S-QRS interval in an unshared non-VT channel was on an average 10ms shorter than in a VT channel (95% CI -18 to -2, p=0.018). The joint annexes to the unshared non-VT channels, identified in 18 channel regions, extended 18±7mm beyond the main length of the channel.

### 2.3.5 Relationship of Channels and Scar Related Electrograms

Abnormal electrograms were frequently identified in low-voltage zones in these patients (Table 2.4). On an average, of all sampled data points, fractionated, late and very late potentials were present at 16±11%, 1.5±0.9% and 0.6±0.8% of sites, respectively. However, of all the fractionated (mean 130±105), late (mean 10±5) and very-late (mean 4±3) potentials, only 21%, 26% and 29%, respectively were recorded in the VT channels. These electrograms had poor sensitivity but high specificity for locating a VT channel; fractionated potential 44% and 86%, late potential 4% and 99%, very late potential 2% and 99%, respectively. There was relatively poor agreement between abnormal electrogram site and a channel location (fractionated potential κ=0.2, late potential κ=0.05 and very late potential κ=0.03). Importantly, however, compared to elsewhere within the scar, VT channels demonstrated longer fractionated potentials (105±2ms vs 95±2ms,p<0.0001), and poorly coupled very late potentials (311±31ms vs 226±23ms, p=0.030), but there was no difference in the coupling intervals of late potentials (p=0.82).

### 2.3.6 Ablation Outcomes

Complete procedural success was achieved in 14 (64%) patients and partial success in 7 (32%) patients. Among those with complete success, three patients with seven VTs had four VTs that could not be successfully mapped but were still eliminated by catheter ablation. Of 8 patients with a partially successful or a failed procedure, five patients including the one failed ablation had VT channels mapped in the basal postero-lateral scar while two had septal circuits. One patient had apical inferior VT channel that could not be ablated. Only four patients continued anti-arrhythmic medications post procedure. Over long-term follow-up of 16±6 months, three patients died of heart failure, and five (23%) had recurrence of VT. Of those with VT recurrence, two patients had had a completely successful and three patients a partially successful first procedure.

#### Inducible Ventricular Tachycardia During Repeat Procedures

Four patients underwent repeat catheter ablation a median of 2 months following the first ablation. During repeat procedures, there were eleven inducible VTs (3±2 VTs per patient), of which eight were completely new, two matched a previous VT, and one matched a previous shared non-VT channel morphology. None of the new VTs during repeat procedures matched a previous unshared non-VT channel morphology.

## 2.4 Discussion

### 2.4.1 Major findings of the study

This study used a high density of sampling and rigorous pace mapping with small bipoles to characterize the ventricular scar. It showed significant differences in the

electroanatomic properties between VT supporting and non-VT channels in patients with ICM and monomorphic VT. Compared with non-VT channels, VT channels were:

1) more commonly located within dense scar;

2) longer in length;

3) had slower conduction velocity with longer conduction times; and

4) more commonly co-located with islets of relatively preserved voltages.

In addition, abnormal electrograms were abundant in the scar but only a small proportion were located in the region of VT channels. Electrograms at these sites displayed a longer duration of fractionation and poorer coupling of very late potentials relative to elsewhere in the scar. These observations may in part explain the difference in propensity of only few surviving myocyte channels in the scar to support reentrant VT.

### 2.4.2 PREVIOUS STUDIES

---

The broad focus of a large body of clinical research in scar related reentry has been on channels supporting VT with a relatively limited representation of the properties of the non-VT channels. Earlier experimental studies have shown that bundles of viable myocytes interwoven with strands of fibrous tissue form preferential conduction channels with slow conduction velocity around 0.25m/s [381, 382]. These channels can be identified during sinus rhythm by endocardial voltage mapping [297] or by mapping of scar areas with pacing [290]. Stimulus-QRS latency ≥40ms during pacing in sinus rhythm is a well-recognized measure of slow conduction and reflects capture in protected zones before breakthrough into larger myocardium. Such slow conducting zones, particularly with latency >80ms, irrespective of the resulting QRS morphology are considered as good markers of locations adjacent to putative isthmuses of clinical VT [288, 289, 297]. Clinical studies involving mapping during hemodynamically stable VT in patients with prior MI report average isthmus lengths of approximately 30 mm [236, 261], with 90% of isthmuses found in the scar, while entrance and exits sites are found in borderzone or normal myocardium [261]. Arenal

et al. identified channels by adjusting voltages within the apparently dense scar (from 0.5 to 0.1 mV), and reported an average channel length of 23±11mm and width of 9±3mm [297]. These corridors of relatively preserved voltages in the dense scar express long paced S-QRS latencies and have been postulated to harbor critical components of VT circuits and their ablation suppresses inducibility of the VT [297, 298].

In this study, we relied largely on pace mapping within the dense scar to track preferential propagation corridors Altering the voltage range to 0.1-0.5mV did not identify VT channels as the majority of the low-voltage area had voltage within this range. The differences in the estimated length (53±5 mm) of VT conducting channels in our study, compared to previous studies, reflect the methodological differences. The longer channel lengths than reported in previous studies are likely due to the higher resolution of scar mapping with up to 10 pacing sites per channel, from a small, closely spaced bipole, enabling identification of the channel course in great detail. However, given that the channels may traverse the scar in a zigzag course, the channel lengths estimated from an orthodromic sequence of high density pace maps would still best reflect only an apparent length [175, 383].

Channels which support VT were found to have distinctive anatomic and electrophysiological properties. These include longer lengths with slower conduction providing the conditions conducive for supporting electrical macroreentry [384]. The differences in the density and orientation of surviving myocytes, introduction of extracellular matrix and fibrous tissue as well as variation in the cellular conductance result in regions of high axial impedance where there is prolonged conduction or block and the activation wavefront follows zigzag patterns [175]. Such regions of highly non-uniform structural framework have been shown to harbor conduction pathways that support reentrant electrical activation [94, 148].

In the present study, the identified non-VT channels outnumbered the VT channels and were widely distributed in the endocardial scar with three-quarters of the non-VT channels in the regions remote to the VT channels. This is in accordance with the widespread inhomogeneous scarring with varying degrees of preservation of

subendocardial myocytes in ICM patients [235, 381]. Interestingly, only a small proportion of the non-VT channels shared segments with the VT channels, and some of these may be exits from the other end of the VT channel [282]. These results may indicate that only certain regions of the ventricular scar develop the necessary properties that are required to sustain reentry.

### 2.4.3 SCAR RELATED ELECTROGRAMS AND VT CHANNELS

The abnormal electrograms observed in sinus rhythm from these surviving myocytes in the scar serve as indirect evidence for the channels with each peak in a multi-deflection bipolar electrogram representing individual myocyte bundle conduction [175, 299, 385]. There are data that suggest that such electrograms are frequently identified at sites where catheter ablation does not terminate VT [304, 305]. Conversely, only 50% of central, proximal or exit sites of reentry isthmuses have abnormal electrograms [306]. The present study confirms these results, that while abnormal electrograms were prevalent within ventricular scar, only a small proportion was related to VT supporting channels. In fact, the majority of abnormal electrograms were unrelated to any channel at all. In the regions of VT supporting channels, compared to elsewhere within the scar, these electrograms were prolonged with poorly coupled potentials, indicating heterogeneity in the ultrastructural properties of the scar tissue.

### 2.4.4 ISLETS OF PRESERVED VOLTAGES AND VT CHANNELS

Previous studies have stressed upon borderzone voltage regions as targets for catheter ablation of VT [237, 240, 263, 296]. The borderzone is not only at the periphery of the dense scar, but it is located at any of the interfaces between the surviving myocardial tissue and dense scar. The voltage threshold of 1.5mV is very specific, but

has limited sensitivity in a low density map, and often fails to detect fine insulated bundles of surviving myocytes within the scar [375, 386]. High density mapping permits identification of some of these surviving tissues as small confluent islets of relatively preserved voltages in an otherwise dense scar. Nakahara et al. reported that 57% of the very late potentials were co-located with these islets and their peripheries, and these were commonly associated with putative isthmus sites [250]. These islets may not necessarily participate in VT circuits; however, they may be markers of proximity to surviving myofibers that have role in perpetuation of VT. In the present study, such islets were nested around the regions of 40% of VT channels and are therefore potential targets for the elimination of VT.

### 2.4.5 Clinical Implications

The contemporary substrate based ablation practices have evolved from linear anchoring ablation [240], short lines [263], to spot ablation targeting areas of long paced-latencies [282], or abnormal scar related electrograms [17, 18]. However, finding and ablating these regions in the expanse of large heterogeneous scar can be time consuming. This and other studies [250, 301] have used multi-electrode catheters enabling rapid collection of ventricular scar related electrograms. There is also interest in a more targeted substrate ablation strategy and identifying regions within the scar important to the development of VT. This study is the first comprehensive report on the differential electroanatomic features of VT supporting and non-VT channels within the scar, and may provide the basis for the development of a more focused substrate ablation. Further analyses are needed to evidently differentiate information in the sinus rhythm electrograms populating VT channels from elsewhere in the scar that may allow ablation of VT during sinus rhythm without extensive pace mapping or mapping during VT.

### 2.4.6 STUDY LIMITATIONS

Most of the VTs were poorly tolerated precluding entrainment mapping and thus, localization of the VT channels relied heavily on paced latencies. Nevertheless, pace mapping is widely considered the best surrogate to locate surviving myocyte channels [282], and ultra high density pace mapping with rigorous matching criteria as was applied in our study reduces this issue. Additionally, as the method for identification of the two groups of channels was identical, the comparisons remain valid. Due to limited feasibility of entrainment mapping, the influence of blind-loop bystander segments could not be adequately resolved. Pace mapping was performed at cycle lengths longer than the VT as rapid pacing is likely to induce VT. Despite pace mapping at slower rates, which can reduce the likelihood of lines of functional block, pace map locations matching one of the induced VT morphology were identified in most patients, signifying functional latencies likely had a limited influence on the QRS morphology in the majority of VTs. Epicardial mapping was not done as all these patients had an ischemic substrate and subendocardial scar, many with previous bypass surgery. It is likely that a proportion of VT and non-VT channels could have had intramural or epicardial circuits. We performed high density pacing from small closely spaced bipoles in preference to unipolar pacing. This design can favorably reduce the influence of anodal capture and capture away from the pacing electrodes [291-293]. The significantly low rate (6%) of non-captured pace maps in the infarct zone reported with unipolar pacing [282], compared to our study, upholds this proposition. Frequent use of antiarrhythmic drugs before ablation can suppress some VT during the procedure. The affect of antiarrhythmic drugs on conduction delays during sinus rhythm was inevitable but regional differences in the scar were still demonstrable. Activation wavefront relation to the direction of orientation of myofibres and fibrous matrix can alter lay out of regions of slow conduction and impulse detouring. This can influence the formation of extracellular electrograms. We did not compare abnormal scar related electrograms during sinus rhythm and RV pacing that could have influenced the morphology and delay in recording of late potentials [297]. Nevertheless, regional differences in electrogram properties would

persist. Ablation was targeted with aim of eliminating scar related electrograms at sites of long paced latencies and the impact of differential ablation of non-VT channels on acute and long-term outcomes was not in the scope of this study. Larger studies with long follow-up are needed to determine if some non-VT channels mature to sustain VT.

### 2.4.7 CONCLUSION

---

High-density mapping in the ventricular scar enables characterization of VT supporting and non-VT channels. Channels supporting VT possess distinctive anatomic and electrophysiological properties that potentially predispose them to perpetuate reentrant VT. Abnormal electrograms are abundant in post-infarction ventricular scar, however the contribution by scar regions harboring clinical VT channels is small. These findings may provide a basis for more limited substrate ablation strategies.

## TABLES

| Table 2.1 | Baseline Characteristics |
|---|---|
| **N** | 22 |
| **Age, years** | 67±10 |
| **Male, n (%)** | 21 (95) |
| **Ejection fraction, %** | 32±8 |
| **Time to first infarction, years** | 14±10 |
| **Coronary bypass surgery, n (%)** | 11 (50) |
| **Rhythm, n (%)** | |
| **Sinus rhythm** | 18 (82) |
| **Atrial fibrillation** | 1 (4) |
| **Ventricular paced rhythm** | 3 (14) |
| **QRS duration, ms** | 143±37 |
| **VT cycle length, ms** | 384±116 |
| **VT storm, n (%)** | 7 (32) |
| **Previous ICD, n (%)** | 19 (86) |
| **Beta blocker, n (%)** | 20 (91) |
| **Amiodarone, n (%)** | 13 (59) |
| **Other antiarrhythmic drugs (Sotalol, Mexilitene), n (%)** | 8 (36) |

VT=Ventricular Tachycardia, ICD=Implantable Cardioverter Defibrillator
Data presented as x±y format represent mean±SD

**Table 2.2** Distribution of pace-maps among VT and Non-VT channels

| Property | VT channels | Non-VT channels | p-value* | Unshared Non-VT channels | p-value* |
|---|---|---|---|---|---|
| **Pace map count** | 428 | 838 | | 613 | |
| **Number per channel** | 7 (5.4,10.2) | 4 (3.1,5.0) | 0.0001 | 4 (2.8,4.5) | <0.0001 |
| **Pace maps with S-QRS ≥ 40ms (%)** | 360 (84) | 774 (92) | | 562 (92) | |
| **Number per channel** | 6 (4.4,8.4) | 4 (2.7,4.5) | 0.0008 | 3 (2.4,4.0) | 0.0001 |
| **Pace maps with S-QRS ≥ 80ms (%)** | 123 (29) | 191 (23) | | 138 (23) | |
| **Number per channel** | 1 (0.7,2.7) | 0.5 (0.3,1.0) | 0.0004 | 0.4 (0.2,0.8) | <0.0001 |

VT= ventricular tachycardia, S-QRS = Stimulus-QRS interval

* versus VT channels

Data presented as x(y,z) format represent mean count (95%CI)

**Table 2.3** **Comparison of Electroanatomic Properties of VT and Non-VT channels**

| Property | VT channels | Non-VT channels | p-value* | Unshared Non-VT channels | p-value* |
|---|---|---|---|---|---|
| **Total number** | 57 | 183 | | 150 | |
| **Number per patient** | 3±1 | 8±6 | <0.001 | 7±5 | <0.001 |
| **Location in Scar, %** | 97 (84,99) | 85 (69,90) | 0.064 | 82 (62,90) | 0.036 |
| **Longest S-QRS, ms** | 130±12 | 85±12 | <0.0001 | 82±12 | <0.0001 |
| **95$^{th}$ percentile value** | 360 | 136 | | 134 | |
| **Any S-QRS, ms** | 73±4 | 63±3 | 0.020 | 63±3 | 0.018 |
| **95$^{th}$ percentile value** | 161 | 108 | | 108 | |
| **Length, mm** | 53±5 | 34±4 | 0.0004 | 33±4 | 0.0003 |
| **Conduction time, ms** | 103±14 | 47±13 | <0.0001 | 43±13 | <0.0001 |
| **Conduction velocity, m/s** | 0.87±0.23 | 1.30±0.21 | 0.022 | 1.39±0.21 | 0.008 |

VT= ventricular tachycardia, S-QRS = Stimulus-QRS interval

*versus VT channels

Data presented as x(y,z) format represent mean proportion (95%CI)

Data presented as x±y format represent mean±SEM, except channel number per patient which is mean±SD

| Table 2.4 | Comparison of Scar Related Electrograms in Channel Regions Versus Rest of Scar | | | | |
|---|---|---|---|---|---|
| **Electrogram type** | | **Electrogram location** | | | |
| | | **VT channels** | **Non-VT channels** | **Rest of Scar** | **p value** |
| **Fractionated potential** | **Total Number (%)** | 607 (21) | 761(27) | 1462 (52) | |
| | **Number Per Channel** | 15 (10.1,22.8) | 16 (13.5,19.3) | | 0.79 |
| | **Duration, ms** | 105±2 | 101±2 | 95±2 | <0.0001* |
| | **Amplitude, mV** | 0.2±0.01 | 0.2±0.01 | 0.2±0.01 | 0.63 |
| **Late potential** | **Total Number (%)** | 59 (26) | 68 (30) | 101(44) | |
| | **Number Per Channel** | 1.3 (0.8,2.1) | 0.9 (0.6,1.2) | | 0.19 |
| | **Coupling interval, ms** | 43±5 | 45±5 | 42±3 | 0.82 |
| **Very late potential** | **Total Number (%)** | 26 (29) | 7(8) | 58 (63) | |
| | **Number Per Channel** | 0.3 (0.2,0.8) | 0.1 (0.04,0.25) | | 0.008 |
| | **Coupling interval, ms** | 311±31 | 250±59 | 226±23 | 0.030† |

VT= ventricular tachycardia

*p=0.004 VT channels versus Non-VT channels, p<0.0001 VT channels versus Rest of scar, p<0.0001 Non-VT channels vs Rest of scar

†p=0.34 VT channels versus Non-VT channels, p=0.0085 VT channels versus Rest of scar, p=0.70 Non-VT channels vs Rest of scar

Data presented as x(y,z) format represent mean count (95%CI)

Data presented as x±y format represent mean±SEM

## FIGURES

### *FIGURE 2.1*

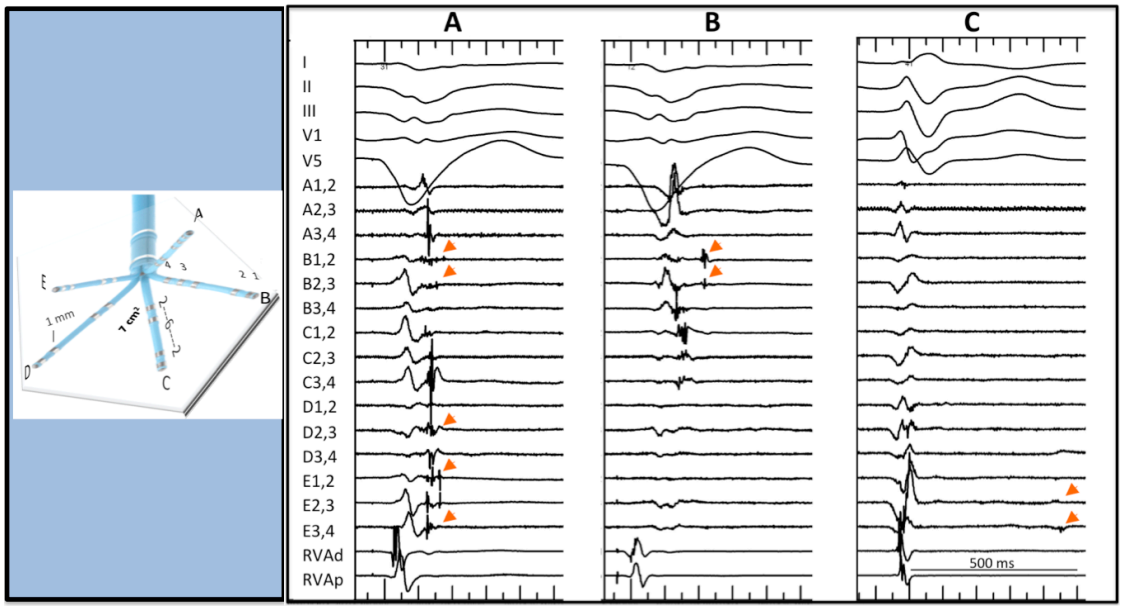


Figure 2.1. Left panel. PentaRay™ mapping catheter deploys twenty 1mm electrodes delivering high-resolution contact mapping covering 7cm$^2$ area. Right panel. Examples of scar related abnormal electrograms. Fractionated (A), late (B) and very late (C) potentials are marked with arrows. Channels from top to bottom are surface ECG (I, II, III, V1, V5), PentaRay™ mapping catheter in left ventricular scar, and right ventricular apical catheter (RVA, d=distal, p=proximal).

***FIGURE 2.2***

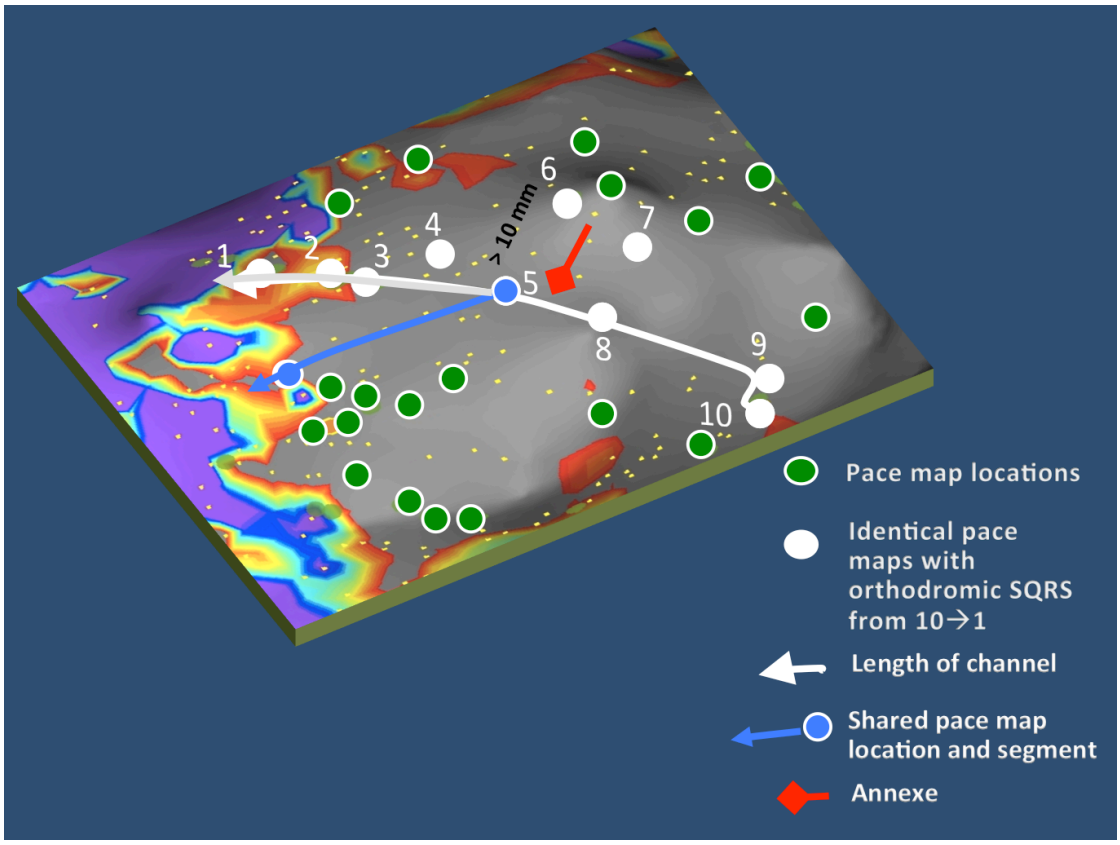


Figure 2.2. Schematic for definitions used in the study. Green circles represent the full set of pace maps performed in dense scar (grey) and borderzone. Pace maps with matching (≥11/12 leads) surface ECG QRS morphology (solid white circles, 1 to 10) are connected in an orthodromic order of S-QRS latency [longest S-QRS(10) to shortest S-QRS(1)] linking at least 6 (60%) identical pace maps in a minimal endocardial pathway (white arrow). This was considered as the length of the channel. The remaining pace maps (6 &7) extending greater than 10mm across channel were considered as joined annexes (red arrow) to the channel. Pace map location with multiple exiting QRS morphology was considered as shared (blue circle, 5) if remote pace maps matching the index QRS morphologies were present.

***FIGURE 2.3***

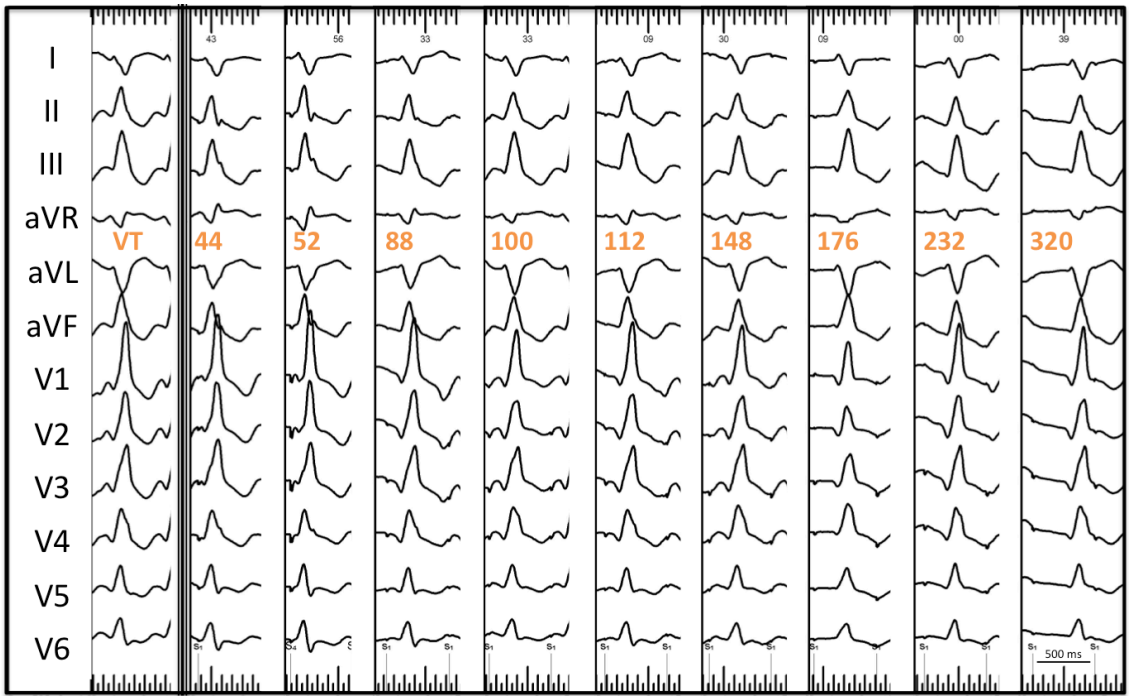


Figure 2.3. Pace map series for an inducible VT. The left panel shows 12-lead ECG QRS morphology of a VT. The right panel shows the set of pace maps with marked stimulus-QRS intervals of ≥40ms in an orthodromic sequence and matching QRS morphology (≥11/12 ECG leads) to the VT. These pace-map sites were joined along a minimal endocardial path to construct the VT channel on the electroanatomic surface.

***FIGURE 2.4***

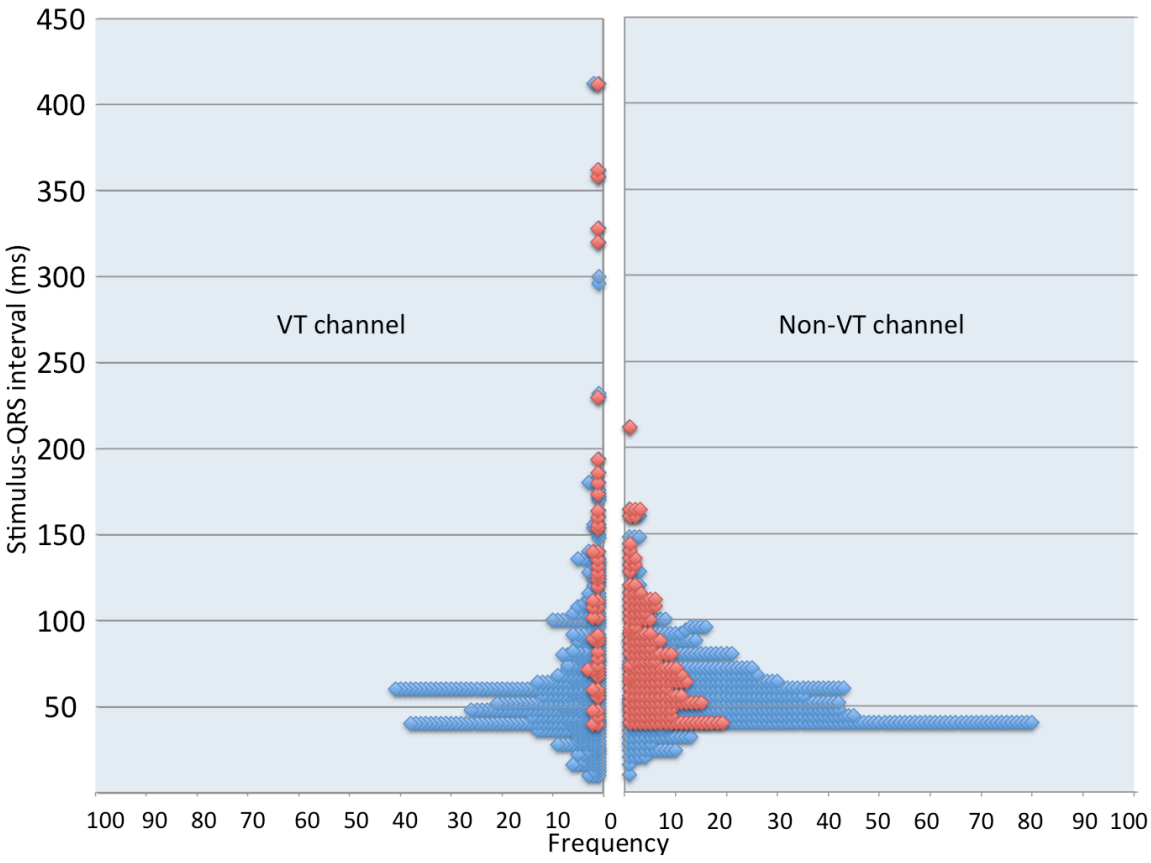


Figure 2.4. Frequency distribution plots of pooled S-QRS interval data for VT and unshared non-VT channels. The blue squares represent all S-QRS intervals in the respective groups of channels. The red squares represent the longest S-QRS interval in individual channels in each group. There is relative tall distribution of the S-QRS intervals in VT channels compared to unshared non-VT channels.

***FIGURE 2.5***

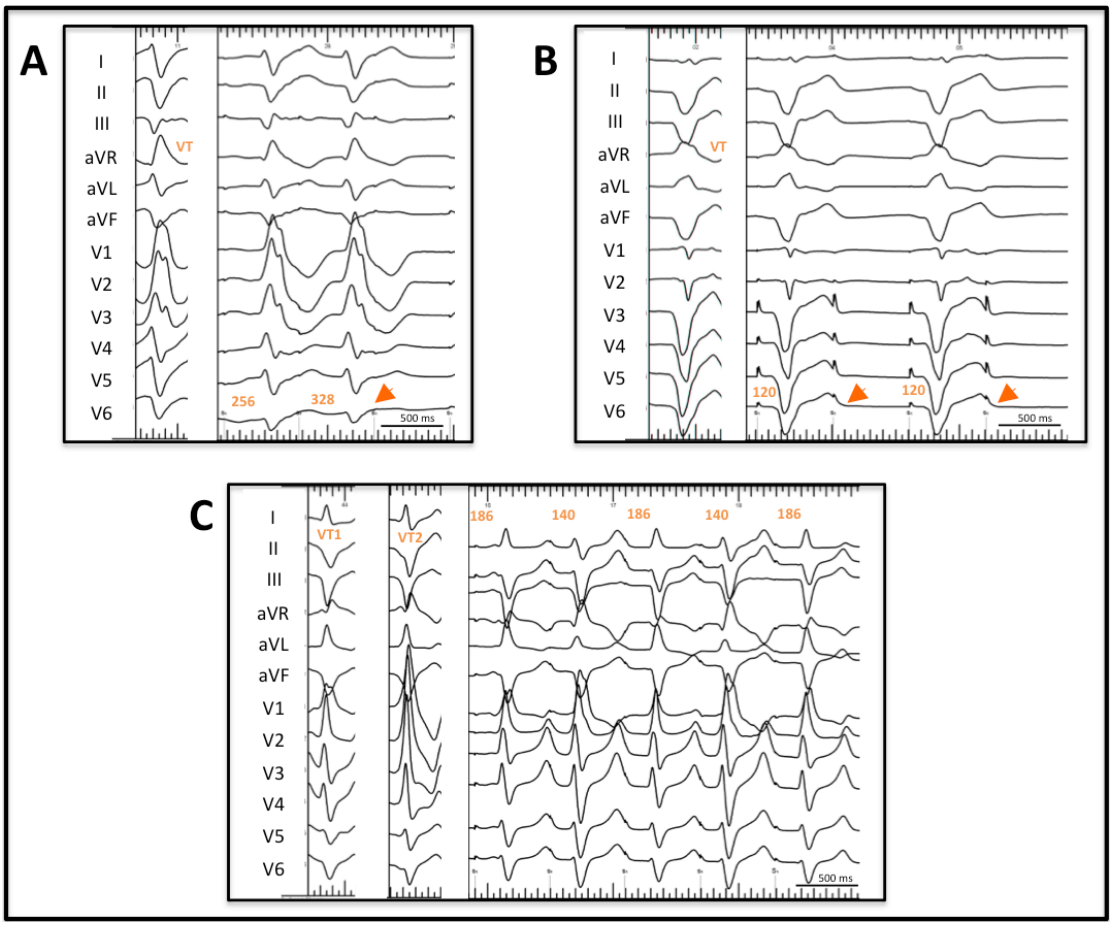


Figure 2.5. Pace map responses. (A) 3:2 Wenckebach type exit block from a pacing site with increasingly long S-QRS intervals (marked) and paced QRS morphology matching VT. Arrow marks the blocked beat. (B) 2:1 exit block from pacing site with long S-QRS interval (marked) and paced QRS morphology matching VT. Arrows mark the blocked beats. (C) Alternating S-QRS interval (marked) and paced QRS morphology matching VT1 and VT2, qualifying as a shared pace map location between these VTs.

***FIGURE 2.6***

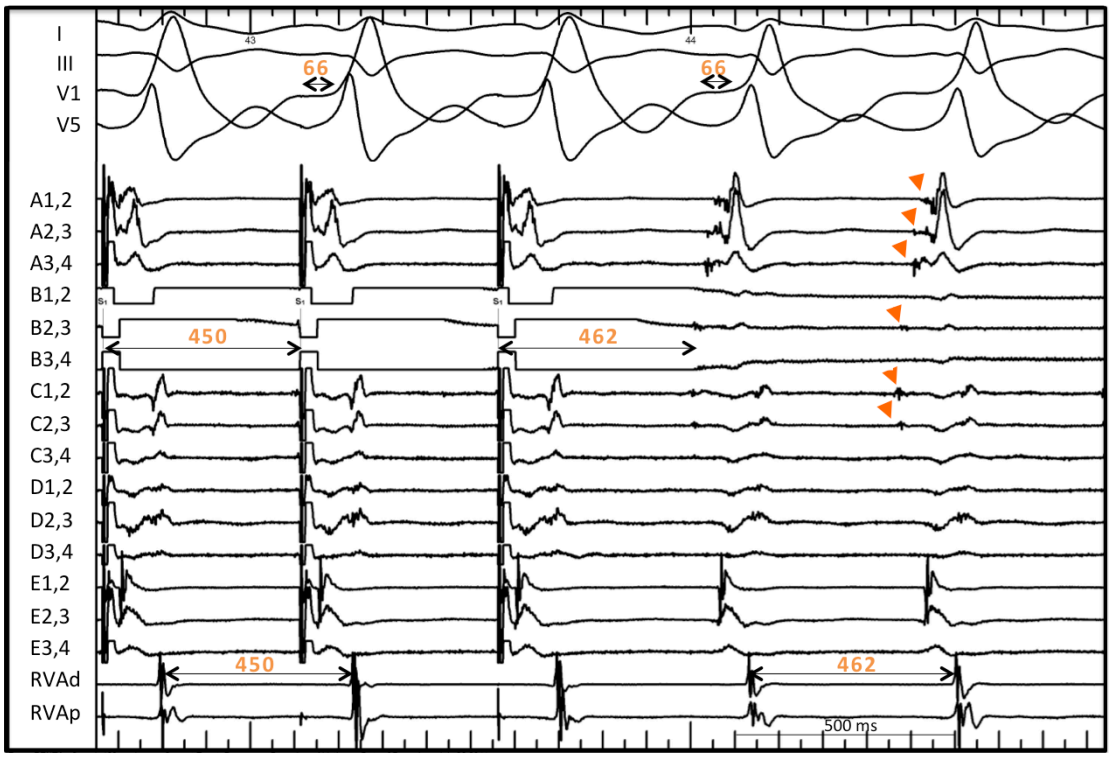


Figure 2.6. Entrainment pacing (channel B2,3) and its termination during a VT. Channels from top to bottom are surface ECG (I, III, V1, V5) , PentaRay™ mapping catheter in left ventricular scar region (A1,2 - E3,4), and right ventricular apex [RVA, distal (d) and proximal (p)]. Intervals are marked in milliseconds. This pacing site entrained the VT with concealed fusion with a S-QRS interval of <30% of the TCL, S-QRS matching the electrogram-QRS interval and the diference between post pacing interval and tachycardia cycle length is zero ms. The diastolic potentials seen on the PentaRay™ channels during tachycardia (arrows) covered 202 ms of the tachycardia cycle length. This site represented isthmus near its exit for this VT.

***FIGURE 2.7***

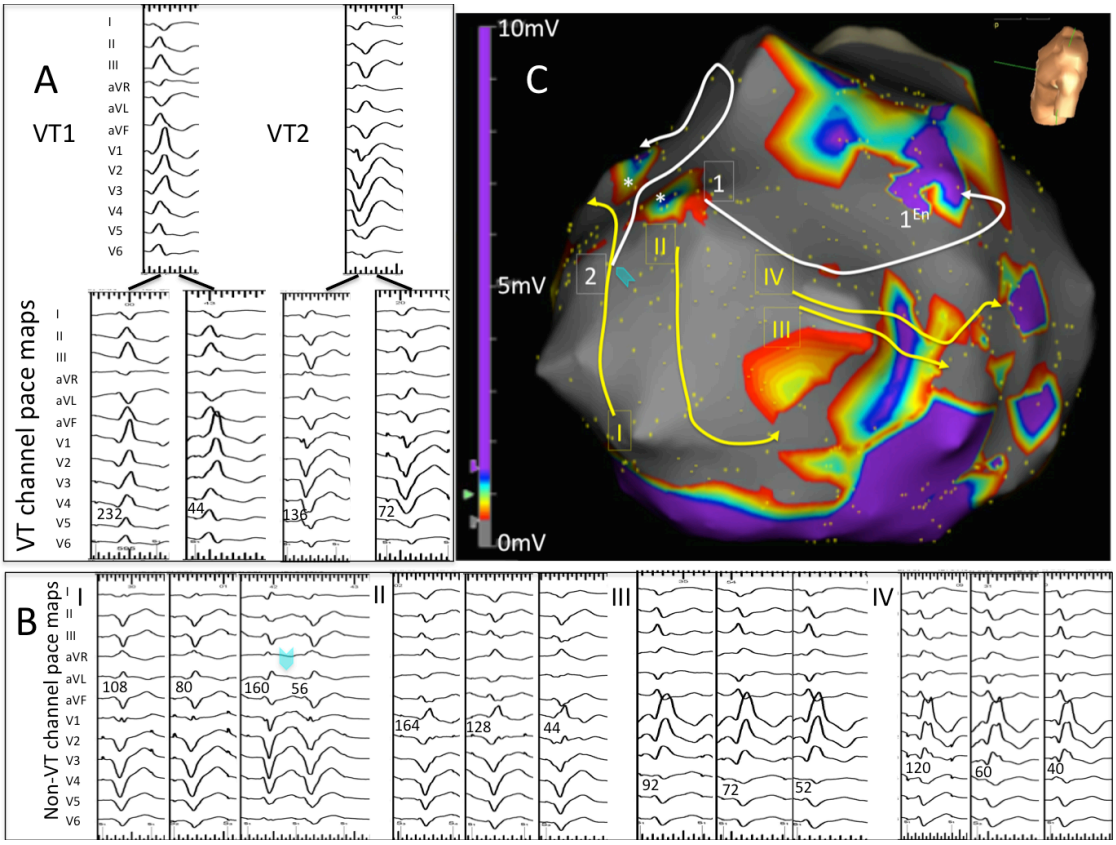


Figure 2.7. Case Example. This figure shows 12 lead ECGs of 2 VT morphologies (VT 1 & 2) and their matching pace map morphologies [Panel A], non-VT channel pace map morphologies (NVT I to IV) [Panel B] and an cranial left anterior oblique view of the associated electroanatomic voltage map [Panel C]. Intervals marked in millisecond in each of the pace maps are stimulus-QRS intervals. The full pace map series pertinent to VT-1 is shown in Figure 2. Four non-VT channels that had multiple matching pace map sites are illustrated in this figure. The 3$^{rd}$-pace map in the NVT-I series shows two exits (marked with arrowhead); the first exit matches VT-2 morphology and the second exit matches with other NVT-I pace maps. NVT-I channel was considered as a shared channel with VT-2. On the voltage map, channels mapped by pace mapping corresponding to VT-1 and VT-2 are displayed as white lines with numbered locations 1 and 2 corresponding to the longest S-QRS pace map location of the respective VTs. The isthmus exit site for VT-1 was confirmed by entrainment mapping, marked as 1$^{En}$. Islets of preserved voltages, marked with asterisks, are adjacent to VT-1 channel. Non-VT channels are displayed as yellow lines with

numbered locations (I to IV) corresponding to the longest S-QRS pace map location of the respective channels. The shared pace map site between NVT-I and VT-2 is marked with an arrowhead.

# CHAPTER 3. DEFINING ARRHYTHMOGENIC VENTRICULAR SCAR USING TIME- AND VOLTAGE-DOMAIN ANALYSIS: A NOVEL APPROACH TO VENTRICULAR TACHYCARDIA CHANNEL LOCALIZATION DURING SINUS RHYTHM

## ABSTRACT

**Background**. In the ventricular scar, the impulse spread is slow as its path is split in multiple zigzag channels of surviving muscle. We aimed to evaluate electrograms in the scar to determine their local delay in relation to onset of heartbeat (activation time) and inequality in voltage splitting (Shannon entropy), and thereby assist channel mapping. We reasoned that unlike short and multi-splitting innocent channels, ventricular tachycardia (VT) supporting channels have very slow impulse spread and possess low entropy due to their longer protected length and relative lack of splitting.

**Methods.** Patients with ischemic cardiomyopathy and multiple inducible VT were studied. In the training stage (16 patients, 58 VT), left ventricular endocardial mapping was performed in sinus rhythm with PentaRay™ catheter and NavX™ mapping system. Detailed pace mapping in the scar was used to identify VT channels. These sites were confirmed, when feasible, by entrainment mapping. The scar electrograms (≤1.5mV) were analyzed in time- and voltage-domains to determine mean activation time, dispersion in activation time and Shannon entropy. The predictive performances of these properties to detect VT channels were tested. In the application stage (6 patients, 17 VT), the novel electrogram properties were prospectively tested to guide catheter ablation of VT.

**Results.** Mean 763±203 sampling points were taken, 451±145 points in dense scar. From 1770 pacemaps, 174 channels were identified, 47 corresponded to inducible

VTs. Entrainment confirmed six of these VT channels. Scar electrograms with latest mean activation time and minimum entropy accurately recognized VT channels in a high activation dispersion region [kappa= 0.89 (95% confidence interval 0.84 to 0.94), sensitivity=86% (76 to 93), specificity=100% (99.8 to 100), positive predictive value=93% (84 to 98) and negative predictive value=100% (99 to 100). Finally, focused ablation within the prospective channel regions eliminated 15/17 inducible VTs.

**Conclusion.** Activation time and entropy mapping mapping of scar accurately identifies VT channels during sinus rhythm. This can expedite recognition of VT channels without pace mapping or mapping during VT and minimize extensive ablation within the scar.

## 3.1 INTRODUCTION

Scar related reentry is the most common mechanism of ventricular arrhythmias in post myocardial infarction patients [36]. Both the extent of scarring and complex assembly of surviving muscle channels makes the myocardium vulnerable to reentrant ventricular (VT) circuits [175, 235, 387]. Radiofrequency ablation is well established as an effective approach for the management of recurrent VT. Entrainment mapping is the foremost method for finding the channels that support VT. However, a number of limitations can significantly constrain its application in the laboratory [262, 277]. As an alternative, substrate based ablation strategies have developed and, in general, now advocate targeting all excitable abnormal electrograms within the scar [290, 301]. However, not all such electrograms reside in the VT supporting channels and, in fact, many are innocuous bystanders [304, 305]. Conversely, only 50% of central, proximal or exit sites of reentry circuits have abnormal electrograms [306]. Based on this, and the fact that substrate ablation can be time consuming in large regions of scar [301, 302], there has been considerable interest into the problem of electrical resolution within the scar [307, 309] and a more targeted substrate ablation approach.

In the ventricular scar, the impulse spread is slow as its path is split in multiple zigzag channels of surviving muscle. We aimed to evaluate electrograms in the scar to determine their local delay in relation to the onset of heartbeat (activation time) and inequality in voltage splitting (Shannon entropy), and thereby assist channel mapping. We reasoned that unlike short and multi-splitting innocent channels, ventricular tachycardia (VT) supporting channels have very slow impulse spread and possess low entropy due to their longer protected length but relative paucity of splitting.

## 3.2 METHODS

In the training stage of the study, patients with ischemic cardiomyopathy (ICM) and recurrent VT underwent conventional substrate characterization and VT channel localization, using a combination of detailed pace mapping. These sites were confirmed when feasible by entrainment mapping. The novel time- and voltage-domain properties of intracardiac scar electrograms were analyzed and correlated with the distribution of VT channels. In the application stage, the novel properties were tested prospectively to guide substrate ablation. The Human Research Ethics Committee of the Royal Adelaide Hospital and the University of Adelaide approved the study.

### 3.2.1 SUBSTRATE CHARACTERIZATION

#### A. PATIENT POPULATION

Sixteen consecutive patients with ICM with recurrent monomorphic VT or VT storm [≥3 episodes or implantable defibrillator (ICD) therapies in 24 hours] undergoing clinically indicated catheter ablation procedure were studied. These patients were common to the study presented Chapter 2. Patients with previous VT ablation, mixed intrinsic and paced (>10%) rhythm, acute coronary event within preceding 1 month, intracardiac thrombus, mechanical prosthetic valve and severe aorto-iliac peripheral vascular disease were excluded.

#### B. ELECTROPHYSIOLOGIC STUDY AND ABLATION

The procedure was done in post-absorptive state under conscious sedation. Briefly, a quadripolar catheter and decapolar catheter were positioned at the right ventricular (RV) apex and coronary sinus, respectively. Programmed ventricular stimulation was done from the RV apex at two drive cycle lengths (600ms and 400ms) with up to

three extrastimuli. All sustained monomorphic VTs induced at baseline, during the course of the study and post-ablation were considered as the clinical VTs.

*a) Substrate mapping*

A 20-pole catheter (PentaRay™, 2-6-2 mm interelectrode spacing, 1mm electrodes, Biosense Webster Inc, Diamond Bar, CA, USA) was introduced either retrogradely using standard sheaths or transeptally using the Agilis™ NxT steerable introducer (St Jude Medical Inc., St Paul, MN, USA) into the left ventricle (LV) for mapping. Activated clotting time was maintained with intravenous unfractionated heparin between 250-300s throughout the course of the study. After obtaining a left ventricular geometry on the electroanatomic mapping system (Ensite NavX™, St Jude Medical), endocardial contact mapping was performed in sinus or a ventricular paced rhythm. At each location, before electrogram acquisition, stability and adequate splaying of the PentaRay™ splines over the endocardium was confirmed fluoroscopically and ventricular ectopic beats were vigilantly excluded. Mapping was targeted as to have dense sampling in regions of low voltage and sufficient sampling elsewhere to have a fill threshold of 15mm. All points projecting > 10mm from geometry were considered of inadequate contact and were excluded. Additional sampling points were taken with the quadripolar ablation catheter in regions of difficult access with the PentaRay™ catheter. Standard definitions were used to describe preserved voltage (>1.5mV), borderzone voltage (0.5-1.5mV) and dense scar (<0.5mV) [240]. The areas of low voltage and dense scar were measured using the integrated software. Bipolar electrograms were filtered between 30 to 500 Hz, notch 50 Hz and presented at sweep speed of 100mm/s (LabSystem PRO v2.4a EP, Bard Inc., Lowell, MA, USA).

*b) VT channel localization*

At sites of low voltage and abnormal electrograms, bipolar pace mapping was performed at a cycle length of 600ms or 50ms faster than the intrinsic rate at a constant output (10mA, 2ms) [290], and pace-map locations were tagged on the

electroanatomic surface. Offline analysis of the digitally stored electrograms and pace maps was performed on the Bard EP system with the use of on-screen calipers at a sweep speed of 200mm/s. Pace-maps were physically searched and matched for at least 11/12-lead matches in the surface ECG QRS morphology. If the morphology matched to a spontaneous or inducible VT, it was classified as a VT channel. Stimulus-QRS (S-QRS) interval was measured manually to the onset of QRS in the ECG lead with the shortest S-QRS [282]. A channel was fashioned from an orthodromically-activated sequence of identical pace maps, including a minimum of two pace maps, with at least one pace map having a S-QRS ≥40ms [288]. So as not to overestimate the channel length, the shortest endocardial distance, joining at least 60% of the pertinent pace maps, was used.

Whenever feasible, entrainment pacing was attempted in the region of abnormal electrograms, to confirm pace map findings. Standard criteria were used to define VT isthmus sites by entrainment mapping [289].

*c) Electrogram analysis*

Electrograms were classified according to the conventional criteria [241, 300] as:
i) Normal (3 or fewer sharp intrinsic deflections from baseline, amplitude ≥3mV, duration <70ms, and/or amplitude: duration >0.046mV/ms),
ii) Fractionated (multiple intrinsic deflections, amplitude ≤0.5mV, duration ≥133ms, and/or amplitude: duration ≤0.005mV/ms),
iii) Late (any electrogram with a duration that extends beyond the end of surface QRS), and
iv) Very late potentials (isolated component ≥100ms after the end of surface QRS).

Any electrogram not fitting into one of these categories were classified as other abnormal electrograms. The locations of the fractionated, late, and very late potentials were registered on the electroanatomic surface. These electrograms were considered related to a VT channel if they resided within 1cm of the channel.

*d) Catheter ablation*

Catheter ablation was performed with 3.5mm tip irrigated ablation catheter (CoolFlex, St Jude Medical or Thermocool Biosense Webster) targeting regions with excitable scar related abnormal electrograms at sites with long S-QRS latencies. A formal programmed ventricular stimulation was repeated following catheter ablation to evaluate the procedural success. Complete success was defined as no inducible VT after ablation, partial success was defined as the abolition of the clinical VT with other VTs inducible, and the inability to eliminate the clinical VT was considered as failure.

**C. FOLLOW-UP**

All patients had or received a new ICD and were monitored clinically three monthly with device interrogation. Recurrence was defined as the occurrence of sustained VT or appropriate ICD therapies.

### 3.2.2 TIME- AND VOLTAGE-DOMAIN ANALYSIS OF ELECTROGRAMS

This approach is a variation of the method of Ciaccio et al [309] and is constructed on the fundamental principles described in the investigative studies by Kucera [176, 177]. We recently learnt that ventricular tachycardia (VT) supporting channels are have longer protected segments and slower conduction during sinus rhythm than channels that do not support VT [388]. Based on these, we propose that the electrical information pertinent to the framework of critical segments of VT channels is reflected in their "activation time" and "voltage distribution (entropy)" patterns during sinus rhythm. The following novel electrogram properties, therefore, are likely to underpin a VT supporting channel:

1. Late mean activation time,
2. High dispersion in activation times, and
3. Narrow voltage distribution (low Shannon entropy).

This is based on the following evidence:

### A. Late Mean Activation Time

The site of the latest activation is the most unperturbed site with greatest likelihood of adjacent altered conduction properties and maximum excitability [310]. This has been shown to be a most sensitive indicator to predict successful ablation sites [305]. Such sites may participate in the reentrant excitation or are in anatomic proximity to the location of functional conduction blocks that are critical for reentry [305, 310]. Figure 3.1 illustrates in a scar model the participation of site of late sinus activation in a potential VT circuit. The delay in activation can be the result of either a discontinuity of conduction (detouring) or slow conduction within the scar [148, 192].

The determination of a unique local activation time in multi-deflection electrograms containing a number of deflections is difficult. Such electrograms indicate that the electrical activity persists near the bipole for the duration of the electrogram. We therefore chose a careful approach for not ignoring individual electrogram deflections. Every deflection in the electrogram was assigned an activation time and the mean of the activation times was calculated according to the method of Ciaccio et al [309] (Figure 3.2). The mean activation times of all electrograms in the left ventricular map were ranked in a descending order to find the top five nodes of latest activation.

### B. High Dispersion in Activation Times

The deflections in a bipolar electrogram reflect the heterogeneity in the ultrastructural properties of the local cardiac scar tissue [148]. The differences in density and orientation of surviving myofibers, extracellular matrix, fibrous tissue and variations in the cellular conductance between adjacent regions, result in regions with impedance mismatches. This produces zigzag patterns of activation propagation in high axial impedance [192]. If a high impedance region in the scar

boundaries with regions of low impedance, the activation wavefront has a window to exit and interact with the larger excitable myocardium. Such regions are likely to harbor conduction pathways that support reentrant electrical activation.

We quantified variable impedance in a region by dispersion in activation time, calculated as the standard deviation of activation times of individual deflections in each electrogram [309]. This was weighted as Z score in the map. After a filling linear interpolation, all regions ($\geq 1$ cm$^2$) with high dispersion in activation (Z score $\geq +1.5$) and their low dispersion interfaces (Z score $\leq -0.5$) were identified.

### C. Low Shannon Entropy

The branching tissue architecture of the post-infarct ventricular scar consists of a complex lattice of surviving muscle strands interwoven with layers of connective tissue fibrosis. Broadly, these muscle strands may be considered as belonging to two groups distinguished by relative differences in current-load relationships and safety of propagation (Figure 3.3). The first group may be strands with extensive open or dead-end branching (branched channel segments) with repetitive current to load mismatches and slowing of conduction [176, 177]. This may place the main strand vulnerable to conduction block at short coupling intervals when the branching is longer (high-load) or when the branching sources invading current (pre-activates) into the main circuit. These channel segments typically show complex notched electrograms with slow upstrokes and a broader split in their voltage distribution due to electrotonic interactions with other fibers near the branch points [176]. The second group of channel segments may be considered as long uninterrupted scaffolding with a relative paucity of branch points and insulated from interactions (protected channel segments). These possess slow conduction in portions far from electrotonic reach of the source current but have a higher safety of propagation at short coupling intervals. These channel segments express relative clean, sharp local electrograms and a narrow split in voltage distribution. We reasoned that such protected channel segments would be: a) preferentially involved in channels

supporting VT circuits compared to branched segments, b) distinguishable from branched segments by having a narrow split in voltage distribution.

To evaluate voltage distribution patterns within the electrograms in ventricular scar, we determined Shannon entropy (ShEn), a fundamental measure for estimating the signal's information content adopted from information theory [311, 389]. It is calculated as a probability distribution within the amplitude histogram of an electrogram. Electrograms arising from a protected channel will have a narrow histogram and low ShEn, compared to branching channel segments. It can thus distinguish a critical channel segment from channels that are unintended to directly support any reentry. This was done in three steps: 1) Each deflection was binned according to its amplitude (0.01 mV fixed amplitude bins) into a voltage histogram 2) The relative probability density *p* was defined as the number of counts in an amplitude bin divided by the sum of bin counts in all bins; 3) The value of ShEn *H* was defined as:

$$H = -\sum_{i=0}^{i=n} p_i \ln p_i,$$

where n is the number of amplitude bins, and p is the probability of any sample falling within a particular amplitude bin. The ShEn values in the map were ranked in an ascending order to identify top five nodes with the minimum ShEn.

In addition to the above-mentioned properties, the region of early sinus activation in the scar is considered relevant. An early-activated region (thus earliest to recover from refractoriness) in a high impedance zone is the preferential path through which, the slowly propagating wavefront during tachycardia exits out of the scar (Figure 3.1) [148, 307].

The novel electrogram properties were analyzed using a custom developed computer program (EPAS, Nucleus Medical, Adelaide) for automated multiple-deflection mapping. The bipolar electrogram location and waveform data from Ensite NavX™ substrate maps were imported. The time- and voltage-domain information within each electrogram deflection was quantified and color-coded left

ventricular maps for each of the individual properties were generated. The location of the VT channels identified by pace and entrainment mapping was then correlated with the individual novel electrogram properties, their various combinations, as well as the conventional abnormal electrograms.

#### D. CHANNEL REGION VALIDATION

The model for prediction of critical channel regions was developed based on assessment of representation of novel electrogram properties in the training stage. When, within a region of high dispersion in activation, a site with latest mean activation time (T) was present adjacent (within 30mm) to a minimum ShEn point (S), a line was drawn along a shortest endocardial path from (T) through (S) to an early activation site near the interface with low dispersion in activation. The anatomic region in proximity to the line (within 1cm) was reasoned as the model region critical to the maintenance of VT(s). The cut-off of 30mm distance between latest activation time and minimum ShEn sites was chosen based on estimated VT isthmus lengths from previous clinical studies [236, 261]. If multiple sites of low ShEn, >10mm apart from each other, existed near to a site of latest mean activation, a line was extended towards each site of low ShEn.

### 3.2.3 PROSPECTIVE APPLICATION

Six patients with ICM presenting for clinically indicated catheter ablation of recurrent VT and consenting for participation were studied. Electroanatomic substrate mapping was performed as previously. The data was imported into and processed in an onsite EPAS equipped computer before attempting catheter ablation. The predicted channel locations from the EPAS were registered manually on the Ensite NavX™map to guide ablation. Limited pace mapping and/or entrainment mapping were done before ablation to validate the predicted location. Ablation was targeted around 1cm of the predicted location. VT inducibility was tested after the regional

ablation. If VT was still inducible, further ablation was performed targeting abnormal electrograms elsewhere in the scar.

### 3.2.4 STATISTICAL ANALYSIS

Continuous variables were reported as mean ± standard deviation and categorical variables were expressed as numbers and percentages. The sensitivity and specificity of abnormal electrograms in the scar for locating a VT channel were calculated. The association between channel locations identified by the two methodologies was evaluated by two-tailed Fisher's exact test. Moreover, a measure of agreement between distributions of channels and electrogram properties was assessed by Cohen's kappa test with values of kappa (κ) from ≥0.4 indicating moderate and ≥0.6 good agreement [390]. The predictive performance of the model properties compared to the channel location was evaluated computing the sensitivity, specificity, positive and negative predictive values (PPV, NPV) with their 95% confidence interval (95% CI) and assessing the best combination of the properties to detect VT supporting channel. A modeled region was considered as a true positive test if a channel inscribed by pace or entrainment mapping was located within the exact region. The latest five mean activation points, the minimum five ShEn sites and all high-low dispersion interfaces within the scar were considered for the sensitivity and PPV analysis. For the purpose of specificity and NPV calculation, true negatives were taken as all the points that were beyond a 1cm radius of an identified channel region. The dispersion in activation and ShEn were analyzed in the pooled data of ventricular maps and differences in the dense scar, borderzone and preserved voltage regions were evaluated by one-way analysis of variance. To account for intrapatient clustering of data and interpatient differences, a linear mixed effects model, clustered by patient (random variable), was used to examine the effect of voltage (fixed variable) on these electrogram properties. All calculations were performed using STATA version 12. A p-value of $< 0.05$ was considered significant.

## 3.3 RESULTS

### 3.3.1 BASELINE CLINICAL CHARACTERISTICS

Baseline characteristics of the sixteen patients are presented in Table 3.1. All patients had undergone a recent non-invasive evaluation or coronary angiography to exclude active ischemia.

### 3.3.2 INDUCIBLE VENTRICULAR TACHYCARDIA

All patients had one or more inducible, or spontaneous sustained monomorphic VT at baseline. Overall, 58 different VTs were inducible, with a mean of 3.6±1.7 VTs per patient with a mean cycle length of 388±103 ms.

### 3.3.3 LEFT VENTRICULAR ENDOCARDIAL VOLTAGE MAPPING

A mean number of 763±203 sampling points were taken per patient with 451±145 points within dense scar. On an average, of the total left ventricular area (319±75cm$^2$), 60±16% (202±80cm$^2$) had low voltage, and 37±11% (129±60cm$^2$) was formed by dense scar.

### 3.3.4 MAPPING OF VENTRICULAR TACHYCARDIA CHANNELS

Pace mapping was performed in low voltage zones at 1770 sites, a mean of 110±55 per patient. Capture was absent at 478 sites. Of the captured sites, 673 sites (42±26 per patient) had a S-QRS interval of ≥40ms. Overall, 307 pace maps corresponded to 47 inducible VTs (8±7 pace maps per VT) (Figure 3.4), of which 97 pace maps (3±2 pace maps per VT) had a S-QRS interval of ≥80ms. The longest S-QRS interval and the

range (longest minus shortest S-QRS) in a VT pace map series averaged 113±75ms and 93±60ms, respectively. Forty-four VTs could be mapped in the LV while 3 had matching pace maps in the RV. The estimated minimal endocardial length along a VT channel was 49±30mm, with 95% of channels residing in the dense scar.

Entrainment mapping was feasible in 8 patients, and isthmus locations could be confirmed in 4 VTs (Figure 2.6). Overall, at these entrainment locations, diastolic potentials covering 44±23% of tachycardia cycle length could be recognized within a PentaRay™ catheter recording area.

### 3.3.5 Relationship of Channels and Scar Related Electrograms

Abnormal electrograms were frequently identified in low-voltage zones in these patients. However, of all the fractionated (mean 114±85), late (mean 10±5) and very-late (mean 3±3) potentials, only 18%, 23% and 35%, respectively were recorded in the VT channels. Table 2 gives the analysis of abnormal electrograms in relation to VT channel locations. These electrograms had high specificity but poor sensitivity for locating a VT channel. There was relatively poor agreement between these abnormal electrogram sites and a channel location ($\kappa<0.1$). Importantly, however, compared to elsewhere within the scar, in the region of VT channels fractionated potentials were longer in duration (102±28ms vs 96±27ms, $p<0.001$), but there were no differences in coupling intervals of the late (18±18ms vs 24±18ms, $p=0.3$) and very late potentials (223±99ms vs 223±145ms, $p=0.6$).

### 3.3.6 Ablation Outcomes

Complete procedural success was achieved in 10 (63%) patients and partial success in 5 (31%) patients. Over long-term follow-up of 15±4 months, three patients died (two heart failure, one sudden death), three had recurrence of VT (two with VT storm), and underwent repeat ablation.

### 3.3.7 Time and Voltage Domain Electrogram Properties

Fractionated and late electrograms, as shown in Figure 3.2, differed in timing and voltage distribution of their multiple deflections as reflected in their mean activation time, dispersion in activation and ShEn. Such differences in electrogram structure were evaluated on individual maps for a predictable pattern and evidence for critical regions for VT maintenance. The latest mean activation time and the minimum ShEn in the maps averaged 614±33ms and 0.15±0.21, respectively. A mean number of 2±1 high activations dispersion regions were identified in these patients. While all the sites with latest mean activation and high activation dispersion resided in the dense scar, approximately one third of least ShEn sites resided in the borderzone (30%) or normal myocardium (6%). When stratified according to the local voltage, the dispersion of activation was highest in the dense scar (2.4±2.3), as compared to the borderzone (1.8±2.2) and preserved (1.1±0.8) voltage regions ($p<0.001$). One unit decrease in voltage was associated with 0.26 unit increase in dispersion in activation (95% CI -0.261 to -0.255, $p<0.001$). As ShEn analyzes electrograms in both time- and voltage-domains, increase in local voltage resulted in higher ShEn due to greater amplitude differences. Unlike dispersion of activation, ShEn was low in the dense scar (1.1±0.4), as compared to borderzone (1.3±0.5) and preserved myocardial voltage (1.6±0.5) ($p<0.001$). One unit increase in voltage was associated with 0.13 unit increase in ShEn (95% CI 0.12 to 0.13, $p<0.001$).

### 3.3.8 Validation of VT Channels Identified by Novel Electrogram Properties

The analysis of novel electrogram properties as a test for identifying a VT channel location is given in Table 3.2. Only left ventricular electroanatomic data was studied and correlated with 44 mapped VT channels. When observed independently, the latest mean activation time, high activation dispersion and minimum ShEn had only moderate agreement with a VT channel location ($\kappa$=0.42, 0.45, and 0.42, respectively, $p<0.01$). However, when present together in a region in various

combinations, the κ-statistic improved, and best agreement was achieved when all the three novel properties were assembled together (κ=0.89, p<0.001). Similarly, the independent PPVs of the three properties for localizing a VT channel were low (58%, 59% and 48%, respectively), but substantially increased to 93% when all the three properties were present together. As an independent parameter, low ShEn had only modest specificity (80%) for localizing a VT channel. However, after pairing with latest mean activation time and high activation dispersion, effectively excluding low ShEn sites outside the scar, its specificity improved to 100% and 96%, respectively. Figure 3.5 and 3.6 illustrate cases where multiple modeled sites for VT channels were identified based on the presence of sites with latest mean activation time and minimum ShEn within a region of high activation dispersion that correlated with the VT channels identified by pace and entrainment mapping.

Three patients did not have any regions in the endocardial left ventricular scar where all three properties assembled. One of these patients who had large left ventricular endocardial scar but did not have a high-low dispersion interface, had VTs mapped only in the RV, while one patient had a failed ablation and the other a partially successful catheter ablation. Subsequently, both had VT recurrences, possibly suggesting epicardial circuits.

### 3.3.9 PROSPECTIVE CASES

Of the six patients (mean age 70±9 years, ejection fraction 33±3%, time to first infarction 18±10 years), one had incessant drug refractory VT while others had frequent monomorphic VT. The mean VT cycle length was 430±146ms. Electroanatomic maps were created (four in sinus rhythm, one atrial fibrillation, one ventricular paced), with 1002±219 sampling points, 566±202 in the dense scar. The average time for time- and voltage-domain analysis from imported Ensite NavX™ data was 19±10 min. A median of one region per patient (range 1 to 3) was identified where the latest mean activation time and least ShEn were assembled together in a high activation dispersion region. Before targeting marked regions with catheter

ablation, pace mapping in these regions demonstrated long S-QRS latencies (121±75ms) with a matching morphology to inducible VTs (Figure 3.7). Entrainment mapping was feasible in three patients where an isthmus exit site could be identified in the marked region (Figure 3.8).

Focused ablation at these sites eliminated 15 of the 17 inducible VTs in these patients. Five patients were rendered non-inducible. In one patient two additional VTs were targeted at areas of long paced latencies elsewhere in the low voltage region, however could not be eliminated. One patient who had an initially successful ablation procedure had an early recurrence within 6 weeks, however was medically managed.

## 3.4 DISCUSSION

### 3.4.1 MAJOR FINDINGS

This study used a novel approach based on time- and voltage-domain analysis of multiple-deflections in the sinus rhythm electrograms to localize VT channels. We have validated three novel electrogram properties (mean time of activation, dispersion in activation times, and Shannon entropy) against the contemporary methods for VT channel localization. The strength of the study lies in the particularly high resolution of sampling and detailed pace mapping within the scar to locate VT channels. The main findings of the study are:

- VT supporting channels have unique electrogram properties distinctive from elsewhere in the scar.
- These channels are generally present within dense scar adjacent to sites of latest activation in a region of high dispersion.
- Despite being located in a region of high dispersion, VT channel regions express low ShEn signifying relatively less complex electrograms.

- There is significant correlation between clinical VT channels recognized by pace and entrainment mapping and channel regions inferred from the model. The indicated regions in the model were highly specific with a high positive predictive value for clinical VT channels.
- The combination model of site of latest activation and low ShEn in a region of high dispersion in activation was the best predictor of the VT channel location, compared to individual electrogram properties.
- In a small test cohort, targeting catheter ablation in the region of the scar identified by the model eliminated the majority of the VTs.

### 3.4.2 SUBSTRATE ABLATION

Ventricular tachycardia ablation is frequently led by the morphology of the VT itself and the distribution of the underlying substrate [283]. While VT morphology is widely emphasized to be relevant in planning ablation targets [282, 288, 289], despite recent advances in substrate characterization [356, 391], identifying surviving myofiber channels by readily applicable and efficient methods has remained a challenge. The contemporary substrate based ablation practices have evolved from linear anchoring ablation [240], short lines [263], to spot ablation targeting areas of long paced-latencies [282], however finding these regions in the expanse of large heterogeneous scar can be tedious. The requirements for a reentrant excitation include the three principle conditions - unidirectional conduction block, slow conduction and re-excitation of the previously blocked myofiber bundle [148]. Only a finite number of sustained VTs ensue in the setting of healed myocardial infarction [380]. Moreover, the critical segments of majority of the new VT morphologies those develop late after prior catheter ablations reside in the previously ablated regions [392]. It is, therefore, reasonable to assume a minimalistic approach that only finite elements of the scar have satisfactory conditions that allow perpetuation of sustained VT. Although there are dynamic components within the substrate that change over time, the development of VT thus seems to be a function of a relatively static set of anatomic

and electrophysiological properties [393]. We have recently shown that channels supporting VT have longer protected segments and slower conduction compared to channels not supporting VT [388]. These properties reflect in the local electrogram morphology and this study explored these morphological differences for any predictable information on the topology of VT supporting channels within the complex interacting system of scar and surviving myofibers.

### 3.4.3 Concept of Multiple-Deflection Mapping and its Relation to VT Channels

The electrograms recorded during sinus rhythm from the areas of surviving myofibers in fibrous scar are often represented as fractionation and late potentials [385]. However, information content pertinent to a VT supporting channel remains obscure in this simplistic way of electrogram classification. The seminal work by Dr de Bakker on human infarct papillary muscle using sub-millimeter electrodes, substantiated that each peak in a multiple-deflection bipolar electrogram represents individual myofiber bundle conduction and that a channel network can be constructed [175]. A previous study using the straight counting of multiple positive deflections has shown a high sensitivity and specificity of electrograms with more than four peaks and amplitude of less than 1mV to co-localize with VT termination sites [394].

Ciaccio et al in their work in post-infarction canine hearts had further developed this concept by assigning individual activation times to all peak deflections (PD) in sinus rhythm bipolar electrograms, and constructed VT channels by the panoramic overlay of maps of mean (MPD) and standard deviation (DPD) of activation times [309]. These were taken as measures of two static properties, the onset, and the duration of local electrical activity within the epicardial scar borderzone. The isthmus trajectory was identified when the last MPD isochrone was associated with sharp transitions in DPD and an activation gradient of <1m/s could be traced in any direction away from the

last MPD activation point. The estimated isthmus overlapped the actual isthmus by ~85%, and in the experiments lacking inducible tachycardia no gradient of <1m/s was identified. Our study extends that of Ciaccio et al. by employing high density mapping in humans and including an analysis of the electrogram complexity in voltage domain, Shannon entropy. This combination of parameters had better correlation with the VT channels than late activation and dispersion of activation together.

### 3.4.4 Contemporary Methods and Future Directives

Entrainment mapping is the foremost way to target isthmus sites by catheter ablation in reentrant VT. However, the necessities for reproducible and tolerated VT limit its routine application in majority of patients who often have multiple unstable VTs. With this realization, substrate based ablation has gained momentum over the last few years. However, its application is often elementary given the inability of the present day mapping methods to reliably distinguish electrograms that populate VT channels from those elsewhere within the scar, and requires extensive pace mapping and catheter ablation within the scar. As the ventricular scar volume can be frequently large, complete elimination of scar related electrograms or scar dechannelization remains difficult.

Given these challenges, facing catheter ablation of reentrant VT in ICM, the new model is anticipated to improve resolution of ventricular scar and identify apparently concealed small regions in the scar that harbor VT channels. This will help reduce excessive ablation employed in the current strategies and promote more focused and targeted ablation. The novel approach appears convenient and is readily applicable in majority of patients; however, the effectiveness of this model must be compared against the prevailing methods of catheter ablation in a large study. We aim to perform a randomized study comparing the novel electrogram properties based and conventional substrate ablation approach.

### 3.4.5 STUDY LIMITATIONS

Large fractions of VT were poorly tolerated, which precluded entrainment mapping and thus, localization of the VT channels relied heavily on paced latencies. Nevertheless, pace mapping is considered as the best surrogate to locate surviving myofiber channels [277], and an ultra high density pace mapping with rigorous matching criteria as was applied in our study, reduces these potential errors. We did not perform epicardial mapping as all these patients had an ischemic substrate, many with previous bypass surgery. It is possible that some of the VTs that could not be mapped endocardially had intramyocardial or epicardial circuits. The presence of epicardial fat and coronary vessels introduce intricacies in electrogram formation. Further studies should evaluate the effectiveness of the model electrogram properties in the epicardial circuits. Nonetheless, the negative predictive value of the model properties was >99% which suggests that absence of regions with all three properties together can potentially identify VT circuits that are not present in the mapped region.

## 3.5 CONCLUSION

Activation time and entropy mapping improves electrical resolution in the ventricular scar. This method of substrate mapping accurately identifies VT channels compared to other frequently employed electrogram characteristics. This can expedite recognition of VT channels without pace mapping or mapping during VT and minimize extensive ablation within the scar.

## TABLES

| Table 3.1 | Baseline Characteristics |
|---|---|
| Number | 16 |
| Age (years) | 67±10 |
| Male, n | 16 |
| Ejection fraction (%) | 31±9 |
| Time to first infarction (years) | 11±15 |
| Coronary bypass surgery, n | 8 |
| Rhythm, n | |
| Sinus rhythm | 14 |
| Atrial fibrillation | 1 |
| Ventricular paced rhythm | 1 |
| QRS duration, ms | 147±36 |
| VT cycle length, ms | 388±103 |
| VT storm, n | 5 |
| Previous ICD, n | 14 |
| Beta blocker, n | 14 |
| Amiodarone, n | 7 |
| Other antiarrhythmic drugs, n | 7 |

ICD=Implantable Cardioverter Defibrillator, VT=Ventricular Tachycardia

| Table 3.2 | Association between electrogram properties with the presence of a ventricular tachycardia channel | | | | | |
|---|---|---|---|---|---|---|
| **Property** | **Kappa** | **Fisher p-value** | **Sensitivity** | **PPV** | **Specificity** | **NPV** |
| **Fractionated potential** | 0.073 | <0.0001 | 0.330 | 0.185 | 0.762 | 0.913 |
| **Late potential** | 0.041 | <0.0001 | 0.044 | 0.232 | 0.980 | 0.911 |
| **Very late potential** | 0.016 | <0.001 | 0.015 | 0.347 | 0.994 | 0.910 |
| **LAT** | 0.424 | <0.0001 | 0.921 | 0.631 | 0.993 | 0.999 |
| **ShEn** | 0.424 | 0.0053 | 0.908, | 0.478 | 0.814 | 0.999 |
| **High low** | 0.453 | <0.0001 | 0.934 | 0.594 | 0.947 | 0.999 |
| **LAT + ShEn** | 0.867 | <0.0001 | 0.868 | 0.868 | 0.998 | 0.998 |
| **LAT + High low** | 0.837 | <0.0001 | 0.895 | 0.791 | 0.997 | 0.999 |
| **ShEn + High low** | 0.540 | <0.0001 | 0.882 | 0.696 | 0.959 | 0.998 |
| **All 3** | 0.889 | <0.0001 | 0.855 | 0.929 | 0.999 | 0.998 |

High-low= high dispersion zone with low dispersion interface, LAT= latest mean activation time, NPV= negative predictive value, PPV= positive predictive value, ShEn= least Shannon entropy

## FIGURES

***Figure 3.1***

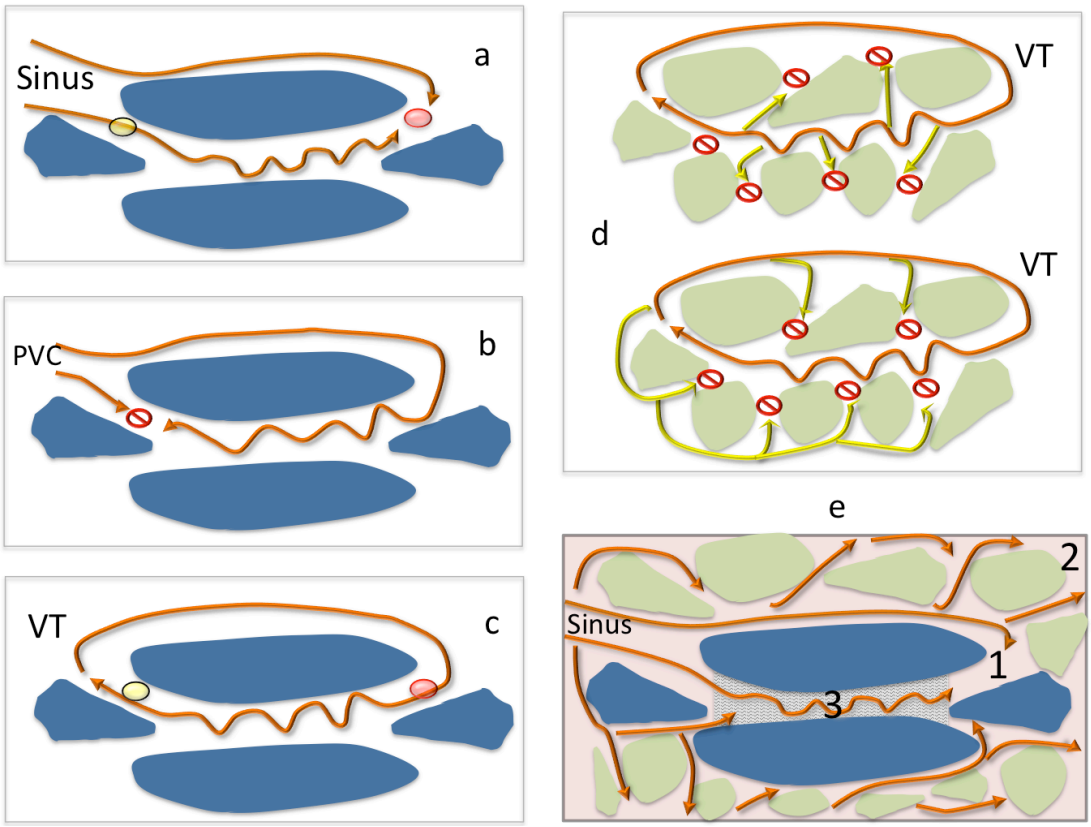


Figure 3.1. a to c. Schematics of a simple scar structure (blue shaded areas) to illustrate that sites of latest (red marker) and relative early activation (yellow marker) in the scar during sinus rhythm participate in a prospective VT circuit. Arrows represent impulse propagation in channels of surviving muscle fibers with undulations representing slow conduction. PVC= premature ventricular complex.

d. Schematics of a complex scar structure (green shaded areas) with branching channel network. This has low anatomic probability to sustain VT due to leakage of charge load (top panel) and/or feeding currents (bottom panel) from and into the central channel segment respectively. Establishment of functional conduction blocks

(no-entry symbols) at numerous sites that protect the central channel segment from side-branch interactions can only sustain a VT.

e. Schematic of a complex scar structure where a relatively long and protected channel (bounded by blue shaded areas) is assembled in a network of branching channel segments (bounded by green shaded areas). The protected channel has highest anatomic probability to sustain VT. The electrical properties of latest activation (1) and low entropy (3) in a region of high dispersion in activation (2) (pink boxed region) during sinus rhythm can together identify the protected channel segment critical for sustaining a VT (grey shaded area).

***Figure 3.2***

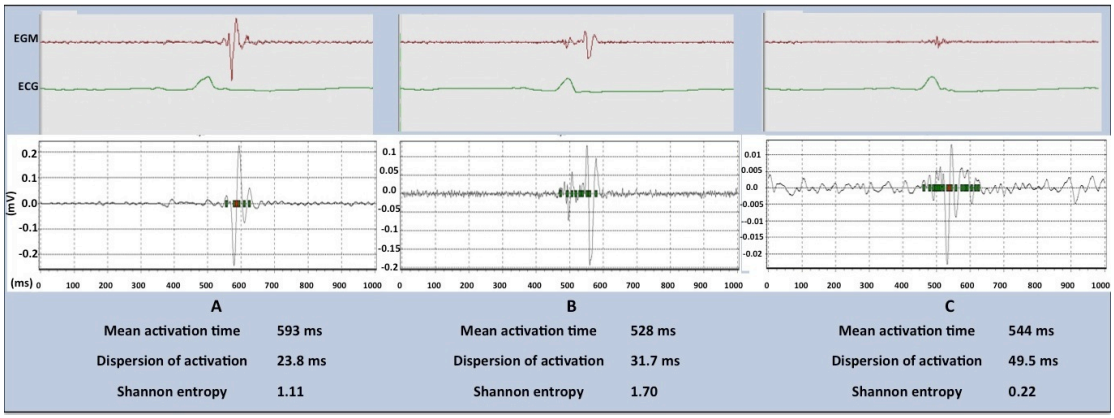


Figure 3.2. Charcteristics of scar electrograms. All three top panels show electrograms obtained from within dense scar with low voltage multiple peak deflections. After filtering at 20Hz low-pass (bottom panels), the electrogram at each location was detected (red marker) at maximum dV/dt adjacent to maximum peak deflection within 30-70% of the recording window of 1-second. Every deflection in the electrogram (peak and trough) (≥1% of the maximum peak deflection, range ≥5ms) in a window of 200ms across maximum dV/dt was assigned an activation time (green markers) relative to start of the window (0ms). The mean and standard deviation of these activation times represent the mean activation time and dispersion of activation at that site, respectively. Shannon entropy (ShEn), a measure of signal amplitude distribution, was estimated for the 30-70% of the recording window at each location (refer text for details). Panel A shows an electrogram with the relative late mean activation time, high dispersion and high ShEn. Panel B shows a relative early mean activation time, high dispersion and high ShEn. Panel C shows a relative early mean activation time, high dispersion and low ShEn.

***Figure 3.3***

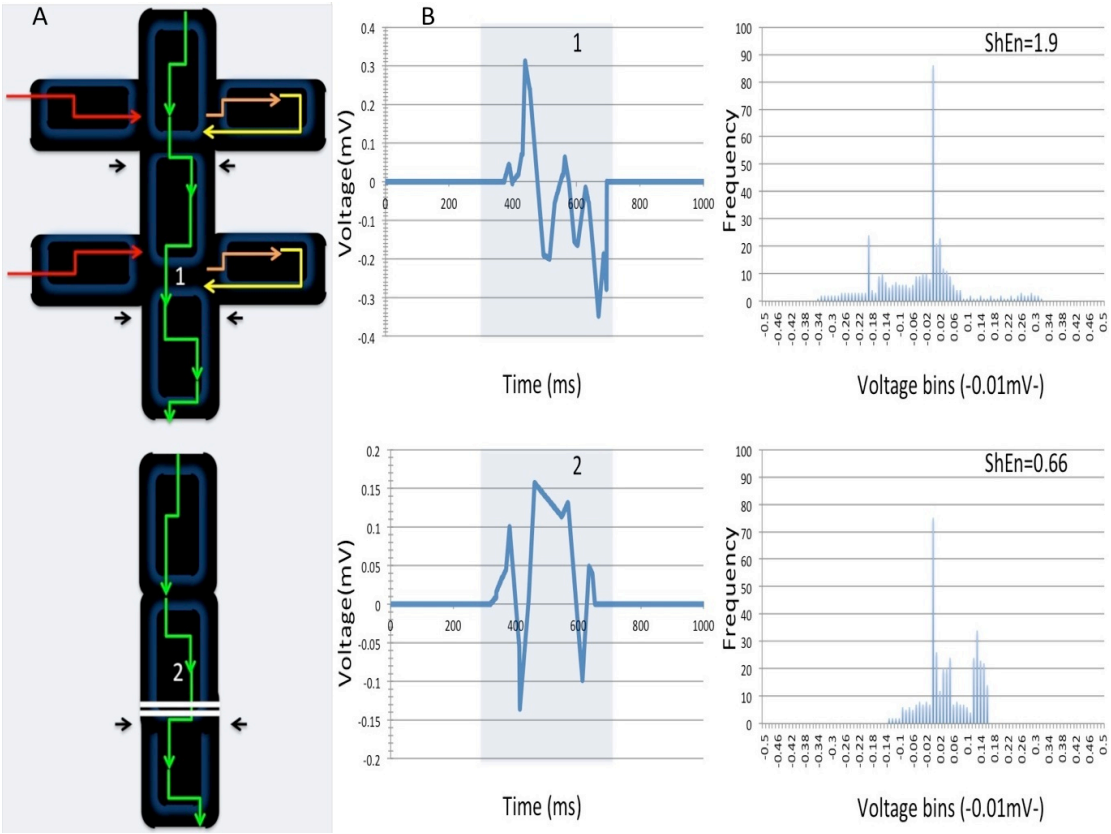


Figure 3.3. Schematic representation for channel segment types, local bipolar electrograms and their Shannon Entropy.

(A) *Top*. Branched channel with multiple side-branches. Green arrows with increasing elbow size depicting downstream slowing of conduction in the main strand. Red arrows denote open-end branches with currents feeding into the main strand. Dead-end branches take current load (orange arrows) away from the main strand and feed electrotonic currents (yellow arrow) back into it. Small black arrows denote sites of branch points and ensuing sections of the main strand at risk of halt in conduction. *Bottom*. Protected long channel with paucity of branches. Green arrows with increasing elbow size depicting downstream slowing of conduction in sections progressively far from the source of current in the main strand. The break in the main strand denotes its long length, and there are no side-branches. Small black arrows mark the section of the main strand at risk of halt in conduction. Numbers 1 and 2 are the sites of bipolar electrogram recordings.

(B) Bipolar electrograms, 1 and 2, from respective sites in panel A. Voltage in each of the deflections within 30-70% of the recording window (shaded) was sampled at 2kHz and binned into 0.01mV bins.

*Top.* Electrogram 1 from branched channel shows multiple intrinsic deflections with wide range in voltage distribution and high Shannon entropy (ShEn). *Bottom.* Electrogram 2 from protected channel shows fewer intrinsic deflections and a relative limited range in voltage distribution and low ShEn.

***Figure 3.4***

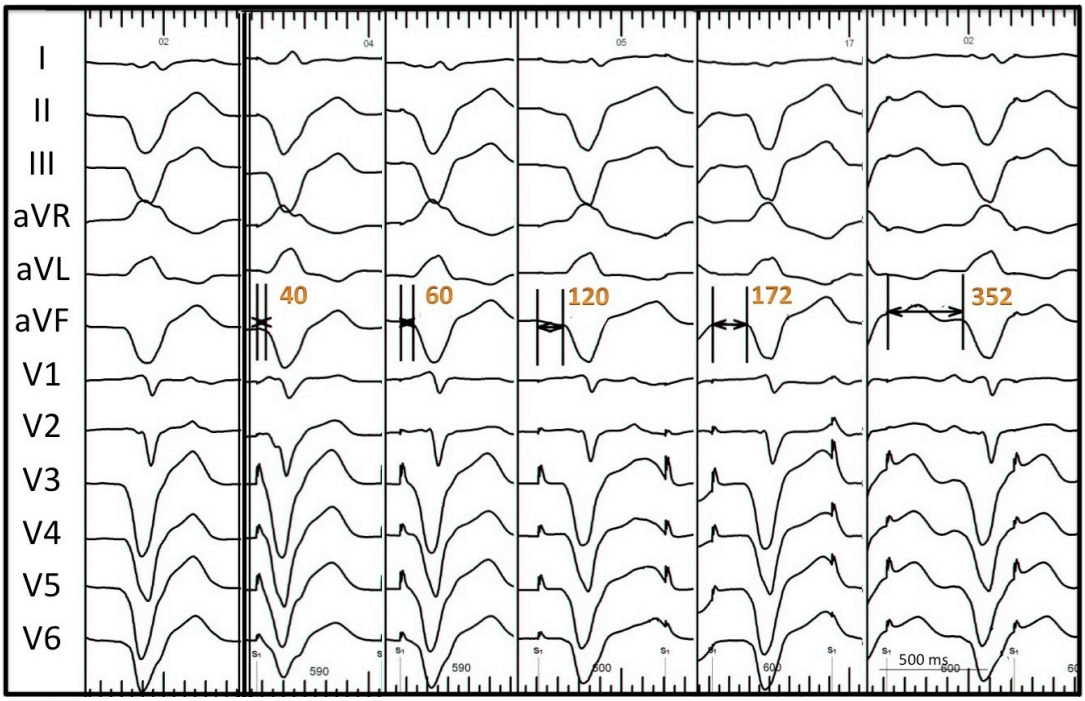


Figure 3.4. The left panel shows 12-lead QRS morphology of a VT. The right panel shows the set of pace maps with marked stimulus-QRS intervals of ≥40ms in an orthodromic sequence and matching QRS morphology (≥11/12 ECG leads) to the VT. These pace-map sites were joined along a minimal endocardial path to construct the VT channel on the electroanatomic surface.

***Figure 3.5***

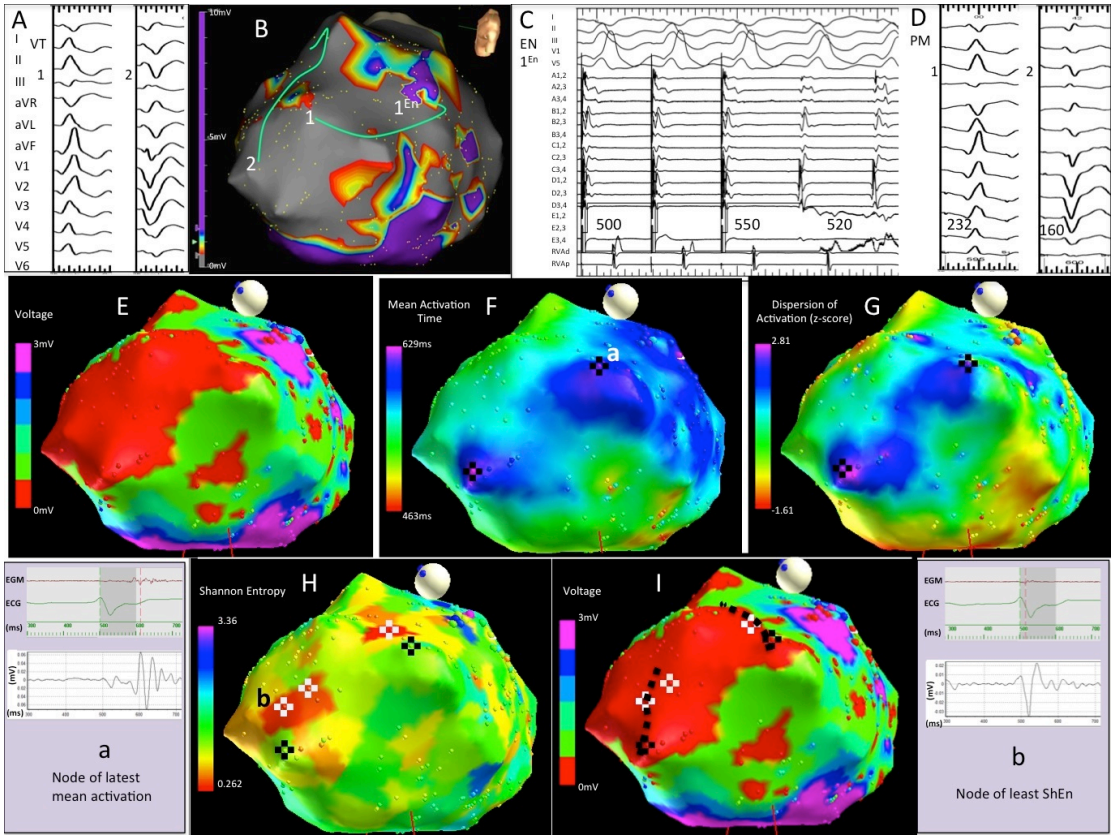


Figure 3.5. Case Example. (A) 12-lead ECG of two Inducible ventricular tachycardias (VT 1 & 2). (B) Voltage map on Ensite NavX™ in left anterior oblique and cranial view showing large scar (grey) in anterior left ventricle. Channels mapped by pace mapping corresponding to VT 1 and 2 are displayed as lines. The isthmus site for VT 1 was confirmed by entrainment mapping, marked as $1^{En}$. (C) Entrainment pacing (EN) for VT1 from site $1^{En}$ (PentaRay™ bipole E2,3) showing concealed fusion with post-pacing interval and tachycardia cycle length difference of 30ms (D) 12-lead ECG of representative pace maps (PM) for VT 1 and 2 from sites corresponding to the numbered locations in panel B. Intervals marked in millisecond in each of the pace maps are stimulus-QRS intervals. (E) Voltage map from the exported data in same view as in panel B with red color representing dense scar. (F) Mean activation time map, with nodes of latest activation highlighted as black-cross. Local electrogram (EGM) at the black-cross marked 'a' is shown in the bottom left panel. (G) Dispersion of activation map, with a high (purple/blue, z≥ +1.5) and low dispersion interface

(green/yellow, z≤ -0.5) within the low voltage region. The nodes of latest activation are residing within the high dispersion zone. (H) Shannon entropy (ShEn) map, with nodes of least ShEn highlighted as white-cross residing within the high dispersion zone. Local electrogram at the white-cross marked ‘b’ is shown in the bottom right panel. (I) Voltage map with putative channel regions identified by projecting lines (broken-black lines) from node of latest activation towards adjacent low ShEn within the high dispersion zone, to nodes of early activation near the high-low dispersion interface. The two regions corresponded with the VT channels identified by pace mapping.

***Figure 3.6***

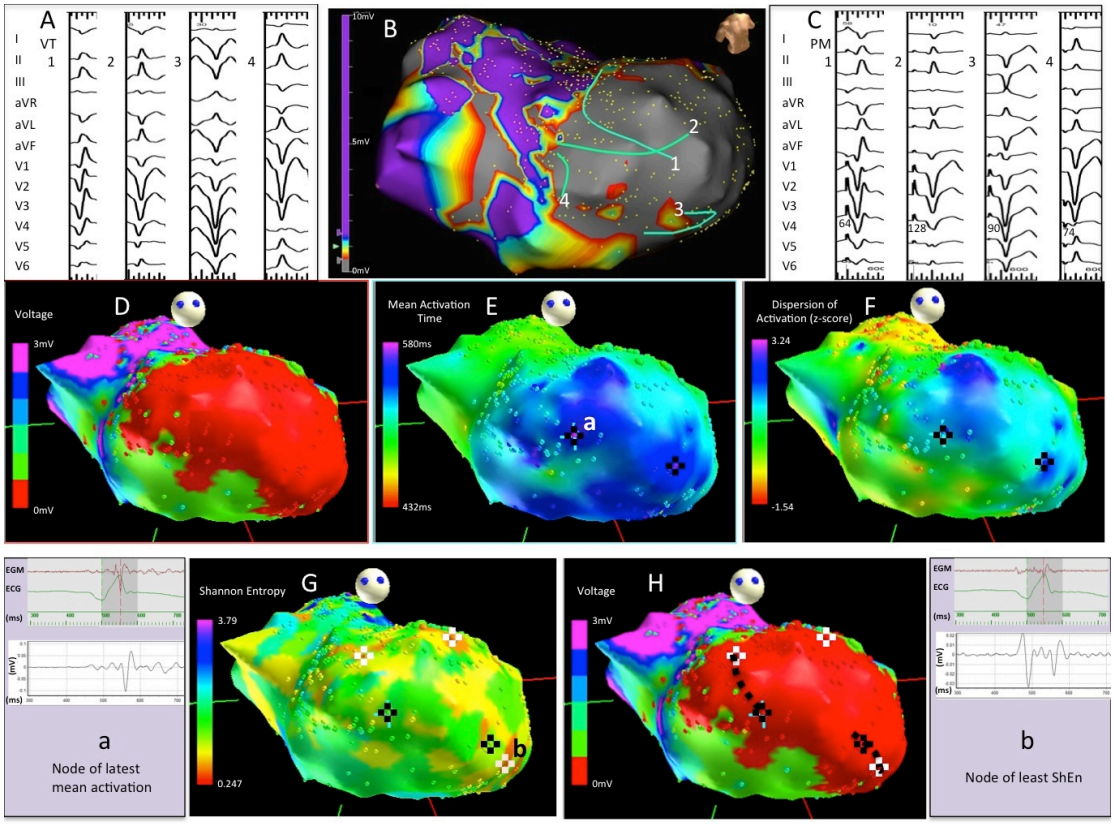


Figure 3.6. Case Example. (A) 12-lead ECG of four Inducible ventricular tachycardias (VT 1 to 4). (B) Voltage map on Ensite NavX™ in right anterior oblique and cranial view showing large scar (grey) in mid-apical left ventricle. Channels mapped by pace mapping corresponding to VT 1 to 4 are displayed as lines. (C) 12-lead ECG of representative pace maps (PM) for VT 1 to 4 from sites corresponding to the numbered locations in panel B. Intervals marked in millisecond in each of the pace maps are stimulus-QRS intervals. (D) Voltage map from the exported data in same view as in panel B with red color representing dense scar. (E) Mean activation time map, with nodes of latest activation highlighted as black-cross. Local electrogram (EGM) at the black-cross marked 'a' is shown in the bottom left panel. (F) Dispersion of activation map, with a high (purple/blue, z≥ +1.5) and low dispersion interface (green/yellow, z≤ -0.5) within the low voltage region. The nodes of latest activation are residing within the high dispersion zone. (G) Shannon entropy (ShEn) map, with nodes of least ShEn highlighted as white-cross residing within the high dispersion

zone. Local electrogram at the white-cross marked ‘b’ is shown in the bottom right panel. (H) Voltage map with putative channel regions identified by projecting lines (broken-black line) from node of latest activation towards adjacent low ShEn within the high dispersion zone, to nodes of early activation near the high-low dispersion interface. The two regions corresponded with the VT channels identified by pace mapping.

***FIGURE 3.7***

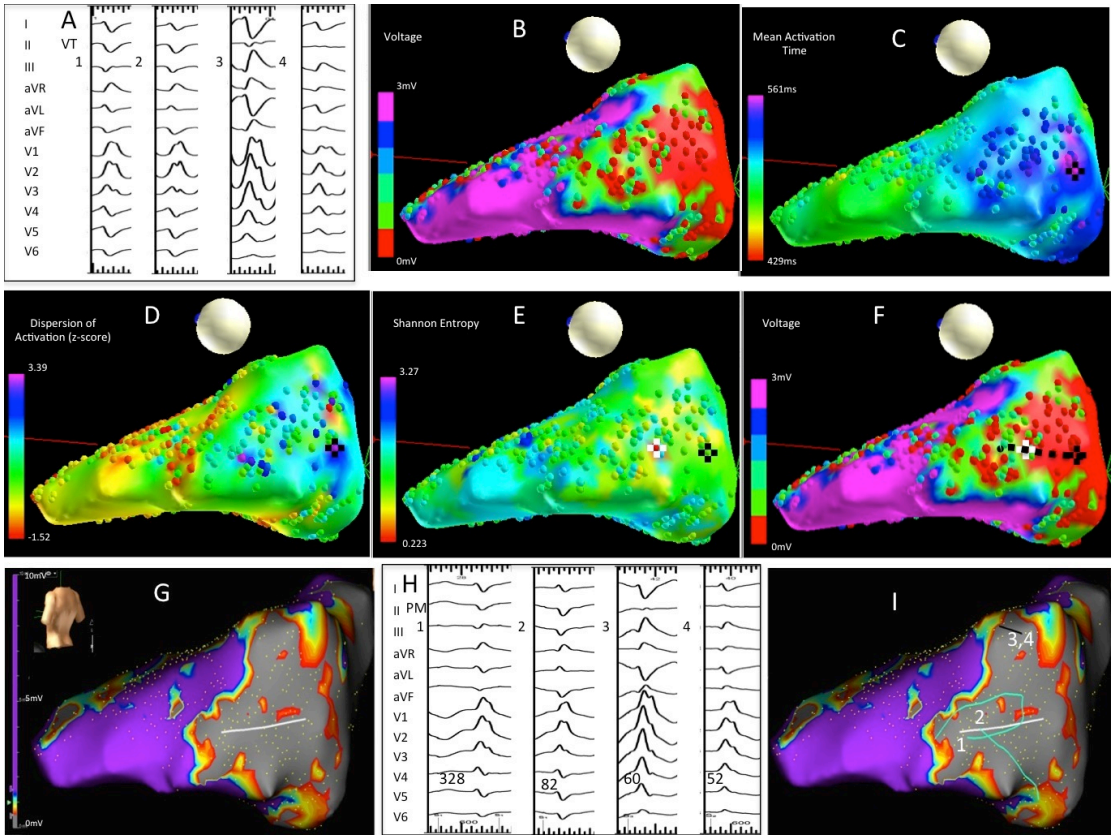


Figure 3.7. Example of a prospective case. (A) 12-lead ECG of four Inducible VTs (1 to 4). (B) Voltage map from the exported data in left posterior lateral view with red color representing dense scar in the basal lateral left ventricle. (C) Mean activation time map, with node of latest activation highlighted as black-cross. (D) Dispersion of activation map, with a high (purple/blue, z≥ +1.5) and low dispersion interface (green/yellow, z≤ -0.5) within the low voltage region. The node of latest activation is residing within the high dispersion zone. (E) Shannon entropy map, with node of least ShEn highlighted as white-cross residing within the high dispersion zone. (F) Voltage map with putative channel region identified by projecting a line (broken-black line) from node of latest activation towards adjacent low ShEn within the high dispersion zone, to a node of early activation near the high low dispersion interface. (G) Voltage map on Ensite NavX™ in same view as in panel B with marked predicted VT channel region (white line). (H) 12-lead ECG of representative pace maps for VT 1 to 4 from sites corresponding to the numbered locations in panel I. Intervals marked in millisecond in each of the pace maps are S-QRS intervals. (I) Voltage map on Ensite

NavX™ showing channels mapped by pace mapping corresponding to VT 1 and 2, displayed as lines. Both these VTs were eliminated by ablation in the predicted region (white line). VT3 and 4 were mapped elsewhere in the scar but could not be eliminated. PM= Pace map, ShEn= Shannon entropy, S-QRS = Stimulus-QRS interval, VT=Ventricular tachycardia.

***Figure 3.8***

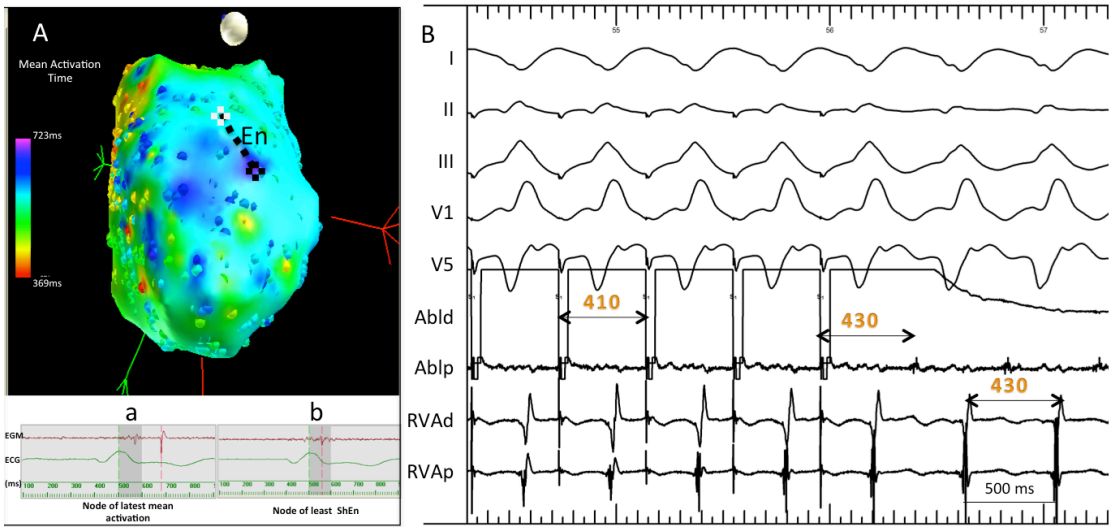


Figure 3.8. Example of a prospective case. Panel A. Mean activation time map. A putative channel region was identified where node of latest mean activation (black-cross) assembled with adjacent low Shannon entropy (white-cross) within the high dispersion region. A concealed entrainment location (marked as En) confirmed participation of this modeled region as the central isthmus site of the VT circuit. Local electrograms at the black-cross marked 'a' and at the white-cross marked 'b' are shown in the bottom panels. Panel B. Entrainment pacing (Abld) during VT. Channels from top to bottom are surface ECG (I, II, III, V1, V5) , ablation catheter (Abl) in mid anterolateral left ventricular scar region (marked En in panel A), and right ventricular apex [RVA, distal (d) and proximal (p)]. Intervals are marked in milliseconds. This pacing site entrained the VT with concealed fusion with post-pacing interval matching tachycardia cycle length. The S-QRS interval (120ms) matched with the diastolic potential (Ablp) to QRS interval. This site represented central isthmus location for this VT.

# CHAPTER 4. A SYSTEMATIC INSIGHT INTO CHANNELS IN ISCHEMIC CARDIOMYOPATHY WITH AND WITHOUT SPONTANEOUS VENTRICULAR TACHYCARDIA USING HIGH DENSITY MAPPING

## ABSTRACT

**Background.** The arrhythmogenic characteristics of surviving myocyte channels in ventricles with post-infarct scarring and sustained monomorphic ventricular tachycardia (VT) compared to post-infarct ventricles without spontaneous VT are unknown.

**Methods.** Patients with ischemic cardiomyopathy (ICM) undergoing catheter ablation of recurrent VT (VT patients; n=22; EF 32±8 %; time to infarct 10±15 years) were compared with stable ICM patients without spontaneous VT (Control group; n=5; 29±6 %; 11±14 years). Left ventricular endocardial mapping was performed with a 20-pole PentaRay™ catheter. Pacing was done from bipoles showing low voltage (≤1.5V) with late potentials and/ or fractionation. A channel was defined as series of matching pacemaps with stimulus (S) to QRS interval ≥ 40ms. Sites were determined to be part of a VT circuit if there were matching pacemaps to the inducible VT morphology. This was confirmed with entrainment mapping when possible. The anatomical and electrophysiologic properties of these channels were evaluated.

**Results**. Seventy-three (range 1 to 7) SMVT were inducible in VT patients compared to two (range 0 to 2) in controls. The sampling density was similar in both groups (760±205 vs 616±104 voltage points, p=NS), with 431±137 vs 310±69 points (p=0.04) within dense scar (≤0.5mV). An average of 114±62 and 104±32 pace maps were performed in the two groups (p=NS). Pacemaps with S-QRS ≥40ms and ≥80ms were

more frequent in VT patients (59% & 20%) than in controls (41% & 1%) ($p<0.01$). Channels in VT patients that were part of VT circuit (n= 57, 3±1 per patient) were lengthier (mean±SEM 53±5 vs 33±4 vs 24±8 mm), had longer S-QRS (73±4 vs 63±3 vs 44±8 ms), longer conduction time (103±13 vs 33±4 vs 24±8 ms) and slower conduction velocity (CV) (0.85±0.21 vs 1.39±0.20 vs 1.31±0.41 m/s) than non-VT channels in VT patients (n=183, 8±6) ($p\leq0.01$) and non-VT channels in controls (n=46, 9±8) ($p\leq0.01$). Additionally, non-VT channels in VT patients had longer S-QRS ($p=0.02$), however there was no difference in length, conduction time or CV compared to non-VT channels in controls. VT channels were more often located within the dense scar than non-VT channels in VT patients (97% vs 77%, $p=0.04$). **Conclusion.** Channels supporting VT in ICM patients with spontaneous VT are lengthier, with longer conduction times and slower CV compared to channels in patients without spontaneous VT. These observations demonstrate why some ICM patients have spontaneous VT and others do not.

## 4.1 INTRODUCTION

Despite more than two decades of research, mapping of scar related ventricular tachycardia (VT) has remained a challenge [365]. This results from complex structure of the scar and expanse of its distribution compounded by multiple clinical VT [175, 380]. The larger reasons why only some patients with ischemic cardiomyopathy (ICM) develop spontaneous VT and majority others do not are not known. It has been suggested that the organization of the scar in ICM patients with spontaneous VT is more complex, with larger area of scarring, greater number of anatomical channels, and more frequent abnormal electrograms than patients without spontaneous VT [235, 241]. However, it is unknown how this complexity relates with the VT channels, and why the large majority of surviving myocyte channels that coexist in the scar never perpetuate VT. It is unclear how these "non-VT channels" differ from VT channels, and why they are nonfunctioning. We therefore embarked on this study in post-infarct ventricles with the objective of exploring electrophysiological properties of the scar using ultra high-density mapping to assess if there are differences in conducting channel properties in patients with and without spontaneous VT.

## 4.2 METHODS

### 4.2.1 PATIENT POPULATION

Twenty-two consecutive patients with ischemic cardiomyopathy (ICM) with recurrent SMVT or VT storm [≥3 episodes or implantable defibrillator (ICD) therapies for VT in 24 hours] undergoing a clinically indicated catheter ablation procedure were studied (VT patients). Five ICM patients undergoing ICD implantation as per sudden cardiac death primary prevention guidelines [84] were studied as controls (Control group). Patients with a previous VT ablation, acute coronary event within the preceding 1month, intracardiac thrombus, mechanical prosthetic valve and severe aorto-iliac peripheral vascular disease were excluded. All patients provided

informed consent, and the study was approved by the Human Research Ethics Committee of the Royal Adelaide Hospital and the University of Adelaide.

### 4.2.2 ELECTROPHYSIOLOGIC STUDY

---

#### A. VENTRICULAR TACHYCARDIA PATIENTS

The procedure was done in post-absorptive state under conscious sedation. Briefly, a quadripolar catheter and decapolar catheter were positioned at the right ventricular (RV) apex and coronary sinus, respectively. Programmed ventricular stimulation was performed from the RV apex at two drive cycle lengths (600ms and 400ms) with up to 3 extrastimuli. All sustained monomorphic VTs induced at baseline, during the course of the study and post-ablation were considered clinical VT [19]. A 20-pole catheter (PentaRay™, Shaft size 7 French, Spline size 3 French, 2-6-2 mm interelectrode spacing, 1mm electrodes, Biosense Webster Inc, Diamond Bar, CA, USA) was introduced either retrogradely using standard sheaths or transeptally using the Agilis™NxT steerable introducer (St Jude Medical Inc., St Paul, MN, USA) into the left ventricle (LV) for mapping. Activated clotting time was maintained, with intravenous unfractionated heparin, between 250-300 seconds throughout the course of the study. After obtaining a left ventricular geometry on the electro-anatomic mapping system (EnsiteNavX™, St Jude Inc., St Paul, MN, USA), an endocardial contact map was acquired in sinus rhythm. At each location, before signal acquisition, stability and adequate splaying of the PentaRay™ splines over the endocardium was confirmed fluoroscopically and ventricular ectopic beats were vigilantly excluded. Mapping was targeted to regions of low voltage (<1.5mV) and sufficient sampling was performed elsewhere to have fill threshold of 15mm. Additional points were taken with quadripolar ablation catheter if there were regions difficult to access with the PentaRay™ catheter. All points projecting > 10mm from the geometry were considered of inadequate contact and were excluded. Regular definitions were used to describe preserved voltage (>1.5mV),

borderzone voltage (0.5-1.5mV) and dense scar (<0.5mV) [240]. Electrograms were classified according to the standard criteria [300] as:

i) normal (3 or fewer sharp intrinsic deflections from baseline, amplitude ≥3mV, duration <70ms, and/or amplitude: duration >0.046),

ii) fractionated (multiple intrinsic deflections and amplitude: duration ≤0.005),

iii) late (isolated component ≥20ms after the end of surface QRS), and

iv) very late potentials (isolated component ≥100ms after the end of surface QRS). Any electrogram not fitting into one of these categories were classified as other abnormal electrograms. Bipolar electrograms were filtered at 30 to 500 Hz, notch 50 Hz and presented at 100mm/s (LabSystem PRO v2.4a EP, Bard Inc., Lowell, MA, USA).

Bipolar pace mapping (MicroPace EPS 320 Cardiac Stimulator, Santa Ana, CA, USA) was performed at each location at 600ms cycle length or 50ms faster than the intrinsic sinus rate at constant output (10mA, 2ms) at sites with low voltage, fractionation and late electrograms. Pace-map locations were tagged on the electroanatomic surface. Entrainment mapping was performed whenever feasible at sites with abnormal electrograms, long S-QRS latencies and a paced QRS morphology matching VT. Standard criteria were used to define VT isthmus sites: concealed fusion with stimulus-QRS (S-QRS) interval that matched the electrogram-QRS interval (±20ms) and post pacing interval tachycardia cycle length difference (PPI-TCL) of ≤30ms [289]. If a mappable VT was rendered transiently non-inducible following PentaRay™ positioning in the zone of interest, entrainment pacing was reattempted with the ablation catheter.

### B. Control Group

The ventricular mapping with PentaRay™ catheter was performed prior to ICD implant. The protocol was similar as in the VT patients, however VT inducibility was tested post ICD implant through non-invasive programmed stimulation. If any VT induced spontaneously during mapping, entrainment mapping was attempted. No additional mapping was done with quadripolar mapping catheter. Heparin reversal was done at the end of ventricular mapping.

### C. POST-PROCESSING OF MAPS

The areas of low voltage and dense scar were measured using the integrated software. Offline analysis of the digitally stored electrograms and pace maps was performed on the Bard EP system with the use of on-screen calipers at a sweep speed of 200mm/s. Electrogram timing, duration and peak-to-peak voltage were measured manually and the locations of fractionated, late and very late potentials were registered on the electroanatomic surface. Pace-maps were physically searched and matched for at least 11/12 lead matches in the surface ECG QRS morphology. If the morphology matched a spontaneous or inducible VT, it was considered as a VT channel; otherwise it was classified as non-VT channel. The S-QRS interval was measured manually to the onset of QRS in the ECG lead with the shortest S-QRS [282]. A channel was fashioned from an orthodromically-activated sequence of identical pace maps when at least two pace maps with matching QRS morphology and dissimilar S-QRS (≥ 5ms) were identified, with at least one pace map having S-QRS ≥40ms [288]. So not to overestimate the channel length, the shortest endocardial distance joining at least 60% of the pertinent pace maps was used. This distance was determined using the incorporated software and was recorded as channel length. The remainder of the pace maps, if any extending beyond 1 cm of the main length, were considered as joint annexes to the channel. In stable VT, a channel was constructed connecting entrainment locations reasoned from inner loop sites in an orthodromic order of S-QRS latencies [223]. Conduction time and conduction velocity in the channel were ascertained as the difference between the longest and shortest S-QRS interval and the ratio of channel length to conduction time, respectively.

A pace-map location with multiple QRS morphologies was considered as a shared segment if remote pace-map locations with QRS morphologies corresponding to the index pace-map existed. Further, if two channels were perceived to cross each other on the anatomic surface, they were considered having a shared endocardial segment. As activation can exit in either direction of a channel with different QRS morphology, this may erroneously classify segments of VT channels as non-VT

channels. To reduce such possibility, the electroanatomic properties of isolated non-VT channels which did not have any shared pace maps or shared anatomic segments with VT channels (referred to as unshared non-VT channels) were separately compared with VT channels and with non-VT channels in the control group.

Small confluent areas (≥2 sampled points) of relatively preserved voltage (>0.5mV) surrounded by dense scar along their perimeter were referred to as islets and their relationship with channels was determined [250]. Fractionated and late potentials were considered presumed related to a channel location if they were sited within 1cm of the channel and their joint annexes.

### 4.2.3 STATISTICAL ANALYSIS

Baseline characteristics in VT patients and controls were presented as mean ± standard deviation for continuous data and counts for categorical data. Comparisons were performed using independent sample Student's *t*-test or chi-square ($\chi^2$) test (or Fischer exact test where applicable), as appropriate. To account for intrapatient clustering of data and interpatient differences, linear and non-linear mixed-effects models, clustered by patient identity (random effect), were used to examine the effect of channel type (fixed effect) on each of the outcomes. As several S-QRS intervals were recorded for each channel, to account for clustering within a channel, channel count within patient was also included as a random effect in the model comparing SQRS interval values between channel types. Linear, logistic and negative binomial mixed-effects models were used to explore the continuous, dichotomous and count outcomes, respectively. The results estimated from models are presented as mean ± standard error of mean for continuous outcomes, proportions with their 95% confidence interval (95% CI) for dichotomous outcomes and mean with 95% CI for count outcomes. The predictive performance of long S-QRS latency >80ms for a clinical channel location is expressed as odds ratio with its 95% CI. A meaningful analysis was not feasible for comparison with control group due to inadequate numbers of long SQRS >80ms in the control group. The S-QRS intervals were ranked

and 95$^{th}$ percentile values were reported for each channel group. The sensitivity and specificity of abnormal electrogram properties compared to VT channel location were computed. Moreover, the measure of agreement between VT channel locations and abnormal electrogram distribution in the scar was evaluated by Cohen's kappa (κ) test, with values of κ>0.4 indicating moderate agreement, and >0.6 good agreement. All calculations were performed using SAS 9.3 (SAS Institute Inc., Cary, NC, USA). A value of $p < 0.05$ was considered statistically significant.

## 4.3 RESULTS

### 4.3.1 BASELINE CLINICAL CHARACTERISTICS

Baseline characteristics of the patients are presented in Table 4.1. VT patients were well matched with the controls with respect to age, time to first infarction, revascularization history, LV function, QRS duration and use of beta-blockers. None of the patients in the control group were receiving amiodarone or other antiarrhythmic drugs at time of study. All patients had undergone a recent non-invasive evaluation or coronary angiography to exclude active ischemia.

### 4.3.2 INDUCIBLE VENTRICULAR TACHYCARDIA

Programmed ventricular stimulation was performed during the study average 3±2.5 times in VT patients and once in controls. All VT patients had one or more inducible, or spontaneous sustained monomorphic VT at baseline. Most patients had additional VTs induced during the course of study. Overall 73 different VTs were inducible, 3.3±1.6 VTs per patient, range 1 to 7, with a mean cycle length of 396±110ms. Only one patient in the control group had inducible sustained monomorphic VT (2VTs), while all others had inducible VF (two with programmed stimulation and two with R on T pacing only).

### 4.3.3 LEFT VENTRICULAR ENDOCARDIAL VOLTAGE MAPPING

The electroanatomic mapping parameters of the groups are shown in Table 4.2. Among VT patients, a mean number of 760±205 sampling points were taken per patient with 431±137 points within dense scar. Of the total left ventricular area (324±69cm$^2$), 60±15% (204±73cm$^2$) had low voltage, and 37±11% (128±56cm$^2$) was formed by dense scar. Islets of relatively preserved voltages (n=3±2.6, mean voltage 1.2±1 mV) were identified within dense scar in most patients.

The sampling density in controls was similar to VT patients. The control patients had similar overall total low voltage (203±88 cm$^2$, p=0.80) and dense scar area (85±48 cm$^2$, p=0.13), however the fraction of dense scar in the low voltage area was smaller in controls (61±16% vs 40±20%, p=0.02)

### 4.3.4 MAPPING OF CHANNELS

#### A. PACE MAPPING

In VT patients, pace mapping was performed in low voltage zones at 2507 sites, 114±62 per patient. Capture was absent at 670 sites (27%), 30±24 per patient. Of the captured sites, 1076 sites (49±42 per patient) had S-QRS interval ≥40ms that led to the assembling of channels. Pacemaps with S-QRS ≥40ms and ≥80ms were more frequent in VT patients (59% & 20%) than in controls (41% & 1%) (p<0.01). The distribution of pace maps among the various channel types is given in Table 4.3 and Figure 4.1. Overall, 428 pace maps corresponded to 57 inducible VT that formed the VT channel group while 838 pace maps belonged to the non-VT channel group. Sixteen inducible VTs could not be pace-mapped. Despite relative uniform pace mapping density in the scar, the average pace map count was higher in the VT channels [8 (95% CI 6.1 to 9.6)] compared to the non-VT channel group [5 (95% CI

3.7 to 5.7), p=0.0001]. Pace maps with S-QRS interval ≥40ms (mean 6, 95% CI 4.4 to 8.5 per channel) and ≥80ms [mean 1 (95% CI 0.7 to 2.7)] were more frequent in VT channels compared to non-VT channels [3 (95% CI 2.7 to 4.4) and 0.5 (95% CI 0.3 to 1.0) respectively, p<0.001]. These differences achieved greater significance when comparison was restricted to the unshared non-VT channels. Beat-to-beat variations in the S-QRS intervals were occasionally observed as varying degrees of exit block at paced sites with long latencies in the VT channel group.

The pace mapping density in controls was similar to VT patients (415 pace maps, 104±32 per patient, p=0.75). Capture was absent at 117 sites (28%), 29±13 per patient. When compared to the VT channels, channels in controls had fewer matching pace maps (mean 3.4, 95% CI 3.0 to 3.7, with less frequent S-QRS interval ≥40ms (mean 3, 95% CI 1.8 to 4.5, and rare S-QRS interval ≥80ms (p<0.01).

### B. ENTRAINMENT MAPPING

Entrainment mapping was feasible in 11 VT patients who had at least one potentially mappable VT. Overall, at the entrainment locations, diastolic potentials covering 52±22% of tachycardia cycle length could be identified within the PentaRay™ mapping catheter area. The participation of these diastolic potentials in the tachycardia circuit was demonstrated and isthmus locations could be confirmed in 6VTs (Figure 2.6 & Figure 4.2).

### C. VT CHANNELS

Fifty-seven VT channels (3±1 per patient) were identified. Fifty-four VTs could be mapped in the LV (Figure 4.3), while 3 had matching pace maps in the RV. Majority (95%) of these channels resided in the dense scar, with 48% of channels having segments extended into the borderzone. Islets of relatively preserved voltages were identified in the close neighborhood of 40% of VT channels. Twenty VT channels (35%) had shared pace map locations (4 channels) or shared anatomic segments (16 channels) with at least one another VT channel. The odds of finding a longest S-QRS

interval of >80ms were 5.9 times greater in a VT channel relative to an unshared non-VT channel (95% CI 2.6 to 13.6, p<0.0001). The joint annexes to the VT channels, identified in 24 VT channel regions, extended 18±7mm beyond the main length of the channel.

### D. NON-VT CHANNELS IN VT PATIENTS

The comparison between electroanatomic properties of VT channels, non-VT channels and unshared non-VT channels are presented in Table 4.4. All non-VT channels were mapped in the LV. Overall, 183 non-VT channels (8±6 channels per patient) were identified, with an average of 4.6 (95% CI 2 to 7) non-VT channels in a patient per VT channel. This included 33 non-VT channels (1±2 channels per patient) that shared pace maps (9 channels) or had shared anatomic segments with a VT channel (24 channels). The remaining 150 non-VT channels (7±5 channels per patient) belonged to the unshared non-VT channel group.

Unlike VT channels, unshared non-VT channels had a wider distribution with as many as 23% found in the borderzone voltage regions (p=0.036). Most of these channels (112/150, 75%) were located beyond 1cm of the VT channel regions. Islets of preserved voltages were infrequently identified adjacent to unshared non-VT channels (40% vs. 15%, p <0.001). Compared to the VT channels, the longest S-QRS interval (p<0.0001) and conduction time (p<0.0001) were shorter, the mapped channel length was shorter (p=0.0003) and conduction velocity (p=0.0008) was faster in unshared non-VT channels. Any S-QRS interval in an unshared non-VT channel was on an average 10ms shorter than in a VT channel (95% CI -18 to -2, p=0.018). The joint annexes to the unshared non-VT channels, identified in 18 channel regions, extended 18±7mm beyond the main length of the channel.

### E. NON-VT CHANNELS IN CONTROL PATIENTS

The conducting channels were abundant in control patients (9±8 per patient), with 11% located in the borderzone voltage regions (p=0.09 vs VT channels) (Figure 4.4).

Islets of preserved voltages were identified adjacent to 24% of non-VT channels (p=0.16 vs VT channels, p= 0.27 vs non-VT channels in VT patients). The longest S-QRS interval expressed from these channels (54±16ms) was significantly shorter compared to both types of channels in the VT patients (p<0.0001). The S-QRS interval in a non-VT channel in controls was 29ms shorter than in a VT channel (95% CI -46 to -12, p=0.0009) and 19ms shorter than in an unshared VT channel (95% CI -36 to -3, p=0.0214) in VT patients. The electroanatomic properties of these channels closely resembled the non-VT channels in VT patients, with shorter channel length, shorter conduction time and faster conduction velocity compared to VT channels (p≤0.01). The joint annexes to the non-VT channels, identified in 14 VT channel regions, extended 16±7mm beyond the main length of the channel.

### 4.3.5 Relationship of Channels and Scar Related Electrograms

Abnormal electrograms were frequently identified in low-voltage zones in VT patients (Table 4.5). However, of all the fractionated (mean 130±105), late (mean 10±5) and very-late (mean 4±3) potentials, only 22%, 30% and 35%, respectively were recorded in the VT channels. These electrograms had poor sensitivity but high specificity for locating a VT channel; fractionated potential 44% and 86%, late potential 4% and 99%, very late potential 2% and 99%, respectively. There was relatively poor agreement between abnormal electrogram site and a channel location (fractionated potential κ=0.2, late potential κ=0.05 and very late potential κ=0.03). Importantly, however, compared to elsewhere within the scar, in the region of VT channels fractionated potentials were longer in duration (105±2ms vs 95±2ms,p<0.0001), and very late potentials were more poorly coupled (311±31ms vs 226±23ms, p=0.030), but there were no differences in the coupling intervals of late potentials (43±5ms vs 45±5ms p=0.82).

There was no difference in the overall prevalence of fractionated (24±10% vs 28±17%, p=0.10), late (1.5±0.9% vs 0.8±1.0%, p=0.18) and very late potentials

(0.6±0.8% vs 0.2±0.1%, p=0.26) between VT patients and controls. However, fewer fractionated and late potentials were observed in the anatomic proximity of non-VT channels in controls than any of the channels in VT patients (p<0.01). Additionally, fractionated potentials were significantly broader (97±26 ms vs 89±18ms p <0.001) and of lower voltage (0.22±0.13 mV vs 0.25±0.15 mV, p <0.001) in VT patients compared to that in controls. Similar differences were observed in fractionated potentials related to channels in the two groups. There was no difference in the coupling intervals of late (42±21 ms vs 56±18 ms, p=0.21) and very late potentials (254±134 ms vs 271±62 ms, p=0.81) between VT patients and controls.

## 4.4 DISCUSSION

### 4.4.1 MAJOR FINDINGS

This study elucidated significant within group and between group differences in the electroanatomic properties of surviving myocyte channels in patients with ICM with and without spontaneous VT. The study bears significance in high-resolution sampling and concentrated pace mapping with a small electrode high-density catheter to demonstrate conducting channels within the ventricular scar. The main findings of the study are:

1. Channels supporting VT are more often located within the dense scar, express longer S-QRS intervals, are longer in length and have slower conduction velocity than channels which do not support VT across all groups of patients with ICM.
2. Channels in patients without spontaneous VT have similar characteristics to non-VT channels in patients with spontaneous VT.
3. Fractionated potentials residing in the VT channels are broader and very late potentials are poorly coupled relative to the non-VT channels.

4. In addition, patients with ICM and previous VT have larger proportion of dense scar in the total low voltage area and broader duration lower voltage fractionated electrograms than matched patients without previous VT.

These observations may explain the relative higher predilection of few selected surviving myocyte channels in the post infarct ventricles to sustain VT.

### 4.4.2 EARLIER STUDIES

Previous studies have evaluated the electroanatomic substrate in cardiomyopathy patients who present with VT in comparison to stable patients without previous VT [235, 241, 395]. All these studies have shown more extensive but non-homogeneous scarring and a higher proportion of abnormal electrograms in VT patients. Although important differences were observed, most of these studies lacked high density characterization of the scar due to relative paucity of sampling points. To the best of our knowledge, none of the previous studies have described properties of conducting channels and their relative differences. Several of the studies postulated frequent anatomically defined channels between fixed boundaries (scar, mitral annulus) as marker for complex substrate in ICM patients with VT [235, 236, 265] without specific evidence for a fitting VT.

Apart from the experimental works [148, 175], only a few clinical studies have looked at the electroanatomy of the channels. Areas of paced latencies ≥40ms in scar are observed to collocate with the isthmuses identified by entrainment mapping in patients with hemodynamically stable VT in ICM [288]. On similar kind, bands of user defined preserved voltages in the scar have been shown to pair with slow conducting zones [261]. These studies in hemodynamically stable VT report average isthmus lengths as 31±7 mm, and width as 16±8 mm [236, 261]. Ninety percent of such isthmuses reside within the scar while entrance and exits sites are found in the peripheral borderzone or normal myocardium. By employing high density mapping, we obtained electrical resolution in the ventricular scar to differentiate conducting

channels and segregate regions with unique electrogram and conduction properties that tend to support VT.

### 4.4.3 Relationship Between Scar And Borderzone

Generally, the arrhythmogenic substrate is not a simple single circuit but rather an extensive array of surviving myocardial fibers in a bed of scar tissue with multiple potential entry and exit points that allow for multiple reentrant paths (and different VTs) to traverse through scar [175, 241]. Although unapparent with the current electroanatomic mapping tools, the borderzone is not only at the periphery of the dense scar, but it is located at any of the interfaces between the surviving myocardial tissue and dense scar. The voltage threshold of 1.5mV is very specific, but has limited sensitivity, and fails to detect surviving myocytes in the scar [365]. These preserved fibers are characterized by abnormal electrophysiologic properties, including decreased cell-to-cell electrical coupling and slower conduction properties [94]. Some of these surviving tissues can be identified as visible small confluent islets of relatively preserved voltages surrounded by the scar. These islets may not necessarily participate in VT circuits [250]; however, they are considered as markers of anatomic proximity to other buried surviving myofibers that may have role in perpetuation of VT. The islets were more frequent in VT patients compared to the control group, and more often nested with regions of VT channels than with non-VT channels. This finding connects with the previous observations that post infarct VT circuits are often pinned at zones with greatest transitions in the thickness of surviving myocardium and resistance mismatches [237].

### 4.4.4 Concept of Channels

The concept that reentry occurs via isolated bundles of surviving myocytes at the border of the infarct and the larger subendocardial muscle mass has been proven in

histological studies in endocardially resected preparations from patients with post infarct VT [381]. The tachycardia route could be reconstructed in the zones of viable myocardial fibers that demonstrated low voltage pre-systolic activity during tachycardia and slow upstroke multiple deflection extracellular electrograms during sinus rhythm. These myocyte bundles are interwoven with strands of fibrous tissue and conduction velocity through the tracts is on the order of 0.25 m/sec [381, 382]. Microelectrode and optical mapping studies in various animal infarct models have also shown slow conduction through the infarct borderzone ranging from 0.015m/s to 0.7m/s that had high rate of VT inducibility [116, 396].

Although pace mapping is widely considered as a surrogate to locate surviving myofiber channels [277], the best channel length and conduction velocity estimated from orthodromic sequence of pacemaps may not strictly identify the actual electroanatomic properties of the channel and would best reflect only an 'apparent length' and an 'apparent conduction velocity'. Nonetheless, pacing in the scar can only identify non-VT channels. Thus, a uniform method for identification of two groups of channels holds these comparisons valid. Exiting QRS morphology while pacing from a VT channel can differ from the tachycardia due to lack of functional blocks during pacing [282, 288, 289]. We minimized selection of such VT channel zones that falsely exhibited non-VT QRS morphology by excluding non-VT QRS morphology channels that shared anatomic segments with VT channels. Expectedly, the differences in the electroanatomic properties among the channels were more robust with this selective omission.

### 4.4.5 Electrogram Properties

The deflections of the local electrogram realistically reflect the heterogeneity in the ultrastructural properties of the cardiac scar tissue [148]. The differences in density and orientation of surviving myofibers, extracellular matrix, fibrous tissue and variations in the cellular conductance between adjacent regions, result in regions with

resistance mismatches. This produces zigzag patterns of activation with high axial impedance [192]. Such regions are likely to harbor conduction pathways that support reentrant electrical activation. If a high resistance region in the scar boundaries with regions of low resistance, the activation wavefront has a window to exit and interact with the larger excitable myocardium. This was fittingly reflected by large population of abnormal electrograms in patients with VT, with broader fractionation and poorly coupled late potentials specifically in the VT channel regions, compared to the non-VT channels and controls. It partly explains lack of inducible VT in control patients, and also suggests that only finite regions within the scar have electrophysiological properties suitable to perpetuate reentrant VT.

### 4.4.6 Clinical Implications

Some components of the anatomic substrate are relatively fixed once infarction has occurred, however, in few patients they continue to evolve with the development of new circuits and advanced heart failure [22]. The incidence of new onset VT in ICM patients is 3% to 5% per year following first year of infarction over the ensuing 15 years [19]. This indicates that surviving myocyte channels present in at least some of the otherwise stable patients may mature favoring development of new VT. No study has tracked this evolution on a long time scale. Given the observed differences in the electroanatomic properties of the conducting channels in VT patients compared to controls, it is likely that during this believed evolution, zones of conduction delay or block coalesce to form longer corridors with slower conduction and thus express surrounding more complex fractionation and poorly coupled electrograms. It would be interesting to know how the electrograms from within the VT supporting channels change compared to their surrounding electrograms. In a similar context, coexisting non-VT channels in VT patients may evolve with progressive remodeling due to changing orientation of myofibers, repeated ischemic insults, chronic inflammation and laying down of fibrosis, and perpetuate new VTs [94].

Aggressive substrate modification by catheter ablation targeting all potential channels can theoretically minimize consequences from adverse remodeling. However appealing it may be, the longstanding arrhythmia free rate has not improved despite extensive ablation within the scar, with ~50% recurrences including new VT [301, 365]. This would suggest either failure of catheter ablation to arrest progressive scar remodeling despite its "apparent" homogenization, or pro-arrhythmic adverse effect of spot ablation in the scar only partially coalescing regions of conduction block. The lasting impact of high incidence of fast VT following catheter ablation on mortality in these patients also needs further investigation [279].

### 4.4.7 STUDY LIMITATIONS

Most VT were poorly tolerated precluding entrainment mapping and thus, localization of the VT channels relied heavily on paced latencies. Nevertheless, pace mapping is widely considered as a best surrogate to locate surviving myocyte channels [282], and an ultra high density pace mapping with rigorous matching criteria as was applied in our study ameliorates the ambiguity against a perfect channel. Additionally, as discussed, the non-VT channels can only be identified by pacing in the scar thus using an identical method for identification of channels held the comparisons valid. Despite relative uniform pace mapping density in the scar, the average pace map count was higher in the VT channels compared to the non-VT channel group. This might have contributed to the higher frequency of pace maps with long S-QRS intervals identified in the VT channel group. Constructively, however, it may essentially mean that while VT channels had long protected segments and thus had higher number of matching pace maps, variations in the QRS morphology were more frequent in non-VT channel regions such that only fewer matching pace maps could be identified in these regions. Pacing was done from closely spaced bipoles with small electrodes. This design favored finding small channels by pace mapping and reduced the size of virtual electrode, potentially eliminating the influence of capture away from the pacing electrodes [292]. We did not

adjust the voltages within dense scar to <0.5mV, a method that has been previously described to recognize and estimate dimensions of the channels [261, 297]. It is unknown if such offsetting of voltage within 0.1-0.5mV reflects greater healthy intramural tissue or absence of subendocardial scar [299]. Epicardial mapping was not done as all these patients had ischemic substrate and subendocardial scar, many with previous bypass surgery. It is likely that few VT and non-VT channels could have had intramural or epicardial circuits. Although non-sustained VT have been shown to possess small isthmus size [397], properties of non-VT channels are not expected to associate with non-sustained VT. The influence of anti-arrhythmic medications in VT patients on the conduction properties of channels has to be conceded. Functional changes in the refractoriness of myofibers and delay in conduction could have suppressed VT inducibility and affected, at least in part, the wider fractionation of electrograms and long S-QRS intervals. However, due to the nature of these patients this was unavoidable.

## 4.5 CONCLUSION

Channels supporting VT in ICM patients with spontaneous VT are lengthier, with longer conduction times and slower CV compared to channels in patients without spontaneous VT. Faster conducting non-VT channels co-exist in VT patients. Electrogram properties in regions of VT channels differ from elsewhere within the scar. These observations demonstrate why some ICM patients have spontaneous VT and others do not.

## TABLES

| Table 4.1 | Baseline Characteristics | | |
|---|---|---|---|
| | VT group | Control group | p value |
| N | 22 | 5 | |
| Age (years) | 67±10 | 62±7 | 0.26 |
| Male, n | 21 | 4 | 0.34 |
| Ejection fraction (%) | 32±8 | 29±6 | 0.49 |
| Time to first infarction (years) | 14±10 | 11±14 | 0.58 |
| Coronary bypass surgery, n | 11 | 3 | 1.00 |
| Rhythm, n | | | |
| Sinus rhythm | 18 | 5 | 0.59 |
| Atrial fibrillation | 1 | | |
| Ventricular paced rhythm | 3 | | |
| QRS duration, ms | 143±37 | 140±21 | 0.85 |
| VT cycle length, ms | 384±116 | | |
| VT storm, n | 7 | | |
| Previous ICD, n | 19 | | |
| Beta blocker, n | 20 | 5 | 1.00 |
| Amiodarone, n | 13 | 0 | 0.04 |
| Other antiarrhythmic drugs (Sotalol, Mexilitene), n | 8 | 0 | 0.28 |

VT=Ventricular Tachycardia, ICD=Implantable Cardioverter Defibrillator
Data presented as x±y format represent mean±SD

| Table 4.2 | Electroanatomic Mapping Data | | |
|---|---|---|---|
| | **VT patients** | **Control** | **p value** |
| **Number of sampling points** | 760±205 | 616±104 | 0.14 |
| **Number of sampling points in dense scar** | 431±137 | 310±69 | 0.04 |
| **Total endocardial area ($cm^2$)** | 324±69 | 303±45 | 0.51 |
| **Endocardial dense scar area ($cm^2$)** | 128±56 | 85±48 | 0.13 |
| **Endocardial dense scar area (%)** | 37±11 | 28±16 | 0.15 |
| **Endocardial total low voltage area ($cm^2$)** | 204±73 | 203±88 | 0.80 |
| **Endocardial total low voltage area (%)** | 60±15 | 66±23 | 0.53 |
| **Endocardial dense scar component of total low voltage area (%)** | 61±16 | 40±20 | 0.02 |
| **Number of high voltage islets** | 3±3 | 2±2 | 0.28 |
| **Fractionated potentials proportion (%)** | 24±10 | 28±17 | 0.46 |
| **Fractionated potentials duration (ms)** | 97±26 | 89±18 | <0.001 |
| **Fractionated potentials amplitude (mV)** | 0.22±0.13 | 0.25±0.15 | <0.001 |
| **Late potentials proportion (%)** | 1.5±0.9 | 0.8±1.0 | 0.18 |
| **Late potentials coupling interval (ms)** | 27±22 | 27±28 | 0.50 |
| **Very late potentials proportion (%)** | 0.6±0.8 | 0.2±0.1 | 0.28 |
| **Very late potentials interval (ms)** | 254±134 | 271±62 | 0.51 |
| **Number of Pace maps** | 114±62 | 104±32 | 0.75 |

VT=Ventricular Tachycardia
Data presented as x±y format represent mean±SD

| Table 4.3 | Distribution of pace-maps among VT and Non-VT channels in VT patients and Controls | | | | | | | |
|---|---|---|---|---|---|---|---|---|
| | VT Group | | | | | Controls | | |
| Property | VT channels | Non-VT channels | p-value* | Unshared Non-VT channels | p-value* | Non-VT channels | p-value | |
| | | | | | | | Vs. VT channels | Vs. Unshared Non-VT channels in VT group |
| Pace map count | 428 | 838 | | 613 | | 155 | | |
| Number per channel | 8 (6.1,9.6) | 5 (3.7,5.7) | 0.0001 | 4 (3.2,5.1) | <0.0001 | 3.4 (3.0,3.7) | <0.0001 | 0.18 |
| Pace maps with S-QRS ≥ 40ms (%) | 360 (84) | 774 (92) | | 562 (92) | | 123 (79) | | |
| Number per channel | 6 (4.4,8.5) | 3 (2.7,4.4) | 0.0008 | 3 (2.4,4.0) | 0.0001 | 3 (1.8,4.5) | 0.002 | 0.74 |
| Pace map with S-QRS ≥ 80ms (%) | 123 (29) | 191 (23) | | 138 (23) | | 2 (1) | | |
| Number per channel | 1.4 (0.7,2.7) | 0.5 (0.3,1.0) | 0.0004 | 0.4 (0.2,0.8) | <0.0001 | 0.03 (0.0,0.2) | <0.0001 | 0.0015 |

VT= ventricular tachycardia, S-QRS = Stimulus-QRS interval

* versus VT channel

Data presented as x(y,z) format represent mean count (95%CI)

| Table 4.4 | Comparison of Properties of VT channels, Non-VT channels in the VT group, and Non-VT channels in the Controls | | | | | | | |
|---|---|---|---|---|---|---|---|---|
| Property | VT group | | | | | Controls | | |
| | VT channels | Non-VT channels | p-value* | Unshared Non-VT channels | p-value* | Non-VT channels | p-values | |
| | | | | | | | Vs. VT channels | Vs. Unshared Non-VT channels in VT group |
| Total number | 57 | 183 | | 150 | | 46 | | |
| Number per patient | 3±1 | 8±6 | <0.001 | 7±5 | <0.001 | 9±8 | 0.001 | 0.65 |
| Location in Scar, % | 97 (87,99) | 81 (63,92) | 0.064 | 77 (54,90) | 0.036 | 89 (67,97) | 0.092 | 0.23 |
| Longest S-QRS, ms | 131±8 | 78±7 | <0.0001 | 75±7 | <0.0001 | 54±16 | <0.0001 | <0.0001 |
| 95$^{th}$percentile value | 360 | 136 | | 134 | | 81 | | |
| Any S-QRS, ms | 73±4 | 63±3 | 0.020 | 63±3 | 0.018 | 44±8 | 0.0009 | 0.021 |
| 95$^{th}$percentile value | 161 | 108 | | 108 | | 72 | | |
| Length, mm | 53±5 | 34±4 | 0.0003 | 33±4 | 0.0002 | 24±8 | 0.0014 | 0.30 |
| Conduction time, ms | 103±13 | 47±12 | <0.0001 | 43±12 | <0.0001 | 29±27 | 0.0134 | 0.63 |
| Conduction velocity, m/s | 0.85±0.21 | 1.29±0.19 | 0.021 | 1.39±0.20 | 0.008 | 1.31±0.41 | 0.005 | 0.87 |

VT= ventricular tachycardia, S-QRS = Stimulus-QRS interval

* versus VT channel

Data presented as x(y,z) format represent mean proportion (95%CI)

Data presented as x±y format represent mean±SEM, except channel number per patient which is mean±SD

**Table 4.5** Comparison of Scar Related Electrograms in Channel Regions Versus Rest of Scar

| Electrogram type | | Electrogram location: VT group | | | | Controls | | | | |
|---|---|---|---|---|---|---|---|---|---|---|
| | | VT channels (X) | Non-VT channels (Y) | Rest of Scar | p value | Non-VT channels | Rest of Scar | p values‡ | | |
| | | | | | | | | Vs. Rest of Scar | Vs. (X) | Vs. (Y) |
| Fractionated potential | Total Number (%) | 607 (22) | 761(28) | 1462 (52) | | 230 (27) | 635 (73) | | | |
| | Number Per Channel | 15 (11,20) | 16 (13,20) | | 0.71 | 8 (6,12) | | | 0.007 | 0.001 |
| | Duration, ms | 105±2 | 101±2 | 95±2 | <0.0001* | 90±5 | 88±4 | 0.20 | 0.004 | 0.038 |
| | Amplitude, mV | 0.22±0.01 | 0.22±0.01 | 0.22±0.01 | 0.25 | 0.26±0.01 | 0.24±0.01 | 0.16 | 0.038 | 0.015 |
| Late potential | Total Number (%) | 59 (30) | 68 (34) | 139 (70) | | 0 | 27(100) | | | |
| | Number Per Channel | 1.3 (0.8,2.1) | 0.9 (0.6,1.2) | | 0.19 | 0 | | | - | - |
| | Coupling interval, ms | 43±5 | 45±5 | 42±3 | 0.81 | - | 56±18 | - | - | - |
| Very late potential | Total Number (%) | 26 (35) | 7(8) | 48 (65) | | 3(75) | 1(25) | | | |
| | Number Per Channel | 0.4 (0.2,0.8) | 0.1 (0.0,0.3) | | 0.009 | 0.1 (0.0,0.4) | | | 0.07 | 0.94 |
| | Coupling interval (ms) | 311±30 | 250±58 | 226±23 | 0.030† | 264±80 | - | - | 0.59 | 0.88 |

VT: ventricular tachycardia

*p=0.0035VT channels versus Non-VT channels, p<0.0001 VT channels versus Rest of scar, p<0.0001 Non-VT channels vs Rest of scar

†p=0.33 VT channels versus Non-VT channels, p=0.008 VT channels versus Rest of scar, p=0.7 Non-VT channels vs Rest of scar

‡ of Non-VT channels in Controls

Data presented as x(y,z) format represent mean count (95%CI)

Data presented as x±y format represent mean±SEM

## FIGURES

### *FIGURE 4.1*

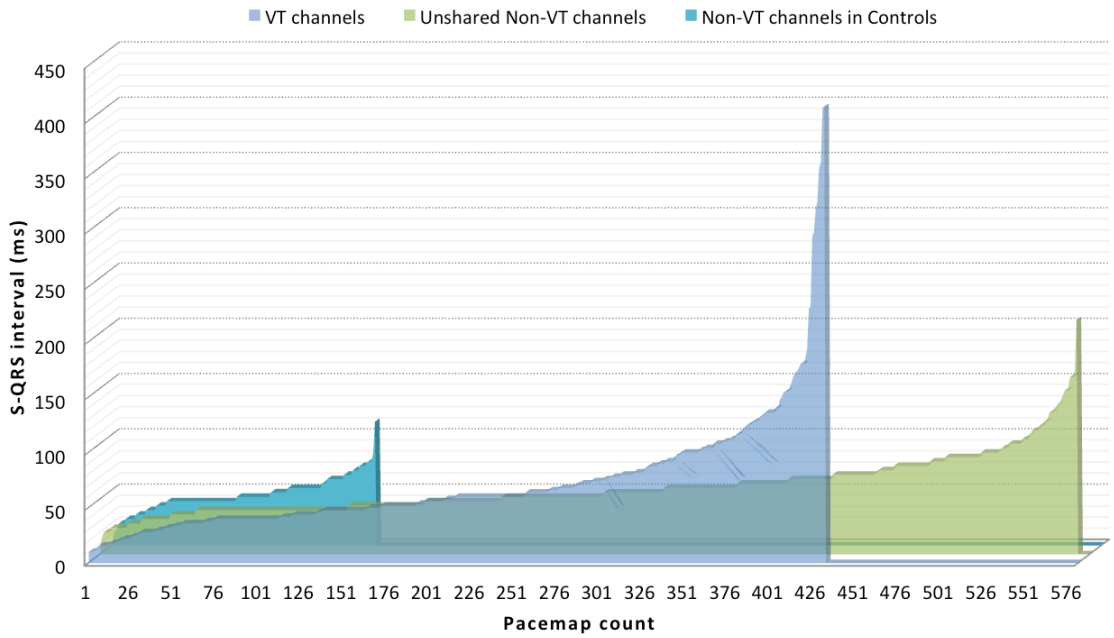


**Figure 4.1.** Stacked S-QRS interval plots for VT, unshared non-VT channels and non-VT channels in controls. The length at each step indicates number of pacemaps while the step height corresponds to the S-QRS interval. There is relative tall distribution of S-QRS intervals in VT channels compared to the unshared non-VT channels and non-VT channels in controls.

***FIGURE 4.2***

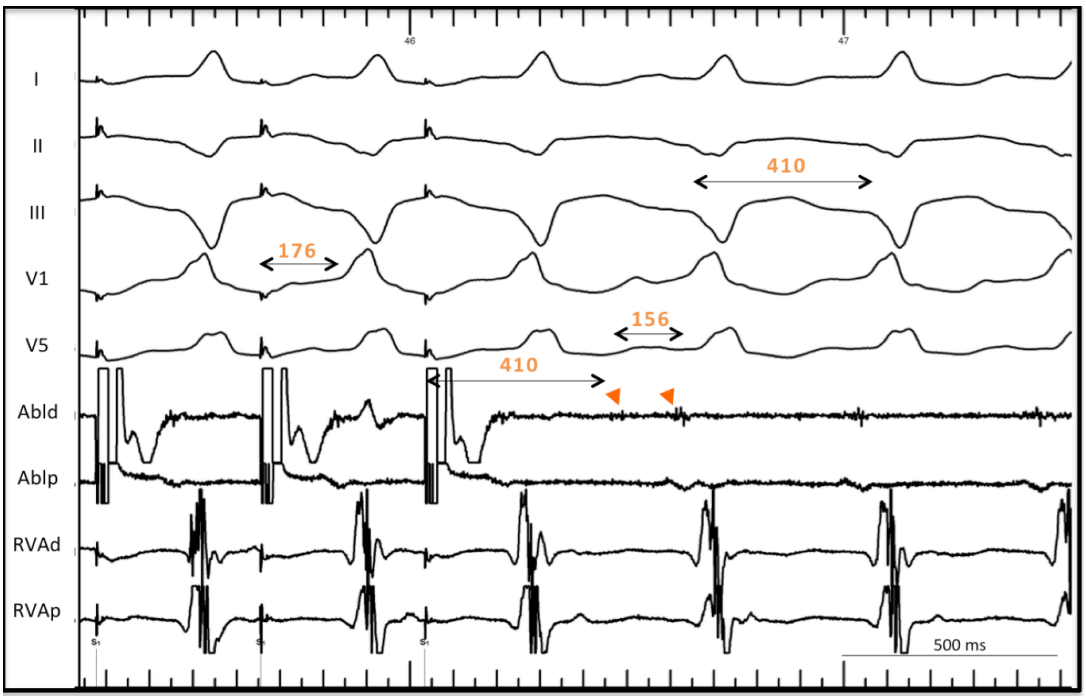


**Figure 4.2.** Entrainment pacing (Abld) and its termination during a VT. Channels shown are surface ECG (I, II, III V1, V5), ablation distal (d) and proximal (p) in left ventricular scar, right ventricular apex [RVA, (d) and (p)]. Intervals are marked in milliseconds. This pacing site entrained the VT with concealed fusion with a S-QRS interval of 43% of the TCL, S-QRS and electrogram-QRS interval difference of 20ms and the diference between post pacing interval and tachycardia cycle length is 0 ms. The diastolic potentials are seen on the Abl(d) during tachycardia (arrows). This site represented the central isthmus for this VT.

***FIGURE 4.3***

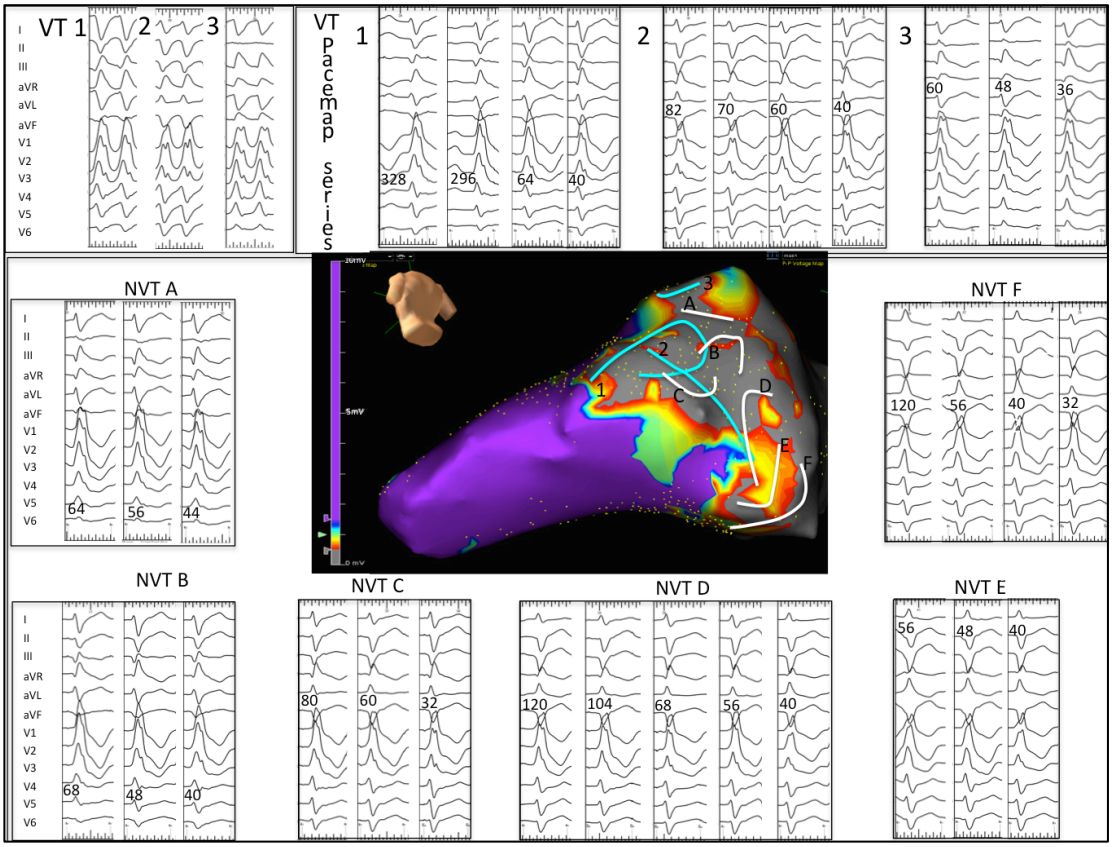


**Figure 4.3.** Case Example of a VT group patient. *Centre.* Voltage map on Ensite NavX™ in left posterior caudal view showing large scar (grey) in the postero-lateral left ventricle. VT (1 to 3) and non-VT channels (A to F) are displayed as lines. *Top*. Three inducible VTs (VT 1 to 3) and their corresponding pace map series. Numbered locations (1 to 3) on the NavX™ voltage map correspond to the first pace map of the respective series. *Centre and Bottom.* Pace map series for six non-VT channels (NVT A to F) with labeled locations on the NavX™ voltage map corresponding to the respective series. NVTs B, C and D shared pace map locations or anatomically crossed with VT channels. Only NVT channels A, E and F were included in the unshared NVT channel group.

***FIGURE 4.4***

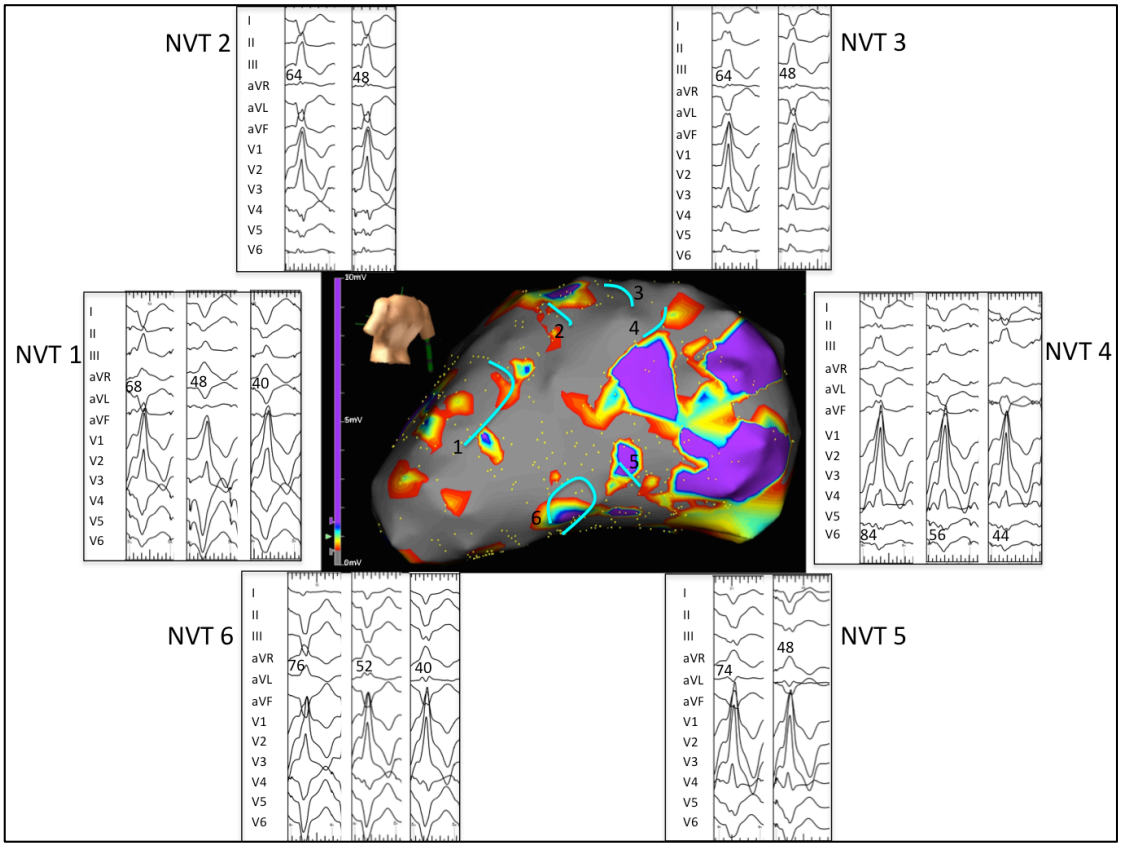


**Figure 4.4** Case Example of a Control patient. Voltage map on Ensite NavX™ in left posterior lateral view showing large scar (grey) in the lateral left ventricle. Pace map series for six non-VT channels (NVT 1 to 6) with numbered locations on the NavX™ voltage map corresponding to the first pace map of the respective series. Non-VT channels (1 to 6) are displayed as lines.

# CHAPTER 5. AUTONOMIC MODULATION OF REPOLARIZATION INSTABILITY IN PATIENTS WITH HEART FAILURE PRONE TO VENTRICULAR TACHYCARDIA

## ABSTRACT

**Background.** QT variability (QTV) signifies repolarization lability and increased QTV is a risk predictor for sudden cardiac death. The aim of this study was to investigate the role of autonomic nervous system activity on QTV.

**Methods.** The study was performed in 29 subjects: 10 heart failure patients with spontaneous ventricular tachycardia [HFVT(+)], 10 heart failure patients without spontaneous VT [HFVT(-)], 9 subjects with structurally normal heart ($H_{Norm}$). Beat-to-beat QT interval was measured by automated analysis on 8-minutes records of surface ECG at baseline and during interventions [atrial pacing at 80bpm and 100bpm, esmolol (0.3 mg/kg/min), isoprenaline (3 μg/min) and atropine (0.04 mg/kg single dose) infusion]. Variability in QT intervals was expressed as the standard deviation of all QT intervals (SDQT) at baseline and in the last 3-minutes during interventions. An index of QTV normalized to heart rate variability (QTV/HRV) was calculated as ratio of SDQT to SDRR.

**Results.** There was a trend towards the baseline QTV/HRV being higher in HFVT(+) group compared to HFVT(-) and $H_{Norm}$ groups (p=0.09). QTV became significantly higher in HFVT(+) and HFVT(-) groups compared to $H_{Norm}$ patients during fixed rate atrial pacing (p=0.008). Compared to baseline, isoprenaline increased QTV in $H_{Norm}$ group (p=0.02), but not in HF patients. QTV remained elevated in HFVT(+) group relative to $H_{Norm}$ group despite acute beta-adrenoceptor blockade with esmolol (p= 0.02).

**Conclusion.** Patients with HF and spontaneous VT have larger fluctuations in beat-to-beat QT intervals. This appears to be a genuine effect that is not solely a consequence of heart rate variation. The effect of acute autonomic nervous system modulation on QTV appears to be limited in HF patients.

## 5.1 INTRODUCTION

Ventricular tachyarrhythmias related to structural heart disease are the most common cause of sudden cardiac death (SCD) in the Western world [36]. Many of these occur in patients with ventricular scarring, related predominantly to coronary artery disease or dilated cardiomyopathies. Such scarring produces non-homogenous myocyte loss, diminished myocyte coupling, ion channel dysfunction, and thus spatial heterogeneity in ventricular action potential repolarization and prolonged $QT_C$ interval that predispose to ventricular arrhythmias and SCD [44-49]. Superimposed on this spatial heterogeneity, temporal (beat-to-beat) variation in cardiac repolarization across the ventricle has been recognized and shown to be elevated in ischemia and heart failure [50-53]. Increased QT variability (QTV) on the surface ECG, which is arguably a marker for compound spatio-temporal heterogeneity in repolarization, was found to predict appropriate device therapies in the MADIT-II (Multicenter Automatic Defibrillator Implantation Trial-II) study, as well as total and arrhythmic deaths in heart failure patients without defibrillators [54-56].

Common mechanisms influencing QTV include heart rate variability, autonomic changes and repolarization reserve, each of which has been studied in normal hearts [58-61]. In contrast, the exact physiologic mechanisms and the role of QTV in arrhythmogenesis in heart failure are poorly understood. There is evidence suggesting that enhanced beat-to-beat fluctuations in repolarization duration in heart failure do not reflect merely incidental changes in heart rate and electrical restitution [50-52]. As interventions that increase sympathetic stimulation shorten ventricular repolarization duration, increase spatial dispersion in repolarization and increase QTV in normal hearts [60, 62], the elevated QT interval variability in heart failure may result from enhanced sympathetic drive and subsequent diminution in repolarization reserve in these patients [63, 64]. On the other hand, primary reduction in repolarization reserve itself, which is commonly seen in structural heart disorders [65, 66] may be the principle driver of elevated QTV in these patients [67]. Given the contrasting differences in the over-all milieu in subjects with normal and myopathic

hearts, it is imperative to understand the central mechanisms underlying elevated QTV in patients with heart failure. In this study, we will therefore examine the effect of arrhythmogenic substrate on QTV in heart failure subjects and whether it can be modulated by autonomic variations.

## 5.2 METHODS

### 5.2.1 PATIENT POPULATION

The study population included 29 patients; ten patients with ischemic or dilated cardiomyopathy undergoing clinically indicated ventricular tachycardia (VT) ablation [HFVT(+) group], 10 patients with ischemic or dilated cardiomyopathy undergoing clinically indicated implantable cardioverter defibrillator (ICD) implantation as per primary prevention guidelines [84] [HFVT(-) group] and 9 patients with structurally normal hearts undergoing electrophysiological study (EPS) and catheter ablation for supraventricular tachycardia ($H_{Norm}$ group). All baseline medications were continued at the time of study. All patients with ischemic cardiomyopathy had undergone a recent non-invasive evaluation or coronary angiography to exclude active ischemia. Patients less than 18 years of age, permanent atrial fibrillation, sinus node disease (resting heart rate <40bpm), ventricular preexcitation, heart block, permanent atrial or ventricular pacing, uncontrolled heart failure, acute coronary event within the preceding 1month and asthma were excluded. All patients provided informed consent, and the study was approved by the Human Research Ethics Committee of the Royal Adelaide Hospital and the University of Adelaide.

### 5.2.2 ECG RECORDING

Body surface 12 lead ECG was recorded before the intended procedure for 8 minutes under resting conditions at a sampling frequency of 1000 Hz with Bard electrophysiology system (LabSystem PRO v2.4a EP, Bard Inc., Lowell, MA, USA). The patients rested for at least 30 minutes before the actual recording started. All procedures were formed under light conscious sedation with intravenous midazolam (1-2mg) and fentanyl (25-50µg).

#### A. PATIENTS UNDERGOING VT ABLATION

Catheters were positioned at right ventricular apex and in the coronary sinus through femoral vein. Atrial pacing was performed at two cycle lengths, 80bpm (Pa80) and 100 bpm (Pa100), (MicroPace EPS 320 Cardiac Stimulator, Santa Ana, CA, USA), each for 8 minutes. If intrinsic rate was fast, maximum pacing rate was allowed up to 90bpm and 110 bpm, respectively. Pharmacological interventions were then individually commenced through a peripheral vein: esmolol (a selective $beta_1$-receptor blocker, 0.05-0.3 mg/kg/min), followed by isoprenaline infusion (1-3 µg/min) and then atropine (0.04 mg/kg single dose). This sequence of drug administration was followed in all subjects, in accordance with rapid elimination pharmacokinetics of esmolol and isoprenaline compared to atropine [398]. The ECG during each intervention was recorded continuously for 8 minutes [399]. The infusion of esmolol and isoprenaline were rapidly up titrated to achieve their respective maximal dose within the first 3 minutes, which then continued until the end of each recording. A compulsory time gap of at least 5 minutes was allowed for drug washout after each intervention with end-point as return of heart rate to baseline value. The presence of atrial or ventricular ectopy and pacing was permitted unless such beats represented >5% of all beats over a 5-minute period. Programmed ventricular stimulation was then performed to assess the inducibility of VT and the procedure for VT ablation continued as per the institutional protocol.

#### B. PATIENTS UNDERGOING ICD IMPLANTATION

The experimental protocol was similar to that applied in the HFVT(+) group; however, atrial pacing was performed through the pacing lead of the implanting device, temporarily positioned in the right atrium, using a compatible pacing system. Pharmacological interventions were performed post ICD implantation. Programmed ventricular stimulation was then performed through non-invasive EPS to assess for inducibility of VT.

#### C. PATIENTS UNDERGOING ELECTROPHYSIOLOGICAL STUDY

Catheters were positioned through femoral vein in the coronary sinus and right ventricle. The experimental protocol was similar to that of the HFVT(+) group; however, pharmacological interventions were performed post EPS and catheter ablation.

### 5.2.3 QT INTERVAL VARIABILITY ANALYSIS

---

The recorded ECG data was stored on removable media for semi-automated offline analysis. To obtain QT intervals, usually lead I was chosen. If the signal was bad in lead I, then an alternative lead with tall T wave was preferred. The algorithm proposed by Berger et al. [50] was used to measure beat-to-beat QT intervals. The operator defines a template QT interval on the chosen ECG channel by selecting the beginning of the QRS complex and the end of the T wave ($T_{end}$) for one beat. The algorithm then finds the QT interval of all other beats by determining how much each T wave must be stretched or compressed in time to best match the template (Figure 5.1). As this method takes into account the whole T wave instead of determining $T_{end,}$ it is less susceptible to the measurement noise associated with beat-to-beat delineation of $T_{end}$ [400]. To account for slow adaptation of the QT interval to the heart rate and intervention, only last 3 minutes of each 8-minute recording

was used for the purpose of analysis in the study [58]. Ventricular ectopic and paced beats were detected automatically based on ECG QRS morphology, and were excluded from analysis.

Variability in the beat-to-beat QT intervals was quantified using the standard deviation of QT intervals (SDQT) during the 3-minute epochs [401, 402]. QTV relative to heart rate variability (QTV/HRV) was computed as the ratio of standard deviations of QT to RR intervals (SDQT/SDRR) [401]. Rather than separating QTV from HRV, this metric can be regarded as a composite measure of heart rate and QT variability. Definition and data on additional metrics of repolarization variability [Normalized QTV (QTVN), QTV index (QTVi), short term variability ratio ($STV_{Ratio}$)] are presented in the supplemental data.

### 5.2.4 STATISTICAL ANALYSIS

Baseline demographic variables are presented as means ± standard deviation for continuous data and counts for the categorical data. Comparisons between the three groups: HFVT(+), HFVT(-) and $H_{Norm}$, were carried out using one way analysis of variance with post hoc multiple comparisons by Bonferroni method, or by chi-square ($\chi^2$) test (or Fisher's exact test) as applicable.

To test for a difference in electrocardiographic parameters at baseline between the three groups, one way analysis of variance was used. To test if changes in ECG measurements from baseline to pacing or pharmacological intervention differ between groups, a linear mixed-effects model was used. Within these models, intervention (e.g. basal/ P80/P100 or basal/esmolol/isoprenaline/atropine) and group [HFVT(+), HFVT(-), $H_{Norm}$] were included as fixed effects and patient ID was included as a random effect to account for dependence within a patient. Initially an interaction term between intervention and group was included in the linear mixed-effects models. However, in every case this interaction term was not significant so

the final models contained only main effects, for which means and post hoc contrasts are presented. Results are presented as means ± standard error of means (SEM). Plots of model estimated means are shown for each ECG measure by pacing or pharmacological intervention.

The statistical software used was SAS 9.3 (SAS Institute Inc., Cary, NC, USA). Two-sided $P < 0.05$ was considered statistically significant.

## 5.3 RESULTS

### 5.3.1 PATIENT CHARACTERISTICS

The demographic characteristics of the patient groups are presented in Table 5.1. Other than VT inducibility, the baseline features in HFVT(+) group were closely matched with the HFVT(-) group. Majority of patients in HF groups (19/20 patients) were on long-term stable dose of an oral beta-blocker before investigation. The $H_{Norm}$ group patients were younger, predominantly women, and most patients (6/9 patients) were not taking any medications.

The effects of pacing and pharmacological interventions in the three groups of patients have been summarized in Table 5.2, and further illustrated with respective means plots in Figures 5.2 and 5.3.

### 5.3.2 HEART RATE RESPONSE

The mean basal RR interval was longer in HFVT(+) patients compared to the $H_{Norm}$ group (p=0.01). In all the three groups, compared to the basal RR interval, the mean RR interval increased marginally with esmolol (p=0.09), shortened significantly after

isoprenaline (p=0.02) and with atropine (p<0.001). The relative baseline difference between HFVT(+) and $H_{Norm}$ patients was maintained during all pharmacological interventions (p=0.04).

### 5.3.3 HEART RATE VARIABILITY

Basal mean heart rate variability (mean SDRR) was <50 ms in both the HF groups but this was not significantly different to the $H_{Norm}$ group (p=0.26). Atrial pacing abolished HRV in all groups of patients (p<0.001). There was a trend towards improvement in HRV after beta-blockade with esmolol (p=0.08) mainly in the HFVT(+) group. It did not change with isoprenaline (p=0.63), but reduced drastically after atropine (p=0.001) in all the three groups.

### 5.3.4 QT RESPONSE

The mean basal uncorrected QT interval was longer in HFVT(+) patients compared to HFVT(-) (p=0.02) and $H_{Norm}$ (p=0.004) groups. Compared to the basal state, mean QT interval shortened with atrial pacing at 80 bpm (p=0.001) and 100bpm (p<0.001), with isoprenaline (p=0.03) and atropine (p=0.02) in all the three groups. The relative baseline differences among HFVT(+), HFVT(-) and $H_{Norm}$ groups were maintained during all pharmacological interventions (p=0.02).

### 5.3.5 QT VARIABILITY

Group mean values in basal QTV were higher in HF patients compared to the $H_{Norm}$ group, but these differences were not significant (p=0.21). Atrial pacing augmented

these differences in QTV. Both HF groups had significantly higher QTV than $H_{Norm}$ group during atrial pacing [p=0.008; p=0.006 for HFVT(+) vs $H_{Norm}$ and p=0.007 HFVT(-) vs $H_{Norm}$]. Considered independently, atrial pacing did not reduce QTV in any of the patient groups (p=0.1). Esmolol (p=0.47) and atropine (p=0.42) failed to produce any significant change in QTV in HF subjects, and it remained higher than $H_{Norm}$ patients (p=0.02). Isoprenaline increased QTV in $H_{Norm}$ patients (p=0.02) but not in the HF groups (overall main effect of intervention p=0.39).

### 5.3.6 QT VARIABILITY/HEART RATE VARIABILITY RATIO

In the basal state, there was a trend towards the QTV/HRV ratio being higher in HFVT(+) patients compared to HFVT(-) and $H_{Norm}$ patients (p=0.09). While esmolol (p=0.51) and isoprenaline (p=0.50) had a neutral effect, QTV/HRV increased considerably after atropine (p=0.001), principally due to a reduction in HRV in all the three groups.

## 5.4 DISCUSSION

### 5.4.1 MAJOR FINDINGS

This study explored the physiologic mechanisms involved in electrocardiographic beat-to-beat QTV in heart failure subjects and their differences compared to the normal hearts. The main findings from the study are:

1. Beat-to-beat repolarization instability is high in patients with heart failure, who are prone to recurrent VT.
2. This appears to be independent of HRV, and remains high despite uncoupling the effect of heart rate.
3. Acute therapy with a beta-blocker improves HRV, however fails to reduce QTV.

### 5.4.2 PREVIOUS STUDIES

Short-term variability in QT intervals is considered a surrogate marker of subtle fluctuations in repolarization duration between consecutive beats [403]. The control of sinus node activity via sympatho-vagal modulation resulting in HRV is well established [404]. In contrast, the physiologic mechanisms that give rise to or alter QTV are not fully recognized. In healthy hearts, interventions that increase sympathetic tone such as sudden standing and infusion of isoprenaline were shown to increase QTV [60], while pharmacological blockade of beta-adrenoreceptors reduces QTV [405]. Similarly, hypertensive subjects with otherwise normal heart were shown to have high QTV that correlated with their cardiac norepinephrine spillover and systolic blood pressure [400]. A recent study in dogs also showed that QT variability was related to left stellate-ganglion activity, but only after the dogs had developed heart failure [406]. As sympathetic tone is elevated in heart failure [407], and QTV is elevated in heart failure [50], it is appealing to believe that autonomic influences have bearing on ventricular repolarization lability in these patients. However, Baumert et al recently challenged the notion that QTV provides an assessment of the cardiac autonomic activity, when resting QT variability measures did not correlate with norepinephrine levels in blood sampled from the coronary sinus in subjects with depression and panic disorder [403]. It is possible that in normal subjects during rest, the sympathetic tone is too low to affect QTV and it needs stimulation to stage a proportionate change above background QTV.

In our study, augmented beta-blockade with esmolol failed to bring down repolarization instability in both HFVT(+) and HFVT(-) patients. This suggests that other local competing mechanisms possibly override sympathetic influences on QTV in electrically remodeled hearts. The down-regulation and desensitization of $beta_1$-adrenoceptors in chronic heart failure [408, 409] can only partly explain the lack of efficacy of acute beta-adrenoceptor blockade on QTV as trend towards heart rate slowing in HF patients observed following esmolol was comparable to the $H_{Norm}$ subjects. Stable chronic therapy with beta-blockers and/or antiarrhythmic drugs in

HF patients may have attenuated the affect of supplementary beta-blockade in these patients. Nonetheless, high baseline QTV in chronically treated HF patients, as observed in our as well as in previous studies [56], suggests that even long-term beta-blockade therapy is probably insufficient to bring down high repolarization instability at least in some of these patients.

As observed in previous studies [60], we were able to replicate the increase in QTV with isoprenaline in $H_{Norm}$ subjects. However, this alteration was absent in HF groups, strengthening the notion that sympathetic influences may only have limited influence on beat-to-beat repolarization stability [403, 410]. Additionally, as protracted sympathetic stimulation in chronic heart failure reduces repolarization reserve [63], the autonomic status presumably ceases to notably affect QTV. Furthermore, in $H_{Norm}$ patients, we were not able to demonstrate reduction in QTV from baseline values by beta-blockade with esmolol. It is possible that high repolarization reserve in these patients from functionally normal ion currents raises threshold for repolarization lability that fails to get significantly modulated with pharmacological sympathetic blockade. It is also conceivable that QTV, especially during rest, is already at its nadir in normal hearts and sympathetic tone is low, so beta blockade would not have a significant effect. This is also in line with the observation that QTV did not correlate with left stellate ganglion activity in dogs with normal heart [406]. The contrasting results in a previous study [405] where beta-blockade with propranolol reduced QTV in individuals with structurally normal hearts, is likely due to methodological differences. The effect of propanolol was evaluated during fixed rate atrial pacing, hence propanolol expectedly only abolished the effects of the incidental surge in sympathetic outflow that was associated with cardiac pacing [411].

### 5.4.3 Relation with Heart Rate Variability

The QT interval is intimately linked to heart rate, reflecting the adaptation of ventricular action potentials to the diastolic interval under physiological conditions

(electrical restitution) [58]. The QT interval adaptation to heart rate changes comprises an immediate response to RR interval change paralleled by a slow, more gradual change that may take several minutes [412]. Constant pacing can abolish the effect of physiological HRV on QTV; residual variance in QT despite no HRV likely indicates genuine fluctuations in ventricular activity independent of changes in heart rate [413]. These may be due to direct autonomic influence, respiration or underlying ventricular pathology [414]. Increased short term QTV uncoupled with HRV has been shown in the setting of ischemic and non-ischemic heart disease [50-53] and is an independent predictor of future VT and SCD in these patients [54-56]. Alongside this strong evidence, a recent study detected changes in RR and QT dynamics during the few hours preceding malignant ventricular arrhythmias [415].

We demonstrated persistently high QTV in HFVT(+) group during short-term fixed rate atrial pacing suggesting mechanisms other than HRV may have a dominant role in QT regulation in these patients. Although inconclusive from this study, it is likely that the arrhythmia risk associated with high QTV cannot be evaded with pacing. This observation is in accordance with the results of the DAVID (Dual Chamber and VVI Implantable Defibrillator) trial where chronic prophylactic atrio-ventricular pacing at 70bpm in ICD recipients without indications for anti-bradycardia pacing, had no advantage or was even detrimental compared to back-up VVI pacing [416]. However, these results cannot be interpreted to biventricular pacing in HF patients. Reverse ventricular remodeling achieved with cardiac resynchronization may improve dynamics of ventricular repolarization and bring down QTV and thus the arrhythmia risk in these patients [417, 418].

Heart rate variability tended to improve following acute beta-blockade with esmolol in HF patients, and reduced rapidly during vagal blockade by atropine. In comparison, both these drugs had neutral effect on high QTV in these patients. This dichotomy in response of sinus node activity and ventricular repolarization to pharmacologic autonomic modulation reinforces the impression of mostly independent physiological mechanisms controlling impulse formation and conduction in HF patients.

### 5.4.4 Clinical Significance and Future Directions

The characteristics of QTV in the HFVT(-) group were more comparable to those of HFVT(+) patients than $H_{Norm}$ subjects. This indirectly demonstrates the progression of spatio-temporal heterogeneity in ventricular repolarization observed as high beat-to-beat QTV in ventricles with cardiomyopathy at high risk for ventricular tachyarrhythmia. Beta-blockers are the mainstay of therapy in patients with systolic dysfunction, and were shown to improve survival in these patients in large studies [74]. The antiarrhythmic effect of beta-blockers is mainly achieved by suppression of triggers for ventricular arrhythmias, improved HRV, and secondary to improved coronary perfusion and cardiovascular dynamics. This study suggests that beta-blockers are ineffective in reducing cardiac repolarization labiality at least on the short-term. Nonetheless, this failure to achieve desirable changes in ventricular repolarization, cannot be translated for gradual adaptive changes in QTV that may occur slowly with long-term beta-blocker therapy and resultant heart failure improvement [76, 408]. However, high baseline QTV in HF patients despite chronic treatment with beta-blockers suggests that long-term beta-blockade may only have limited effect on QTV. A key implication from this analysis is that since increased QTV is a risk predictor in HF, QTV reduction may in fact be a clinical target for improving life expectancy. However, increased QTV is not altered by acutely varying the autonomic outflow to the myopathic heart. This entails that autonomic modulation alone may be insufficient and perhaps high QTV in HF needs its own different set of possible interventions beyond purely neurohumoral management.

### 5.4.5 Study limitations

While various metrics (e.g. SDQT [401], Normalized QTV (QTVN) [54], QTV index (QTVi) [50], Short-term variability Ratio ($STV_{Ratio}$) [419], $T_{peak}$-$T_{end}$ interval variability [420] have been proposed to quantify beat-to-beat repolarization variability, the association of

individual measures with future adverse events has been inconsistent among studies [54-56]. Nevertheless, SDQT has been shown to correlate significantly with QTVN and QTVi in HF patients [55]. Due to ethical constraints of studying high-risk patient populations with HF, pharmacologic interventions could not be performed at higher maximal doses and longer infusion periods in these patients. For similar reasons, the regular beta-blocker therapy was not withheld before the planned interventions. The lack of response to esmolol due to an insufficient dosage is possible. Esmolol bolus and high-dose infusion, however, frequently produce hypotension [421] that can smudge the effects on QT variability and were suitably avoided. A drug specific ineffectiveness of esmolol to reduce QTV is unlikely as the efficacy of beta-blockers was shown to be a class effect than that of a generic drug [422]. Patients with normal heart were significantly younger and predominant females compared with the other study groups, which is in accordance with the general demographic profile of patients with SVT without other cardiovascular diseases [423]. However, QTV has been found to be relatively insensitive to age and does not differ between healthy younger and older adults [424, 425] Although gender differences in QTV have been insufficiently investigated, as with the rate corrected QT interval [426], QTV [425] and QTV/HRV [424] were shown to be higher in women than in men. A higher proportion of females in the $H_{Norm}$ group may therefore have diminished the observed differences in QTV and QTV/HRV between $H_{Norm}$ and HF groups. Beat-to-beat fluctuations in the QT interval are typically small, and measurement noise might have a considerable impact on QT variability measures. In this study, we mostly used lead I, which is characterized by relatively tall T waves and a good signal-to-noise ratio. Although larger number of patients could possibly have unequivocally demonstrated the interaction between groups and interventions, we could still reveal clinically relevant observations and trends in HF patients. The sample size was inadequate to demonstrate small differences between HFVT(+) and HFVT(-) patients that may exist. The duration of ECG recording for the assessment of QTV was based on recommendations for short-term HRV analysis [399]. The suitability of this duration for the assessment of short-term QT variability has not been systematically investigated. Longer periods of recording may be required to allow lengthier time for adaptation of QT interval, which may be a case in HF patients.

## 5.5 CONCLUSION

Patients with HF and spontaneous VT have larger fluctuations in beat-to-beat QT intervals. This repolarization instability appears to persist despite uncoupling the effect of heart rate. The effect of acute autonomic nervous system modulation on QTV appears to be limited in HF patients.

## TABLES

| Table 5.1 | Patient Characteristics | | | |
|---|---|---|---|---|
| | HFVT(+) group | HFVT(-) group | $H_{Norm}$ group | p value |
| **N** | 10 | 10 | 9 | |
| **Age (years)** | 63±12 | 54±13 | 36±19 | 0.004* |
| **Male, n** | 9 | 10 | 2 | 0.002† |
| **Cardiomyopathy, n** | | | | |
| **Ischemic** | 8 | 8 | - | 1.00 |
| **Non-ischemic** | 2 | 2 | | |
| **Ejection fraction (%)** | 30±10 | 29±8 | 63±3 | <0.001† |
| **NYHA Class I** | 2 | 4 | 9 | |
| **II** | 7 | 5 | | 0.01 |
| **III** | 1 | 1 | | |
| **Time to first infarction (years)** | 19±12 | 10±8 | - | 0.17 |
| **Coronary bypass surgery, n** | 5 | 2 | - | 0.35 |
| **QRS duration, ms** | 140±25 | 128±33 | 95±11 | 0.03† |
| **Inducible VT** | 10 | 1 | - | <0.001 |
| **Beta blocker, n** | 9 | 10 | 3 | 0.002 |
| **Amiodarone, n** | 3 | 0 | 0 | 0.07 |
| **Other antiarrhythmic drugs (Sotalol, Mexilitene)** | 2 | 0 | 0 | 0.18 |

VT=Ventricular Tachycardia, HFVT (+)= Heart failure with VT, HFVT (-)= Heart failure without VT

* HFVT(+) group vs $H_{Norm}$ group

† HFVT(+) group and HFVT(-) group vs $H_{Norm}$ group

| Table 5.2 | Effect of Various Interventions on ECG Parameters in the Three Study Groups | | | | | | | | | |
|---|---|---|---|---|---|---|---|---|---|---|
| Intervention ➔ Property and Study group ➔ | Baseline | Pacing80 | | Pacing100 | | Esmolol | | Isoprenaline | | Atropine | |
| | Mean±SEM | Mean±SEM | p value* | Mean±SEM | p value* | Mean±SEM | p value* | Mean±SEM | p value* | Mean±SEM | p value* |
| **meanRR (ms)** | | | | | | | | | | | |
| HFVT(+) | 1001±58[§] | 743±14 | | 594±12 | | 1027±70[§] | | 979±58[§] | | 731±56[§] | |
| HFVT(-) | 891±56 | 748±14 | <0.001 | 600±11 | <0.001 | 926±69 | 0.091 | 847±58 | 0.02 | 611±55 | <0.001 |
| $H_{Norm}$ | 823±59 | 711±14 | | 572±11 | | 867±73 | | 707±62 | | 589±58 | |
| p value[†] | 0.03 | 0.21 | | 0.21 | | 0.04 | | 0.04 | | 0.04 | |
| **SDRR (ms)** | | | | | | | | | | | |
| HFVT(+) | 36±8 | 4±1 | | 3±1 | | 83±17 | | 45±10 | | 16±6 | |
| HFVT(-) | 34±8 | 4±1 | <0.001 | 5±1 | <0.001 | 42±16 | 0.085 | 48±10 | 0.3 | 18±6 | 0.001 |
| $H_{Norm}$ | 51±9 | 3±1 | | 2±1 | | 52±17 | | 49±11 | | 17±6 | |
| p value[†] | 0.26 | 0.25 | | 0.25 | | 0.63 | | 0.63 | | 0.63 | |
| **meanQT (ms)** | | | | | | | | | | | |
| HFVT(+) | 509±21[‡§] | 441±16[§] | | 425±17[§] | | 498±23[‡§] | | 498±21[‡§] | | 460±29[‡§] | |
| HFVT(-) | 445±21 | 437±16[§] | 0.001 | 423±16[§] | <0.001 | 447±22 | 0.45 | 425±21 | 0.03 | 433±28 | 0.02 |
| $H_{Norm}$ | 429±22 | 398±17 | | 381±17 | | 414±24 | | 404±28 | | 404±30 | |
| p value[†] | 0.009 | 0.08 | | 0.08 | | 0.02 | | 0.02 | | 0.02 | |

| Intervention ➔ Property and Study group ➘ | Baseline | Pacing80 | | Pacing100 | | Esmolol | | Isoprenaline | | Atropine | |
|---|---|---|---|---|---|---|---|---|---|---|---|
| | Mean±SEM | Mean±SEM | p value* | Mean±SEM | p value* | Mean±SEM | p value* | Mean±SEM | p value* | Mean±SEM | p value* |
| **SDQT (ms)** | | | | | | | | | | | |
| **HFVT(+)** | 12±3 | 11±2§ | | 11±2§ | 0.35 | 16±2§ | | 14±2§ | | 13±3§ | |
| **HFVT(-)** | 13±3 | 10±1§ | 0.099 | 11±2§ | | 13±2 | 0.47 | 12±2 | 0.39 | 15±3 | 0.42 |
| **$H_{Norm}$** | 7±3 | 5±1 | | 5±2 | | 7±2 | | 11±2‖ | | 8±3 | |
| **p value†** | 0.21 | 0.008 | | 0.008 | | 0.02 | | 0.02 | | 0.02 | |
| **SDQT/SDRR** | | | | | | | | | | | |
| **HFVT(+)** | 0.54±0.10 | | | | | 0.33±0.11 | | 0.37±0.09 | | 1.03±0.25 | |
| **HFVT(-)** | 0.37±0.10 | | | | | 0.37±0.11 | 0.51 | 0.38±0.09 | 0.50 | 1.13±0.24 | 0.001 |
| **$H_{Norm}$** | 0.24±0.10 | | | | | 0.29±0.11 | | 0.26±0.10 | | 0.80±0.25 | |
| **p value†** | 0.094 | | | | | 0.30 | | 0.30 | | 0.30 | |

*: Intervention effect

†: Group effect

‡: compared to HF without VT

§: compared to Normal heart

‖:p=0.02 compared to baseline (linear regression)

## FIGURES

***FIGURE 5.1.***

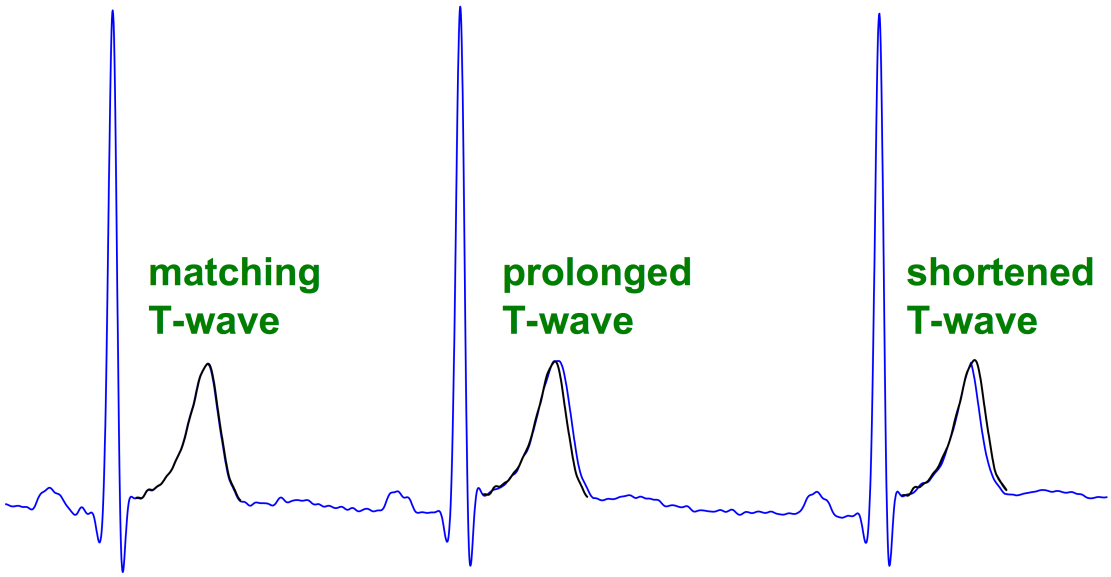


Figure 5.1. Beat-to-beat QT interval measurement. QT interval is calculated by selecting the beginning of the QRS complex and the end of the T wave for each beat. To calculate the end of T wave, an operator-defined template of the whole T wave (bold) is compared with the T wave of each heartbeat by cross-correlation. The change in QT interval is calculated from the degree of compression or expansion of the template T wave to best match at each beat. (Adapted from Baumert et al. [403] )

***FIGURE 5.2.***

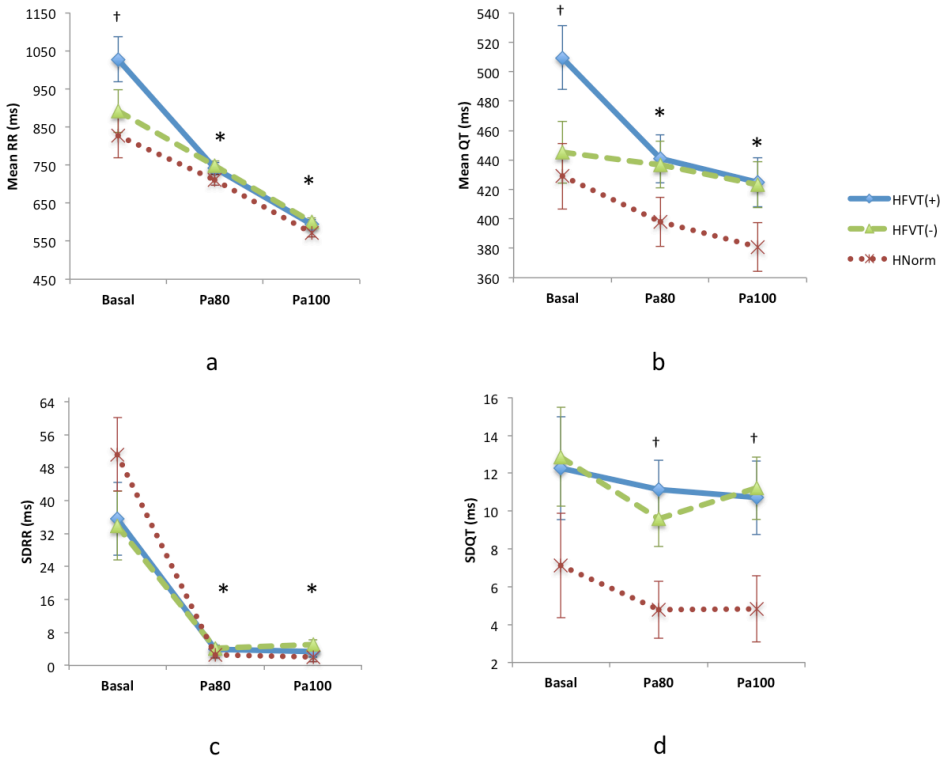


Figure 5.2. Effect of atrial pacing (Pa) at 80bpm and 100bpm. (a) Mean RR: *p <0.001 (intervention effect); †p <0.05 (group effect); post-hoc test, p<0.05 [HFVT(+) vs $HF_{Norm}$]. (b) Mean QT: *p <0.001 (intervention effect); †p <0.05 (group effect); post-hoc test, p<0.05 [HFVT(+) vs HFVT(-) and HFVT(+) vs $HF_{Norm}$ ]. (c) SDRR: *p <0.001 (intervention effect). (d) SDQT: †p <0.05 (group effect); post-hoc test, p<0.05 [HFVT(+) vs $HF_{Norm}$ and HFVT(-) vs $HF_{Norm}$ ].

***FIGURE 5.3***

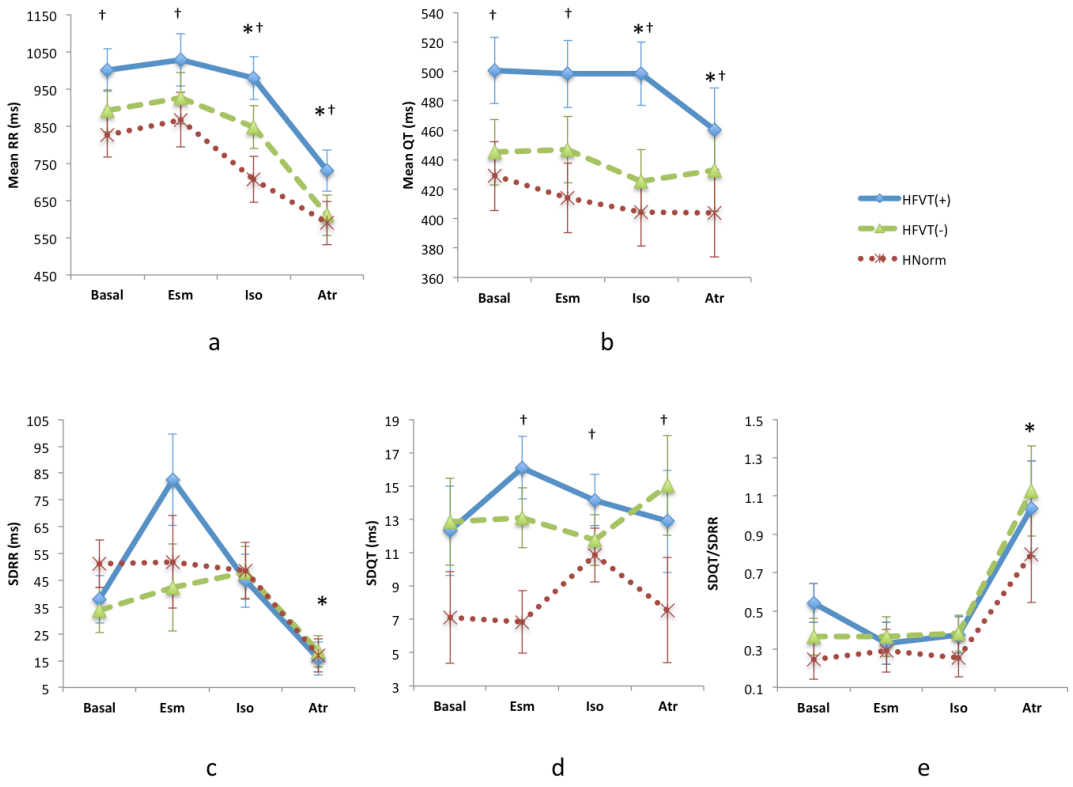


Figure 5.3. Effect of drugs (Esm= esmolol, Iso= isoprenaline, Atr= atropine). (a) Mean RR: *p <0.05 (intervention effect Iso); *p <0.001 (intervention effect Atr); †p <0.05 (group effect); post-hoc test, p<0.05 [HFVT(+) vs $HF_{Norm}$]. (b) Mean QT: *p <0.05 (intervention effect); †p <0.05 (group effect); post-hoc test, p<0.05 [HFVT(+) vs HFVT(-) and HFVT(+) vs $HF_{Norm}$ ]. (c) SDRR: *p <0.001 (intervention effect). (d) SDQT: †p <0.05 (group effect); post-hoc test, p<0.05 [HFVT(+) vs $HF_{Norm}$]. (e) SDQT/SDRR ratio: *p =0.001 (intervention effect).

## 5.6 SUPPLEMENTARY DATA

*Additional QT variability metrics*

**1. Normalized QT variability (QTVN)** was calculated as the variance of all QT intervals ($QT_v$) divided by the square of the mean QT interval ($QT_m$).

$$QTVN = QT_v / QT_m{}^2$$

For each patient, QT and RR sequences at baseline (3-minutes) and last 3-minutes epoch during each of the interventions were analyzed.

**2. QT variability index (QTVi)** was calculated defined as in Berger et al [50]:

$$QTVi = log_{10}[QTVN)/(RR_v/RR_m{}^2)]$$

where the numerator contains the QTVN. The denominator contains the variance of all RR intervals ($RR_v$) divided by the square of the mean RR interval ($RR_m$).

**3. Short-term variability (STV)** was calculated defined as in Oosterhoff et al [419].

$$STV_{QT},\ STV_{RR} = \sum_{1\ldots N}|D_n - D_{n-1}| \ / \left(N * \sqrt{2}\right)$$

where *D* is QT or RR interval and N is number of beats at baseline (3-minutes) and last 3-minutes epoch during each of the interventions. $STV_{Ratio}$ was calculated as:

$$STV_{Ratio} = STV_{QT} / \ STV_{RR}$$

*Results*

The results on the additional QT variability metrics are summarized in the supplementary data table.

*Normalized QT variability*

Group mean values in basal QTVN were higher in HF patients compared to the $H_{Norm}$ group, but these differences were not significant (p=0.34). Atrial pacing augmented the group differences in QTVN (p=0.085) however considered independently, atrial pacing did not alter QTVN in any of the patient groups (p=0.14). Esmolol (p=0.39)

and atropine (p=0.21) infusion failed to produce any significant change in QTVN. Isoprenaline tended to increase QTVN in $H_{Norm}$ patients (p=0.09) but not in the HF groups (overall main effect of intervention p=0.26).

*QT variability index*

In the basal state, QTVi was higher in HFVT(+) patients compared to HFVT(-) and $H_{Norm}$ patients (p=0.0015). While esmolol (p=0.29) and isoprenaline (p=0.44) had a neutral effect, QTVi increased considerably after atropine (p=0.036) infusion, principally due to a reduction in RR variance in all the three groups.

*Short term QT variability*

Group mean values in basal $STV_{QT}$ tended to be higher in HF patients compared to the $H_{Norm}$ group (p=0.062). Atrial pacing augmented the group differences in $STV_{QT}$ (p=0.004). Considered independently, atrial pacing reduced $STV_{QT}$ in all the patient groups (p=0.022 vs Pa80, p=0.032 vs Pa100) without a group specific effect (Group*Intervention p= 0.76). Esmolol (p=0.51), isoprenaline (p=0.17) and atropine (p=0.16) infusion failed to produce any significant change in $STV_{QT}$ in HF subjects, for which it remained higher than in $H_{Norm}$ patients (p=0.031).

*Short term variability ratio*

In the basal state, there was a trend for a higher $STV_{Ratio}$ in HFVT(+) patients compared to $H_{Norm}$ patients (p=0.056). While esmolol (p=0.62) and isoprenaline (p=0.66) had a neutral effect, $STV_{Ratio}$ increased considerably after atropine (p<0.001), principally due to a reduction in $STV_{RR}$ in all the three groups.

| Supplementary Data Table | Effect of Various Interventions on Additional ECG Parameters in the Three Study Groups | | | | | | | | | | | |
|---|---|---|---|---|---|---|---|---|---|---|---|---|
| **Intervention ➔ Property and Study group ⬇** | **Baseline** | **Pacing80** | | **Pacing100** | | **Esmolol** | | **Isoprenaline** | | **Atropine** | |
| | **Mean±SEM** | **Mean±SEM** | **p value*** | **Mean±SEM** | **p value*** | **Mean±SEM** | **p value*** | **Mean±SEM** | **p value*** | **Mean±SEM** | **p value*** |
| **QTVN (x $10^{-4}$)** | | | | | | | | | | | |
| **HFVT(+)** | 7±4 | 7±1 | | 8±3 | | 14±3 | | 10±3 | | 8±4 | |
| **HFVT(-)** | 11±3 | 6±1 | 0.25 | 10±3 | 0.91 | 10±2 | 0.39 | 8±3 | 0.26 | 14±3 | 0.21 |
| **$H_{Norm}$** | 3±4 | 2±1 | | 2±3 | | 4±3 | | 8±3[‖] | | 4±4 | |
| **p value[†]** | 0.34 | 0.085 | | 0.085 | | 0.19 | | 0.19 | | 0.19 | |
| **QTVi** | | | | | | | | | | | |
| **HFVT(+)** | 0.08±0.21[§] | | | | | -0.46±0.23[§] | | -0.34±0.15[§] | | 0.20±0.19[§] | |
| **HFVT(-)** | -0.46±0.18 | | | | | -0.38±0.21 | 0.29 | -0.50±0.17 | 0.44 | 0.25±0.18 | 0.0036 |
| **$H_{Norm}$** | -0.98±0.21 | | | | | -1.00±0.22 | | -0.79±0.16 | | -0.11±0.19 | |
| **p value[†]** | 0.0015 | | | | | 0.02 | | 0.02 | | 0.02 | |
| **$STV_{RR}$ (ms)** | | | | | | | | | | | |
| **HFVT(+)** | 23.5±6.6 | 2.9±0.5 | | 2.5±0.6 | | 43.2±12.3 | | 20.0±3.7 | | 4.5±1.9 | |
| **HFVT(-)** | 13.9±6.6 | 2.9±0.5 | <0.001 | 2.8±0.5 | <0.001 | 15.7±11.7 | 0.39 | 12.9±3.7 | 0.05 | 5.8±1.8 | 0.0005 |
| **$H_{Norm}$** | 27.8±7.0 | 1.4±0.5 | | 1.3±0.6 | | 24.3±12.4 | | 11.0±3.9 | | 3.6±1.9 | |
| **p value[†]** | 0.33 | 0.059 | | 0.059 | | 0.23 | | 0.23 | | 0.23 | |

| Intervention ➔ Property and Study group ➓ | Baseline Mean±SEM | Pacing80 Mean±SEM | p value* | Pacing100 Mean±SEM | p value* | Esmolol Mean±SEM | p value* | Isoprenaline Mean±SEM | p value* | Atropine Mean±SEM | p value* |
|---|---|---|---|---|---|---|---|---|---|---|---|
| **$STV_{QT}$ (ms)** | | | | | | | | | | | |
| **HFVT(+)** | 9.8±1.9§ | 5.6±1.0§ | | 5.5±0.9§ | | 10.1±1.2§ | | 7.3±1.0§ | | 6.6±1.5§ | |
| **HFVT(-)** | 8.7±1.9 | 6.5±1.0§ | 0.022 | 5.9±0.7§ | 0.032 | 8.5±1.2§ | 0.51 | 6.6±1.0§ | 0.17 | 7.9±1.4§ | 0.16 |
| **$H_{Norm}$** | 3.6±2.0 | 2.6±1.0 | | 2.5±0.8 | | 3.0±1.3 | | 4.1±1.1 | | 3.2±1.5 | |
| **p value†** | 0.062 | 0.004 | | 0.004 | | 0.031 | | 0.031 | | 0.031 | |
| **$STV_{Ratio}$** | | | | | | | | | | | |
| **HFVT(+)** | 0.76±0.14§ | | | | | 0.45±0.34 | | 0.59±0.17 | | 2.3±0.7 | |
| **HFVT(-)** | 0.62±0.14 | | | | | 0.76±0.32 | 0.62 | 0.78±0.17 | 0.66 | 2.9±0.7 | <0.001 |
| **$H_{Norm}$** | 0.30±0.14 | | | | | 0.73±0.34 | | 0.43±0.18 | | 2.2±0.7 | |
| **p value†** | 0.056 | | | | | 0.16 | | 0.16 | | 0.16 | |

*: Intervention effect

†: Group effect

‡: compared to HF without VT

§: compared to Normal heart

||:p=0.09 compared to baseline (linear regression)

# CHAPTER 6. VENTRICULAR ARRHYTHMIA STORM ABLATION- A SYSTEMATIC REVIEW AND META-ANALYSIS

## ABSTRACT

**Aims** Ablation has substantial evidence base in the management of ventricular arrhythmia (VA). It can be a "lifesaving" procedure in the acute setting of VA storm. Current reports on ablation in VA storm are in the form of small series and has relative small representation in large observational series. The purpose of this study was to systematically synthesize the available literature to appreciate the efficacy and safety of ablation in the setting of VA storm.

**Methods and results** The medical electronic databases through January 31st, 2012 were searched. VA storm was defined as recurrent (≥3 episodes or defibrillator therapies in 24 hours) or incessant (continuous > 12 hours) VA. Studies reporting data on VA storm patients at individual or study level were included. A total of 471 VA storm patients from 39 publications were collated for the analysis. All VAs were successfully ablated in 72% [95% confidence interval (CI) 71 to 89%] and 9% (95% CI 3 to 10%) had a failed procedure. Procedure related mortality occurred in 3 patients (0.6%). Only 6% patients had recurrence of VA storm. The recurrence of VA was significantly higher after ablation for arrhythmic storm of monomorphic VT relative to VF or polymorphic VT with underlying cardiomyopathy (odds ratio 3.76; 95% CI 1.65 to 8.57; p=0.002). During follow-up (61±37 weeks), 17% of patients died (heart failure 62%, arrhythmias 23%, non-cardiac 15%) with 55% deaths occurring within 12 weeks of intervention. The odds of death were 4.0 times higher after a failed

procedure compared to those with a successful procedure (95% CI 2.04 to 8.01, p<0.001).

**Conclusion** VA storm ablation has high acute success rates, with a low rate of recurrent storms. Heart failure is the dominant cause of death in the long term. Failure of the acute procedure carries a high mortality.

## 6.1 INTRODUCTION

Ventricular arrhythmia (VA) storm is increasingly being recognized as a distinctive arrhythmia syndrome with its specific management issues and prognostic consequences that differ from ventricular tachycardia (VT) and ventricular fibrillation (VF) episodes unrelated to storm [326, 327]. Implantable cardioverter defibrillator (ICD) is recommended as primary or secondary prevention of sudden death in patients with cardiomyopathy and life threatening genetic cardiac disorders [35, 36, 325, 427]. However, despite the presence of an ICD, the appearance of a VA storm still portends a high mortality [327-330]. The AVID study which followed secondary prevention ICD recipients observed a 5.6 fold relative increase in mortality in the first 12 weeks following development of VA storm and 2.4 fold over 3 years as compared to those who had VA episodes unrelated to storm [327]. Indeed every defibrillator shock therapy multiplies the mortality risk [428, 429] and the impact of multiple therapies over a short period can have unpredictable consequences.

Radiofrequency catheter ablation (RFA) is evolving as the standard care in patients with VA storm, with VT free long term survival improved with early invasive intervention [331]. Other approaches such as transcoronary ethanol ablation generally remain as a treatment of last resort after failure of RFA [332]. Most of the published data on VA storm ablation are single center small series or case reports and has relative small representation within large multicenter VT ablation series [279, 316]. Therefore, given the lack of large data, interpretability of reported information on survival outcomes in VA storm management remains contentious. Despite this relatively modest supporting evidence, current guidelines endorse the role of catheter ablation for VA storm management with a consensus on early intervention [326]. We therefore undertook this systematic review to organize the published data on high-risk VA storm patients and examine the efficacy and safety of VA storm ablation.

## 6.2 METHODS

The protocol for conducting this systematic review was made following the guidelines by NHS Centre for Reviews and Dissemination (CRD) report [430]. All published case series documenting invasive electrophysiology data and follow up on VA storm patients were sought. For purpose of this review the term VA storm was defined as (i) recurrent VA in a short time (≥3 separate episodes in 24 hours, each requiring termination by intervention), (ii) frequent defibrillator therapies (≥3 separate episodes separated by 5 min in 24 hours), or (iii) incessant VA (continuous VA that recurred promptly despite intervention for termination over > 12 hours) [325, 326].

### 6.2.1 IDENTIFICATION OF RESEARCH

The medical scientific electronic databases (MEDLINE, Web of Science, Science Direct, Cochrane Register, EMBASE) were comprehensively searched using the search terms “ventricular tachycardia” or “ventricular fibrillation” and “ablation”. No limits of start date or language were applied. The search was conducted up through January 31st, 2012. The retrieved data were then filtered for terms “storm” or “recurrent” or “incessant” anywhere in the title or abstract. Reference lists from the review articles were assessed for any other relevant publications missed in the search. The January 2012 issues of all major medical and electrophysiology journals were reviewed for latest articles not available on the databases. The studies from non-English journals were included if adequate information was available in the translated abstract or full text [431-433]. As a study on invasive VA storm management is more likely to be published based on significance of the results, this bias arising in the published literature was minimized by including all published reports irrespective of the ranking of the journal citations. All single case reports were excluded. Whenever publications were identified as parallel repetition of a patient series from the same author group, only one was selected on the merit of its quality.

### 6.2.2 Quality Assessment And Selection Of Studies

All studies retrieved after filtering were hand-searched in their full texts for data on VA storm patients. Table 6.1 gives the details of selection criteria applied for inclusion of a study. Authors with subject expertise (SN, ANG) and methodological expertise (AGB) assessed inclusion of individual studies to minimize the uncertainty of study selection. No pre-specified criteria on the approach of invasive management were applied and no definition of procedural success was stipulated.

### 6.2.3 Data Extraction

All demographic data on baseline characteristics, nature of VA, ablation or other intervention methodology, acute outcomes, complications, follow-up, recurrences and mortality were extracted by two researchers independently (SN, ANG). Discrete data and events were recorded as total numbers (sex, underlying heart disease, nature of VA, type of intervention, procedural success, complication, number of procedures, VA recurrence, mortality) while continuous data were recorded either as mean [age, ejection fraction (EF), VT cycle length] or a median value (follow-up duration, time of recurrence, time of death). For the purpose of assessing effect of predictor variables such as age, EF, underlying heart disease, nature of VA and procedural success on the incidence of outcomes of VA recurrence and mortality, individual patient demographic and survival data were retrieved whenever detailed in the study. Hazard ratio (HR), odds ratio (OR) and confidence intervals (CI) for predictor variables were extracted whenever individual data was not explicit. Studies where VA morphology was not specified, it was assumed as monomorphic VT. Polymorphic VT (pVT) and VF were treated together for the purpose of analysis.

The primary outcome was all cause mortality. Secondary outcomes assessed were cardiac mortality, VA recurrence and VA storm recurrence. The VA recurrences were labeled as unspecified morphology if reported only as ICD therapies.

### 6.2.4 Data Synthesis And Statistical Analysis

Descriptive data were reported as mean and standard deviation (or median and range for skewed observations) for continuous variables and absolute frequencies with 95% CI for categorical variables. Heterogeneity in nature of VA, ablation methodology and reporting of procedural result among studies was qualitatively described. Studies with >5 patients reporting individual level demographic predictor data (age, ejection fraction) and outcomes (time to recurrence of VA, time to death, recurrence of VA, death) were grouped for predictor analysis. The association between these predictors and outcomes within each study was analyzed using Cox proportional hazards and logistic regression models. The natural logarithm of the hazard ratio (HR) and odds ratio (OR), and their lower and upper 95% confidence limits were then pooled across studies using a random effects meta-analysis model. Heterogeneity in the study estimates was assessed using the I-squared statistic and a $\chi^2$-test of goodness of fit test. A formal meta-analysis of comparison between studies was not feasible for association among underlying heart disease, type of VA, procedural result and outcomes because of skewed distribution of number of patients in each category in different studies. This was therefore assessed using a logistic regression model after ignoring individual studies and treating the data as if obtained from a single study. All calculations were performed using Stata version 12.

## 6.3 Results

### 6.3.1 Identification Of Literature

The elementary online database search on “ventricular tachycardia” or “ventricular fibrillation” and “ablation” identified 3646 unique publications. After filtering this data in titles and abstract, 218 potential publications of VA storm were retained for secondary review. Out of these, 179 publications were excluded on general criteria as detailed in Figure 6.1. Twelve of these excluded publications collectively reported

ablation outcomes in 628 VA patients but did not adequately provide separate breakdown of their 261 VA storm patients [279, 316, 331, 332, 434-441]. Finally, 39 publications were included for purpose of this systematic review.

The studies included in this analysis were all published after 1991, and had collectively reported data on 519 patients (range 2-95, median 8) [274, 296, 431-433, 442-475]. Of these, 471 patients were with VA storm and their data were extracted for statistical analysis. Table 6.2 summarizes the data of individual studies included in this systematic review. Twenty-eight publications with 206 VA storm patients provided individual level data while the remaining 11 publications [433, 448, 449, 452-454, 460, 466, 468, 471, 472] withheld individual level data.

### 6.3.2 Basic Clinical And Demographic Data

Data of 39 publications with 471 patients were pooled together as study population. Table 6.3 summarizes their basic clinical and demographic features. The mean age was 61±7 years (range 38-71), with 85% males. The underlying heart disease was ischemic cardiomyopathy [ICM (68%)], idiopathic dilated cardiomyopathy [DCM (17%)], arrhythmogenic right ventricular dysplasia [ARVD (5%)], no structural heart disease [NSHD (6%)], others (4%). The mean left ventricular EF in patients with structural heart disease was 30±8%.

VA storm was present due to incessant VA in 37% of patients; the rest had frequent episodes of VA fulfilling the criteria for VA storm. On average, these patients had received 47±50 ICD therapies as reported in 7 publications and most studies reported failure of drug therapy. Monomorphic VT storm occurred in 77% patients with 1.6±0.8 morphologies per patient, while VF storm occurred in 11% and pVT in 7%. VT morphology was unspecified in 5%. Among VF storm patients, 45% (24/53) had NSHD while rest had a form of cardiomyopathy.

### 6.3.3 PROCEDURAL STRATEGY

VA storm related instability and multiple cardioversions necessitated deep sedation with mechanical ventilation (13%), inotropic support (11%), intraaortic balloon counterpulsation (1.5%), extracorporeal membrane oxygenation (2%) or ventricular assist device (0.4%) in 23 % patients before or during electrophysiologic procedure.

#### A. NON-RFA METHODS.

Non-RFA invasive methods were reported in 57 (12%) patients, that included ethanol ablation [442, 473], surgical ablation [473], electrofulgration [446, 476], cervical sympathetic ganglionectomy [469, 475], thoracic epidural anesthesia [469, 475] and renal denervation [474]. These were mostly desperate measures after failure of medical therapy and radiofrequency ablation. However, few studies reported cases that were managed only with non-RFA invasive strategies due to severe instability, multiple or non-mappable VTs [469] or polymorphic VT [474, 475]. Three papers published in the era before RFA became widely available described electrofulgration [446, 476] and ethanol ablation [442] as the primary treatment for incessant VT.

#### B. CATHETER BASED RFA.

Catheter based RFA was the primary mode of invasive management in 88% of patients. Among these, irrigated RFA was used in 65% of patients. The use of 3D mapping was cited in 21 publications after year 2003. Two publications [465, 468] tested the utility of magnetic navigation and irrigated tip catheter ablation in VA storm. Whereas 90% of patients underwent left or right ventricular endocardial mapping and ablation, a combined endo-epicardial approach was performed in 9% of patients due to arrhythmia recurrence after the first procedure [432, 451, 452, 460, 467, 471-473, 475]. Three patients (1%) underwent only epicardial ablation because of the presence of an intraventricular thrombus [451, 452].

### 6.3.4 ELECTROPHYSIOLOGIC CHARACTERISTICS

Scar related reentry was the commonest mechanism of VA storm seen in 83% of patients. Recurrent VA triggered by Purkinje related or myocardial premature ventricular complexes (PVC) was present in 14% [432, 448-450, 453, 456, 459, 464, 466, 470, 472]. Macrorentry within the His-Purkinje system was responsible for VA storm in 3% of patients [443, 458, 462, 467, 472]. None of the publications clearly reported any focal VA. Most of the patients underwent combined activation and substrate mapping guided ablation. Mapping generally included entrainment mapping for targeting isthmus sites, pace mapping for exit sites, and activation mapping for triggering PVC and Purkinje potentials. Substrate mapping and ablation targeted scar related late and fractionated potentials. Ablation guided by activation mapping alone was reported in 23% [274, 431, 432, 445, 447-449, 451-454, 456, 458, 459, 462, 464, 472], while substrate modification alone was done in 12% patients due to unstable nature of VA [432, 455, 463, 472]. Majority of polymorphic VT and VF were targeted at triggering PVC (88%) while the remainder underwent substrate modification.

### 6.3.4 PROCEDURAL RESULT

#### A. DEFINITION OF SUCCESS

Most of the studies reported results as complete success (no inducible VT), partial success (no inducible clinical VT) and failure (inducible clinical VT) based on formal induction at the end of the procedure. However, in some studies, including a few with catheter based RFA, the inducibility of VA was not assessed and outcomes were reported as complete suppression of clinical VA, partial suppression of clinical arrhythmia or failure [448, 449, 454, 466, 469, 470, 474-476]. One study reported success as elimination of scar related electrograms [455]. None of these studies were excluded for the assessment of procedural success or failure as a predictor of mortality. One study that did not report acute procedural outcomes in adequate detail was excluded for this analysis [432].

### B. Acute Procedural Result

In the 447 patients, all VA were successfully ablated in 72% (95% CI 71 to 89%) with the clinical VA ablated in 91% (95% CI 90 to 97%). Multiple procedures, including more than one mode of intervention, were required in 91 (19%) patients resulting in average 1.3±0.4 procedures per patient. The clinical VA remained inducible in 9% patients (95% CI 3 to 10%).

The procedure related complication rate was low, with 10 (2%) patients having significant complications that included death (3 patients, 0.6%, cause of deaths reported as myocardial infarction, pericardial tamponade and electromechanical dissociation), stroke (3 patients, 0.6%), heart block (3 patients, 0.6%), and cardiac tamponade (1 patient, 0.2%) [296, 432, 442, 446, 452, 460, 472, 473].

## 6.3.5 Follow-Up, Recurrence Of VA And Mortality

---

The mean follow up duration reported was 61±37 weeks (median 58, range 4 – 156). Ventricular arrhythmia recurred in 188 (40%, 95% CI 27 to 47%) patients after the first procedure, while a recurrence after the last procedure occurred in 133 (28%, 95% CI 17 to 34%) patients [296, 431, 432, 442, 444-446, 448, 451-453, 455, 457, 458, 460, 462, 463, 467-476].
The time to first recurrence, reported in 19 publications, ranged from the first week to 104 weeks with a median of 8 weeks. Among those who had recurrences, the clinical VA recurred in 17%, a non-clinical VA recurred in 11%, while 72% had recurrences of unspecified morphology as ICD interventions. Only 19% patients of these patients (6% of the overall population) had a recurrence as storm while the others had recurrences as isolated episodes of VA. Among 24 patients with VF storm and NSHD, only 2 had recurrence of VF [448, 449].

Seventy-eight deaths (17%, 95% CI 12 to 23%) were reported on follow up [296, 431, 432, 442, 444-446, 452, 453, 455-461, 463, 467-472, 475]. Most deaths were due to non-sudden cardiac causes (mostly progressive heart failure, 62%, 10% of overall population) while only

a minority died due to intractable arrhythmia recurrence (23%, 4% of overall population). Non-cardiac mortality (stroke, pneumonia, cancer, pancreatitis) was reported in 15%. No deaths occurred in patients with VF storm with NSHD, while 24% patients with VF or polymorphic VT storm and underlying heart disease died on follow-up. Two studies did not separate deaths in VF or polymorphic VT storm patients [432, 472]. The time of death after the last procedure, reported in 23 publications with 77 deaths, ranged from first week to 90 weeks (median 12 weeks). The median time to death was ≤ 12 weeks in 55% of these patients.

### 6.3.6 Impact Of Incessant VA On Procedural Outcome, Mortality And VA Recurrence

Incessant VA was present in 37% of patients before procedure. Apart from 2 studies [432, 471], all other studies reported adequate details in relation to incessant VA patients. Among these patients the underlying heart disease were ICM (80%), DCM (15%) and ARVD + others (5%). Hemodynamic instability and multiple cardioversions necessitated deep sedation and various other support measures more often in patients with incessant VA (43%) than with non-incessant VA storm (7%) ($p<0.001$). The odds of having a procedural failure were 3.4 times higher in the incessant VA relative to arrhythmic storm of frequent VA (OR=3.40, 95% CI 1.63 to 7.12, p=0.001). Further, the odds of VA recurrence were 42% higher in the incessant VA patients (OR=0.58, 95% CI 0.38 to 0.90, p=0.01), however the odds of arrhythmic death did not differ relative to arrhythmic storm of frequent VA (OR=0.54, 95% CI 0.19 to 1.52, p=0.24).

### 6.3.7 Other Demographic Predictors Of Mortality And VA Recurrence

Eleven studies which included more than 5 patients each [296, 431, 432, 442, 446, 451, 459, 467, 469, 470, 475] and provided individual level demographic, recurrence and death data on

145 patients were included in this analysis. Additionally, the largest study [460] with 95 patients that detailed the HR and its 95% CI for predictors of cardiac mortality was also included. Other studies with less than 5 patients or not providing HR or OR with their 95% CI were excluded. None of the studies on VF storm ablation in NSHD provided these data [448, 449].

The odds of death and VA recurrence did not appear to be associated with age or EF when pooled across the usable studies (Table 6.4). The pooled hazard ratio for the association between EF and time to cardiac death was 0.96, indicating that a one unit increase in EF was associated with a 4% reduction in the risk of cardiac death, however the overall association was not statistically significant (95% CI 0.92 to 1.00, p=0.067) (Figure 6.2). The I-squared statistic was estimated to be 0.0%, indicating that the heterogeneity between studies did not exceed what would have been expected due to chance.

There was no difference in the odds of death (p=0.31) and VA recurrence (p=0.34) between the three disease groups of ICM, DCM and ARVD + others (Table 6.5). Although the odds of death and recurrence were 49% (OR=0.51, 95% CI 0.22 to 1.22, p=0.13) and 35% (OR=0.65, 95% CI 0.29 to 1.43, p=0.28) lower in ICM group relative to DCM group, the difference between groups did not achieve statistical significance. Importantly, among studies with individual level data, 8 of 13 patients who had failed ablations belonged to the non-ICM groups suggesting higher failure rates in these groups.

The odds of VA recurrence were 3.8 times higher after ablation for arrhythmic storm of monomorphic VT relative to arrhythmic storm of VF or polymorphic VT with underlying cardiomyopathy (OR=3.76, 95% CI 1.65 to 8.57, p=0.002), however, the odds of death did not differ between them (OR=0.69, 95% CI 0.34 to 1.40, p=0.31).

### 6.3.8 Relationship Between Procedural Outcome, Mortality And VA Recurrence

VA recurrence and mortality data in relation to individual procedural outcome was available from 38 studies (447 patients) and 37 studies (417 patients) respectively. Two studies [432, 468] did not provide this data. Among those who had recurrence of arrhythmia after last procedure 20% (26/129) (95% CI 16 to 43%) died while there were 15% (49/318) (95% CI 8 to 23%) deaths in those who did not have a recurrence. The odds of death were 28% lower in those without a recurrence, but the difference between the groups was not statistically significant (OR=0.72, 95% CI 0.42 to 1.22, p=0.22). The mortality rate was 42% (17/41) (95% CI 12 to 51%) in those who had a failed procedure and 15% (56/376) (95% CI 10 to 23%) following complete or a partially successful procedure. The odds of death were 4.0 times higher in those with a failed procedure compared to those with a successful procedure (OR=4.05, 95% CI 2.04 to 8.01; p<0.001). When confining this analysis to incessant VT patients only, the odds of death increased to 6.0 times following a failed procedure compared to those with a successful procedure. (OR=6.19, 95% CI 2.30 to 16.63; p<0.001).

## 6.4 Discussion

This systematic review describes the largest pooled database of 39 studies with 471 VA storm patients with structural and non-structural heart disease who underwent invasive management. It contributes evidence supporting the protective role of intervention in the entire spectrum of VA storm patients who have impending risk of death, including interventions not limited to catheter ablation. Patients with idiopathic and ion-channel disorder related VF and polymorphic VT storm (24 patients) [448, 449] were included because of their comparable clinical implications (sudden death risk and defibrillator therapies) to VA in structural heart disease [325, 477, 478]. Likewise non-ischemic non-dilated cardiomyopathies (40 patients) [431, 432, 452, 456, 460, 463, 469, 471, 473-475] such as ARVD, hypertrophic cardiomyopathy and sarcoidosis

were included being high risk subgroups for VA related sudden cardiac death [479-481]. As observed in this review, the frequency of these conditions was not as high as that of ICM or DCM which makes prospective randomized trials difficult to perform, and can possibly be evaluated only by exploring non-randomized observational studies in an alike method [482].

### 6.4.1 Appraising Available Multicenter Studies, Meta-Analysis And Reviews

Most of the previously published data on VA storm ablation are single center small series or case reports and there is relative small representation of VA storm patients in larger studies of VT ablation. The largest VT ablation study to-date, the multicenter Thermocool VT ablation trial that included 231 recurrent VT patients with ICM treated with catheter ablation [279], had only 37 (16%) patients with incessant VT before ablation. In this cohort of incessant VT at 1 year following ablation 49% had recurrence of VT, 24% had recurrences of VT storm and 11% died. Despite these sobering outcomes, the investigators concluded incessant VT to be a predictor of better primary outcome following ablation compared to those with intermittent VT (OR 0.33, 95% CI 0.13 to 0.86, p=0.02). However, since the description of primary end point was different for patients with incessant VT (recurrence of incessant VT) and intermittent VT (recurrence of any VT), the interpretation of this conclusion should be done cautiously. This paper was excluded from this systematic review as demographic and procedural outcome data of incessant VT were not reported separately. Other multicenter studies, the Euro-VT study (14 out of 63 patients) [316] and epicardial VT ablation study (95 out of 218 patients) [440], were also not explicit in reporting demographics and outcomes in the patients with VA storm. In a recent meta-analysis of studies on VT catheter ablation as adjunct to medical therapy combining 457 patients [369], where 20% of patient population were VA storm, catheter ablation group showed only a trend towards reduction of arrhythmia in VA storm patients (p=0.06). The paper did not report the effect of VT ablation on survival for VA storm patients separately however, overall there was no reduction in mortality. All the previously available reviews [432, 483, 484]

had summarized the primary research with no attempt to extract and systematically analyze the data.

### 6.4.2 Major Findings From The Systematic Review

---

The most important finding from this study is the high acute success rate of invasive management of VA storm, with 91% of patients having elimination of the clinical VA and 72% of patients having all inducible VA eliminated. Importantly, 94% patients were free from VA storm on follow-up and arrhythmic sudden deaths were rare (4%). This is quite significant considering the life threatening status and cardiogenic shock present in many of these patients. It is, however, at the cost of multiple procedures (1.3±0.4 per patient), non-conventional modes of intervention such as ethanol ablation, sympathetic denervation, surgical ablation and 23% patients requiring major invasive hemodynamic support during procedure. Despite these, the reported complication rate was fairly low (2%) and procedure related deaths were only rare (<1%).

#### A. Palliation Or Mortality Benefit

The largest study in the review by Carbucicchio et al [460] that compared VA storm catheter ablation outcomes in stable patients with those presenting with hemodynamic instability showed comparable acute success rate in both the groups. However the latter had a greater number of recurrences and subsequent sudden deaths. This suggests that a proportion of patients with VA storm probably achieve only palliative benefit from the invasive intervention and their long-term outcomes remain poor. Overall, VA storm ablation appears to have a role beyond acute palliation and improves long-term outcomes. This is indicated by 17% all-cause mortality at 1.2 years follow-up in our pooled database against comparable data on medically managed historic controls of VA storm who had 27% all-cause mortality at 1.6 years [329] and 38% at 3 years [327]. Further, if reduction in mortality is real, it is

unclear whether this is secondary to reduction in arrhythmic or overall cardiac death. In this pooled analysis, arrhythmic sudden deaths accounted for 23% of deaths, while progressive heart failure accounted for 62%. This is compared with 25% unspecified deaths and 58% heart failure deaths in medically managed controls [329].

A key implication of this analysis is that all patients with VA storm are possibly suitable and should be offered ablation. However, even a successful procedure does not equate with even medium term survival, as many of these patients still die of progressive heart failure. This entails that ablation alone is insufficient for some and perhaps high arrhythmia frequency heralds pre-terminal pump failure with its own different set of possible interventions beyond purely anti-arrhythmic management.

### B. Predictors Of Outcomes: Mortality And VA Recurrence

#### *i) EF and Underlying Substrate*

There did not appear to be any significant predictors in baseline characteristics that indicate higher risk of death or arrhythmia recurrence on follow-up. Only the EF appeared to have small inverse association with the secondary outcome of cardiac mortality, but it was not statistically significant. The possibility for this lack of importance of EF could be that, depending on when the measure for EF was made, it might include patients whose measures were temporarily depressed by arrhythmia frequency / shocks as well as those whose function was permanently low, thus confounding the prognostic implication of very low systolic function. The odds of death following ablation were lowest for ICM compared with other forms of structural heart disease. This might be due in part to the predominantly endocardial location of VT isthmus sites in most ICM patients, as compared to a higher incidence of epicardial sites in DCM and ARVD [485, 486]. Studies by Carbucicchio et al [460] and Kozeluhova et al [471] reported an association between EF (HR 0.4; 95% CI 0.15-0.99, for 10% unit increment) and LV end-diastolic diameter (OR 1.18; 95% CI 1.03, 1.35) with cardiac mortality. However Arya et al [468] could not demonstrate a similar

association. Non-ICM was a significant predictor of cardiac mortality in the study by Carbucicchio et al (HR 13.69; 95% CI) as compared to ICM, however the outcomes were not different between ICM and ARVD.

*ii) Incessant VA*

Storm due to incessant VA predicted poor outcomes compared to arrhythmic storm of frequent VA. These patients had more than 3-times worse procedural outcomes and higher recurrence of any VA (42% increase), although there was no difference in sudden death. Incessant VA is likely to compound the hemodynamic instability as was reflected in many of these patients requiring multiple major support measures. Although not obvious in the studies, such patients generally have advanced disease, resistance to antiarrhythmic drugs, tolerate very narrow window for adequate mapping and are more likely to have procedures done at off-hours, with limited auxiliary support, and shorter procedure times. All these elements could have perhaps produced the poor outcomes observed in these patients.

*iii) Monomorphic VT versus pVT and VF*

In our study, among patients with a form of cardiomyopathy, VA recurrence was significantly lower in VF and pVT storm group compared with arrhythmic storm of monomorphic VT. This could be related to the differences in amount and composition of underlying scar in these patterns, with VF and pVT patients possibly having less confluent anatomic scarring with surviving Purkinje fibers compared to large confluent scarring often seen with monomorphic VT [23, 487]. Furthermore, VF storm with NSHD had dramatic reduction in VF episodes following ablation with only 2 isolated VA recurrences among 24 patients on long-term follow up to 2 years. None of these patients died which was congruent with the fact that none had heart failure.

*iv) Failed Procedure*

Failure of the acute procedure presages high mortality on follow-up. The leading study in the review from Carbucicchio et al [460] reported high cardiac mortality following failed catheter ablation (HR15.23, 95%CI 2.05-112.83, p=0.008). In our study, the odds of death were 4.0 times higher in those with a failed procedure compared to those with a successful procedure. This potentially may be due to a pre-existing advanced stage of the disease and multiple VA or a detrimental effect of prolonged multiple failed procedures that contribute to the morbidity of heart failure and VA. Patients in whom ablation is failing are likely to have greater number of ablation lesions with the potential of adversely affecting the ventricular function, although this hypothesis has not been proven in prior studies [488]. Importantly, in this study, 55% of the deaths that followed invasive intervention occurred in the first 3 months. This is much higher than medically managed VA storm patients where only 29% die in the first 3 months after its development [327].

Taken together, the findings provide a simple validation of the clinical impression that the majority of patients presenting with VA storm should undergo ablation as part of their overall management. The available data suggests that successful invasive intervention has favorable impact on long-term outcomes, however those who have failed procedures might have modest increase in death. None of the studies could address the question of which patient will benefit most from ablation. Given these important questions on the relative benefit of invasive VA storm management, it is worthwhile investigating long-term outcomes in VA storm population in a randomized controlled trial.

### 6.4.4 STUDY LIMITATIONS

The most important limitation of this systematic review is all the studies were primarily observational small series and only a few studies were usable for meaningful survival and meta-analysis (12/39 studies; 240 / 471 patients). Notably,

only 11 publications with more than 5 patients compiled individual level data and only one publication with study level data provided adequate predictor analysis data. It reduced the opportunity for a greater detailed analysis to explore the strength of effect association of different predictors on recurrence of VA, all cause morality and cardiac mortality. But the estimation of survival outcomes in relation with acute procedural result was more robust as data were available on 37 studies (417 patients). The lack of uniformity in assessing procedural result with 10 studies not including a formal VA inducibility testing at the end of the procedure, cannot be rejected. The differences in the conduct of ablation present among these studies motivate the need of a standard practice that future studies on invasive management in VA storm should promptly follow [489]. Nonetheless, as our focus was not on comparative outcome assessment of different substrates and strategies, the results demonstrate the effectiveness of ablation in VA storm and not as a guide to which patient will benefit from VA storm ablation. Due to lack of any randomized controlled trial data, it was impossible to compare and contrast medical therapy versus intervention in these patients. The study cannot unequivocally advocate that ablation is superior to other therapies to enhance survival in patients with VA storm and further randomized controlled studies are needed to investigate this proposition. Although patients with NSHD, ARVD and other miscellaneous cardiac disorders were included, these conditions, whenever feasible, were dealt separately and their outcomes compared with the more common ICM and DCM.

The bearing of the largest study from Carbucicchio et al [460] influencing the results has to be accepted. Nevertheless, the method of systematic review and meta-analysis typically aggregates results from all data in the literature meeting inclusion criteria so as to facilitate rapid synthesis of adequately powered evidence and generation of new hypothesis. Data from 261 VA storm patients from 12 publications [279, 316, 331, 332, 434-441] was not included in the analysis, as it could not be separated from non-storm patients. These papers, though not explicitly on VA storm patients, possibly could have influenced the overall results and added important predictive information. Briefly, these discussed the use of irrigated ablation [316], experience of epicardial ablation [434, 439-441], ethanol ablation after failed catheter ablation [332], ablation in

biopsy proven viral myocarditis [441], ablation in post cardiac valve surgery [438], the comparative usefulness of entrainment mapping versus substrate mapping [437], the need for early intervention [331], palliative rather than curative role of ablation [436], and 1 year and 5 year outcomes of VA ablation in ICM [279, 435]. All these publications had commended the role of ablation in these patients. The pertinent issues of advantage of entrainment mapping over substrate based ablation and whether the epicardium should be accessed in all or selected patients with VA storm during the first procedure, could not be resolved in this review.

The publication bias was minimized by including all the published reports irrespective of the ranking of the journal citations and excluding single case reports.

## 6.5 CONCLUSION

VA storm ablation has high acute success rates, with a low rate of recurrent storms. It is a "lifesaving" approach with acceptable efficacy and safety profile with low complication rate and should be considered in patients not responsive to the available medical management. Heart failure is the dominant cause of death in the long-term in patients having a successful procedure. Failure of the acute procedure carries a high mortality.

## TABLES

| Table 6.1 | Study Selection Criteria | |
|---|---|---|
| **Selection Criteria** | **Inclusion Criteria** | **Exclusion Criteria** |
| Population | Definition of VA storm fulfilled | Recurrent VA not fulfilling the definition of storm. |
| | Underlying structural heart disease, or VF storm with or without structural heart disease | Idiopathic outflow tract VT and fascicular VT |
| Intervention | Invasive management | Medical management only or time delay of several weeks before invasive management. |
| Study design | Observational or Case control series; ≥ 2 patients | Single patient case reports, review articles, conference abstracts, statements, editorials. |
| Study quality | Data on VA storm patients detailed adequately | Composite data on VA storm and non-storm patients that cannot be manipulated separately for VA storm patients. |
| | Outcome and follow up data available | No data on outcome or follow up |

VA: Ventricular arrhythmia, VF: Ventricular Fibrillation, VT: Ventricular tachycardia

**Table 6.2** **Summary of Studies Included in this Systematic Review**

| No | First Author | Year | n* | Underlying Heart disease, n | Age† (yrs) | EF† (%) | Arrhythmia,n | Acute success, n (%) | Follow-up (weeks) | Recurrence of VA, n (%) | Death, n (%) |
|---|---|---|---|---|---|---|---|---|---|---|---|
| 1 | Trappe | 1991 | 11 | ICM,10; DCM,1 | 60 | | VT,11 | 9 (82) | 124 | 6 (55) | 0 (0) |
| 2 | Nellens | 1992 | 12 | ICM,12 | 62 | | VT12 | 10 (83) | 24 | 3 (25) | 3 (25) |
| 3 | Morady | 1993 | 1 | ICM,1 | 71 | 20 | VT,1 | 1 (100) | 44 | 0 (0) | 0 (0) |
| 4 | Ometto | 1993 | 1 | ICM,1 | 66 | 19 | VT,1 | 1 (100) | 56 | 0 (0) | 0 (0) |
| 5 | Willems | 1993 | 4 | ICM,4 | 58 | 43 | VT,4 | 3 (75) | 32 | 3 (75) | 1 (25) |
| 6 | Kottkamp | 1995 | 4 | DCM,4 | 55 | 27 | VT,4 | 3 (75) | 29 | 4 (100) | 1 (25) |
| 7 | Cao | 1996 | 17 | ICM,15; DCM,2 | 65 | 31 | VT,17 | 16 (94) | 120 | 6 (35) | 4 (24) |
| 8 | Sato | 1997 | 1 | DCM,1 | 53 | 30 | VT,1 | 1 (100) | 92 | 0 (0) | 0 (0) |
| 9 | Haissaguerre | 2002 | 19 | NSHD,19 | 43 | 60 | VF,19 | 19 (100) | 104 | 2 (11) | 0 (0) |
| 10 | Haissaguerre | 2003 | 5 | NSHD,5 | 38 | | VF,5 | 5 (100) | 68 | 0 (0) | 0 (0) |
| 11 | Bansch | 2003 | 4 | ICM,4 | 66 | 29 | VF,4 | 4 (100) | 58 | 0 (0) | 0 (0) |
| 12 | Brugada | 2003 | 10 | ICM,8; DCM,1; NSHD,1 | 68 | 28 | VT,10 | 9 (90) | 72 | 1 (10) | 0 (0) |
| 13 | Kottkamp | 2003 | 28 | ICM,28 | 64 | 29 | VT,28 | 26 (93) | 60 | 10 (36) | 2 (7) |
| 14 | Silva | 2004 | 15 | ICM,9; DCM,4; | 63 | 31 | VT,15 | 12 (80) | 12 | 2 (13) | 4 (27) |

| | | | | | | | | | | | |
|---|---|---|---|---|---|---|---|---|---|---|---|
| | | | | ARVD,1; NSHD,1 | | | | | | | |
| 15 | Marrouche | 2004 | 8 | ICM,8 | 65 | 15 | VF,8 | 8 (100) | 40 | 2 (25) | 1 (13) |
| 16 | Szumowski | 2004 | 5 | ICM,5 | 61 | 32 | pVT,5 | 5 (100) | 64 | 0 (0) | 0 (0) |
| 17 | Montijano | 2005 | 11 | ICM,10; ARVD,1 | 67 | 29 | VT,11 | 8 (72) | 156 | 9 (82) | 2 (18) |
| 18 | Schrejeck | 2005 | 5 | ICM,5 | 61 | 18 | VT,5 | 5 (100) | 76 | 2 (40) | 2 (40) |
| 19 | Micochova | 2006 | 2 | Amyloid,2 | 56 | 40 | VF,2 | 2 (100) | 18 | 0 (0) | 1 (50) |
| 20 | Dandamudi | 2007 | 3 | ICM,2; DCM,1 | 51 | 30 | VT,3 | 3 (100) | 29 | 1 (34) | 1 (33) |
| 21 | Riethmann | 2007 | 4 | ICM,2; DCM,1; NSHD,1 | 68 | 40 | VT,4 | 4 (100) | 36 | 2 (50) | 1 (25) |
| 22 | Bode | 2008 | 7 | ICM,4; DCM,2; Valv,1 | 55 | 38 | pVT,7 | 7 (100) | 32 | 0 (0) | 2 (29) |
| 23 | Carbucicchio | 2008 | 95 | ICM,72; DCM,10; ARVD,13 | 64 | 36 | VT,95 | 85 (89) | 88 | 32 (34) | 15 (16) |
| 24 | Nayak | 2008 | 4 | ICM,4 | 71 | 17 | VT,4 | 4 (100) | 4 | 0 (0) | 3 (75) |
| 25 | Sakata | 2008 | 6 | ICM,1; DCM,5 | 62 | 26 | VT,6 | 6 (100) | 112 | 1 (17) | 0 (0) |
| 26 | Uusimaa | 2008 | 2 | Sarcoid,2 | 48 | 55 | VT,2 | 2 (100) | 88 | 1 (50) | 1 (50) |
| 27 | Enjoji | 2009 | 4 | ICM,4 | 65 | 32 | VT,2; VF,2 | 4 (100) | 104 | 0 (0) | 0 (0) |
| 28 | Haghjoo | 2009 | 4 | ICM,4 | 68 | 25 | VT,4 | 4 (100) | 16 | 0 (0) | 0 (0) |
| 29 | Sinha | 2009 | 4 | DCM,4 | 61 | 35 | VF,4 | 4 (100) | 48 | 0 (0) | 0 (0) |

| | | | | | | | | | | | |
|---|---|---|---|---|---|---|---|---|---|---|---|
| 30 | Arya | 2010 | 13 | DCM,13 | 57 | 33 | VT,13 | 13 (100) | 92 | 5 (38) | 4 (31) |
| 31 | Arya | 2010 | 30 | ICM,30 | 70 | 30 | VT,30 | 30 (100) | 32 | 9 (30) | 1 (3) |
| 32 | Bourke | 2010 | 14 | ICM,4; DCM,4; ARVD,1; Sarcoid,2; HCM,3 | 54 | 35 | VT,10; pVT,4 | 9 (64) | 24 | 4 (29) | 6 (43) |
| 33 | Piechi | 2010 | 9 | ICM,9 | 62 | 27 | pVT,9 | 8 (89) | 52 | 2 (22) | 2 (22) |
| 34 | Kozeluhova | 2011 | 41 | ICM,30; DCM,5; ARVD,6 | 59 | 29 | VT,38; pVT,3 | 35 (85) | 72 | 7 (17) | 12 (29) |
| 35 | Deneke | 2011 | 32 | ICM,17; DCM,15 | 68 | 28 | VT,29; VF,3 | 30 (94) | 60 | 10 (31) | 3 (9) |
| 36 | Kozluk | 2011 | 24 | ICM,18; DCM,3; HCM,1; Valv,1; NC,1 | 63 | 27 | VT,15; pVT,3; VF,6 | | 112 | 5 (21) | 3 (13) |
| 37 | Ueda | 2011 | 4 | HCM,4 | 64 | 39 | VT,4 | 4 (100) | 76 | 1 (25) | 0 (0) |
| 38 | Ukena | 2012 | 2 | DCM,1; HCM,1 | 62 | 34 | VT,1; pVT,1 | 2 (100) | 24 | 1 (50) | 0 (0) |
| 39 | Ajijola | 2012 | 6 | DCM,4; ARVD,1; Sarcoid,1 | 60 | 26 | VT,5; pVT,1 | 5 (83) | 14 | 2 (33) | 3 (50) |

VT: Ventricular tachycardia, pVT: Polymorphic VT, VF: Ventricular fibrillation, VA: Ventricular arrhythmia, EF: Ejection Fraction, ICM: Ischemic cardiomyopathy, DCM: Dilated cardiomyopathy, ARVD: Arrhythmogenic right ventricular dysplasia, NSHD: No structural heart disease, HCM: Hypertrophic cardiomyopathy, Valv: Valvular cardiomyopathy; NC: Non-compaction.

* represents VT storm cases only , † mean value

| Table 6.3 | Baseline clinical & demographic data |
|---|---|
| Study population VA storm, n | 471 |
| Age (mean ± SD), years | 61 ± 7 |
| Gender (Males,%) | 85 |
| EF (mean ± SD), %* | 30 ± 8 |
| Underlying heart disease, n (%) | |
| ICM | 321 (68) |
| DCM | 81 (17) |
| ARVD | 22 (5) |
| NSHD | 27 (6) |
| Others (Sarcoid, HCM, Valvular, Amyloid, NC) | 18 (4) |
| Nature of VA storm, n (%) | |
| Monomorphic VT | 362 (77) |
| pVT | 33 (7) |
| VF | 53 (11) |
| Unspecified | 23 (5) |
| Incessant VA | 172 (37) |
| Number of VT morphologies in monomorphic VT group (mean ± SD) | 1.6 ± 0.8 |
| VT cycle length (mean ± SD) | 395 ± 48 |
| ICD shocks per patient | 47 ± 50 |

* excluding patients with NSHD.

VT: Ventricular tachycardia, pVT: Polymorphic VT, VF: Ventricular fibrillation, VA: Ventricular arrhythmia, EF: Ejection fraction, ICM: Ischemic cardiomyopathy, DCM: Dilated cardiomyopathy, ARVD: Arrhythmogenic right ventricular dysplasia, NSHD: No structural heart disease, HCM: Hypertrophic cardiomyopathy, NC: Non-compaction, ICD: Implantable cardioverter defibrillator

| Table 6.4 | Odds of death and recurrence of ventricular arrhythmia after ablation in relation to baseline age and ejection fraction* | | | | |
|---|---|---|---|---|---|
| **Statistical model variables** | **Number of usable studies** | **Study references** | **Hazard Ratio (95% CI)** | **p value** | **Heterogeneity ($I^2$), %** |
| Age vs. Time to death | 9 | 431, 432, 442, 446, 459, 467, 469, 470, 475 | 1.03 (0.99, 1.07) | 0.15 | 0.0 |
| EF vs. Time to death | 8 | 431, 432, 446, 459, 467, 469, 470, 475 | 0.98 (0.94, 1.02) | 0.32 | 0.0 |
| Age vs. Time to cardiac death | 9 | 431, 432, 442, 446, 459, 460, 467, 469, 470, 475 | 1.05 (0.99, 1.11) | 0.12 | 34.2 |
| EF vs. Time to cardiac death | 8 | 431, 432, 446, 459, 460, 467, 469, 470, 475 | 0.96 (0.92, 1.00) | 0.07 | 0.0 |
| Age vs. Time to recurrence of VA | 8 | 431, 432, 446, 459, 467, 469, 470, 475 | 1.03 (0.99, 1.07) | 0.32 | 0.0 |
| EF vs. Time to recurrence of VA | 8 | 431, 432, 446, 459, 460, 467, 469, 470, 475 | 1.01 (0.98,1.04) | 0.54 | 0.0 |

| **Statistical model variables** | **Number of usable studies** | **Study references** | **Odds Ratio (95% CI)** | **p value** | **Heterogeneity ($I^2$), %** |
|---|---|---|---|---|---|
| Age vs. death | 7 | 431, 432, 442, 446, 459, 467, 469, 470, 475 | 1.02 (0.98, 1.07) | 0.33 | 0.0 |
| EF vs. death | 7 | 431, 432, 446, 459, 467, 469, 470, 475 | 0.96 (0.91, 1.02) | 0.15 | 0.0 |
| Age vs. recurrence of VA | 8 | 296, 431, 432, 446, 459, 467, 469, 470, 475 | 0.97 (0.93, 1.01) | 0.17 | 0.0 |
| EF vs recurrence of VA | 9 | 296, 431, 432, 446, 451, 459, 467, 469, 470, 475 | 0.96 (0.90, 1.02) | 0.15 | 10.6 |

* one % unit increment

VA: Ventricular Arrhythmia, EF: Ejection fraction, CI: Confidence interval

| Table 6.5 | Odds of recurrence of ventricular arrhythmia and death after ablation in relation to underlying heart disease. |
|---|---|

| Disease group comparison | Death | | Recurrence | |
|---|---|---|---|---|
| | Odds Ratio (95% CI) | p-value | Odds Ratio (95% CI) | p-value |
| ICM vs DCM | 0.51 (0.22,1.22) | 0.13 | 0.65 (0.29, 1.43) | 0.28 |
| ICM vs ARVD + Others | 0.69 (0.24, 2.01) | 0.50 | 0.57 (0.23, 1.40) | 0.22 |
| DCM vs ARVD + Others | 1.36 (0.43, 4.2) | 0.60 | 0.89 (0.30,2.54) | 0.82 |
| | | 0.31 | | 0.34 |

ICM: Ischemic cardiomyopathy, DCM: Dilated cardiomyopathy, ARVD: Arrhythmogenic right ventricular dysplasia, CI: Confidence interval

## FIGURES

***FIGURE 6.1***

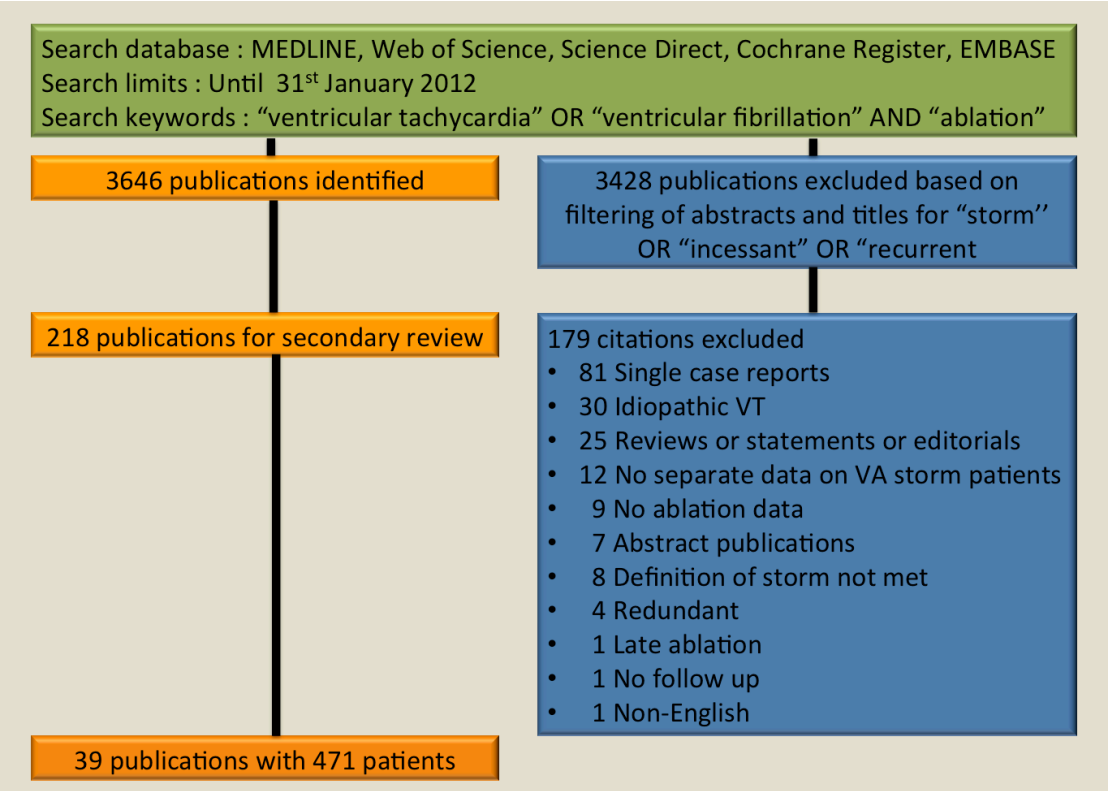


Figure 6.1. Schematic of database search and identification of studies. VT: ventricular tachycardia, VA: ventricular arrhythmia

***FIGURE 6.2***

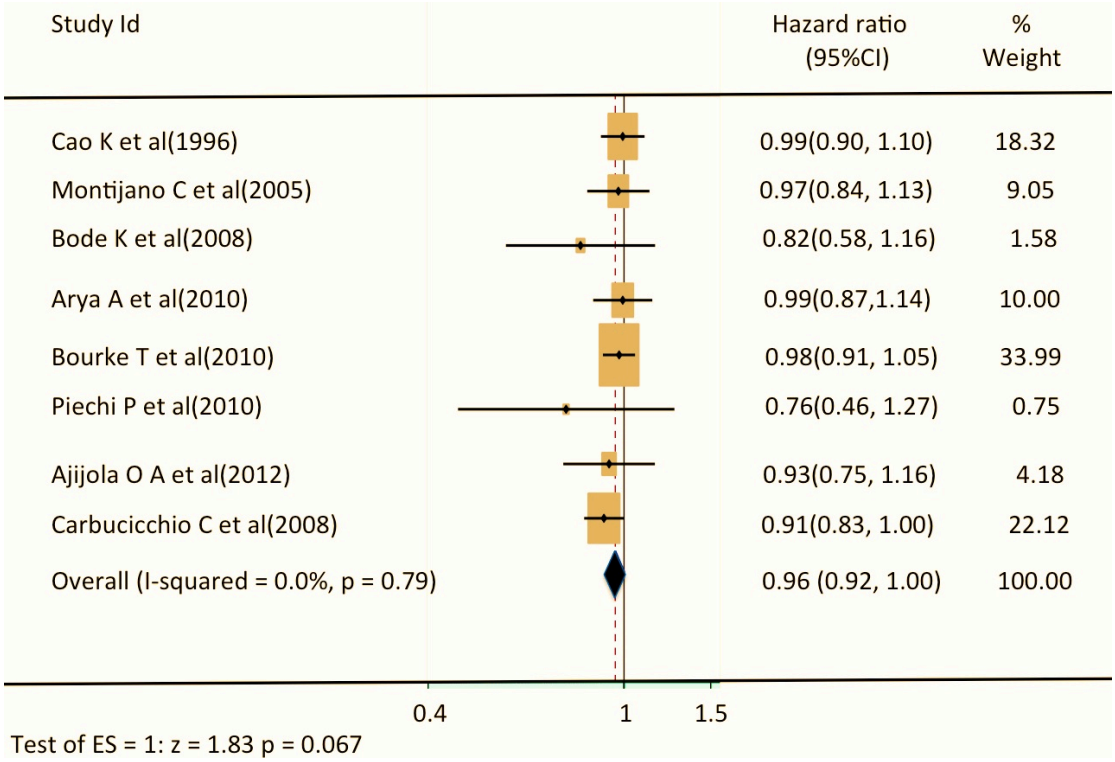


Figure 6.2. Association between ejection fraction (one unit increase) and instantaneous risk of cardiac death after ventricular arrhythmia storm.

# CHAPTER 7. FINAL DISCUSSION

This thesis has examined the electrophysiological properties of surviving myocyte channels in patients with ischemic cardiomyopathy and scar related ventricular tachycardia (VT). Whereas large body of clinical research has focused on the properties of channels critical for maintenance of VT circuits, no previous studies have characterized and compared electrophysiologic properties of VT channels, non-VT channels and rest of the scar. Using high density catheter mapping with enhanced resolution of scar, our studies have elucidated differential electrophysiological features of VT and non-VT channels. This information is critical to understand why some channels perpetuate VT and others do not. It will help lead clinicians to observe prudence while targeting these channels by catheter ablation.

Chapter 1 reviewed the basic principles of cardiac impulse propagation and development of reentrant VT. The rapidly growing body of scientific literature at the molecular and cellular level has integrated isolated elements of knowledge into a system that can now predict the electrical behavior of cardiac tissue. The complex interactions among many molecular events determine the structural and functional phenotype of electrograms observed at the regional heart level. The limitations in the current systems for mapping electrograms and VT circuits, and sobering long-term outcomes after catheter ablation reflect that we have achieved only limited translation of scientific knowledge to clinical practice and there is an opportunity for significant improvement.

The broad focus of a large body of clinical research in scar related reentry has been on channels supporting VT with a relatively limited representation of the properties of the non-VT channels. Chapter 2 described the use of high density of sampling and rigorous pace mapping with small bipoles to characterize the ventricular scar. It showed significant differences in the electroanatomic properties between VT supporting and non-VT channels in patients with ischemic cardiomyopathy and VT.

In addition, abnormal electrograms were abundant in the scar but only a small proportion were located in the region of VT channels. Electrograms at these sites displayed a longer duration of fractionation and poorer coupling of very late potentials relative to elsewhere in the scar. These observations may in part explain the difference in propensity of only few surviving myocyte channels in the scar to support reentrant VT.

The electrograms recorded during sinus rhythm from the areas of surviving myofibers in fibrous scar are often represented as fractionation and late potentials. However, information content pertinent to a VT supporting channel remains obscure in this simplistic way of composite electrogram classification. Chapter 3 details the development and use of a novel approach based on multiple-deflection time- and voltage-domain mapping of the intrinsic electrograms to localize VT channels. The strength of the study lied in the particularly high resolution of sampling and rigorous pace mapping within the dense scar to locate VT channels. This study, for the first time, described Shannon entropy, as a measure of information contained in a bipolar electrogram, in the ventricular scar. The electrogram properties: mean activation time, high-low dispersion interface and Shannon entropy (ShEn), were validated in a step-wise model against the contemporary methods for channel localization. The combination of latest site of activation, a zone of high dispersion of activation and low ShEn was the best predictor of the VT channel location, compared to individual electrogram properties. Despite being located in a zone of high dispersion, VT channel regions expressed low ShEn signifying relatively less complex electrograms. This novel strategy for substrate based mapping of scar related VT can be a significant leap forward towards individualized and potentially focused catheter ablation.

Some components of the anatomic substrate are relatively fixed once infarction has occurred, however, in few patients they continue to evolve with the development of new circuits and advanced heart failure. This indicates that surviving myocyte channels present in patients with previous VT differ in maturity compared to otherwise stable patients without spontaneous VT. No studies have compared this

evolution of myocyte channels to VT supporting channels. Chapter 4 elucidates the differences in the electroanatomic properties of conducting channels in VT patients compared to patients without spontaneous VT. These results are hypothesis generating that during the believed evolution towards establishment of VT circuits, zones of conduction delay or block coalesce to form longer corridors with slower conduction and thus express surrounding more complex fractionation and poorly coupled electrograms.

Besides the fixed anatomic scarring, spatio-temporal fluctuations in myocyte activation and recovery time increase risk of development of ventricular arrhythmias in these patients. There is evidence suggesting that beat-to-beat fluctuations in repolarization duration in heart failure are enhanced, however, the exact physiologic mechanisms in heart failure are poorly understood. Chapter 5 demonstrated that this high repolarization instability could not be modulated acutely by pacing or pharmacologic interventions in these patients, suggesting that autonomic modulation alone may be insufficient and perhaps high repolarization instability needs its own different set of possible interventions beyond purely neurohumoral management.

Finally, the life-saving role of catheter ablation in the setting of ventricular arrhythmia storms was critically analyzed in a systematic review of literature and emphasized its palliative role in these high-risk patients. This systematic review described the largest pooled database of ventricular arrhythmia storm patients with structural and non-structural heart disease who underwent invasive management. It contributes evidence supporting the protective role of intervention in the entire spectrum of VA storm patients who have impending risk of death, including interventions not limited to catheter ablation. It showed that these patients have only modest long-term survival advantage despite having a successful procedure, however, failure of the acute procedure carries a high short-term mortality.

# CHAPTER 8. FUTURE DIRECTIONS

Chapter 2 is the first comprehensive report on the differential electroanatomic features of VT supporting and non-VT channels within the scar, and may provide the basis for the development of a more focused substrate ablation. Further analyses are needed to evidently differentiate information in the sinus rhythm electrograms populating VT channels from elsewhere in the scar that may allow ablation of VT during sinus rhythm without extensive pace mapping or mapping during VT. Ablation was targeted with aim of eliminating scar related electrograms at sites of long paced latencies and the impact of differential ablation of non-VT channels on acute and long-term outcomes was not in the scope of this study. Larger studies with long follow-up are needed to determine if some non-VT channels mature to sustain VT.

As the ventricular scar volume can be frequently large, complete elimination of scar related electrograms or scar dechannelization remains difficult. Given this challenge facing catheter ablation of reentrant VT, the new model of mapping presented in Chapter 3 is anticipated to improve resolution of ventricular scar and identify apparently concealed small regions in the scar that harbor VT channels. This will help reduce excessive ablation employed in the current strategies and foster more focused and targeted ablation. The new approach appears convenient and is readily applicable in majority of patients; however, the effectiveness of this model must be compared against the prevailing methods of catheter ablation in a large study. We did not perform epicardial mapping. It is possible that some of the VTs that could not be mapped endocardially had intramyocardial or epicardial circuits. The presence of epicardial fat and coronary vessels introduce intricacies in electrogram formation. Further studies should evaluate the effectiveness of the model electrogram properties in the epicardial circuits.

Longer corridors with long latencies and slow conduction, broader fractionation, poorly coupled late potentials specifically in the VT channel regions described in Chapter 4, partly explains lack of inducible VT in patients without spontaneous VT. It

also suggests that only finite regions within the scar have electrophysiological properties suitable to perpetuate reentrant VT. However, longitudinal studies are needed to track the evolution of substrate in patients without spontaneous VT and appraise maturation of some of their channels to VT supporting channels. Aggressive substrate modification by catheter ablation targeting all potential channels can theoretically minimize consequences from adverse remodeling. However, it has failed to have any significant impact on long-term outcomes in these patients. This would suggest either failure of catheter ablation to arrest progressive scar remodeling despite its "apparent" homogenization, or pro-arrhythmic adverse effect of spot ablation in the scar only partially coalescing regions of conduction block. The lasting impact of high incidence of fast VT following catheter ablation on mortality in these patients also needs further investigation.

Beta-blockers are the mainstay of therapy in patients with systolic dysfunction, and were shown to improve survival in heart failure patients in large studies. The study presented in Chapter 5 has shown that beta-blockers are ineffective in reducing cardiac repolarization labiality in these patients at least on the short-term. This failure to achieve favorable changes in ventricular repolarization cannot be translated for gradual adaptive changes in repolarization lability that may occur slowly with long-term beta-blocker therapy and heart failure improvement. The insights gained from this work should stimulate further investigation and guide the development of clinical experiments to further assess if neuro-pharmacological augmentation of repolarization stability is feasible, and if responders have improved arrhythmia free survival.

The findings in Chapter 6 provide validation to the clinical belief that the majority of patients presenting with ventricular arrhythmia storm should undergo ablation as part of their overall management. The available data suggests that successful invasive intervention has favorable impact on long-term outcomes, however those who have failed procedures might have modest increase in death. The differences in the conduct of ablation present among these studies motivate the need of a standard practice that future studies on invasive management in VA storm should

promptly follow. None of the studies could address the question of which patient will benefit most from ablation. Due to lack of any randomized controlled trial data, it was impossible to compare and contrast medical therapy versus intervention in these patients. The study cannot unequivocally advocate that ablation is superior to other therapies to enhance survival in patients with VA storm and further randomized controlled studies are needed to investigate these propositions.

## BIBLIOGRAPHY


1. McWilliam JA: Cardiac Failure and Sudden Death. *Br Med J*. 1889; 1:6-8.

2. Rosamond W, Flegal K, Furie K, Go A, Greenlund K, Haase N, Hailpern SM, Ho M, Howard V, Kissela B, Kittner S, Lloyd-Jones D, McDermott M, Meigs J, Moy C, Nichol G, O'Donnell C, Roger V, Sorlie P, Steinberger J, Thom T, Wilson M, Hong Y: Heart disease and stroke statistics--2008 update: a report from the American Heart Association Statistics Committee and Stroke Statistics Subcommittee. *Circulation*. 2008; 117:e25-146.

3. Centers for Disease Control and Prevention CDC: State-specific mortality from sudden cardiac death--United States, 1999. *MMWR Morbidity and mortality weekly report*. 2002; 51:123-126.

4. Chugh SS, Jui J, Gunson K, Stecker EC, John BT, Thompson B, Ilias N, Vickers C, Dogra V, Daya M, Kron J, Zheng ZJ, Mensah G, McAnulty J: Current burden of sudden cardiac death: multiple source surveillance versus retrospective death certificate-based review in a large U.S. community. *J Am Coll Cardiol*. 2004; 44:1268-1275.

5. Bunch TJ, White RD: Trends in treated ventricular fibrillation in out-of-hospital cardiac arrest: ischemic compared to non-ischemic heart disease. *Resuscitation*. 2005; 67:51-54.

6. Fox CS, Evans JC, Larson MG, Kannel WB, Levy D: Temporal trends in coronary heart disease mortality and sudden cardiac death from 1950 to 1999: the Framingham Heart Study. *Circulation*. 2004; 110:522-527.

7. Mukharji J, Rude RE, Poole WK, Gustafson N, Thomas LJ, Jr., Strauss HW, Jaffe AS, Muller JE, Roberts R, Raabe DS, Jr., et al.: Risk factors for sudden death after acute myocardial infarction: two-year follow-up. *Am J Cardiol*. 1984; 54:31-36.

8. Ford ES, Ajani UA, Croft JB, Critchley JA, Labarthe DR, Kottke TE, Giles WH, Capewell S: Explaining the decrease in U.S. deaths from coronary disease, 1980-2000. *N Engl J Med*. 2007; 356:2388-2398.

9. AVID Investigators: Causes of death in the Antiarrhythmics Versus Implantable Defibrillators (AVID) Trial. *J Am Coll Cardiol*. 1999; 34:1552-1559.

10. Hua W, Niu H, Fan X, Ding L, Xu YZ, Wang J, Chen K, Wang F, Zhang S: Preventive effectiveness of implantable cardioverter defibrillator in reducing sudden cardiac death in the Chinese population: a multicenter trial of ICD therapy versus non-ICD therapy. *J Cardiovasc Electrophysiol*. 2012; 23 Suppl 1:S5-9.

11. Greenberg H, Case RB, Moss AJ, Brown MW, Carroll ER, Andrews ML: Analysis of mortality events in the Multicenter Automatic Defibrillator Implantation Trial (MADIT-II). *J Am Coll Cardiol*. 2004; 43:1459-1465.

12. Packer DL, Prutkin JM, Hellkamp AS, Mitchell LB, Bernstein RC, Wood F, Boehmer JP, Carlson MD, Frantz RP, McNulty SE, Rogers JG, Anderson J, Johnson GW, Walsh MN, Poole JE, Mark DB, Lee KL, Bardy GH: Impact of implantable cardioverter-defibrillator, amiodarone, and placebo on the mode of death in stable patients with heart failure: analysis from the sudden cardiac death in heart failure trial. *Circulation*. 2009; 120:2170-2176.

13. Myerburg RJ, Kessler KM, Zaman L, Conde CA, Castellanos A: Survivors of prehospital cardiac arrest. *JAMA*. 1982; 247:1485-1490.

14. Kjekshus J: Arrhythmias and mortality in congestive heart failure. *Am J Cardiol*. 1990; 65:42I-48I.

15. Doval HC, Nul DR, Grancelli HO, Perrone SV, Bortman GR, Curiel R: Randomised trial of low-dose amiodarone in severe congestive heart failure. Grupo de Estudio de la Sobrevida en la Insuficiencia Cardiaca en Argentina (GESICA). *Lancet*. 1994; 344:493-498.

16. Bolick DR, Hackel DB, Reimer KA, Ideker RE: Quantitative analysis of myocardial infarct structure in patients with ventricular tachycardia. *Circulation*. 1986; 74:1266-1279.

17. Adhar GC, Larson LW, Bardy GH, Greene HL: Sustained ventricular arrhythmias: differences between survivors of cardiac arrest and patients with recurrent sustained ventricular tachycardia. *J Am Coll Cardiol*. 1988; 12:159-165.

18. Moss AJ, Hall WJ, Cannom DS, Daubert JP, Higgins SL, Klein H, Levine JH, Saksena S, Waldo AL, Wilber D, Brown MW, Heo M: Improved survival with an implanted defibrillator in patients with coronary disease at high risk for ventricular arrhythmia. Multicenter Automatic Defibrillator Implantation Trial Investigators. *N Engl J Med*. 1996; 335:1933-1940.

19. Josephson M. Clinical Cardiac Electrophysiology: Techniques and Interpretations. 3rd ed. Philadelphia: Lippincott Williams & Wilkins; 2002. pp. 425-610.

20. Roy D, Marchand E, Theroux P, Waters DD, Pelletier GB, Cartier R, Bourassa MG: Long-term reproducibility and significance of provokable ventricular arrhythmias after myocardial infarction. *J Am Coll Cardiol*. 1986; 8:32-39.

21. Marchlinski FE, Waxman HL, Buxton AE, Josephson ME: Sustained ventricular tachyarrhythmias during the early postinfarction period: electrophysiologic findings and prognosis for survival. *J Am Coll Cardiol*. 1983; 2:240-250.

22. Daubert JP, Zareba W, Hall WJ, Schuger C, Corsello A, Leon AR, Andrews ML, McNitt S, Huang DT, Moss AJ: Predictive value of ventricular arrhythmia inducibility for subsequent ventricular tachycardia or ventricular fibrillation in Multicenter Automatic Defibrillator Implantation Trial (MADIT) II patients. *J Am Coll Cardiol*. 2006; 47:98-107.

23. Wijnmaalen AP, Schalij MJ, von der Thusen JH, Klautz RJ, Zeppenfeld K: Early reperfusion during acute myocardial infarction affects ventricular tachycardia characteristics and the chronic electroanatomic and histological substrate. *Circulation*. 2010; 121:1887-1895.

24. Myerburg RJ, Kessler KM, Castellanos A: Sudden cardiac death: epidemiology, transient risk, and intervention assessment. *Ann Intern Med*. 1993; 119:1187-1197.

25. Solomon SD, Zelenkofske S, McMurray JJ, Finn PV, Velazquez E, Ertl G, Harsanyi A, Rouleau JL, Maggioni A, Kober L, White H, Van de Werf F, Pieper K, Califf RM, Pfeffer MA: Sudden death in patients with myocardial infarction and left ventricular dysfunction, heart failure, or both. *N Engl J Med*. 2005; 352:2581-2588.

26. Tavazzi L, Volpi A: Remarks about postinfarction prognosis in light of the experience with the Gruppo Italiano per lo Studio della Sopravvivenza nell' Infarto Miocardico (GISSI) trials. *Circulation*. 1997; 95:1341-1345.

27. Krumholz HM, Chen J, Chen YT, Wang Y, Radford MJ: Predicting one-year mortality among elderly survivors of hospitalization for an acute myocardial infarction: results from the Cooperative Cardiovascular Project. *J Am Coll Cardiol*. 2001; 38:453-459.

28. Goldenberg I, Vyas AK, Hall WJ, Moss AJ, Wang H, He H, Zareba W, McNitt S, Andrews ML: Risk stratification for primary implantation of a cardioverter-

defibrillator in patients with ischemic left ventricular dysfunction. *J Am Coll Cardiol*. 2008; 51:288-296.

29. Camm A, Katrisis D. Risk stratification of patients with ventricular arrhythmias. . In: Zipes D, Jalife J, editors. Cardiac electrophysiology: from cell to bedside Philadelphia: W.B. Saunders Co.; 2000. pp. 808–828.

30. Kober L, Torp-Pedersen C, Elming H, Burchardt H: Use of left ventricular ejection fraction or wall-motion score index in predicting arrhythmic death in patients following an acute myocardial infarction. The TRACE Study Group. *Pacing Clin Electrophysiol*. 1997; 20:2553-2559.

31. Naccarella F, Lepera G, Rolli A: Arrhythmic risk stratification of post-myocardial infarction patients. *Curr Opin Cardiol*. 2000; 15:1-6.

32. Buxton AE, Lee KL, Hafley GE, Pires LA, Fisher JD, Gold MR, Josephson ME, Lehmann MH, Prystowsky EN: Limitations of ejection fraction for prediction of sudden death risk in patients with coronary artery disease: lessons from the MUSTT study. *J Am Coll Cardiol*. 2007; 50:1150-1157.

33. Zipes DP, Wellens HJ: Sudden cardiac death. *Circulation*. 1998; 98:2334-2351.

34. Buxton AE, Lee KL, Fisher JD, Josephson ME, Prystowsky EN, Hafley G: A randomized study of the prevention of sudden death in patients with coronary

artery disease. Multicenter Unsustained Tachycardia Trial Investigators. *N Engl J Med*. 1999; 341:1882-1890.

35. Moss AJ, Zareba W, Hall WJ, Klein H, Wilber DJ, Cannom DS, Daubert JP, Higgins SL, Brown MW, Andrews ML: Prophylactic implantation of a defibrillator in patients with myocardial infarction and reduced ejection fraction. *N Engl J Med*. 2002; 346:877-883.

36. Bardy GH, Lee KL, Mark DB, Poole JE, Packer DL, Boineau R, Domanski M, Troutman C, Anderson J, Johnson G, McNulty SE, Clapp-Channing N, Davidson-Ray LD, Fraulo ES, Fishbein DP, Luceri RM, Ip JH: Amiodarone or an implantable cardioverter-defibrillator for congestive heart failure. *N Engl J Med*. 2005; 352:225-237.

37. Gomes JA, Cain ME, Buxton AE, Josephson ME, Lee KL, Hafley GE: Prediction of long-term outcomes by signal-averaged electrocardiography in patients with unsustained ventricular tachycardia, coronary artery disease, and left ventricular dysfunction. *Circulation*. 2001; 104:436-441.

38. Bailey JJ, Berson AS, Handelsman H, Hodges M: Utility of current risk stratification tests for predicting major arrhythmic events after myocardial infarction. *J Am Coll Cardiol*. 2001; 38:1902-1911.

39. Ikeda T, Sakata T, Takami M, Kondo N, Tezuka N, Nakae T, Noro M, Enjoji Y, Abe R, Sugi K, Yamaguchi T: Combined assessment of T-wave alternans and late

potentials used to predict arrhythmic events after myocardial infarction. A prospective study. *J Am Coll Cardiol*. 2000; 35:722-730.

40. Bloomfield DM, Steinman RC, Namerow PB, Parides M, Davidenko J, Kaufman ES, Shinn T, Curtis A, Fontaine J, Holmes D, Russo A, Tang C, Bigger JT, Jr.: Microvolt T-wave alternans distinguishes between patients likely and patients not likely to benefit from implanted cardiac defibrillator therapy: a solution to the Multicenter Automatic Defibrillator Implantation Trial (MADIT) II conundrum. *Circulation*. 2004; 110:1885-1889.

41. Kleiger RE, Miller JP, Bigger JT, Jr., Moss AJ: Decreased heart rate variability and its association with increased mortality after acute myocardial infarction. *Am J Cardiol*. 1987; 59:256-262.

42. Bilchick KC, Fetics B, Djoukeng R, Fisher SG, Fletcher RD, Singh SN, Nevo E, Berger RD: Prognostic value of heart rate variability in chronic congestive heart failure (Veterans Affairs' Survival Trial of Antiarrhythmic Therapy in Congestive Heart Failure). *Am J Cardiol*. 2002; 90:24-28.

43. Nolan J, Batin PD, Andrews R, Lindsay SJ, Brooksby P, Mullen M, Baig W, Flapan AD, Cowley A, Prescott RJ, Neilson JM, Fox KA: Prospective study of heart rate variability and mortality in chronic heart failure: results of the United Kingdom heart failure evaluation and assessment of risk trial (UK-heart). *Circulation*. 1998; 98:1510-1516.

44. Beuckelmann D, Nabauer M, Erdmann E: Intracellular calcium handling in isolated ventricular myocytes from patients with terminal heart failure. *Circulation*. 1992; 85:1046-1055.

45. Beuckelmann D, Nabauer M, Erdmann E: Alterations of K+ currents in isolated humanventricular myocytes from patients with terminal heart failure
. *Circulation*. 1993; 73:379-385.

46. Antzelevitch C, Fish J: Electrical heterogeneity within the ventricular wall. *Basic Res Cardiol*. 2001; 96:517-527.

47. Schwartz PJ, Wolf S: QT interval prolongation as predictor of sudden death in patients with myocardial infarction. *Circulation*. 1978; 57:1074-1077.

48. Chugh SS, Reinier K, Singh T, Uy-Evanado A, Socoteanu C, Peters D, Mariani R, Gunson K, Jui J: Determinants of prolonged QT interval and their contribution to sudden death risk in coronary artery disease: the Oregon Sudden Unexpected Death Study. *Circulation*. 2009; 119:663-670.

49. Karwatowska-Prokopczuk E, Wang W, Cheng ML, Zeng D, Schwartz PJ, Belardinelli L: The risk of sudden cardiac death in patients with non-ST elevation acute coronary syndrome and prolonged QTc interval: effect of ranolazine. *Europace*. 2013; 15:429-436.

50. Berger R, Kasper E, Baughman K, Marban E, Calkins H, Tomaselli G: Beat-to-beat QT interval variability: novel evidence for repolarization lability in ischemic and nonischemic dilated cardiomyopathy. *Circulation*. 1997; 96:1557-1565.

51. Murabayashi T, Fetics B, Kass D, Nevo E, Gramatikov B, Berger R: Beat-to-beat QT interval variability associated with acute myocardial ischemia. *J Electrocardiol*. 2002; 35:19-25.

52. Piccirillo G, Magnanti M, Matera S, Di Carlo S, De Laurentis T, Torrini A, Marchitto N, Ricci R, Magrí D: Age and QT variability index during free breathing, controlled breathing and tilt in patients with chronic heart failure and healthy control subjects *Transl Res*. 2006; 148:72-78.

53. Hinterseer M, Beckmann BM, Thomsen MB, Pfeufer A, Ulbrich M, Sinner MF, Perz S, Wichmann HE, Lengyel C, Schimpf R, Maier SK, Varro A, Vos MA, Steinbeck G, Kaab S: Usefulness of short-term variability of QT intervals as a predictor for electrical remodeling and proarrhythmia in patients with nonischemic heart failure. *Am J Cardiol*. 2010; 106:216-220.

54. Haigney M, Zareba W, Gentlesk P, Goldstein R, Illovsky M, McNitt S, Andrews M, Moss A: QT interval variability and spontaneous ventricular tachycardia or fibrillation in the Multi- center Automatic Defibrillator Implantation Trial (MADIT) II patients. *J Am Coll Cardiol*. 2004; 44:1481-1487.

55. Piccirillo G, Magri D, Matera S, Magnanti M, Torrini A, Pasquazzi E, Schifano E, Velitti S, Marigliano V, Quaglione R, Barillà F: QT variability strongly predicts sudden cardiac death in asymptomatic subjects with mild or moderate left ventricular systolic dysfunction: a prospective study. *Eur Heart J*. 2007; 28:1344-1350.

56. Tereshchenko LG, Cygankiewicz I, McNitt S, Vazquez R, Bayes-Genis A, Han L, Sur S, Couderc JP, Berger RD, de Luna AB, Zareba W: Predictive value of beat-to-beat QT variability index across the continuum of left ventricular dysfunction: competing risks of noncardiac or cardiovascular death and sudden or nonsudden cardiac death. *Circ Arrhythm Electrophysiol*. 2012; 5:719-727.

57. Dobson CP, La Rovere MT, Pinna GD, Goldstein R, Olsen C, Bernardinangeli M, Veniani M, Midi P, Tavazzi L, Haigney M: QT variability index on 24-hour Holter independently predicts mortality in patients with heart failure: analysis of Gruppo Italiano per lo Studio della Sopravvivenza nell'Insufficienza Cardiaca (GISSI-HF) trial. *Heart Rhythm*. 2011; 8:1237-1242.

58. Zaza A, Malfatto G, Schwartz PJ: Sympathetic modulation of the relation between ventricular repolarization and cycle length. *Circ Res*. 1991; 68:1191-1203.

59. Roden DM: Taking the "idio" out of "idiosyncratic": predicting torsades de pointes. *Pacing Clin Electrophysiol*. 1998; 21:1029-1034.

60. Yeragani V, Pohl R, Jampala V, Balon R, Kay J, Igel G: Effect of posture and isoproterenol on beat-to-beat heart rate and QT variability. *Neuropsychobiology*. 2000; 41:113-123.

61. Cheng A, Dalal D, Fetics BJ, Angkeow P, Spragg DD, Calkins H, Tomaselli GF, Berger RD: Ibutilide-induced changes in the temporal lability of ventricular repolarization in patients with and without structural heart disease. *J Cardiovasc Electrophysiol*. 2009; 20:873-879.

62. Ajijola OA, Vaseghi M, Zhou W, Yamakawa K, Benharash P, Hadaya J, Lux RL, Mahajan A, Shivkumar K: Functional differences between junctional and extrajunctional adrenergic receptor activation in mammalian ventricle. *Am J Physiol Heart Circ Physiol*. 2013; 304:H579-588.

63. Roden DM, Yang T: Protecting the Heart Against Arrhythmias: Potassium Current Physiology and Repolarization Reserve. *Circulation*. 2005; 112:1376-1378.

64. Vaseghi M, Lux RL, Mahajan A, Shivkumar K: Sympathetic stimulation increases dispersion of repolarization in humans with myocardial infarction. *Am J Physiol Heart Circ Physiol*. 2012; 302:H1838-1846.

65. Antzelevitch C, Dumaine R. Electrical heterogeneity in the heart: physiological, pharmacological and clinical implications. . In: Page E, Fozzard HA, Solaro RJ, editors. The Handbook of Physiology. New York: Oxford Univ. Press; 2002. pp. 654–692.

66. Akar FG, Wu RC, Juang GJ, Tian Y, Burysek M, Disilvestre D, Xiong W, Armoundas AA, Tomaselli GF: Molecular mechanisms underlying K+ current downregulation in canine tachycardia-induced heart failure. *Am J Physiol Heart Circ Physiol*. 2005; 288:H2887-2896.

67. Lengyel C, Varro A, Tabori K, Papp JG, Baczko I: Combined pharmacological block of I(Kr) and I(Ks) increases short-term QT interval variability and provokes torsades de pointes. *Br J Pharmacol*. 2007; 151:941-951.

68. Lymperopoulos A, Rengo G, Koch WJ: Adrenergic nervous system in heart failure: pathophysiology and therapy. *Circ Res*. 2013; 113:739-753.

69. Pepper GS, Lee RW: Sympathetic activation in heart failure and its treatment with beta-blockade. *Arch Intern Med*. 1999; 159:225-234.

70. Iaccarino G, Tomhave ED, Lefkowitz RJ, Koch WJ: Reciprocal in vivo regulation of myocardial G protein-coupled receptor kinase expression by beta-adrenergic receptor stimulation and blockade. *Circulation*. 1998; 98:1783-1789.

71. Osadchii OE, Norton GR, McKechnie R, Deftereos D, Woodiwiss AJ: Cardiac dilatation and pump dysfunction without intrinsic myocardial systolic failure following chronic beta-adrenoreceptor activation. *Am J Physiol Heart Circ Physiol*. 2007; 292:H1898-1905.

72. Adamson PB, Gilbert EM: Reducing the risk of sudden death in heart failure with beta-blockers. *J Card Fail*. 2006; 12:734-746.

73. Rengo G, Lymperopoulos A, Zincarelli C, Femminella G, Liccardo D, Pagano G, de Lucia C, Cannavo A, Gargiulo P, Ferrara N, Perrone Filardi P, Koch W, Leosco D: Blockade of beta-adrenoceptors restores the GRK2-mediated adrenal alpha(2) -adrenoceptor-catecholamine production axis in heart failure. *Br J Pharmacol*. 2012; 166:2430-2440.

74. Fauchier L, Pierre B, de Labriolle A, Babuty D: Comparison of the beneficial effect of beta-blockers on mortality in patients with ischaemic or non-ischaemic systolic heart failure: a meta-analysis of randomised controlled trials. *Eur J Heart Fail*. 2007; 9:1136-1139.

75. Furukawa Y, Shimizu H, Hiromoto K, Kanemori T, Masuyama T, Ohyanagi M: Circadian variation of beat-to-beat QT interval variability in patients with prior myocardial infarction and the effect of beta-blocker therapy. *Pacing Clin Electrophysiol*. 2006; 29:479-486.

76. Piccirillo G, Quaglione R, Nocco M, Naso C, Moise A, Lionetti M, Di Carlo S, Marigliano V: Effects of long-term beta-blocker (metoprolol or carvedilol) therapy on QT variability in subjects with chronic heart failure secondary to ischemic cardiomyopathy. *Am J Cardiol*. 2002; 90:1113-1117.

77. Wellens HJ: Value and limitations of programmed electrical stimulation of the heart in the study and treatment of tachycardias. *Circulation*. 1978; 57:845-853.

78. Josephson ME, Almendral JM, Buxton AE, Marchlinski FE: Mechanisms of ventricular tachycardia. *Circulation*. 1987; 75:III41-47.

79. Buxton AE, Waxman HL, Marchlinski FE, Untereker WJ, Waspe LE, Josephson ME: Role of triple extrastimuli during electrophysiologic study of patients with documented sustained ventricular tachyarrhythmias. *Circulation*. 1984; 69:532-540.

80. Rothman SA, Hsia HH, Cossu SF, Chmielewski IL, Buxton AE, Miller JM: Radiofrequency catheter ablation of postinfarction ventricular tachycardia: long-term success and the significance of inducible nonclinical arrhythmias. *Circulation*. 1997; 96:3499-3508.

81. Stevenson WG, Friedman PL, Kocovic D, Sager PT, Saxon LA, Pavri B: Radiofrequency catheter ablation of ventricular tachycardia after myocardial infarction. *Circulation*. 1998; 98:308-314.

82. Yoshida K, Liu TY, Scott C, Hero A, Yokokawa M, Gupta S, Good E, Morady F, Bogun F: The value of defibrillator electrograms for recognition of clinical ventricular tachycardias and for pace mapping of post-infarction ventricular tachycardia. *J Am Coll Cardiol*. 2010; 56:969-979.

83. Buxton AE, Lee KL, DiCarlo L, Gold MR, Greer GS, Prystowsky EN, O'Toole MF, Tang A, Fisher JD, Coromilas J, Talajic M, Hafley G: Electrophysiologic testing to identify patients with coronary artery disease who are at risk for sudden death. Multicenter Unsustained Tachycardia Trial Investigators. *N Engl J Med*. 2000; 342:1937-1945.

84. Epstein AE, Dimarco JP, Ellenbogen KA, Estes NA, 3rd, Freedman RA, Gettes LS, Gillinov AM, Gregoratos G, Hammill SC, Hayes DL, Hlatky MA, Newby LK, Page RL, Schoenfeld MH, Silka MJ, Stevenson LW, Sweeney MO: ACC/AHA/HRS 2008 guidelines for Device-Based Therapy of Cardiac Rhythm Abnormalities: executive summary. *Heart Rhythm*. 2008; 5:934-955.

85. Rudy Y. The cardiac ventricular action potential. In: Page E, Fozzard HA, Solaro RJ, editors. The Handbook of Physiology The Cardiovascular System The Heart Bethesda, MD: Am. Physiol. Soc.; 2002. pp. 531–547.

86. Coraboeuf E, Weidmann S: Potentiels d'action du muscle cardiaque obtenus a` l'aide de microe´ le´ctrodes intracellulaires. Pre´sence d'une inversion du potentiel. . *C R Se´ances Soc Biol* 1949; 143:1360.

87. Hodgkin AL, Huxley AF: A quantitative description of membrane current and its application to conduction and excitation in nerve. *J Physiol*. 1952; 117:500-544.

88. Weidmann S: The electrical constants of Purkinje fibres. *J Physiol*. 1952; 118:348-360.

89. Weidmann S: Electrical constants of trabecular muscle from mammalian heart. *J Physiol*. 1970; 210:1041-1054.

90. Neher E, Sakmann B: Single-channel currents recorded from membrane of denervated frog muscle fibres. *Nature*. 1976; 260:799-802.

91. Reuter H: Calcium channel modulation by neurotransmitters, enzymes and drugs. *Nature*. 1983; 301:569-574.

92. Reuter H, Scholz H: [On the influence of the extracellular Ca concentration on membrane potential and contraction of isolated heart preparations during graded depolarization]. *Pflugers Archiv fur die gesamte Physiologie des Menschen und der Tiere*. 1968; 300:87-107.

93. Marban E: Cardiac channelopathies. *Nature*. 2002; 415:213-218.

94. Kleber A, Rudy Y: Basic Mechanisms of Cardiac Impulse Propagation and Associated Arrhythmias. *Physiol Rev*. 2004; 84:431-488.

95. Heath B, Gingrich K, Kass R. Ion channels in the heart: cellular and molecular properties of cardiac Na, Ca and K channels. In: Page E, Fozzard HA, Solaro RJ, editors. The Handbook of Physiology The Cardiovascular System The Heart. Bethesda, MD: Am. Physiol. Soc; 2002. pp. 548–567.

96. Fozzard HA: Membrane capacity of the cardiac Purkinje fibre. *J Physiol*. 1966; 182:255-267.

97. Luo CH, Rudy Y: A model of the ventricular cardiac action potential. Depolarization, repolarization, and their interaction. *Circ Res*. 1991; 68:1501-1526.

98. Luo CH, Rudy Y: A dynamic model of the cardiac ventricular action potential. I. Simulations of ionic currents and concentration changes. *Circ Res*. 1994; 74:1071-1096.

99. Berman MF, Camardo JS, Robinson RB, Siegelbaum SA: Single sodium channels from canine ventricular myocytes: voltage dependence and relative rates of activation and inactivation. *J Physiol*. 1989; 415:503-531.

100. Hadley RW, Lederer WJ: Ca2+ and voltage inactivate Ca2+ channels in guinea-pig ventricular myocytes through independent mechanisms. *J Physiol*. 1991; 444:257-268.

101. Sipido KR, Callewaert G, Carmeliet E: Inhibition and rapid recovery of Ca2+ current during Ca2+ release from sarcoplasmic reticulum in guinea pig ventricular myocytes. *Circ Res*. 1995; 76:102-109.

102. Noble D, Rudy Y: Models of cardiac ventricular action potentials: iterative interaction between experiment and simulation. *PhilosTrans R Soc Lond* 2001; 359:1127–1142.

103. LeGrice IJ, Smaill BH, Chai LZ, Edgar SG, Gavin JB, Hunter PJ: Laminar structure of the heart: ventricular myocyte arrangement and connective tissue architecture in the dog. *Am J Physiol*. 1995; 269:H571-582.

104. Shaw RM, Rudy Y: Electrophysiologic effects of acute myocardial ischemia: a theoretical study of altered cell excitability and action potential duration. *Cardiovasc Res*. 1997; 35:256-272.

105. Spach MS, Kootsey JM: Relating the sodium current and conductance to the shape of transmembrane and extracellular potentials by simulation: effects of propagation boundaries. *IEEE Trans Biomed Eng*. 1985; 32:743-755.

106. Spach MS, Barr RC, Serwer GS, Johnson EA, Kootsey JM: Collision of excitation waves in the dog Purkinje system. Extracellular identification. *Circ Res*. 1971; 29:499-511.

107. Wang Y, Rudy Y: Action potential propagation in inhomogeneous cardiac tissue: safety factor considerations and ionic mechanism. *Am J Physiol Heart Circ Physiol*. 2000; 278:H1019-1029.

108. Fast VG, Kleber AG: Cardiac tissue geometry as a determinant of unidirectional conduction block: assessment of microscopic excitation spread by optical mapping in patterned cell cultures and in a computer model. *Cardiovasc Res*. 1995; 29:697-707.

109. Joyner RW: Effects of the discrete pattern of electrical coupling on propagation through an electrical syncytium. *Circ Res*. 1982; 50:192-200.

110. Joyner RW, van Capelle FJ: Propagation through electrically coupled cells. How a small SA node drives a large atrium. *Biophys J*. 1986; 50:1157-1164.

111. Shaw RM, Rudy Y: Ionic mechanisms of propagation in cardiac tissue. Roles of the sodium and L-type calcium currents during reduced excitability and decreased gap junction coupling. *Circ Res*. 1997; 81:727-741.

112. Fast VG, Kleber AG: Role of wavefront curvature in propagation of cardiac impulse. *Cardiovasc Res*. 1997; 33:258-271.

113. Zykov VS, Morozova OL: Rate of impulse propagation in a two-dimensional excitable medium. *Biofizika*. 1979; 24:717-722.

114. Roberts DE, Hersh LT, Scher AM: Influence of cardiac fiber orientation on wavefront voltage, conduction velocity, and tissue resistivity in the dog. *Circ Res*. 1979; 44:701-712.

115. Kadish A, Shinnar M, Moore EN, Levine JH, Balke CW, Spear JF: Interaction of fiber orientation and direction of impulse propagation with anatomic barriers in anisotropic canine myocardium. *Circulation*. 1988; 78:1478-1494.

116. Spear JF, Michelson EL, Moore EN: Cellular electrophysiologic characteristics of chronically infarcted myocardium in dogs susceptible to sustained ventricular tachyarrhythmias. *J Am Coll Cardiol*. 1983; 1:1099-1110.

117. Kleber A, Janse M, Fast V. Normal and abnomal conduction in the heart. . In: Page E, Fozzard HA, Solaro RJ, editors. The Handbook of Physiology The Cardiovascular System The Heart Bethesda, MD: Am. Physiol. Soc; 2002. pp. 455–530.

118. Draper MH, Mya-Tu M: A comparison of the conduction velocity in cardiac tissues of various mammals. *Q J Exp Physiol Cogn Med Sci* 1959; 44:91-109.

119. Saffitz JE, Kanter HL, Green KG, Tolley TK, Beyer EC: Tissue-specific determinants of anisotropic conduction velocity in canine atrial and ventricular myocardium. *Circ Res*. 1994; 74:1065-1070.

120. Davis LM, Kanter HL, Beyer EC, Saffitz JE: Distinct gap junction protein phenotypes in cardiac tissues with disparate conduction properties. *J Am Coll Cardiol*. 1994; 24:1124-1132.

121. Fast VG, Kleber AG: Anisotropic conduction in monolayers of neonatal rat heart cells cultured on collagen substrate. *Circ Res*. 1994; 75:591-595.

122. Spach MS, Heidlage JF, Dolber PC, Barr RC: Electrophysiological effects of remodeling cardiac gap junctions and cell size: experimental and model studies of normal cardiac growth. *Circ Res*. 2000; 86:302-311.

123. Fleischhauer J, Lehmann L, Kleber AG: Electrical resistances of interstitial and microvascular space as determinants of the extracellular electrical field and velocity of propagation in ventricular myocardium. *Circulation*. 1995; 92:587-594.

124. Willecke K, Eiberger J, Degen J, Eckardt D, Romualdi A, Guldenagel M, Deutsch U, Sohl G: Structural and functional diversity of connexin genes in the mouse and human genome. *Biol Chem*. 2002; 383:725-737.

125. Spach MS, Dolber PC, Heidlage JF: Influence of the passive anisotropic properties on directional differences in propagation following modification of the sodium conductance in human atrial muscle. A model of reentry based on anisotropic discontinuous propagation. *Circ Res*. 1988; 62:811-832.

126. Cottrell GT, Burt JM: Heterotypic gap junction channel formation between heteromeric and homomeric Cx40 and Cx43 connexons. *Am J Physiol Cell Physiol*. 2001; 281:C1559-1567.

127. Peters NS, Wit AL: Gap junction remodeling in infarction: does it play a role in arrhythmogenesis? *J Cardiovasc Electrophysiol*. 2000; 11:488-490.

128. Smith JH, Green CR, Peters NS, Rothery S, Severs NJ: Altered patterns of gap junction distribution in ischemic heart disease. An immunohistochemical study of human myocardium using laser scanning confocal microscopy. *Am J Pathol*. 1991; 139:801-821.

129. Luke RA, Saffitz JE: Remodeling of ventricular conduction pathways in healed canine infarct border zones. *J Clin Invest*. 1991; 87:1594-1602.

130. Glukhov AV, Fedorov VV, Kalish PW, Ravikumar VK, Lou Q, Janks D, Schuessler RB, Moazami N, Efimov IR: Conduction remodeling in human end-stage nonischemic left ventricular cardiomyopathy. *Circulation*. 2012; 125:1835-1847.

131. Peters NS: New insights into myocardial arrhythmogenesis: distribution of gap-junctional coupling in normal, ischaemic and hypertrophied human hearts. *Clin Sci* 1996; 90:447-452.

132. Cohen SA: Immunocytochemical localization of rH1 sodium channel in adult rat heart atria and ventricle. Presence in terminal intercalated disks. *Circulation*. 1996; 94:3083-3086.

133. Gathercole DV, Colling DJ, Skepper JN, Takagishi Y, Levi AJ, Severs NJ: Immunogold-labeled L-type calcium channels are clustered in the surface plasma membrane overlying junctional sarcoplasmic reticulum in guinea-pig myocytes-implications for excitation-contraction coupling in cardiac muscle. *J Mol Cell Cardiol*. 2000; 32:1981-1994.

134. Anselme F, Saoudi N, Redonnet M, Letac B: Atrioatrial conduction after orthotopic heart transplantation. *J Am Coll Cardiol*. 1994; 24:185-189.

135. Lefroy DC, Fang JC, Stevenson LW, Hartley LH, Friedman PL, Stevenson WG: Recipient-to-donor atrioatrial conduction after orthotopic heart transplantation: surface electrocardiographic features and estimated prevalence. *Am J Cardiol*. 1998; 82:444-450.

136. Miragoli M, Gaudesius G, Rohr S: Electrotonic modulation of cardiac impulse conduction by myofibroblasts. *Circ Res*. 2006; 98:801-810.

137. Fast VG, Kleber AG: Microscopic conduction in cultured strands of neonatal rat heart cells measured with voltage-sensitive dyes. *Circ Res*. 1993; 73:914-925.

138. Fast VG, Darrow BJ, Saffitz JE, Kleber AG: Anisotropic activation spread in heart cell monolayers assessed by high-resolution optical mapping. Role of tissue discontinuities. *Circ Res*. 1996; 79:115-127.

139. Cabo C, Yao J, Boyden PA, Chen S, Hussain W, Duffy HS, Ciaccio EJ, Peters NS, Wit AL: Heterogeneous gap junction remodeling in reentrant circuits in the epicardial border zone of the healing canine infarct. *Cardiovasc Res*. 2006; 72:241-249.

140. Kieken F, Mutsaers N, Dolmatova E, Virgil K, Wit AL, Kellezi A, Hirst-Jensen BJ, Duffy HS, Sorgen PL: Structural and molecular mechanisms of gap junction

remodeling in epicardial border zone myocytes following myocardial infarction. *Circ Res*. 2009; 104:1103-1112.

141. Powell DW, Mifflin RC, Valentich JD, Crowe SE, Saada JI, West AB: Myofibroblasts. I. Paracrine cells important in health and disease. *Am J Physiol*. 1999; 277:C1-9.

142. Baum JR, Long B, Cabo C, Duffy HS: Myofibroblasts cause heterogeneous Cx43 reduction and are unlikely to be coupled to myocytes in the healing canine infarct. *Am J Physiol Heart Circ Physiol*. 2012; 302:H790-H800.

143. Henriquez CS, Muzikant AL, Smoak CK: Anisotropy, fiber curvature, and bath loading effects on activation in thin and thick cardiac tissue preparations: simulations in a three-dimensional bidomain model. *J Cardiovasc Electrophysiol*. 1996; 7:424-444.

144. Spach MS, Heidlage JF: The stochastic nature of cardiac propagation at a microscopic level. Electrical description of myocardial architecture and its application to conduction. *Circ Res*. 1995; 76:366-380.

145. Hoffman BF, Cranefield PF, Lepeschkin E, Surawicz B, Herrlich HC: Comparison of cardiac monophasic action potentials recorded by intracellular and suction electrodes. *Am J Physiol*. 1959; 196:1297-1301.

146. Maglaveras N, De Bakker JM, Van Capelle FJ, Pappas C, Janse MJ: Activation delay in healed myocardial infarction: a comparison between model and experiment. *Am J Physiol*. 1995; 269:H1441-1449.

147. Rudy Y, Quan W: Propagation Delays Across Cardiac Gap Junctions and their Reflection in Extracellular Potentials: A Simulation Study. *J Cardiovasc Electrophysiol*. 1991; 2:299-315.

148. Dillon SM, Allessie MA, Ursell PC, Wit AL: Influences of anisotropic tissue structure on reentrant circuits in the epicardial border zone of subacute canine infarcts. *Circ Res*. 1988; 63:182-206.

149. Spach MS, Dolber PC: Relating extracellular potentials and their derivatives to anisotropic propagation at a microscopic level in human cardiac muscle. Evidence for electrical uncoupling of side-to-side fiber connections with increasing age. *Circ Res*. 1986; 58:356-371.

150. Downar E, Janse MJ, Durrer D: The effect of acute coronary artery occlusion on subepicardial transmembrane potentials in the intact porcine heart. *Circulation*. 1977; 56:217-224.

151. Kleber AG, Janse MJ, Wilms-Schopmann FJ, Wilde AA, Coronel R: Changes in conduction velocity during acute ischemia in ventricular myocardium of the isolated porcine heart. *Circulation*. 1986; 73:189-198.

152. Kodama I, Wilde A, Janse MJ, Durrer D, Yamada K: Combined effects of hypoxia, hyperkalemia and acidosis on membrane action potential and excitability of guinea-pig ventricular muscle. *J Mol Cell Cardiol*. 1984; 16:247-259.

153. Buchanan JW, Jr., Saito T, Gettes LS: The effects of antiarrhythmic drugs, stimulation frequency, and potassium-induced resting membrane potential changes on conduction velocity and dV/dtmax in guinea pig myocardium. *Circ Res*. 1985; 56:696-703.

154. Bezzina C, Veldkamp MW, van Den Berg MP, Postma AV, Rook MB, Viersma JW, van Langen IM, Tan-Sindhunata G, Bink-Boelkens MT, van Der Hout AH, Mannens MM, Wilde AA: A single Na(+) channel mutation causing both long-QT and Brugada syndromes. *Circ Res*. 1999; 85:1206-1213.

155. Kagiyama Y, Hill JL, Gettes LS: Interaction of acidosis and increased extracellular potassium on action potential characteristics and conduction in guinea pig ventricular muscle. *Circ Res*. 1982; 51:614-623.

156. Rohr S, Kucera JP, Kleber AG: Slow conduction in cardiac tissue, I: effects of a reduction of excitability versus a reduction of electrical coupling on microconduction. *Circ Res*. 1998; 83:781-794.

157. Janse MJ, Kleber AG: Electrophysiological changes and ventricular arrhythmias in the early phase of regional myocardial ischemia. *Circ Res*. 1981; 49:1069-1081.

158. Janse MJ, Wit AL: Electrophysiological mechanisms of ventricular arrhythmias resulting from myocardial ischemia and infarction. *Physiol Rev*. 1989; 69:1049-1169.

159. Kleber AG: Resting membrane potential, extracellular potassium activity, and intracellular sodium activity during acute global ischemia in isolated perfused guinea pig hearts. *Circ Res*. 1983; 52:442-450.

160. Kleber AG, Riegger CB, Janse MJ: Electrical uncoupling and increase of extracellular resistance after induction of ischemia in isolated, arterially perfused rabbit papillary muscle. *Circ Res*. 1987; 61:271-279.

161. Coronel R, Wilms-Schopman FJ, Fiolet JW, Opthof T, Janse MJ: The relation between extracellular potassium concentration and pH in the border zone during regional ischemia in isolated porcine hearts. *J Mol Cell Cardiol*. 1995; 27:2069-2073.

162. Janse MJ, van Capelle FJ, Morsink H, Kleber AG, Wilms-Schopman F, Cardinal R, d'Alnoncourt CN, Durrer D: Flow of "injury" current and patterns of excitation during early ventricular arrhythmias in acute regional myocardial ischemia in isolated porcine and canine hearts. Evidence for two different arrhythmogenic mechanisms. *Circ Res*. 1980; 47:151-165.

163. Gettes LS, Reuter H: Slow recovery from inactivation of inward currents in mammalian myocardial fibres. *J Physiol*. 1974; 240:703-724.

164. Peters NS, Green CR, Poole-Wilson PA, Severs NJ: Reduced content of connexin43 gap junctions in ventricular myocardium from hypertrophied and ischemic human hearts. *Circulation*. 1993; 88:864-875.

165. Riegger CB, Alperovich G, Kleber AG: Effect of oxygen withdrawal on active and passive electrical properties of arterially perfused rabbit ventricular muscle. *Circ Res*. 1989; 64:532-541.

166. Ek-Vitorin JF, Calero G, Morley GE, Coombs W, Taffet SM, Delmar M: PH regulation of connexin43: molecular analysis of the gating particle. *Biophys J*. 1996; 71:1273-1284.

167. Firek L, Weingart R: Modification of gap junction conductance by divalent cations and protons in neonatal rat heart cells. *J Mol Cell Cardiol*. 1995; 27:1633-1643.

168. Noma A, Tsuboi N: Dependence of junctional conductance on proton, calcium and magnesium ions in cardiac paired cells of guinea-pig. *J Physiol*. 1987; 382:193-211.

169. Zhuang J, Yamada KA, Saffitz JE, Kleber AG: Pulsatile stretch remodels cell-to-cell communication in cultured myocytes. *Circ Res*. 2000; 87:316-322.

170. Darrow BJ, Fast VG, Kleber AG, Beyer EC, Saffitz JE: Functional and structural assessment of intercellular communication. Increased conduction velocity and

enhanced connexin expression in dibutyryl cAMP-treated cultured cardiac myocytes. *Circ Res*. 1996; 79:174-183.

171. Rohr S, Kucera JP, Fast VG, Kleber AG: Paradoxical improvement of impulse conduction in cardiac tissue by partial cellular uncoupling. *Science*. 1997; 275:841-844.

172. Kumar R, Joyner RW: Calcium currents of ventricular cell pairs during action potential conduction. *Am J Physiol*. 1995; 268:H2476-2486.

173. Sugiura H, Joyner RW: Action potential conduction between guinea pig ventricular cells can be modulated by calcium current. *KAm J Physiol*. 1992; 263:H1591-1604.

174. Joyner RW, Kumar R, Wilders R, Jongsma HJ, Verheijck EE, Golod DA, Van Ginneken AC, Wagner MB, Goolsby WN: Modulating L-type calcium current affects discontinuous cardiac action potential conduction. *Biophys J*. 1996; 71:237-245.

175. de Bakker J, van Capelle F, Janse M, Tasseron S, Vermeulen J, de Jonge N, Lahpor J: Slow conduction in the infarcted human heart. 'Zigzag' course of activation. *Circulation*. 1993; 88:915-926.

176. Kucera JP, Kléber AG, Rohr S: Slow Conduction in Cardiac Tissue, II: Effects of Branching Tissue Geometry. *Circ Res*. 1998; 83:795-805.

177. Kucera JP, Rudy Y: Mechanistic Insights Into Very Slow Conduction in Branching Cardiac Tissue: A Model Study. *Circ Res*. 2001; 89:799-806.

178. Quan W, Rudy Y: Unidirectional block and reentry of cardiac excitation: a model study. *Circ Res*. 1990; 66:367-382.

179. Shaw RM, Rudy Y: The vulnerable window for unidirectional block in cardiac tissue: characterization and dependence on membrane excitability and intercellular coupling. *J Cardiovasc Electrophysiol*. 1995; 6:115-131.

180. Rudy Y: Reentry: insights from theoretical simulations in a fixed pathway. *J Cardiovasc Electrophysiol*. 1995; 6:294-312.

181. Coronel R, Fiolet JW, Wilms-Schopman FJ, Schaapherder AF, Johnson TA, Gettes LS, Janse MJ: Distribution of extracellular potassium and its relation to electrophysiologic changes during acute myocardial ischemia in the isolated perfused porcine heart. *Circulation*. 1988; 77:1125-1138.

182. Pinto JM, Boyden PA: Electrical remodeling in ischemia and infarction. *Cardiovasc Res*. 1999; 42:284-297.

183. Kaab S, Dixon J, Duc J, Ashen D, Nabauer M, Beuckelmann DJ, Steinbeck G, McKinnon D, Tomaselli GF: Molecular basis of transient outward potassium current downregulation in human heart failure: a decrease in Kv4.3 mRNA correlates with a reduction in current density. *Circulation*. 1998; 98:1383-1393.

184. Beuckelmann DJ, Nabauer M, Erdmann E: Alterations of K+ currents in isolated human ventricular myocytes from patients with terminal heart failure. *Circ Res*. 1993; 73:379-385.

185. Priori SG, Barhanin J, Hauer RN, Haverkamp W, Jongsma HJ, Kleber AG, McKenna WJ, Roden DM, Rudy Y, Schwartz K, Schwartz PJ, Towbin JA, Wilde AM: Genetic and molecular basis of cardiac arrhythmias: impact on clinical management parts I and II. *Circulation*. 1999; 99:518-528.

186. Overholt ED, Joyner RW, Veenstra RD, Rawling D, Wiedmann R: Unidirectional block between Purkinje and ventricular layers of papillary muscles. *Am J Physiol*. 1984; 247:H584-595.

187. Spach MS, Kootsey JM: The nature of electrical propagation in cardiac muscle. *Am J Physiol*. 1983; 244:H3-22.

188. Delgado C, Steinhaus B, Delmar M, Chialvo DR, Jalife J: Directional differences in excitability and margin of safety for propagation in sheep ventricular epicardial muscle. *Circ Res*. 1990; 67:97-110.

189. Girouard SD, Pastore JM, Laurita KR, Gregory KW, Rosenbaum DS: Optical mapping in a new guinea pig model of ventricular tachycardia reveals mechanisms for multiple wavelengths in a single reentrant circuit. *Circulation*. 1996; 93:603-613.

190. Danse PW, Garratt CJ, Allessie MA: Flecainide widens the excitable gap at pivot points of premature turning wavefronts in rabbit ventricular myocardium. *J Cardiovasc Electrophysiol*. 2001; 12:1010-1017.

191. Fast VG, Kleber AG: Block of impulse propagation at an abrupt tissue expansion: evaluation of the critical strand diameter in 2- and 3-dimensional computer models. *Cardiovasc Res*. 1995; 30:449-459.

192. Cabo C, Pertsov AM, Baxter WT, Davidenko JM, Gray RA, Jalife J: Wave-front curvature as a cause of slow conduction and block in isolated cardiac muscle. *Circ Res*. 1994; 75:1014-1028.

193. Rohr S, Salzberg BM: Characterization of impulse propagation at the microscopic level across geometrically defined expansions of excitable tissue: multiple site optical recording of transmembrane voltage (MSORTV) in patterned growth heart cell cultures. *J Gen Physiol*. 1994; 104:287-309.

194. Rohr S, Kucera JP: Involvement of the calcium inward current in cardiac impulse propagation: induction of unidirectional conduction block by nifedipine and reversal by Bay K 8644. *Biophysical journal*. 1997; 72:754-766.

195. Ortiz J, Nozaki A, Shimizu A, Khrestian C, Rudy Y, Waldo AL: Mechanism of interruption of atrial flutter by moricizine. Electrophysiological and multiplexing studies in the canine sterile pericarditis model of atrial flutter. *Circulation*. 1994; 89:2860-2869.

196. Mines GR: On dynamic equilibrium in the heart. *J Physiol*. 1913; 46:349-383.

197. Mines G: On circulating excitations in heart muscles and their possible relation to tachycardia and fibrillation. *Trans R Soc Can*. 1914; 4:43–52.

198. Allessie MA, Bonke FI, Schopman FJ: Circus movement in rabbit atrial muscle as a mechanism of tachycardia. *Circ Res*. 1973; 33:54-62.

199. Smeets JL, Allessie MA, Lammers WJ, Bonke FI, Hollen J: The wavelength of the cardiac impulse and reentrant arrhythmias in isolated rabbit atrium. The role of heart rate, autonomic transmitters, temperature, and potassium. *Circ Res*. 1986; 58:96-108.

200. Allessie MA, Bonke FI, Schopman FJ: Circus movement in rabbit atrial muscle as a mechanism of tachycardia. III. The "leading circle" concept: a new model of circus movement in cardiac tissue without the involvement of an anatomical obstacle. *Circ Res*. 1977; 41:9-18.

201. Winfree AT: Electrical turbulence in three-dimensional heart muscle. *Science*. 1994; 266:1003-1006.

202. Vaquero M, Calvo D, Jalife J: Cardiac fibrillation: from ion channels to rotors in the human heart. *Heart Rhythm*. 2008; 5:872-879.

203. Jalife J, Berenfeld O: Molecular mechanisms and global dynamics of fibrillation: an integrative approach to the underlying basis of vortex-like reentry. *J Theor Biol*. 2004; 230:475-487.

204. Allessie MA, Bonke FI, Schopman FJ: Circus movement in rabbit atrial muscle as a mechanism of tachycardia. II. The role of nonuniform recovery of excitability in the occurrence of unidirectional block, as studied with multiple microelectrodes. *Circ Res*. 1976; 39:168-177.

205. van Capelle FJ, Durrer D: Computer simulation of arrhythmias in a network of coupled excitable elements. *Circ Res*. 1980; 47:454-466.

206. Zykov V, Morozova O: Speed of spread of excitation in two-dimensional excitable medium *Biofizika*. 1979; 24:739–744.

207. Cabo C, Pertsov AM, Davidenko JM, Baxter WT, Gray RA, Jalife J: Vortex shedding as a precursor of turbulent electrical activity in cardiac muscle. *Biophysical journal*. 1996; 70:1105-1111.

208. Winfree A. Rotors, fibrillation, and dimensionality. In: Panfilov A, Holden A, editors. Computational Biology of the Heart. Chichester, UK: Wiley; 1996. pp. 101–135.

209. Agladze K, Keener JP, Muller SC, Panfilov A: Rotating spiral waves created by geometry. *Science*. 1994; 264:1746-1748.

210. Allessie MA, Schalij MJ, Kirchhof CJHJ, Boersma L, Huybers M, Hollen J: Experimental electrophysiology and arrhythmogenicity. Anisotropy and ventricular tachycardia. *Eur Heart J*. 1989; 10:2-8.

211. Spach MS, Josephson ME: Initiating reentry: the role of nonuniform anisotropy in small circuits. *J Cardiovasc Electrophysiol*. 1994; 5:182-209.

212. Boersma L, Brugada J, Kirchhof C, Allessie M: Entrainment of reentrant ventricular tachycardia in anisotropic rings of rabbit myocardium. Mechanisms of termination, changes in morphology, and acceleration. *Circulation*. 1993; 88:1852-1865.

213. Almendral JM, Stamato NJ, Rosenthal ME, Marchlinski FE, Miller JM, Josephson ME: Resetting response patterns during sustained ventricular tachycardia: relationship to the excitable gap. *Circulation*. 1986; 74:722-730.

214. Bernstein RC, Frame LH: Ventricular reentry around a fixed barrier. Resetting with advancement in an in vitro model. *Circulation*. 1990; 81:267-280.

215. Brugada J, Boersma L, Kirchhof CJ, Heynen VV, Allessie MA: Reentrant excitation around a fixed obstacle in uniform anisotropic ventricular myocardium. *Circulation*. 1991; 84:1296-1306.

216. Pertsov AM, Davidenko JM, Salomonsz R, Baxter WT, Jalife J: Spiral waves of excitation underlie reentrant activity in isolated cardiac muscle. *Circ Res*. 1993; 72:631-650.

217. Peters NS, Coromilas J, Hanna MS, Josephson ME, Costeas C, Wit AL: Characteristics of the temporal and spatial excitable gap in anisotropic reentrant circuits causing sustained ventricular tachycardia. *Circ Res*. 1998; 82:279-293.

218. Peters NS, Coromilas J, Severs NJ, Wit AL: Disturbed connexin43 gap junction distribution correlates with the location of reentrant circuits in the epicardial border zone of healing canine infarcts that cause ventricular tachycardia. *Circulation*. 1997; 95:988-996.

219. Waldo AL, Plumb VJ, Arciniegas JG, MacLean WA, Cooper TB, Priest MF, James TN: Transient entrainment and interruption of the atrioventricular bypass pathway type of paroxysmal atrial tachycardia. A model for understanding and identifying reentrant arrhythmias. *Circulation*. 1983; 67:73-83.

220. MacLean WA, Plumb VJ, Waldo AL: Transient entrainment and interruption of ventricular tachycardia. *Pacing Clin Electrophysiol*. 1981; 4:358-366.

221. Frazier DW, Stanton MS: Resetting and transient entrainment of ventricular tachycardia. *Pacing Clin Electrophysiol*. 1995; 18:1919-1946.

222. Waldecker B, Coromilas J, Saltman AE, Dillon SM, Wit AL: Overdrive stimulation of functional reentrant circuits causing ventricular tachycardia in the infarcted canine heart. Resetting and entrainment. *Circulation*. 1993; 87:1286-1305.

223. Stevenson W, Khan H, Sager P, Saxon L, Middlekauff H, Natterson P, Wiener I: Identification of reentry circuit sites during catheter mapping and radiofrequency ablation of ventricular tachycardia late after myocardial infarction. *Circulation*. 1993; 88:1647-1670.

224. Schalij MJ, Boersma L, Huijberts M, Allessie MA: Anisotropic reentry in a perfused 2-dimensional layer of rabbit ventricular myocardium. *Circulation*. 2000; 102:2650-2658.

225. El-Sherif N. Reentrant mechanisms in ventricular arrhythmias. In: Zipes DP, Jalife J, editors. Cardiac Electrophysiology: From Cell to Bedside. Philadelphia, PA: Saunders; 1995. pp. 567–582.

226. Frazier DW, Wolf PD, Wharton JM, Tang AS, Smith WM, Ideker RE: Stimulus-induced critical point. Mechanism for electrical initiation of reentry in normal canine myocardium. *J Clin Invest*. 1989; 83:1039-1052.

227. Simson MB, Spear JF, Moore EN: Stability of an experimental atrioventricular reentrant tachycardia in dogs. *Am J Physiol*. 1981; 240:H947-953.

228. Vinet A, Roberge FA: The dynamics of sustained reentry in a ring model of cardiac tissue. *Ann Biomed Eng*. 1994; 22:568-591.

229. Hund TJ, Otani NF, Rudy Y: Dynamics of action potential head-tail interaction during reentry in cardiac tissue: ionic mechanisms. *Am J Physiol Heart Circ Physiol*. 2000; 279:H1869-1879.

230. Qu Z, Weiss JN, Garfinkel A: Cardiac electrical restitution properties and stability of reentrant spiral waves: a simulation study. *Am J Physiol*. 1999; 276:H269-283.

231. Moe G: On the multiple wavelet hypothesis of atrial fibrillation. *Arch Int Pharmacodyn Ther* 1962; 140:183–188.

232. Riccio ML, Koller ML, Gilmour RF, Jr.: Electrical restitution and spatiotemporal organization during ventricular fibrillation. *Circ Res*. 1999; 84:955-963.

233. Davidenko JM, Pertsov AV, Salomonsz R, Baxter W, Jalife J: Stationary and drifting spiral waves of excitation in isolated cardiac muscle. *Nature*. 1992; 355:349-351.

234. Davidenko JM: Spiral wave activity: a possible common mechanism for polymorphic and monomorphic ventricular tachycardias. *J Cardiovasc Electrophysiol*. 1993; 4:730-746.

235. Haqqani HM, Kalman JM, Roberts-Thomson KC, Balasubramaniam RN, Rosso R, Snowdon RL, Sparks PB, Vohra JK, Morton JB: Fundamental differences in electrophysiologic and electroanatomic substrate between ischemic cardiomyopathy patients with and without clinical ventricular tachycardia. *J Am Coll Cardiol*. 2009; 54:166-173.

236. de Chillou C, Lacroix D, Klug D, Magnin-Poull I, Marquie C, Messier M, Andronache M, Kouakam C, Sadoul N, Chen J, Aliot E, Kacet S: Isthmus characteristics of reentrant ventricular tachycardia after myocardial infarction. *Circulation*. 2002; 105:726-731.

237. Ciaccio EJ, Ashikaga H, Kaba RA, Cervantes D, Hopenfeld B, Wit AL, Peters NS, McVeigh ER, Garan H, Coromilas J: Model of reentrant ventricular tachycardia based on infarct border zone geometry predicts reentrant circuit features as determined by activation mapping. *Heart Rhythm*. 2007; 4:1034-1045.

238. Miura M, Nishio T, Hattori T, Murai N, Stuyvers BD, Shindoh C, Boyden PA: Effect of nonuniform muscle contraction on sustainability and frequency of triggered arrhythmias in rat cardiac muscle. *Circulation*. 2010; 121:2711-2717.

239. Cassidy DM, Vassallo JA, Marchlinski FE, Buxton AE, Untereker WJ, Josephson ME: Endocardial mapping in humans in sinus rhythm with normal left ventricles: activation patterns and characteristics of electrograms. *Circulation*. 1984; 70:37-42.

240. Marchlinski FE, Callans DJ, Gottlieb CD, Zado E: Linear ablation lesions for control of unmappable ventricular tachycardia in patients with ischemic and nonischemic cardiomyopathy. *Circulation*. 2000; 101:1288-1296.

241. Cassidy D, Vassallo J, Miller J, Poll D, Buxton A, Marchlinski F, Josephson M: Endocardial catheter mapping during sinus rhythm: Relation of underlying heart disease and ventricular arrhythmia. . *Circulation*. 1986; 73:645-652.

242. Kienzle MG, Doherty JU, Cassidy D, Buxton AE, Marchlinski FE, Waxman HL, Josephson ME: Electrophysiologic sequelae of chronic myocardial infarction: local refractoriness and electrographic characteristics of the left ventricle. *Am J Cardiol*. 1986; 58:63-69.

243. Callans DJ, Ren JF, Michele J, Marchlinski FE, Dillon SM: Electroanatomic left ventricular mapping in the porcine model of healed anterior myocardial infarction. Correlation with intracardiac echocardiography and pathological analysis. *Circulation*. 1999; 100:1744-1750.

244. Reddy VY, Wrobleski D, Houghtaling C, Josephson ME, Ruskin JN: Combined epicardial and endocardial electroanatomic mapping in a porcine model of healed myocardial infarction. *Circulation*. 2003; 107:3236-3242.

245. Wrobleski D, Houghtaling C, Josephson ME, Ruskin JN, Reddy VY: Use of electrogram characteristics during sinus rhythm to delineate the endocardial scar in

a porcine model of healed myocardial infarction. *J Cardiovasc Electrophysiol*. 2003; 14:524-529.

246. Brunckhorst CB, Delacretaz E, Soejima K, Maisel WH, Friedman PL, Stevenson WG: Impact of changing activation sequence on bipolar electrogram amplitude for voltage mapping of left ventricular infarcts causing ventricular tachycardia. *J Interv Card Electrophysiol*. 2005; 12:137-141.

247. Hutchinson MD, Gerstenfeld EP, Desjardins B, Bala R, Riley MP, Garcia FC, Dixit S, Lin D, Tzou WS, Cooper JM, Verdino RJ, Callans DJ, Marchlinski FE: Endocardial unipolar voltage mapping to detect epicardial ventricular tachycardia substrate in patients with nonischemic left ventricular cardiomyopathy. *Circ Arrhythm Electrophysiol*. 2011; 4:49-55.

248. Campos B, Jauregui ME, Park KM, Mountantonakis SE, Gerstenfeld EP, Haqqani H, Garcia FC, Hutchinson MD, Callans DJ, Dixit S, Lin D, Riley MP, Tzou W, Cooper JM, Bala R, Zado ES, Marchlinski FE: New unipolar electrogram criteria to identify irreversibility of nonischemic left ventricular cardiomyopathy. *J Am Coll Cardiol*. 2012; 60:2194-2204.

249. Spears DA, Suszko AM, Dalvi R, Crean AM, Ivanov J, Nanthakumar K, Downar E, Chauhan VS: Relationship of bipolar and unipolar electrogram voltage to scar transmurality and composition derived by magnetic resonance imaging in patients with nonischemic cardiomyopathy undergoing VT ablation. *Heart Rhythm*. 2012; 9:1837-1846.

250. Nakahara S, Tung R, Ramirez RJ, Gima J, Wiener I, Mahajan A, Boyle NG, Shivkumar K: Distribution of late potentials within infarct scars assessed by ultra high-density mapping. *Heart Rhythm*. 2010; 7:1817-1824.

251. Littmann L, Svenson RH, Gallagher JJ, Selle JG, Zimmern SH, Fedor JM, Colavita PG: Functional role of the epicardium in postinfarction ventricular tachycardia. Observations derived from computerized epicardial activation mapping, entrainment, and epicardial laser photoablation. *Circulation*. 1991; 83:1577-1591.

252. Sosa E, Scanavacca M, d'Avila A, Oliveira F, Ramires JA: Nonsurgical transthoracic epicardial catheter ablation to treat recurrent ventricular tachycardia occurring late after myocardial infarction. *J Am Coll Cardiol*. 2000; 35:1442-1449.

253. Svenson RH, Littmann L, Gallagher JJ, Selle JG, Zimmern SH, Fedor JM, Colavita PG: Termination of ventricular tachycardia with epicardial laser photocoagulation: a clinical comparison with patients undergoing successful endocardial photocoagulation alone. *J Am Coll Cardiol*. 1990; 15:163-170.

254. Soejima K, Stevenson W, Sapp J, Selwyn A, Couper G, Epstein L: Endocardial and epicardial radiofrequency ablation of ventricular tachycardia associated with dilated cardiomyopathy: the importance of low-voltage scars. *J Am Coll Cardiol*. 2004; 43:1834-1842.

255. Yamada T, Doppalapudi H, McElderry HT, Okada T, Murakami Y, Inden Y, Yoshida Y, Yoshida N, Murohara T, Epstein AE, Plumb VJ, Litovsky SH, Kay GN:

Electrocardiographic and electrophysiological characteristics in idiopathic ventricular arrhythmias originating from the papillary muscles in the left ventricle: relevance for catheter ablation. *Circ Arrhythm Electrophysiol*. 2010; 3:324-331.

256. Chen PS, Karagueuzian HS, Kim YH: Papillary muscle hypothesis of idiopathic left ventricular tachycardia. *J Am Coll Cardiol*. 2001; 37:1475-1476.

257. Bogun F, Desjardins B, Crawford T, Good E, Jongnarangsin K, Oral H, Chugh A, Pelosi F, Morady F: Post-infarction ventricular arrhythmias originating in papillary muscles. *J Am Coll Cardiol*. 2008; 51:1794-1802.

258. Abouezzeddine O, Suleiman M, Buescher T, Kapa S, Friedman PA, Jahangir A, Mears JA, Ladewig DJ, Munger TM, Hammill SC, Packer DL, Asirvatham SJ: Relevance of endocavitary structures in ablation procedures for ventricular tachycardia. *J Cardiovasc Electrophysiol*. 2010; 21:245-254.

259. Kim YH, Xie F, Yashima M, Wu TJ, Valderrabano M, Lee MH, Ohara T, Voroshilovsky O, Doshi RN, Fishbein MC, Qu Z, Garfinkel A, Weiss JN, Karagueuzian HS, Chen PS: Role of papillary muscle in the generation and maintenance of reentry during ventricular tachycardia and fibrillation in isolated swine right ventricle. *Circulation*. 1999; 100:1450-1459.

260. Valderrabano M, Lee MH, Ohara T, Lai AC, Fishbein MC, Lin SF, Karagueuzian HS, Chen PS: Dynamics of intramural and transmural reentry during ventricular fibrillation in isolated swine ventricles. *Circ Res*. 2001; 88:839-848.

261. Hsia H, Lin D, Sauer W, Callans D, Marchlinski F: Anatomic characterization of endocardial substrate for hemodynamically stable reentrant ventricular tachycardia: Identification of endocardial conducting channels. *Heart Rhythm*. 2006; 3:503-512.

262. Stevenson WG, Friedman PL, Sager PT, Saxon LA, Kocovic D, Harada T, Wiener I, Khan H: Exploring postinfarction reentrant ventricular tachycardia with entrainment mapping. *J Am Coll Cardiol*. 1997; 29:1180-1189.

263. Soejima K, Suzuki M, Maisel W, Brunckhorst C, Delacretaz E, Blier L, Tung S, Khan H, Stevenson W: Catheter ablation in patients with multiple and unstable ventricular tachycardias after myocardial infarction: short ablation lines guided by reentry circuit isthmuses and sinus rhythm mapping. *Circulation*. 2001; 104:664-669.

264. Soejima K, Stevenson WG, Maisel WH, Delacretaz E, Brunckhorst CB, Ellison KE, Friedman PL: The N + 1 difference: a new measure for entrainment mapping. *J Am Coll Cardiol*. 2001; 37:1386-1394.

265. Bogun F, Bahu M, Knight BP, Weiss R, Goyal R, Daoud E, Man KC, Strickberger SA, Morady F: Response to pacing at sites of isolated diastolic potentials during ventricular tachycardia in patients with previous myocardial infarction. *J Am Coll Cardiol*. 1997; 30:505-513.

266. Fontaine G, Frank R, Tonet J, Grosgogeat Y: Identification of a zone of slow conduction appropriate for VT ablation: theoretical and practical considerations. *Pacing Clin Electrophysiol*. 1989; 12:262-267.

267. Tung S, Soejima K, Maisel WH, Suzuki M, Epstein L, Stevenson WG: Recognition of far-field electrograms during entrainment mapping of ventricular tachycardia. *J Am Coll Cardiol*. 2003; 42:110-115.

268. Almendral JM, Gottlieb CD, Rosenthal ME, Stamato NJ, Buxton AE, Marchlinski FE, Miller JM, Josephson ME: Entrainment of ventricular tachycardia: explanation for surface electrocardiographic phenomena by analysis of electrograms recorded within the tachycardia circuit. *Circulation*. 1988; 77:569-580.

269. Waldo AL, Henthorn RW: Use of transient entrainment during ventricular tachycardia to localize a critical area in the reentry circuit for ablation. *Pacing Clin Electrophysiol*. 1989; 12:231-244.

270. Okumura K, Henthorn RW, Epstein AE, Plumb VJ, Waldo AL: Further observations on transient entrainment: importance of pacing site and properties of the components of the reentry circuit. *Circulation*. 1985; 72:1293-1307.

271. Bogun F, Bahu M, Knight BP, Weiss R, Paladino W, Harvey M, Goyal R, Daoud E, Man KC, Strickberger SA, Morady F: Comparison of effective and ineffective target sites that demonstrate concealed entrainment in patients with coronary artery disease undergoing radiofrequency ablation of ventricular tachycardia. *Circulation*. 1997; 95:183-190.

272. Calkins H, Epstein A, Packer D, Arria AM, Hummel J, Gilligan DM, Trusso J, Carlson M, Luceri R, Kopelman H, Wilber D, Wharton JM, Stevenson W: Catheter

ablation of ventricular tachycardia in patients with structural heart disease using cooled radiofrequency energy: results of a prospective multicenter study. Cooled RF Multi Center Investigators Group. *J Am Coll Cardiol*. 2000; 35:1905-1914.

273. Kim RJ, Wu E, Rafael A, Chen EL, Parker MA, Simonetti O, Klocke FJ, Bonow RO, Judd RM: The use of contrast-enhanced magnetic resonance imaging to identify reversible myocardial dysfunction. *N Engl J Med*. 2000; 343:1445-1453.

274. Morady F, Harvey M, Kalbfleisch SJ, el-Atassi R, Calkins H, Langberg JJ: Radiofrequency catheter ablation of ventricular tachycardia in patients with coronary artery disease. *Circulation*. 1993; 87:363-372.

275. O'Callaghan P, Poloniecki J, Sosa-Suarez G, Ruskin J, McGovern B, H. G: Long term clinical outcome of patients with prior myocardial infarction after palliative radiofrequency ablation for frequent ventricular tachycardia. *Am J Cardiol*. 2001; 87:975-979.

276. Della Bella P, De Ponti R, Uriarte J, Tondo C, Klersy C, Carbucicchio C, Storti C, Riva S, Longobardi M: Catheter ablation and antiarrhythmic drugs for hemodynamically tolerated post-infarction ventricular tachycardia. Long term outcome in relation to acute electrophysiological findings. *Eur Heart J*. 2002; 23:414-424.

277. Stevenson W, Soejima K: Catheter ablation for ventricular tachycardia. *Circulation*. 2007; 115:2750-2760.

278. Callans DJ, Zado E, Sarter BH, Schwartzman D, Gottlieb CD, Marchlinski FE: Efficacy of radiofrequency catheter ablation for ventricular tachycardia in healed myocardial infarction. *Am J Cardiol*. 1998; 82:429-432.

279. Stevenson WG, Wilber DJ, Natale A, Jackman WM, Marchlinski FE, Talbert T, Gonzalez MD, Worley SJ, Daoud EG, Hwang C, Schuger C, Bump TE, Jazayeri M, Tomassoni GF, Kopelman HA, Soejima K, Nakagawa H: Irrigated radiofrequency catheter ablation guided by electroanatomic mapping for recurrent ventricular tachycardia after myocardial infarction: the multicenter thermocool ventricular tachycardia ablation trial. *Circulation*. 2008; 118:2773-2782.

280. Miller MA, Dukkipati SR, Mittnacht AJ, Chinitz JS, Belliveau L, Koruth JS, Gomes JA, d'Avila A, Reddy VY: Activation and entrainment mapping of hemodynamically unstable ventricular tachycardia using a percutaneous left ventricular assist device. *J Am Coll Cardiol*. 2011; 58:1363-1371.

281. Bunch TJ, Darby A, May HT, Ragosta M, Lim DS, Taylor AM, DiMarco JP, Ailawadi G, Revenaugh JR, Weiss JP, Mahapatra S: Efficacy and safety of ventricular tachycardia ablation with mechanical circulatory support compared with substrate-based ablation techniques. *Europace*. 2012; 14:709-714.

282. Brunckhorst CB, Delacretaz E, Soejima K, Maisel WH, Friedman PL, Stevenson WG: Identification of the ventricular tachycardia isthmus after infarction by pace mapping. *Circulation*. 2004; 110:652-659.

283. Miller JM, Marchlinski FE, Buxton AE, Josephson ME: Relationship between the 12-lead electrocardiogram during ventricular tachycardia and endocardial site of origin in patients with coronary artery disease. *Circulation*. 1988; 77:759-766.

284. Josephson ME, Callans DJ: Using the twelve-lead electrocardiogram to localize the site of origin of ventricular tachycardia. *Heart Rhythm*. 2005; 2:443-446.

285. Patel VV, Rho RW, Gerstenfeld EP, Hsia HH, Callans DJ, Marchlinski FE: Right bundle-branch block ventricular tachycardias: septal versus lateral ventricular origin based on activation time to the right ventricular apex. *Circulation*. 2004; 110:2582-2587.

286. Berruezo A, Mont L, Nava S, Chueca E, Bartholomay E, Brugada J: Electrocardiographic recognition of the epicardial origin of ventricular tachycardias. *Circulation*. 2004; 109:1842-1847.

287. Martinek M, Stevenson W, Inada K, Tokuda M, Tedrow UB: QRS characteristics fail to reliably identify ventricular tachycardias that require epicardial ablation in ischemic heart disease. *J Cardiovasc Electrophysiol*. 2012; 23:188-193.

288. Stevenson WG, Sager PT, Natterson PD, Saxon LA, Middlekauff HR, Wiener I: Relation of pace mapping QRS configuration and conduction delay to ventricular tachycardia reentry circuits in human infarct scars. *J Am Coll Cardiol*. 1995; 26:481-488.

289. Brunckhorst CB, Stevenson WG, Soejima K, Maisel WH, Delacretaz E, Friedman PL, Ben-Haim SA: Relationship of slow conduction detected by pace-mapping to ventricular tachycardia re-entry circuit sites after infarction. *J Am Coll Cardiol*. 2003; 41:802-809.

290. Soejima K, Stevenson W, Maisel W, Sapp J, Epstein L: Electrically unexcitable scar mapping based on pacing threshold for identification of the reentry critical isthmus: Feasibility for guiding ventricular tachycardia ablation. *Circulation*. 2002; 106:1678-1683.

291. Kadish AH, Schmaltz S, Morady F: A comparison of QRS complexes resulting from unipolar and bipolar pacing: implications for pace-mapping. *Pacing Clin Electrophysiol*. 1991; 14:823-832.

292. Wikswo JP, Jr., Wisialowski TA, Altemeier WA, Balser JR, Kopelman HA, Roden DM: Virtual cathode effects during stimulation of cardiac muscle. Two-dimensional in vivo experiments. *Circ Res*. 1991; 68:513-530.

293. Biffi M, Foerster L, Eastman W, Eggen M, Grenz NA, Sommer J, De Santo T, Haddad T, Varbaro A, Yang Z: Effect of bipolar electrode spacing on phrenic nerve stimulation and left ventricular pacing thresholds: an acute canine study. *Circ Arrhythm Electrophysiol*. 2012; 5:815-820.

294. Eitel C, Hindricks G, Dagres N, Sommer P, Piorkowski C: EnSite Velocity cardiac mapping system: a new platform for 3D mapping of cardiac arrhythmias. *Expert Rev Med Devices*. 2010; 7:185-192.

295. Reddy VY, Neuzil P, Taborsky M, Ruskin JN: Short-term results of substrate mapping and radiofrequency ablation of ischemic ventricular tachycardia using a saline-irrigated catheter. *J Am Coll Cardiol*. 2003; 41:2228-2236.

296. Kottkamp H, Wetzel U, Schirdewahn P, Dorszewski A, Gerds-Li JH, Carbucicchio C, Kobza R, Hindricks G: Catheter ablation of ventricular tachycardia in remote myocardial infarction: substrate description guiding placement of individual linear lesions targeting noninducibility. *J Cardiovasc Electrophysiol*. 2003; 14:675-681.

297. Arenal A, del Castillo S, Gonzalez-Torrecilla E, Atienza F, Ortiz M, Jimenez J, Puchol A, Garcia J, Almendral J: Tachycardia-related channel in the scar tissue in patients with sustained monomorphic ventricular tachycardias: influence of the voltage scar definition. *Circulation*. 2004; 110:2568-2574.

298. Mountantonakis SE, Park RE, Frankel DS, Hutchinson MD, Dixit S, Cooper J, Callans D, Marchlinski FE, Gerstenfeld EP: Relationship between voltage map "channels" and the location of critical isthmus sites in patients with post-infarction cardiomyopathy and ventricular tachycardia. *J Am Coll Cardiol*. 2013; 61:2088-2095.

299. Miller JM, Tyson GS, Hargrove WCr, Vassallo JA, Rosenthal ME, Josephson ME: Effect of subendocardial resection on sinus rhythm endocardial electrogram abnormalities. *Circulation*. 1995; 91:2385-2391.

300. Bogun F, Good E, Reich S, Elmouchi D, Igic P, Lemola K, Tschopp D, Jongnarangsin K, Oral H, Chugh A, Pelosi F, Morady F: Isolated Potentials During Sinus Rhythm and Pace-Mapping Within Scars as Guides for Ablation of Post-Infarction Ventricular Tachycardia. *J Am Coll Cardiol*. 2006; 47:2013-2019.

301. Jais P, Maury P, Khairy P, Sacher F, Nault I, Komatsu Y, Hocini M, Forclaz A, Jadidi AS, Weerasooryia R, Shah A, Derval N, Cochet H, Knecht S, Miyazaki S, Linton N, Rivard L, Wright M, Wilton SB, Scherr D, Pascale P, Roten L, Pederson M, Bordachar P, Laurent F, Kim SJ, Ritter P, Clementy J, Haissaguerre M: Elimination of local abnormal ventricular activities: a new end point for substrate modification in patients with scar-related ventricular tachycardia. *Circulation*. 2012; 125:2184-2196.

302. Vergara P, Trevisi N, Ricco A, Petracca F, Baratto F, Cireddu M, Bisceglia C, Maccabelli G, Della Bella P: Late Potentials Abolition as an Additional Technique for Reduction of Arrhythmia Recurrence in Scar Related Ventricular Tachycardia Ablation. *J Cardiovasc Electrophysiol* 2012; 23:621-627.

303. Cassidy DM, Vassallo JA, Buxton AE, Doherty JU, Marchlinski FE, Josephson ME: The value of catheter mapping during sinus rhythm to localize site of origin of ventricular tachycardia. *Circulation*. 1984; 69:1103-1110.

304. Harada T, Stevenson WG, Kocovic DZ, Friedman PL: Catheter ablation of ventricular tachycardia after myocardial infarction: relation of endocardial sinus rhythm late potentials to the reentry circuit. *J Am Coll Cardiol*. 1997; 30:1015-1023.

305. Schilling RJ, Davies DW, Peters NS: Characteristics of sinus rhythm electrograms at sites of ablation of ventricular tachycardia relative to all other sites: a noncontact mapping study of the entire left ventricle. *J Cardiovasc Electrophysiol*. 1998; 9:921-933.

306. Kocovic D, Harada T, Friedman P, Stevenson W: Characteristics of electrograms recorded at reentry circuit sites and bystanders during ventricular tachycardia after myocardial infarction. *J Am Coll Cardiol*. 1999; 34:381-388.

307. Ciaccio EJ, Tosti AC, Scheinman MM: Relationship between sinus rhythm activation and the reentrant ventricular tachycardia isthmus. *Circulation*. 2001; 104:613-619.

308. Ciaccio EJ, Chow AW, Davies DW, Wit AL, Peters NS: Localization of the isthmus in reentrant circuits by analysis of electrograms derived from clinical noncontact mapping during sinus rhythm and ventricular tachycardia. *J Cardiovasc Electrophysiol*. 2004; 15:27-36.

309. Ciaccio EJ, Tosti AC, Scheinman MM: Method to Predict Isthmus Location in Ventricular Tachycardia Caused by Reentry with a Double-Loop Pattern. *J Cardiovasc Electrophysiol* 2005; 16:528-536.

310. Assadi M, Restivo M, Gough WB, el-Sherif N: Reentrant ventricular arrhythmias in the late myocardial infarction period: 17. Correlation of activation patterns of sinus and reentrant ventricular tachycardia. *Am Heart J* 1990; 119:1014-1024.

311. Shannon C: A mathematical theory of communication. *Bell System Technical Journal*. 1948; 27:379-423, 623-656.

312. Ganesan AN, Kuklik P, Lau DH, Brooks AG, Baumert M, Lim WW, Thanigaimani S, Nayyar S, Mahajan R, Kalman JM, Roberts-Thomson KC, Sanders P: Bipolar electrogram shannon entropy at sites of rotational activation: implications for ablation of atrial fibrillation. *Circ Arrhythm Electrophysiol*. 2013; 6:48-57.

313. Schilling RJ, Peters NS, Davies DW: Feasibility of a Noncontact Catheter for Endocardial Mapping of Human Ventricular Tachycardia *Circulation*. 1999; 99:2543-2552.

314. Sanders P, Hocini M, Jais P, Hsu L, Takahashi Y, Rotter M, Scavee C, Pasquie J, Sacher F, Rostock T, Nalliah C, Clementy J, Haissaguerre M: Characterization of focal atrial tachycardia using high-density mapping. . *J Am Coll Cardiol*. 2005; 46:2088-2099.

315. Sra J, Bhatia A, Dhala A, Blanck Z, Deshpande S, Cooley R, Akhtar M: Electroanatomically guided catheter ablation of ventricular tachycardias causing multiple defibrillator shocks. *Pacing Clin Electrophysiol*. 2001; 24:1645-1652.

316. Tanner H, Hindricks G, Volkmer M, Furniss S, Kuhlkamp V, Lacroix D, C DEC, Almendral J, Caponi D, Kuck KH, Kottkamp H: Catheter ablation of recurrent scar-related ventricular tachycardia using electroanatomical mapping and irrigated ablation technology: results of the prospective multicenter Euro-VT-study. *J Cardiovasc Electrophysiol*. 2010; 21:47-53.

317. Della Bella P, Baratto F, Tsiachris D, Trevisi N, Vergara P, Bisceglia C, Petracca F, Carbucicchio C, Benussi S, Maisano F, Alfieri O, Pappalardo F, Zangrillo A, Maccabelli G: Management of Ventricular Tachycardia in the Setting of a Dedicated Unit for the Treatment of Complex Ventricular Arrhythmias: Long Term Outcome after Ablation. *Circulation*. 2013.

318. Reddy VY, Reynolds MR, Neuzil P, Richardson AW, Taborsky M, Jongnarangsin K, Kralovec S, Sediva L, Ruskin JN, Josephson ME: Prophylactic catheter ablation for the prevention of defibrillator therapy. *N Engl J Med*. 2007; 357:2657-2665.

319. Kuck KH, Schaumann A, Eckardt L, Willems S, Ventura R, Delacretaz E, Pitschner HF, Kautzner J, Schumacher B, Hansen PS: Catheter ablation of stable ventricular tachycardia before defibrillator implantation in patients with coronary heart disease (VTACH): a multicentre randomised controlled trial. *Lancet*. 2010; 375:31-40.

320. Camm AJ, Pratt CM, Schwartz PJ, Al-Khalidi HR, Spyt MJ, Holroyde MJ, Karam R, Sonnenblick EH, Brum JM: Mortality in patients after a recent myocardial

infarction: a randomized, placebo-controlled trial of azimilide using heart rate variability for risk stratification. *Circulation*. 2004; 109:990-996.

321. Pacifico A, Hohnloser SH, Williams JH, Tao B, Saksena S, Henry PD, Prystowsky EN: Prevention of implantable-defibrillator shocks by treatment with sotalol. d,l-Sotalol Implantable Cardioverter-Defibrillator Study Group. *N Engl J Med*. 1999; 340:1855-1862.

322. Wathen MS, Sweeney MO, DeGroot PJ, Stark AJ, Koehler JL, Chisner MB, Machado C, Adkisson WO: Shock reduction using antitachycardia pacing for spontaneous rapid ventricular tachycardia in patients with coronary artery disease. *Circulation*. 2001; 104:796-801.

323. Pauriah M, Cismaru G, Magnin-Poull I, Andronache M, Sellal J-M, Schwartz J, Brembilla-Perrot B, Sadoul N, Aliot E, de Chillou C: A Stepwise Approach to the Management of Post-Infarct Ventricular Tachycardia Using Catheter Ablation as the First Line Treatment: A Single Center Experience. *Circ Arrhythm Electrophysiol*. 2013; 6:351-356.

324. Callans D, Josephson ME. Ventricular tachycardia in patients with coronary artery disease. In: Zipes DP, Jalife J, editors. Cardiac electrophysiology: From cell to bedside. 3 ed. Philadelphia: Saunders; 2004. pp. 569-574.

325. Zipes DP, Camm AJ, Borggrefe M, Buxton AE, Chaitman B, Fromer M, Gregoratos G, Klein G, Moss AJ, Myerburg RJ, Priori SG, Quinones MA, Roden DM,

Silka MJ, Tracy C, Smith SC, Jr., Jacobs AK, Adams CD, Antman EM, Anderson JL, Hunt SA, Halperin JL, Nishimura R, Ornato JP, Page RL, Riegel B, Blanc JJ, Budaj A, Dean V, Deckers JW, Despres C, Dickstein K, Lekakis J, McGregor K, Metra M, Morais J, Osterspey A, Tamargo JL, Zamorano JL: ACC/AHA/ESC 2006 guidelines for management of patients with ventricular arrhythmias and the prevention of sudden cardiac death: a report of the American College of Cardiology/American Heart Association Task Force and the European Society of Cardiology Committee for Practice Guidelines (Writing Committee to Develop Guidelines for Management of Patients With Ventricular Arrhythmias and the Prevention of Sudden Cardiac Death). *J Am Coll Cardiol*. 2006; 48:e247-346.

326. Aliot EM, Stevenson WG, Almendral-Garrote JM, Bogun F, Calkins CH, Delacretaz E, Della Bella P, Hindricks G, Jais P, Josephson ME, Kautzner J, Kay GN, Kuck KH, Lerman BB, Marchlinski F, Reddy V, Schalij MJ, Schilling R, Soejima K, Wilber D: EHRA/HRS Expert Consensus on Catheter Ablation of Ventricular Arrhythmias: developed in a partnership with the European Heart Rhythm Association (EHRA), a Registered Branch of the European Society of Cardiology (ESC), and the Heart Rhythm Society (HRS); in collaboration with the American College of Cardiology (ACC) and the American Heart Association (AHA). *Heart Rhythm*. 2009; 6:886-933.

327. Exner DV, Pinski SL, Wyse DG, Renfroe EG, Follmann D, Gold M, Beckman KJ, Coromilas J, Lancaster S, Hallstrom AP: Electrical Storm Presages Nonsudden Death : The Antiarrhythmics Versus Implantable Defibrillators (AVID) Trial. *Circulation*. 2001; 103:2066-2071.

328. Sesselberg HW, Moss AJ, McNitt S, Zareba W, Daubert JP, Andrews ML, Hall WJ, McClinitic B, Huang DT: Ventricular arrhythmia storms in postinfarction patients with implantable defibrillators for primary prevention indications: A MADIT-II substudy. *Heart Rhythm*. 2007; 4:1395-1402.

329. Verma A, Kilicaslan F, Marrouche NF, Minor S, Khan M, Wazni O, Burkhardt JD, Belden WA, Cummings JE, Abdul-Karim A, Saliba W, Schweikert RA, Tchou PJ, Martin DO, Natale A: Prevalence, predictors, and mortality significance of the causative arrhythmia in patients with electrical storm. *J Cardiovasc Electrophysiol*. 2004; 15:1265-1270.

330. Gatzoulis KA, Andrikopoulos GK, Apostolopoulos T, Sotiropoulos E, Zervopoulos G, Antoniou J, Brili S, Stefanadis CI: Electrical storm is an independent predictor of adverse long-term outcome in the era of implantable defibrillator therapy. *Europace*. 2005; 7:184-192.

331. Frankel DS, Mountantonakis SE, Robinson MR, Zado ES, Callans DJ, Marchlinski FE: Ventricular Tachycardia Ablation Remains Treatment of Last Resort in Structural Heart Disease: Argument for Earlier Intervention. *J Cardiovasc Electrophysiol*. 2011; 22:1123-1128.

332. Tokuda M, Sobieszczyk P, Eisenhauer AC, Kojodjojo P, Inada K, Koplan BA, Michaud GF, John RM, Epstein LM, Sacher F, Stevenson WG, Tedrow UB: Transcoronary ethanol ablation for recurrent ventricular tachycardia after failed catheter ablation: an update. *Circ Arrhythm Electrophysiol*. 2011; 4:889-896.

333. Zipes DP, Camm AJ, Borggrefe M, Buxton AE, Chaitman B, Fromer M, Gregoratos G, Klein G, Moss AJ, Myerburg RJ, Priori SG, Quinones MA, Roden DM, Silka MJ, Tracy C, Smith SC, Jr., Jacobs AK, Adams CD, Antman EM, Anderson JL, Hunt SA, Halperin JL, Nishimura R, Ornato JP, Page RL, Riegel B, Blanc JJ, Budaj A, Dean V, Deckers JW, Despres C, Dickstein K, Lekakis J, McGregor K, Metra M, Morais J, Osterspey A, Tamargo JL, Zamorano JL: ACC/AHA/ESC 2006 Guidelines for Management of Patients With Ventricular Arrhythmias and the Prevention of Sudden Cardiac Death: a report of the American College of Cardiology/American Heart Association Task Force and the European Society of Cardiology Committee for Practice Guidelines (writing committee to develop Guidelines for Management of Patients With Ventricular Arrhythmias and the Prevention of Sudden Cardiac Death): developed in collaboration with the European Heart Rhythm Association and the Heart Rhythm Society. *Circulation*. 2006; 114:e385-484.

334. Soejima K, Delacretaz E, Suzuki M, Brunckhorst CB, Maisel WH, Friedman PL, Stevenson WG: Saline-cooled versus standard radiofrequency catheter ablation for infarct-related ventricular tachycardias. *Circulation*. 2001; 103:1858-1862.

335. Nakagawa H, Yamanashi WS, Pitha JV, Arruda M, Wang X, Ohtomo K, Beckman KJ, McClelland JH, Lazzara R, Jackman WM: Comparison of in vivo tissue temperature profile and lesion geometry for radiofrequency ablation with a saline-irrigated electrode versus temperature control in a canine thigh muscle preparation. *Circulation*. 1995; 91:2264-2273.

336. Haines DE, Watson DD: Tissue heating during radiofrequency catheter ablation: a thermodynamic model and observations in isolated perfused and superfused canine right ventricular free wall. *Pacing Clin Electrophysiol*. 1989; 12:962-976.

337. Matsudaira K, Nakagawa H, Wittkampf FH, Yamanashi WS, Imai S, Pitha JV, Lazzara R, Jackman WM: High incidence of thrombus formation without impedance rise during radiofrequency ablation using electrode temperature control. *Pacing Clin Electrophysiol*. 2003; 26:1227-1237.

338. Callans DJ, Ren JF, Narula N, Michele J, Marchlinski FE, Dillon SM: Effects of linear, irrigated-tip radiofrequency ablation in porcine healed anterior infarction. *J Cardiovasc Electrophysiol*. 2001; 12:1037-1042.

339. Fernández-Armenta J, Berruezo A, Andreu D, Camara O, Silva E, Serra L, Barbarito V, Carotenutto L, Evertz R, Ortiz-Pérez JT, De Caralt TM, Perea RJ, Sitges M, Mont L, Frangi A, Brugada J: Three-dimensional Architecture of Scar and Conducting Channels Based on High Resolution ce-CMR: Insights for Ventricular Tachycardia Ablation. *Circ Arrhythm Electrophysiol*. 2013.

340. Reddy VY, Malchano ZJ, Holmvang G, Schmidt EJ, d'Avila A, Houghtaling C, Chan RC, Ruskin JN: Integration of cardiac magnetic resonance imaging with three-dimensional electroanatomic mapping to guide left ventricular catheter manipulation: feasibility in a porcine model of healed myocardial infarction. *J Am Coll Cardiol*. 2004; 44:2202-2213.

341. Codreanu A, Odille F, Aliot E, Marie PY, Magnin-Poull I, Andronache M, Mandry D, Djaballah W, Regent D, Felblinger J, de Chillou C: Electroanatomic characterization of post-infarct scars comparison with 3-dimensional myocardial scar reconstruction based on magnetic resonance imaging. *J Am Coll Cardiol*. 2008; 52:839-842.

342. Dukkipati SR, Mallozzi R, Schmidt EJ, Holmvang G, d'Avila A, Guhde R, Darrow RD, Slavin G, Fung M, Malchano Z, Kampa G, Dando JD, McPherson C, Foo TK, Ruskin JN, Dumoulin CL, Reddy VY: Electroanatomic mapping of the left ventricle in a porcine model of chronic myocardial infarction with magnetic resonance-based catheter tracking. *Circulation*. 2008; 118:853-862.

343. Ector J, De Buck S, Adams J, Dymarkowski S, Bogaert J, Maes F, Heidbuchel H: Cardiac three-dimensional magnetic resonance imaging and fluoroscopy merging: a new approach for electroanatomic mapping to assist catheter ablation. *Circulation*. 2005; 112:3769-3776.

344. Andreu D, Berruezo A, Ortiz-Perez JT, Silva E, Mont L, Borras R, de Caralt TM, Perea RJ, Fernandez-Armenta J, Zeljko H, Brugada J: Integration of 3D electroanatomic maps and magnetic resonance scar characterization into the navigation system to guide ventricular tachycardia ablation. *Circ Arrhythm Electrophysiol*. 2011; 4:674-683.

345. Estner HL, Zviman MM, Herzka D, Miller F, Castro V, Nazarian S, Ashikaga H, Dori Y, Berger RD, Calkins H, Lardo AC, Halperin HR: The critical isthmus sites of

ischemic ventricular tachycardia are in zones of tissue heterogeneity, visualized by magnetic resonance imaging. *Heart Rhythm*. 2011; 8:1942-1949.

346. Sasaki T, Miller CF, Hansford R, Yang J, Caffo BS, Zviman MM, Henrikson CA, Marine JE, Spragg D, Cheng A, Tandri H, Sinha S, Kolandaivelu A, Zimmerman SL, Bluemke DA, Tomaselli GF, Berger RD, Calkins H, Halperin HR, Nazarian S: Myocardial structural associations with local electrograms: a study of postinfarct ventricular tachycardia pathophysiology and magnetic resonance-based noninvasive mapping. *Circ Arrhythm Electrophysiol*. 2012; 5:1081-1090.

347. Bello D, Fieno DS, Kim RJ, Pereles FS, Passman R, Song G, Kadish AH, Goldberger JJ: Infarct morphology identifies patients with substrate for sustained ventricular tachycardia. *J Am Coll Cardiol*. 2005; 45:1104-1108.

348. Schmidt A, Azevedo CF, Cheng A, Gupta SN, Bluemke DA, Foo TK, Gerstenblith G, Weiss RG, Marban E, Tomaselli GF, Lima JA, Wu KC: Infarct tissue heterogeneity by magnetic resonance imaging identifies enhanced cardiac arrhythmia susceptibility in patients with left ventricular dysfunction. *Circulation*. 2007; 115:2006-2014.

349. Yan AT, Shayne AJ, Brown KA, Gupta SN, Chan CW, Luu TM, Di Carli MF, Reynolds HG, Stevenson WG, Kwong RY: Characterization of the peri-infarct zone by contrast-enhanced cardiac magnetic resonance imaging is a powerful predictor of post-myocardial infarction mortality. *Circulation*. 2006; 114:32-39.

350. Crawford T, Cowger J, Desjardins B, Kim HM, Good E, Jongnarangsin K, Oral H, Chugh A, Pelosi F, Morady F, Bogun F: Determinants of postinfarction ventricular tachycardia. *Circ Arrhythm Electrophysiol*. 2010; 3:624-631.

351. Perez-David E, Arenal A, Rubio-Guivernau JL, del Castillo R, Atea L, Arbelo E, Caballero E, Celorrio V, Datino T, Gonzalez-Torrecilla E, Atienza F, Ledesma-Carbayo MJ, Bermejo J, Medina A, Fernandez-Aviles F: Noninvasive identification of ventricular tachycardia-related conducting channels using contrast-enhanced magnetic resonance imaging in patients with chronic myocardial infarction: comparison of signal intensity scar mapping and endocardial voltage mapping. *J Am Coll Cardiol*. 2011; 57:184-194.

352. Komatsu Y, Cochet H, Jadidi A, Sacher F, Shah A, Derval N, Scherr D, Pascale P, Roten L, Denis A, Ramoul K, Miyazaki S, Daly M, Riffaud M, Sermesant M, Relan J, Ayache N, Kim S, Montaudon M, Laurent F, Hocini M, Haïssaguerre M, Jaïs P: Regional Myocardial Wall Thinning at Multi-Detector Computed Tomography Correlates to Arrhythmogenic Substrate in Post-Infarction Ventricular Tachycardia: Assessment of Structural and Electrical Substrate. *Circ Arrhythm Electrophysiol*. 2013.

353. Cochet H, Komatsu Y, Sacher F, Jadidi AS, Scherr D, Riffaud M, Derval N, Shah A, Roten L, Pascale P, Relan J, Sermesant M, Ayache N, Montaudon M, Laurent F, Hocini M, HaÏSsaguerre M, JaÏS P: Integration of Merged Delayed-Enhanced Magnetic Resonance Imaging and Multidetector Computed Tomography for the

Guidance of Ventricular Tachycardia Ablation: A Pilot Study. *J Cardiovasc Electrophysiol*. 2013; 24:419-426.

354. Ng J, Jacobson JT, Ng JK, Gordon D, Lee DC, Carr JC, Goldberger JJ: Virtual electrophysiological study in a 3-dimensional cardiac magnetic resonance imaging model of porcine myocardial infarction. *J Am Coll Cardiol*. 2012; 60:423-430.

355. Sapp JL, Dawoud F, Clements JC, Horacek BM: Inverse solution mapping of epicardial potentials: quantitative comparison with epicardial contact mapping. *Circ Arrhythm Electrophysiol*. 2012; 5:1001-1009.

356. Cuculich PS, Zhang J, Wang Y, Desouza KA, Vijayakumar R, Woodard PK, Rudy Y: The electrophysiological cardiac ventricular substrate in patients after myocardial infarction: noninvasive characterization with electrocardiographic imaging. *J Am Coll Cardiol*. 2011; 58:1893-1902.

357. Ramanathan C, Ghanem RN, Jia P, Ryu K, Rudy Y: Noninvasive electrocardiographic imaging for cardiac electrophysiology and arrhythmia. *Nature medicine*. 2004; 10:422-428.

358. Ramanathan C, Jia P, Ghanem R, Calvetti D, Rudy Y: Noninvasive electrocardiographic imaging (ECGI): application of the generalized minimal residual (GMRes) method. *Ann Biomed Eng*. 2003; 31:981-994.

359. Hocini M, Shah AJ, Denis A, Cochet H, Haissaguerre M: Noninvasive 3D mapping system guided ablation of anteroseptal pathway below the aortic cusp. *Heart Rhythm*. 2013; 10:139-141.

360. Tung L, Zhang Y: Optical imaging of arrhythmias in tissue culture. *J Electrocardiol*. 2006; 39:S2-6.

361. Kadota S, Minami I, Morone N, Heuser JE, Agladze K, Nakatsuji N: Development of a reentrant arrhythmia model in human pluripotent stem cell-derived cardiac cell sheets. *Eur Heart J*. 2012.

362. Kizana E, Chang CY, Cingolani E, Ramirez-Correa GA, Sekar RB, Abraham MR, Ginn SL, Tung L, Alexander IE, Marban E: Gene transfer of connexin43 mutants attenuates coupling in cardiomyocytes: novel basis for modulation of cardiac conduction by gene therapy. *Circ Res*. 2007; 100:1597-1604.

363. Greener ID, Sasano T, Wan X, Igarashi T, Strom M, Rosenbaum DS, Donahue JK: Connexin43 Gene Transfer Reduces Ventricular Tachycardia Susceptibility After Myocardial Infarction. *J Am Coll Cardiol*. 2012; 60:1103-1110.

364. Sasano T, Kelemen K, Greener ID, Donahue JK: Ventricular tachycardia from the healed myocardial infarction scar: validation of an animal model and utility of gene therapy. *Heart Rhythm*. 2009; 6:S91-97.

365. Wissner E, Stevenson WG, Kuck K-H: Catheter ablation of ventricular tachycardia in ischaemic and non-ischaemic cardiomyopathy: where are we today? A clinical review. *Eur Heart J*. 2012.

366. Kuck KH, Reddy VY, Schmidt B, Natale A, Neuzil P, Saoudi N, Kautzner J, Herrera C, Hindricks G, Jais P, Nakagawa H, Lambert H, Shah DC: A novel radiofrequency ablation catheter using contact force sensing: Toccata study. *Heart Rhythm*. 2012; 9:18-23.

367. Yokoyama K, Nakagawa H, Shah DC, Lambert H, Leo G, Aeby N, Ikeda A, Pitha JV, Sharma T, Lazzara R, Jackman WM: Novel contact force sensor incorporated in irrigated radiofrequency ablation catheter predicts lesion size and incidence of steam pop and thrombus. *Circ Arrhythm Electrophysiol*. 2008; 1:354-362.

368. Thiagalingam A, Pouliopoulos J, Barry MA, Boyd AC, Eipper V, Yung T, Ross DL, Kovoor P: Cooled needle catheter ablation creates deeper and wider lesions than irrigated tip catheter ablation. *J Cardiovasc Electrophysiol*. 2005; 16:508-515.

369. Mallidi J, Nadkarni GN, Berger RD, Calkins H, Nazarian S: Meta-analysis of catheter ablation as an adjunct to medical therapy for treatment of ventricular tachycardia in patients with structural heart disease. *Heart Rhythm*. 2011; 8:503-510.

370. Bohnen M, Stevenson WG, Tedrow UB, Michaud GF, John RM, Epstein LM, Albert CM, Koplan BA: Incidence and Predictors of Major Complications from

Contemporary Catheter Ablation to treat Cardiac Arrhythmias. *Heart Rhythm*. 2011; 8:1661-1666.

371. Landymore RW, Gardner MA, McIntyre AJ, Barker RA: Surgical intervention for drug-resistant ventricular tachycardia. *J Am Coll Cardiol*. 1990; 16:37-41.

372. Bourke J, Campbell R, McComb J, Furniss S, Doig J, Hilton C: Surgery for postinfarction ventricular tachycardia in the pre-implantable cardioverter defibrillator era: early and long term outcomes in 100 consecutive patients. *Heart*. 1999; 82:156-162.

373. Khan HH, Maisel WH, Ho C, Suzuki M, Soejima K, Solomon S, Stevenson WG: Effect of radiofrequency catheter ablation of ventricular tachycardia on left ventricular function in patients with prior myocardial infarction. *J Interv Card Electrophysiol*. 2002; 7:243-247.

374. Roberts-Thomson KC, Lau DH, Sanders P: The diagnosis and management of ventricular arrhythmias. *Nat Rev Cardiol*. 2011; 8:311-321.

375. Fenoglio JJ, Jr., Pham TD, Harken AH, Horowitz LN, Josephson ME, Wit AL: Recurrent sustained ventricular tachycardia: structure and ultrastructure of subendocardial regions in which tachycardia originates. *Circulation*. 1983; 68:518-533.

376. Engelman ZJ, Trew ML, Smaill BH: Structural heterogeneity alone is a sufficient substrate for dynamic instability and altered restitution. *Circ Arrhythm Electrophysiol*. 2010; 3:195-203.

377. Tung R, Mathuria N, Michowitz Y, Yu R, Buch E, Bradfield J, Mandapati R, Wiener I, Boyle N, Shivkumar K: Functional pace-mapping responses for identification of targets for catheter ablation of scar-mediated ventricular tachycardia. *Circ Arrhythm Electrophysiol*. 2012; 5:264-272.

378. Tung R, Nakahara S, Maccabelli G, Buch E, Wiener I, Boyle NG, Carbucicchio C, Bella PD, Shivkumar K: Ultra high-density multipolar mapping with double ventricular access: a novel technique for ablation of ventricular tachycardia. *J Cardiovasc Electrophysiol*. 2011; 22:49-56.

379. Berruezo A, Fernandez-Armenta J, Mont L, Zeljko H, Andreu D, Herczku C, Boussy T, Tolosana JM, Arbelo E, Brugada J: Combined endocardial and epicardial catheter ablation in arrhythmogenic right ventricular dysplasia incorporating scar dechanneling technique. *Circ Arrhythm Electrophysiol*. 2012; 5:111-121.

380. Della Bella P, Riva S, Fassini G, Giraldi F, Berti M, Klersy C, Trevisi N: Incidence and significance of pleomorphism in patients with postmyocardial infarction ventricular tachycardia. Acute and long-term outcome of radiofrequency catheter ablation. *Eur Heart J*. 2004; 25:1127-1138.

381. de Bakker J, van Capelle F, Janse M, Wilde A, Coronel R, Becker A, Dingemans K, van Hemel N, Hauer R: Reentry as a cause of ventricular tachycardia in patients with chronic ischemic heart disease: electrophysiologic and anatomic correlation. *Circulation*. 1988; 77:589-606.

382. de Bakker JM, Coronel R, Tasseron S, Wilde AA, Opthof T, Janse MJ, van Capelle FJ, Becker AE, Jambroes G: Ventricular tachycardia in the infarcted, Langendorff-perfused human heart: role of the arrangement of surviving cardiac fibers. *J Am Coll Cardiol*. 1990; 15:1594-1607.

383. Taccardi B, Punske BB, Macchi E, MacLeod RS, Ershler PR: Epicardial and intramural excitation during ventricular pacing: effect of myocardial structure. *Am J Physiol Heart Circ Physiol*. 2008; 294:H1753-H1766.

384. Wit AL, Janse MJ. Basic mechanisms of arrhythmias. In: Wit AL, Janse MJ, editors. The Ventricular Arrhythmias of Ischemia and Infarction. New York, NY: Futura; 1993. pp. 1-160.

385. de Bakker JMT, Wittkampf FHM: The Pathophysiologic Basis of Fractionated and Complex Electrograms and the Impact of Recording Techniques on Their Detection and Interpretation. *Circ Arrhythm Electrophysiol*. 2010; 3:204-213.

386. Wissner E, Stevenson WG, Kuck KH: Catheter ablation of ventricular tachycardia in ischaemic and non-ischaemic cardiomyopathy: where are we today? A clinical review. *Eur Heart J*. 2012; 33:1440-1450.

387. Wilber DJ, Davis MJ, Rosenbaum M, Ruskin JN, Garan H: Incidence and determinants of multiple morphologically distinct sustained ventricular tachycardias. *J Am Coll Cardiol*. 1987; 10:583-591.

388. Nayyar S, Wilson L, Ganesan A, Kuklik P, Sullivan T, Baumert M, Brooks A, Young G, Sanders P, Thomson K: High Density Mapping Of Ventricular Scar: A Comparison Of Ventricular Tachycardia Supporting Channels With Channels That Do Not Support VT. *Circ Arrhythm Electrophysiol*. 2013; In press.

389. Masucci AP, Kalampokis A, Eguiluz VM, Hernandez-Garcia E: Extracting directed information flow networks: an application to genetics and semantics. *Phys Rev E Stat Nonlin Soft Matter Phys* 2011; 83:026103(026101-026106).

390. Landis JR, Koch GG: The measurement of observer agreement for categorical data. *Biometrics*. 1977; 33:159-174.

391. Schneider HE, Schill M, Kriebel T, Paul T: Value of dynamic substrate mapping to identify the critical diastolic pathway in postoperative ventricular reentrant tachycardias after surgical repair of tetralogy of fallot. *J Cardiovasc Electrophysiol*. 2012; 23:930-937.

392. Yokokawa M, Desjardins B, Crawford T, Good E, Morady F, Bogun F: Reasons for recurrent ventricular tachycardia after catheter ablation of post-infarction ventricular tachycardia. *J Am Coll Cardiol*. 2013; 61:66-73.

393. Cherry EM, Fenton FH, Gilmour RF: Mechanisms of ventricular arrhythmias: a dynamical systems-based perspective. *Am J Physiol Heart Circ Physiol*. 2012; 302:H2451-H2463.

394. Zeppenfeld K, Kies P, Wijffels MC, Bootsma M, van Erven L, Schalij MJ: Identification of successful catheter ablation sites in patients with ventricular tachycardia based on electrogram characteristics during sinus rhythm. *Heart Rhythm*. 2005; 2:940-950.

395. Wiener I, Mindich B, Pitchon R: Determinants of ventricular tachycardia in patients with ventricular aneurysms: results of intraoperative epicardial and endocardial mapping. *Circulation*. 1982; 65:856-861.

396. Ding C, Gepstein L, Nguyen DT, Wilson E, Hulley G, Beaser A, Lee RJ, Olgin J: High-resolution optical mapping of ventricular tachycardia in rats with chronic myocardial infarction. *Pacing Clin Electrophysiol*. 2010; 33:687-695.

397. Ciaccio EJ, Chow AW, Kaba RA, Davies DW, Segal OR, Peters NS: Detection of the diastolic pathway, circuit morphology, and inducibility of human postinfarction ventricular tachycardia from mapping in sinus rhythm. *Heart Rhythm*. 2008; 5:981-991.

398. Goodman and Gilman's The Pharmacological Basis of Therapeutics. 12 ed. Brunton L, Chabner B, Knollman B, editors. New York: McGraw-Hill Professional; 2011.

399. Heart rate variability: standards of measurement, physiological interpretation and clinical use. Task Force of the European Society of Cardiology and the North American Society of Pacing and Electrophysiology. *Circulation*. 1996; 93:1043-1065.

400. Baumert M, Schlaich MP, Nalivaiko E, Lambert E, Sari CI, Kaye DM, Elser MD, Sanders P, Lambert G: Relation between QT interval variability and cardiac sympathetic activity in hypertension. *Am J Physiol Heart Circ Physiol*. 2011; 300:H1412-1417.

401. Jensen BT, Larroude CE, Rasmussen LP, Holstein-Rathlou NH, Hojgaard MV, Agner E, Kanters JK: Beat-to-beat QT dynamics in healthy subjects. *Ann Noninvasive Electrocardiol*. 2004; 9:3-11.

402. Starc V, Schlegel TT: Real-time multichannel system for beat-to-beat QT interval variability. *J Electrocardiol*. 2006; 39:358-367.

403. Baumert M, Lambert G, Dawood T, Lambert E, Esler M, McGrane M, Barton D, Nalivaiko E: QT interval variability and cardiac norepinephrine spillover in patients with depression and panic disorder. *Am J Physiol Heart Circ Physiol* 2008; 295:H962-968.

404. Lombardi F, Malliani A, Pagani M, Cerutti S: Heart rate variability and its sympatho-vagal modulation. *Cardiovasc Res*. 1996; 32:208-216.

405. Mine T, Shimizu H, Hiromoto K, Furukawa Y, Kanemori T, Nakamura H, Masuyama T, Ohyanagi M: Beat-to-beat QT interval variability is primarily affected by the autonomic nervous system. *Ann Noninvasive Electrocardiol*. 2008; 13:228-233.

406. Piccirillo G, Magrı D, Ogawa M, Song J, Chong V, Han S, Joung B, Choi E, Hwang S, Chen L, Lin S, Chen P: Autonomic nervous system activity measured directly and QT interval variability in normal and pacing-induced tachycardia heart failure dogs. *J Am Coll Cardiol*. 2009; 54:840-850.

407. Kaye D, Lefkovits J, Jennings G, Bergin P, Broughton A, Esler M: Adverse consequences of high sympathetic nervous activity in the failing human heart. *J Am Coll Cardiol*. 1995; 26:1257-1263.

408. Bristow MR: beta-adrenergic receptor blockade in chronic heart failure. *Circulation*. 2000; 101:558-569.

409. Feldman DS, Carnes CA, Abraham WT, Bristow MR: Mechanisms of disease: beta-adrenergic receptors--alterations in signal transduction and pharmacogenomics in heart failure. *Nat Clin Pract Cardiovasc Med*. 2005; 2:475-483.

410. Desai N, Raghunandan DS, Mallavarapu M, Berger RD, Yeragani VK: Beat-to-beat heart rate and QT variability in patients with congestive cardiac failure: blunted response to orthostatic challenge. *Ann Noninvasive Electrocardiol*. 2004; 9:323-329.

411. Berglund H, Edlund A, Theodorsson E, Vallin H: Haemodynamic and hormonal responses to cardiac pacing in humans: influence of different stimulation sequences and rates. *Clin Sci*. 1995; 88:165-172.

412. Franz MR, Swerdlow CD, Liem LB, Schaefer J: Cycle length dependence of human action potential duration in vivo. Effects of single extrastimuli, sudden sustained rate acceleration and deceleration, and different steady-state frequencies. *J Clin Invest*. 1988; 82:972-979.

413. Lombardi F, Sandrone G, Porta A, Torzillo D, Terranova G, Baselli G, Cerutti S, Malliani A: Spectral analysis of short term R-Tapex interval variability during sinus rhythm and fixed atrial rate. *Eur Heart J* 1996; 17:769-778.

414. Porta A, Tobaldini E, Gnecchi-Ruscone T, Montano N: RT variability unrelated to heart period and respiration progressively increases during graded head-up tilt. *Am J Physiol Heart Circ Physiol*. 2010; 298:H1406-1414.

415. Chen X, Hu Y, Fetics BJ, Berger RD, Trayanova NA: Unstable QT interval dynamics precedes ventricular tachycardia onset in patients with acute myocardial infarction: a novel approach to detect instability in QT interval dynamics from clinical ECG. *Circ Arrhythm Electrophysiol*. 2011; 4:858-866.

416. Wilkoff BL, Cook JR, Epstein AE, Greene HL, Hallstrom AP, Hsia H, Kutalek SP, Sharma A: Dual-chamber pacing or ventricular backup pacing in patients with an

implantable defibrillator: the Dual Chamber and VVI Implantable Defibrillator (DAVID) Trial. *JAMA*. 2002; 288:3115-3123.

417. Tereshchenko LG, Henrikson CA, Berger RD: Strong coherence between heart rate variability and intracardiac repolarization lability during biventricular pacing is associated with reverse electrical remodeling of the native conduction and improved outcome. *J Electrocardiol*. 2011; 44:713-717.

418. Ouellet G, Huang DT, Moss AJ, Hall WJ, Barsheshet A, McNitt S, Klein H, Zareba W, Goldenberg I: Effect of cardiac resynchronization therapy on the risk of first and recurrent ventricular tachyarrhythmic events in MADIT-CRT. *J Am Coll Cardiol*. 2012; 60:1809-1816.

419. Oosterhoff P, Tereshchenko LG, van der Heyden MAG, Ghanem RN, Fetics BJ, Berger RD, Vos MA: Short-term variability of repolarization predicts ventricular tachycardia and sudden cardiac death in patients with structural heart disease: a comparison to QT variability index. *Heart Rhythm*. 2011; 8:1584-1590.

420. Piccirillo G, Rossi P, Mitra M, Quaglione R, Dell'Armi A, Di Barba D, Maisto D, Lizio A, Barilla F, Magri D: Indexes of temporal myocardial repolarization dispersion and sudden cardiac death in heart failure: any difference? *Ann Noninvasive Electrocardiol*. 2013; 18:130-139.

421. Wiest DB, Haney JS: Clinical pharmacokinetics and therapeutic efficacy of esmolol. *Clin Pharmacokinet*. 2012; 51:347-356.

422. Chatterjee S, Biondi-Zoccai G, Abbate A, D'Ascenzo F, Castagno D, Van Tassell B, Mukherjee D, Lichstein E: Benefits of beta blockers in patients with heart failure and reduced ejection fraction: network meta-analysis. *BMJ (Clinical research ed)*. 2013; 346:f55.

423. Orejarena LA, Vidaillet H, Jr., DeStefano F, Nordstrom DL, Vierkant RA, Smith PN, Hayes JJ: Paroxysmal supraventricular tachycardia in the general population. *J Am Coll Cardiol*. 1998; 31:150-157.

424. Krauss TT, Mauser W, Reppel M, Schunkert H, Bonnemeier H: Gender effects on novel time domain parameters of ventricular repolarization inhomogeneity. *Pacing Clin Electrophysiol*. 2009; 32 Suppl 1:S167-172.

425. Hasan MA, Abbott D, Baumert M: Relation between beat-to-beat QT interval variability and T-wave amplitude in healthy subjects. *Ann Noninvasive Electrocardiol*. 2012; 17:195-203.

426. Nakagawa M, Ooie T, Ou B, Ichinose M, Takahashi N, Hara M, Yonemochi H, Saikawa T: Gender differences in autonomic modulation of ventricular repolarization in humans. *J Cardiovasc Electrophysiol*. 2005; 16:278-284.

427. Myerburg RJ, Castellanos A: Clinical trials of implantable defibrillators. *N Engl J Med*. 1997; 337:1621-1623.

428. Larsen GK, Evans J, Lambert WE, Chen Y, Raitt MH: Shocks burden and increased mortality in implantable cardioverter-defibrillator patients. *Heart Rhythm*. 2011; 8:1881-1886.

429. Shepard RK, Ellenbogen KA: Predicting outcome after implantable cardioverter-defibrillator therapy: a new piece to the puzzle? *J Am Coll Cardiol*. 2009; 54:829-831.

430. Centre for Reviews and Dissemination. Undertaking systematic reviews of research on effectiveness: CRD's guidance for carrying out or commissioning reviews. 2nd ed. Khan KS, Riet Gt, Glanville J, Sowden AJ, Kleijnen J, editors. York: NHS Centre for Reviews and Dissemination, University of York; 2001.

431. Montijano Cabrera nM, Barrera Cordero A, Alzueta Rodrìguez J, Robledo Carmona J, de Teresa Galv·n E: Radiofrequency Catheter Ablation of Ventricular Tachycardia in Patients With an Implantable Defibrillator. Long-Term Follow-up. *Revista Espanola de Cardiologia*. 2005; 58:491-498.

432. Kozluk E, Gaj S, Kiliszek M, Lodzinski P, Piatkowska A, Opolski G: Efficacy of catheter ablation in patients with an electrical storm. *Kardiol Pol*. 2011; 69:665-670.

433. Trappe HJ, Klein H, Wenzlaff P, Lichtlen PR: [Significance of catheter ablation as emergency intervention in patients with sustained monomorphic ventricular tachycardia]. *Z Kardiol*. 1991; 80:720-726.

434. Sosa E, Scanavacca M, d'Avila A, Oliveira F, Ramires JA: Nonsurgical transthoracic epicardial catheter ablation to treat recurrent ventricular tachycardia occurring late after myocardial infarction. *J Am Coll Cardiol*. 2000; 35:1442-1449.

435. O'Callaghan PA, Poloniecki J, Sosa-Suarez G, Ruskin JN, McGovern BA, Garan H: Long-term clinical outcome of patients with prior myocardial infarction after palliative radiofrequency catheter ablation for frequent ventricular tachycardia. *Am J Cardiol*. 2001; 87:975-979.

436. Fiala M, Chovanzik J, Neuwirth R, Nykl I, Szymeczek H, Nevralova R, Jiravsky O, Branny M: [Sustained monomorphic ventricular tachycardia in patients with structural heart disease. Different arrhythmogenic substrates, different options of palliative and curative treatment in the era of three-dimensional mapping]. *Vnitr Lek*. 2006; 52:577-589.

437. Volkmer M, Ouyang F, Deger F, Ernst S, Goya M, Bansch D, Berodt K, Kuck KH, Antz M: Substrate mapping vs. tachycardia mapping using CARTO in patients with coronary artery disease and ventricular tachycardia: impact on outcome of catheter ablation. *Europace*. 2006; 8:968-976.

438. Eckart RE, Hruczkowski TW, Tedrow UB, Koplan BA, Epstein LM, Stevenson WG: Sustained ventricular tachycardia associated with corrective valve surgery. *Circulation*. 2007; 116:2005-2011.

439. Grimard C, Lacotte J, Hidden-Lucet F, Duthoit G, Gallais Y, Frank R: Percutaneous epicardial radiofrequency ablation of ventricular arrhythmias after failure of endocardial approach: a 9-year experience. *J Cardiovasc Electrophysiol*. 2010; 21:56-61.

440. Della Bella P, Brugada J, Zeppenfeld K, Merino J, Neuzil P, Maury P, Maccabelli G, Vergara P, Baratto F, Berruezo A, Wijnmaalen AP: Epicardial ablation for ventricular tachycardia: a European multicenter study. *Circ Arrhythm Electrophysiol*. 2011; 4:653-659.

441. Russo AD, Casella M, Pieroni M, Pelargonio G, Bartoletti S, Santangeli P, Zucchetti M, Innocenti E, Di Biase L, Carbucicchio C, Bellocci F, Fiorentini C, Natale A, Tondo C: Drug-Refractory Ventricular Tachycardias After Myocarditis / Clinical Perspective. *Circ Arrhythm Electrophysiol*. 2012; 5:492-498.

442. Nellens P, Gursoy S, Andries E, Brugada P: Transcoronary chemical ablation of arrhythmias. *Pacing Clin Electrophysiol*. 1992; 15:1368-1373.

443. Ometto R, Bedogni F, La Vecchia L, Finocchi G, Mosele GM, Vincenzi M: Radiofrequency catheter ablation of the slow reentrant pathway of sustained ventricular tachycardia. *Pacing Clin Electrophysiol*. 1993; 16:1898-1905.

444. Willems S, Borggrefe M, Shenasa M, Chen X, Hindricks G, Haverkamp W, Wietholt D, Block M, Breithardt G: Radiofrequency catheter ablation of ventricular

tachycardia following implantation of an automatic cardioverter defibrillator. *Pacing Clin Electrophysiol*. 1993; 16:1684-1692.

445. Kottkamp H, Hindricks G, Chen X, Brunn J, Willems S, Haverkamp W, Block M, Breithardt G, Borggrefe M: Radiofrequency Catheter Ablation of Sustained Ventricular-Tachycardia in Idiopathic Dilated Cardiomyopathy. *Circulation*. 1995; 92:1159-1168.

446. Cao K, Gonska BD: Catheter ablation of incessant ventricular tachycardia: acute and long-term results. *Eur Heart J*. 1996; 17:756-763.

447. Sato M, Sakurai M, Yotsukura A, Betsuyaku T, Ito T, Yoshida I, Kitabatake A: The efficacy of radiofrequency catheter ablation for the treatment of ventricular tachycardia associated with cardiomyopathy. *Jpn Circ J*. 1997; 61:55-63.

448. Haissaguerre M, Shoda M, Jais P, Nogami A, Shah DC, Kautzner J, Arentz T, Kalushe D, Lamaison D, Griffith M, Cruz F, de Paola A, Gaita F, Hocini M, Garrigue S, Macle L, Weerasooriya R, Clementy J: Mapping and ablation of idiopathic ventricular fibrillation. *Circulation*. 2002; 106:962-967.

449. Haissaguerre M, Extramiana F, Hocini M, Cauchemez B, Jais P, Cabrera JA, Farre J, Leenhardt A, Sanders P, Scavee C, Hsu LF, Weerasooriya R, Shah DC, Frank R, Maury P, Delay M, Garrigue S, Clementy J: Mapping and ablation of ventricular fibrillation associated with long-QT and Brugada syndromes. *Circulation*. 2003; 108:925-928.

450. Bansch D, Oyang F, Antz M, Arentz T, Weber R, Val-Mejias JE, Ernst S, Kuck KH: Successful catheter ablation of electrical storm after myocardial infarction. *Circulation*. 2003; 108:3011-3016.

451. Brugada J, Berruezo A, Cuesta A, Osca J, Chueca E, Fosch X, Wayar L, Mont L: Nonsurgical transthoracic epicardial radiofrequency ablation: An alternative in incessant ventricular tachycardia. *J Am Coll Cardiol*. 2003; 41:2036-2043.

452. Silva RM, Mont L, Nava S, Rojel U, Matas M, Brugada J: Radiofrequency catheter ablation for arrhythmic storm in patients with an implantable cardioverter defibrillator. *Pacing Clin Electrophysiol*. 2004; 27:971-975.

453. Marrouche NF, Verma A, Wazni O, Schweikert RA, Martin DO, Saliba W, Kilicaslan F, Cummings JE, Burkhardt DJ, Bhargava M, Bash D, Brachmann J, Guenther J, Hao S, Beheiry S, Rossillo A, Raviele A, Themistoclakis S, Natale A: Mode of Initiation and Ablation of Ventricular Fibrillation Storms In Patients With Ischemic Cardiomyopathy. *J Am Coll Cardiol*. 2004; 43:1715-1720.

454. Szumowski L, Sanders P, Walczak F, Hocini M, Jais P, Kepski R, Szufladowicz E, Urbanek P, Derejko P, Bodalski R, Haissaguerre M: Mapping and ablation of polymorphic ventricular tachycardia after myocardial infarction. *J Am Coll Cardiol*. 2004; 44:1700-1706.

455. Schreieck J, Zrenner B, Deisenhofer I, Schmitt C: Rescue ablation of electrical storm in patients with ischemic cardiomyopathy: A potential-guided ablation

approach by modifying substrate of intractable, unmappable ventricular tachycardias. *Heart Rhythm*. 2005; 2:10-14.

456. Mlcochova H, Saliba WI, Burkhardt DJ, Rodriguez RE, Cummings JE, Lakkireddy D, Patel D, Natale A: Catheter Ablation of Ventricular Fibrillation Storm in Patients with Infiltrative Amyloidosis of the Heart. *J Cardiovasc Electrophysiol*. 2006; 17:426-430.

457. Dandamudi G, Ghumman WS, Das MK, Miller JM: Endocardial catheter ablation of ventricular tachycardia in patients with ventricular assist devices. *Heart Rhythm*. 2007; 4:1165-1169.

458. Reithmann C, Hahnefeld A, Oversohl N, Ulbrich M, Remp T, Steinbeck G: Reinitiation of ventricular macroreentry within the His-Purkinje system by back-up ventricular pacing - A mechanism of ventricular tachycardia storm. *Pacing Clin Electrophysiol*. 2007; 30:225-235.

459. Bode K, Hindricks G, Piorkowski C, Sommer P, Janousek J, Dagres N, Arya A: Ablation of Polymorphic Ventricular Tachycardias in Patients with Structural Heart Disease. *Pacing Clin Electrophysiol*. 2008; 31:1585-1591.

460. Carbucicchio C, Santamaria M, Trevisi N, Maccabelli G, Giraldi F, Fassini G, Riva S, Moltrasio M, Cireddu M, Veglia F, Della Bella P: Catheter ablation for the treatment of electrical storm in patients with Implantable cardioverter-defibrillators

- Short- and long-term outcomes in a prospective single-center study. *Circulation*. 2008; 117:462-469.

461. Nayak HM, Verdino RJ, Russo AM, Gerstenfeld EP, Hsia HH, Lin D, Dixit S, Cooper JM, Callans DJ, Marchlinski FE: Ventricular tachycardia storm after initiation of biventricular pacing: Incidence, clinical characteristics, management, and outcome. *J Cardiovasc Electrophysiol*. 2008; 19:708-715.

462. Sakata T, Tanner H, Stuber T, Delacretaz E: His-Purkinje system re-entry in patients with clustering ventricular tachycardia episodes. *Europace*. 2008; 10:289-293.

463. Uusimaa P, Ylitalo K, Anttonen O, Kerola T, Virtanen V, Paakko E, Raatikainen P: Ventricular tachyarrhythmia as a primary presentation of sarcoidosis. *Europace*. 2008; 10:760-766.

464. Enjoji Y, Mizobuchi M, Muranishi H, Miyamoto C, Utsunomiya M, Funatsu A, Kobayashi T, Nakamura S: Catheter ablation of fatal ventricular tachyarrhythmias storm in acute coronary syndrome-role of Purkinje fiber network. *J Interv Card Electrophysiol*. 2009; 26:207-215.

465. Haghjoo M, Hindricks G, Bode K, Piorkowski C, Bollmann A, Arya A: Initial clinical experience with the new irrigated tip magnetic catheter for ablation of scar-related sustained ventricular tachycardia: a small case series. *J Cardiovasc Electrophysiol*. 2009; 20:935-939.

466. Sinha AM, Schmidt M, Marschang H, Gutleben K, Ritscher G, Brachmann J, Marrouche NF: Role of Left Ventricular Scar and Purkinje-Like Potentials During Mapping and Ablation of Ventricular Fibrillation in Dilated Cardiomyopathy. *Pacing Clin Electrophysiol*. 2009; 32:286-290.

467. Arya A, Bode K, Piorkowski C, Bollmann A, Sommer P, Gaspar T, Wetzel U, Husser D, Kottkamp H, Hindricks G: Catheter ablation of electrical storm due to monomorphic ventricular tachycardia in patients with nonischemic cardiomyopathy: acute results and its effect on long-term survival. *Pacing Clin Electrophysiol*. 2010; 33:1504-1509.

468. Arya A, Eitel C, Bollmann A, Wetzel U, Sommer P, Gaspar T, Husser D, Piorkowski C, Hindricks G: Catheter Ablation of Scar-Related Ventricular Tachycardia in Patients with Electrical Storm Using Remote Magnetic Catheter Navigation. *Pacing Clin Electrophysiol*. 2010; 33:1312-1318.

469. Bourke T, Vaseghi M, Michowitz Y, Sankhla V, Shah M, Swapna N, Boyle NG, Mahajan A, Narasimhan C, Lokhandwala Y, Shivkumar K: Neuraxial modulation for refractory ventricular arrhythmias: value of thoracic epidural anesthesia and surgical left cardiac sympathetic denervation. *Circulation*. 2010; 121:2255-2262.

470. Peichl P, Cihak R, Kozeluhova M, Wichterle D, Vancura V, Kautzner J: Catheter ablation of arrhythmic storm triggered by monomorphic ectopic beats in patients with coronary artery disease. *J Interv Card Electrophysiol*. 2010; 27:51-59.

471. Kozeluhova M, Peichl P, Cihak R, Wichterle D, Vancura V, Bytesnik J, Kautzner J: Catheter ablation of electrical storm in patients with structural heart disease. *Europace*. 2011; 13:109-113.

472. Deneke T, Shin DI, Lawo T, Bosche L, Balta O, Anders H, Bunz K, Horlitz M, Grewe PH, Lemke B, Mugge A: Catheter ablation of electrical storm in a collaborative hospital network. *Am J Cardiol*. 2011; 108:233-239.

473. Ueda A, Fukamizu S, Soejima K, Tejima T, Nishizaki M, Nitta T, Kobayashi Y, Hiraoka M, Sakurada H: Clinical and electrophysiological characteristics in patients with sustained monomorphic reentrant ventricular tachycardia associated with dilated-phase hypertrophic cardiomyopathy. *Europace*. 2012; 14:734-740.

474. Ukena C, Bauer A, Mahfoud F, Schreieck J, Neuberger HR, Eick C, Sobotka PA, Gawaz M, Bohm M: Renal sympathetic denervation for treatment of electrical storm: first-in-man experience. *Clin Res Cardiol*. 2012; 101:63-67.

475. Ajijola OA, Lellouche N, Bourke T, Tung R, Ahn S, Mahajan A, Shivkumar K: Bilateral cardiac sympathetic denervation for the management of electrical storm. *J Am Coll Cardiol*. 2012; 59:91-92.

476. Trappe HJ, Klein H, Wenzlaff P, Lichtlen PR: The Value of Catheter Ablation as Emergency Treatment in Patients with Sustained Monomorphic Ventricular-Tachycardia. *Heart*. 1991; 80:720-726.

477. Tikkanen JT, Anttonen O, Junttila MJ, Aro AL, Kerola T, Rissanen HA, Reunanen A, Huikuri HV: Long-term outcome associated with early repolarization on electrocardiography. *N Engl J Med*. 2009; 361:2529-2537.

478. Haissaguerre M, Derval N, Sacher F, Jesel L, Deisenhofer I, de Roy L, Pasquie JL, Nogami A, Babuty D, Yli-Mayry S, De Chillou C, Scanu P, Mabo P, Matsuo S, Probst V, Le Scouarnec S, Defaye P, Schlaepfer J, Rostock T, Lacroix D, Lamaison D, Lavergne T, Aizawa Y, Englund A, Anselme F, O'Neill M, Hocini M, Lim KT, Knecht S, Veenhuyzen GD, Bordachar P, Chauvin M, Jais P, Coureau G, Chene G, Klein GJ, Clementy J: Sudden cardiac arrest associated with early repolarization. *N Engl J Med*. 2008; 358:2016-2023.

479. Tavernier R, Gevaert S, De Sutter J, De Clercq A, Rottiers H, Jordaens L, Fonteyne W: Long term results of cardioverter-defibrillator implantation in patients with right ventricular dysplasia and malignant ventricular tachyarrhythmias. *Heart*. 2001; 85:53-56.

480. Maron BJ, Spirito P, Shen WK, Haas TS, Formisano F, Link MS, Epstein AE, Almquist AK, Daubert JP, Lawrenz T, Boriani G, Estes NA, 3rd, Favale S, Piccininno M, Winters SL, Santini M, Betocchi S, Arribas F, Sherrid MV, Buja G, Semsarian C, Bruzzi P: Implantable cardioverter-defibrillators and prevention of sudden cardiac death in hypertrophic cardiomyopathy. *JAMA*. 2007; 298:405-412.

481. Lubitz SA, Goldbarg SH, Mehta D: Sudden cardiac death in infiltrative cardiomyopathies: sarcoidosis, scleroderma, amyloidosis, hemachromatosis. *Prog Cardiovasc Dis*. 2008; 51:58-73.

482. Passman R, Kadish A: Sudden Death Prevention With Implantable Devices. *Circulation*. 2007; 116:561-571.

483. Littmann L, Rennyson SL: Electrical storm: clinical manifestations and management. *Minerva Med*. 2007; 98:489-501.

484. Proietti R, Sagone A: Electrical storm: Incidence, Prognosis and Therapy. *Indian Pacing Electrophysiol J*. 2011; 11:34-42.

485. Nakahara S, Tung R, Ramirez RJ, Michowitz Y, Vaseghi M, Buch E, Gima J, Wiener I, Mahajan A, Boyle N, Shivkumar K: Characterization of the arrhythmogenic substrate in ischemic and nonischemic cardiomyopathy Implications for catheter ablation of hemodynamically unstable ventricular tachycardia. *J Am Coll Cardiol*. 2010; 55:2355-2365.

486. Bai R, Di Biase L, Shivkumar K, Mohanty P, Tung R, Santangeli P, Saenz LC, Vacca M, Verma A, Khaykin Y, Mohanty S, Burkhardt JD, Hongo R, Beheiry S, Dello Russo A, Casella M, Pelargonio G, Santarelli P, Sanchez J, Tondo C, Natale A: Ablation of ventricular arrhythmias in arrhythmogenic right ventricular dysplasia/cardiomyopathy: arrhythmia-free survival after endo-epicardial substrate based mapping and ablation. *Circ Arrhythm Electrophysiol*. 2011; 4:478-485.

487. Dosdall DJ, Tabereaux PB, Kim JJ, Walcott GP, Rogers JM, Killingsworth CR, Huang J, Robertson PG, Smith WM, Ideker RE: Chemical ablation of the Purkinje system causes early termination and activation rate slowing of long-duration ventricular fibrillation in dogs. *Am J Physiol Heart Circ Physiol*. 2008; 295:H883-H889.

488. Khan HH, Maisel WH, Ho C, Suzuki M, Soejima K, Solomon S, Stevenson WG: Effect of radiofrequency catheter ablation of ventricular tachycardia on left ventricular function in patients with prior myocardial infarction. *J Interv Card Electrophysiol*. 2002; 7:243-247.

489. Frankel DS, Mountantonakis SE, Zado ES, Anter E, Bala R, Cooper JM, Deo R, Dixit S, Epstein AE, Garcia FC, Gerstenfeld EP, Hutchinson MD, Lin D, Patel VV, Riley MP, Robinson MR, Tzou WS, Verdino RJ, Callans DJ, Marchlinski FE: Noninvasive programmed ventricular stimulation early after ventricular tachycardia ablation to predict risk of late recurrence. *J Am Coll Cardiol*. 2012; 59:1529-1535.